

# An annotated and illustrated identification guide to common mesophotic reef sponges (Porifera, Demospongiae, Hexactinellida, and Homoscleromorpha) inhabiting Flower Garden Banks National Marine Sanctuary and vicinities

Maria Cristina Díaz<sup>1</sup>, Marissa Nuttall<sup>2,3</sup>, Shirley A. Pomponi<sup>1</sup>, Klaus Rützler<sup>4</sup>, Sarah Klontz<sup>5</sup>, Christi Adams<sup>2</sup>, Emma L. Hickerson<sup>2</sup>, G. P. Schmahl<sup>2</sup>

**1** Harbor Branch Oceanographic Institute, Florida Atlantic University, Fort Pierce, FL, USA **2** Flower Garden Banks National Marine Sanctuary, Galveston, TX, USA **3** CPC Inc, Galveston, TX, USA **4** National Museum of Natural History, Smithsonian Institution, Washington D.C., USA **5** Genetic Disease Research Branch, NHGRI, NIH, Bethesda, MD, USA

Corresponding author: Maria Cristina Díaz ([taxochica@gmail.com](mailto:taxochica@gmail.com))

---

Academic editor: Pavel Stoev | Received 23 August 2022 | Accepted 1 January 2023 | Published 11 May 2023

---

<https://zoobank.org/4CE0D6C5-C304-4F74-8387-FCC71F8F8AC0>

---

**Citation:** Díaz MC, Nuttall M, Pomponi SA, Rützler K, Klontz S, Adams C, Hickerson EL, Schmahl GP (2023) An annotated and illustrated identification guide to common mesophotic reef sponges (Porifera, Demospongiae, Hexactinellida, and Homoscleromorpha) inhabiting Flower Garden Banks National Marine Sanctuary and vicinities. ZooKeys 1161: 1–68. <https://doi.org/10.3897/zookeys.1161.93754>

---

## Abstract

Sponges are recognized as a diverse and abundant component of mesophotic and deep-sea ecosystems worldwide. In Flower Garden Banks National Marine Sanctuary region within the northwestern Gulf of Mexico, sponges thrive among diverse biological and geological habitats between 16–200+ m deep (i.e., coral reefs and communities, algal nodules, and coralline algae reefs, mesophotic reefs, patch reefs, scarps, ridges, soft substrate, and rocky outcrops). A synoptic guide is presented, developed by studying common sponge species in the region, through direct sampling and *in-situ* photographic records. A total of 64 species is included: 60 are Demospongiae (14 orders), two are Hexactinellida (one order), and two are Homoscleromorpha (one order). Thirty-four taxa are identified to species and 13 were identified to have affinity with, but were not identical to, a known species. Fifteen taxa could only be identified to genus level, and the species remain as uncertain (*incerta sedis*), with the potential to represent new species or variants of known species. One specimen received only a family assignment. This study extends

geographic or mesophotic occurrence data for eleven known species and includes several potentially new species. This work improves our knowledge of Gulf of Mexico sponge biodiversity and highlights the importance of the region for scientists and resource managers.

### **Keywords**

Algal reefs, biodiversity, Gulf of Mexico, mesophotic reefs, Porifera, sponges

## **Introduction**

Flower Garden Banks National Marine Sanctuary consists of portions of 17 topographic features in the northwestern Gulf of Mexico. The reefs and banks occur along the continental shelf, from 70–120 miles off the coast of Texas and Louisiana (Fig. 1), range in depth from 16–220 m, and harbor coral reefs, coral communities, coralline algal reefs, rhodolith beds, and deep mesophotic communities. Extensive remotely operated vehicle explorations within the region have been conducted during the past 30 years by National Oceanic and Atmospheric Administration's (NOAA's) Flower Garden Banks National Marine Sanctuary (FGBNMS) and partners, including NOAA's Deep-Sea Coral Research and Technology Program (ONMS 2016). More than 50,000 geo-referenced images, 900 hours of video, and 38 annotation logs have been collected during those expeditions, and multiple databases have been produced. This prior work discovered that the region consists of a series of unique and interconnected habitats of banks, coral reefs, patch reefs, scarps, and ridges, featuring algal dominated areas, soft substrate features, mesophotic and deep coral communities and rocky outcrops (Schmahl et al. 2008). A comprehensive review of the biology and ecology of coral reefs, coral communities, and mesophotic habitats in this region, including the area within the sanctuary boundaries, have documented four major reef-related habitats: i) a “coral reef zone” from approximately 0–70 m that includes the actively accreting hermatypic coral assemblages and a shallow mesophotic coral community, ii) a “coral community zone” that occurs primarily in depths less than 50 m where hermatypic coral species are present at low densities but are not dominant, iii) a “coralline algae” or mid-mesophotic zone occurring in depths 60–120 m and characterized by rocky outcrops with a predominance of crustose coralline algal nodules, and iv) a lower mesophotic reef occurring between 90–200 m, characterized by antipatharian and alcyonarian corals, crinoids, bryozoans, sponges, azooxanthellate branching corals, and small, solitary hard corals (Schmahl et al. 2008; Semmler et al. 2016; Nuttall et al. 2022). These complex underwater features provide feeding areas, spawning sites and habitat for critical life history stages for a variety of reef organisms (Schmahl et al. 2008).

Sponges are recognized as a diverse and abundant component of mesophotic and deep-sea ecosystems (Pomponi et al. 2019, Slattery et al. 2017; Schmahl et al. 2012), and in 2017 the development of field guides was identified as a priority in NOAA's Science Plan for the Southeast Deep Coral Initiative (Wagner et al. 2017). Hickerson and Schmahl (2012) created a quick reference photo guide poster for 37 species studied

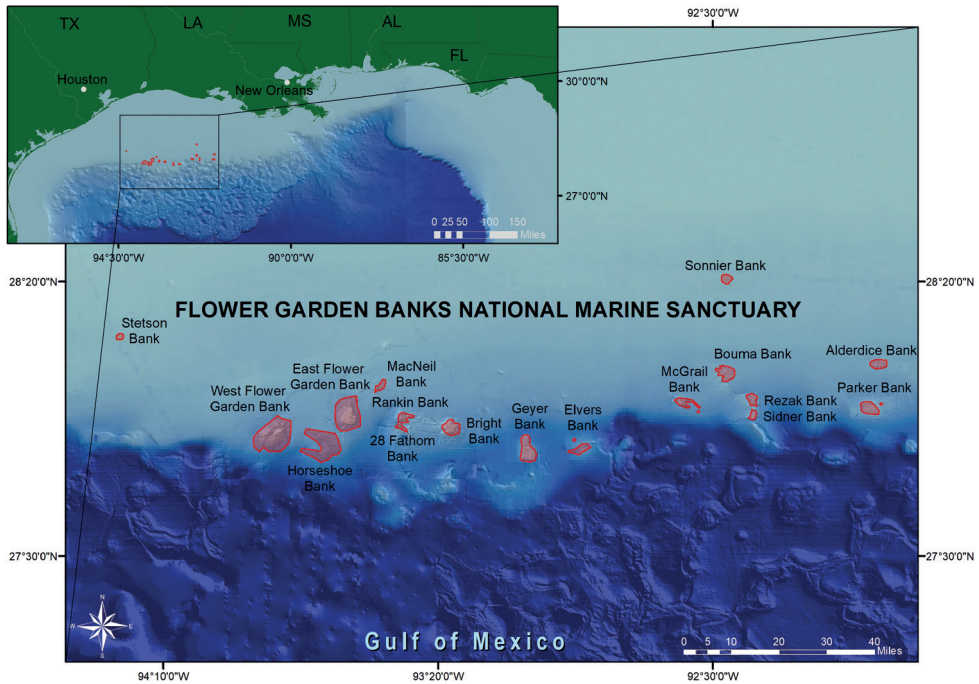


**Figure 1.** Map of Flower Garden Banks National Marine Sanctuary.

and identified by KR, SWK, and CA that had been documented during exploratory dives between 50 and 110 m deep within the northwestern Gulf of Mexico. More surveys have been conducted since 2012, resulting in additional sponge specimens and imagery that required further investigation. These expeditions investigated areas that were under consideration for sanctuary expansion and officially became part of the sanctuary in 2021 (15 CFR Part 922 – Subpart L, 2021). Twenty-seven morphospecies of emergent sponges from the Classes Demospongiae and Hexactinellida and an unaccounted number of thin encrusting species were documented during an expedition in 2019. This study expanded the recognized sponge biodiversity of Flower Garden Banks National Marine Sanctuary region by 17 species (<https://flowergarden.noaa.gov/about/spongelist.html>) and includes at least six species potentially new to science: *Pleraplysilla* sp. 2, *Geodia* sp. 1, *Cinachyrella* sp. 1, *Auletta* sp. 1, *Petrosia* sp. 1, and *Xestospongia* sp. 1.

The major goal of this study was to update current knowledge of Porifera biodiversity from mesophotic depths at the sanctuary region and to promote this knowledge among major stakeholders. We have developed a synoptic identification guide that can be used by a wide range of end-users (i.e., marine scientists and students, conservationists, environmental managers, naturalists, recreational divers, etc.). This identification guide summarizes the current taxonomic status and distinct features for 63 species distinguished of the common sponge species encountered in the region. This work

will improve our knowledge of sponge biodiversity in the Gulf of Mexico and enhance studies of sponges from mesophotic and deep-water ecosystems in the region. Furthermore, this first illustrated guide to species at mesophotic depths in the northwestern Gulf of Mexico will facilitate the comparisons with recently studied mesophotic sponge fauna from other deep mesophotic habitats occurring at Pulley Ridge in the southeast Gulf of Mexico (MCD unpublished data), Cuba (Reed et al. 2018; Díaz et al. 2019) and southeast USA Deep Ecosystems in Marine Protected Areas (Díaz et al. 2021; Reed et al. 2021). The potential discovery of new species and its importance will be discussed herein.

## Materials and methods

### Area of study

This study focused on topographic features in the northwestern Gulf of Mexico in and around Flower Garden Banks National Marine Sanctuary located on the continental shelf edge in the northwestern Gulf of Mexico in the USA (Fig. 1). Samples presented in this study were collected both within and adjacent to the sanctuary boundaries and occurred within one of the six habitats (coral reefs, coral communities, algal nodules, coralline algae reefs, lower mesophotic reefs, and soft substrates) described by Schmahl et al. (2008) and Semmler et al. (2016). The waters in the region are typically oligotrophic, warm tropical water that is transported from the Caribbean into the eastern Gulf of Mexico via the Loop Current and travels to the western Gulf through the action of spin-off eddies (see Schmahl et al. 2008: fig. 6.6). The offshore location (60–130 miles off the continental coast) of these habitats typically separates them from turbid, brackish, coastal waters and the influence of coastal runoff and nearshore eutrophication. However, sporadic coastal water intrusion events have been documented in the region (Kealoha et al. 2020).

### Collection methods and data

Collections were made using one of three remotely operated vehicles (ROV), including Phantom S2, owned and operated by University of North Carolina at Wilmington (UNCW) Undersea Vehicle Program, MOHAWK, owned by the National Marine Sanctuary Foundation and operated by UNCW Undersea Vehicle Program, and YOGI, owned and operated by the Global Foundation for Ocean Exploration. Specimens were photographed in situ using a variety of digital still cameras with scale lasers in the field of view set at 10 cm (Fig. 2). Sponges were collected using a manipulator on the ROV and either brought directly to the surface in the manipulator or placed in a sample box mounted on the ROV. Once on the surface, sponges were photographed in the lab using a digital still camera prior to preservation. Sample metadata, including location (latitude and longitude), depth, and habitat were recorded into a Microsoft



**Figure 2.** Sample collection DFH33-542A using a manipulator mounted on an ROV. Green scale lasers, 10 cm apart seen in the field of view, were used to estimate the size of the specimen.

Excel database archived at Flower Garden Banks National Marine Sanctuary offices in Galveston, TX. Specimens were either preserved in 95% ethanol, and occasionally in 10% formalin in sea water for histological evaluation when specimens were potential new species. Samples were stored at the Flower Garden Banks National Marine Sanctuary offices in Galveston, TX, except for samples collected in 2019, which are archived at Florida Atlantic University – Harbor Branch Oceanographic Institute, Marine Biotechnology Reference Collection (<http://hboi-marine-biomedical-and-biotechnology-reference-collection.fau.edu/app/data-portal>). Suppl. material 1 lists all species included in this guide, location of observations, and their abundance at each site.

## Species data and morphological characterization

Each species within this guide is represented by an *in-situ* image, the lowest available scientific name, species author/date, higher taxonomy, depth, and sample number (indicated in the figure legend). The species data are divided in six sections: “Diagnostic features” describes distinctive morphologic features; Similar species with which it might be confused; “Distribution and abundance” refers to overall regional distribution from the World Porifera Database and other recent references (Pomponi et al. 2019) indicating countries and/or regions where the species occur as well as the number of sites within the sanctuary (i.e., East Flower Garden Bank, Geyer Bank, etc.) in which the species was observed and a qualitative range of abundances (Suppl. material 1); “Ecology” mentions the habitat(s) where each species occurs; “ID” indicates the individual(s) who identified the sample by their initials, and “References” provides literature where the reader can get a more detailed description including other characters such as spicules, skeletal architecture, or genetic information.

Fifty-two of the 64 species included on this study were identified by the analysis of one or more samples. Therefore, the majority (~ 84%) of the identifications were

confirmed by evaluation of skeletal morphology (skeleton type, size, and architecture) as well as features of the external morphology. Skeleton analysis was carried out using methods described in Díaz and Pomponi (2018) but using a rapid tissue digestion in bleach instead of nitric acid. The taxonomic assignation for each morphotype reflects the most current classification of the World Porifera Database (de Voogd et al. 2023). The occurrence and qualitative estimate of abundance was made within an approximate area of 259 sq. miles (the core biological zone that FGB uses to bound explorations; Office of National Marine Sanctuaries 2020). The occurrence at each site is characterized according to the approximate number of specimens observed as: Single (**S**) if only one specimen was observed, Few (**F**) 2–10 specimens, Many (**M**) 10–100 specimens, and Abundant (**A**) more than 100 specimens.

We use the same criteria to describe the external morphology as in the recent guide to sponges from deep marine protected areas from the southeastern USA (Diaz et al. 2021). Each morphospecies is characterized by its external appearance (shape, surface features, color patterns, oscula). Sponge shapes are described according to their 3-dimensional growth as encrusting (thin or thick but following the contour of the substrate) or massive (the sponge develops away from the substrate). The shape may represent a particular geometry (tubular, cylindrical, globular or sub-globular, cup, or fan) or a particular pattern (bushy, arborescent, amorphous). “Surface” refers to details of the outer appearance; it may be smooth, convoluted, rugose, velvet, porous, or have projections that might be cone-shaped (conulose), hairy (hispid), or with digitated hollow blind projections (fistulose). The smaller, incurrent water apertures (ostia) may be aggregated in papillae, clumps, or porocalices. The larger excurrent water apertures usually represent oscula or pseudo-oscula and are described by morphology (shape, presence of a membrane or collar, etc.), abundance (sparse, common, or abundant), location (apical, regularly distributed, in clumps, on a sieve plate), size (diameter, measured when they are visible), and the presence and nature of a membrane (flush, elevated, collar, transparent, colored). The sponge consistency, ranging from soft, compressible, cartilaginous, crumbly, or hard, is also a useful feature to characterize sponge species. These are useful details to characterize and distinguish the majority of sponge species. Definition of these descriptive terms for sponge external morphology can be found in the Sponge Thesaurus (Boury-Esnault and Rützler 1997).

## Species checklist terms and abbreviations

- aff.**           affinis; the species might appear similar but is not that species. Implies a higher degree of uncertainty compared to cf. (Sigovini et al. 2016);
- cf.**           confer; to be compared with. Indicates that most of the diagnostic characters correspond to a given species, but some characters are unclear. The identification is provisional but is likely to be definitive after comparing with reference material or consulting a specialist of the taxon (Sigovini et al. 2016);
- FGBNMS**   Flower Garden Banks National Marine Sanctuary;
- GOM**        Gulf of Mexico;

- sp. nov.** new species to science. Specimen has unique characters that can support our interpretation about its distinct and unique identity;
- spp.** species in plural. Refers to multiple species from a particular genus.

## Results

### Taxonomic scope

Sixty-four species were identified from a collection of 54 samples with photographs and ten photographs (without samples) from inside and around Flower Garden Banks National Marine Sanctuary (Suppl. material 1), and 63 are synoptically described below (Figs 3–65). Two species belong to the class Hexactinellida (order Hexasterophora). Two species, *Plakortis* cf. *simplex* and *Plakina versatilis* (not represented in the present guide, but a sample was studied by KR, SK, and CA) represent the class Homoscleromorpha (order Homosclerophorida), and 60 species represent the class Demospongiae (14 orders). The most diverse orders in terms of family diversity and species richness are: Tetractinellida (11 spp. within 5 families), Dictyoceratida (9 spp. within 4 families), Haplosclerida (10 spp. within 5 families), Axinellida (5 spp. within 4 families), and Bubarida (5 spp. within 1 family). The most species-rich genus with several undescribed species is *Ircinia* with five species distinguished. Forty-seven species are identified either to species level or with a probable intraspecific variation of a known species (12 spp. as cf.), or with affinity to a known species (one sp. as aff.). Fifteen species were given only a generic assignment; many of those probably represent undescribed species or require deeper taxonomic studies, such as museum type comparisons or molecular evaluation to confirm a species identification. One morphotype could only be identified to the family level: a skeletal-less member of the family Ianthellidae that thinly encrusted a portion of an Hexactinellida. If this taxonomic identification is correct, it would constitute the first association of this type ever reported.

### Geographic scope

Eleven species included in this study are either first reports for the occurrence of that species at mesophotic depths, or first occurrences in the Gulf of Mexico or specifically in the northwestern Gulf of Mexico. *Biemna cribaria*, *Placosphaerastra antillensis*, *Batzella rubra*, and *Erylus trisphaerus* are here reported at mesophotic depths (> 50 m deep) for the first time. First reports in the Gulf of Mexico include *Stellettinopsis megastylifera*, *Erylus alleni*, and *Erylus goffrilleri*. First reports in the northwestern area of the Gulf of Mexico include *Agelas dilatata*, *Neophrissospongia* cf. *nolitangere*, *Erylus trisphaerus*, and *Ircinia campana*.

The occurrence and qualitative abundance estimate for most of the species in this study, along 17 banks or features in Flower Garden Banks National Marine Sanctuary and vicinity are summarized in the Suppl. material 1.

## Taxonomic accounts

### Phylum Porifera

### Class Demospongiae

### Subclass Heteroscleromorpha

### Order Agelasida

### Family Agelasidae

#### *Agelas* cf. *citrina* Gotera & Alcolado, 1987

Fig. 3

**Diagnostic features.** Massive amorphous to thick crust ( $\leq 3$  cm thick), bright orange to reddish externally. The surface is convoluted with irregular folds and depressions. Oscula round, sparse, 2–5 mm wide.

**Similar species.** *Agelas clathrodes* has key-holed and round oscula. *Agelas cerebriformis* has a convoluted surface but it is brown and tubular.

**Distribution and abundance.** *Agelas citrina* occurs on shallow coral reefs throughout the Caribbean and the Florida Keys. Found on mesophotic reefs at FGBNMS, Cuba (50–61 m deep), and South Carolina MPA (52 m depth). At FGBNMS, rare to moderate in abundance and a widespread distribution occurring at 11 sites.

**Ecology.** Lower mesophotic reefs and heavily silted reefs in FGBNMS region. A strong, particular garlic-like odor is associated with all regional variants. This morphotype is referred to as cf. since it does not have the typical flabellate shape nor the orangish color.

**Identification.** KR, SK, CA, MCD.

**References.** Diaz et al. 2019, 2021; Parra-Velandia et al. 2014; Zea et al. 2014.



**Figure 3.** *Agelas* cf. *citrina*, 50 m deep. Sample DFH9-7E.

***Agelas clathrodes* (Schmidt, 1870)**

Fig. 4

**Diagnostic features.** Massive, flabellate, orange reddish in color. The surface is rugose, irregularly riddled by round (1–10 mm wide) and key-holed (1–4 cm long) oscula.

**Similar species.** *Agelas citrina* flabellate specimens are similar but lack key holed oscula and usually have a paler pinkish or yellowish color.

**Distribution and abundance.** Common in shallow and mesophotic reefs in North and South Carolina, eastern Florida, throughout the Caribbean, the Guyana shelf, and Brazil.

**Ecology.** Coral reefs, coral communities, and coralline algae reefs in FGBNMS region.

**Identification.** MCD, MFN.

**References.** Diaz et al. 2019; Parra-Velandia et al. 2014

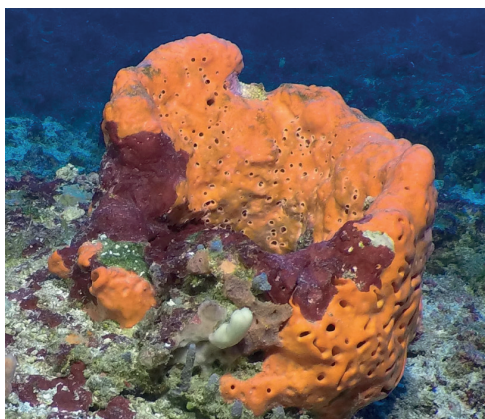


**Figure 4.** *Agelas clathrodes*, 61 m deep. Photo code YG1901L3\_IMG\_20190831T212309Z.

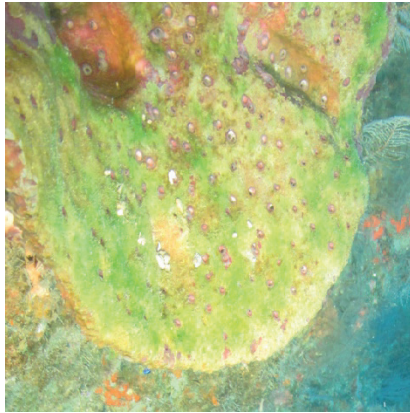
***Agelas dilatata* (Duchassaing & Michelotti, 1864)**

Fig. 5

**Diagnostic features.** Flabellate to fan- and cup-shaped, < 3 cm thick, sometimes pedunculated. Brown in color. The surface is smooth with abundant and homogeneously arranged round oscula (4–10 mm) on the upper side, and small unevenly dispersed ostia (1–2 mm wide) on the underside.

**Similar species.** *Agelas dispar*, a fan-shaped brown species, which is thicker and possesses mostly key-holed oscula.

**Distribution and abundance.** Previously considered restricted to the Bahamian-Greater Antilles shallow coral reefs (18–30 m deep) and Cuba (90–115 m). This is the first report for the NW GOM, where it is rare at Sonnier Bank.



**Figure 5.** *Agelas dilatata*, 46 m deep. Photo code SP-49.

**Ecology.** Coralline algae reefs. Specimen is overgrown by a film of green algae. A unique alkaloid isolated from a Yucatan specimen is bioactive against a multidrug-resistant pathogen *Pseudomonas aeruginosa* (Pech-Puch et al. 2020).

**Identification.** MCD.

**References.** Diaz et al. 2019; Parra-Velandia et al. 2014.

## Order Axinellida

### Family Axinellidae

#### *Ptilocaulis* cf. *walpersii* (Duchassaing & Michelotti, 1864)

Fig. 6

**Diagnostic features.** Flagelliform branching; single or multiple branches (ca. 1–2 cm wide,  $\leq$  50 cm height). Red to orange in color. Branches have different lengths, and they can be straight, bent, or laterally fused forming flabellate bodies. Surface rugose and porous, with flattened or rounded processes. Oscula are sparse along the side of branches, hardly visible. Branches are compressible and firm. The identification given to this specimen is based on the external morphology and observations of the live photo.

**Similar species.** *Ptilocaulis marquezii* (with oxeads and styles) and *Higginsia coralloides* (with acanthose micro-oxeads added to large oxeads and styles). *Ptilocaulis walpersii* has only styles as spicules. The cf. is placed since the spicules could not be corroborated. *Higginsia coralloides* consists of shorter ( $\leq$  10 cm height) and thicker branches (3–5 cm wide).

**Distribution and abundance.** *Ptilocaulis walpersii* is widely distributed on shallow coral reefs throughout the Caribbean, Florida, and Bermuda (0.5–35 m); recently reported at the southern GOM, 4–20 m deep (Ugalde et al. 2021). This is the first report from the northwestern GOM on mesophotic reefs. Common on Cuban mesophotic reefs. At FGBNMS, rare abundance and documented only at West Flower Garden Bank.



**Figure 6.** *Ptilocaulis* cf. *walpersii*, 60 m deep, Photo code SP-01.

**Ecology.** Coralline algae reefs.

**Identification.** MCD, CA.

**References.** Alvarez et al. 1998; Ugalde et al. 2021.

## Order Axinellida

### Family Heteroxyidae

#### *Myrmekioderma gyroderma* (Alcolado, 1984)

Fig. 7

**Diagnostic features.** Massive amorphous to thick encrusting (3.5 cm thick). Brown reddish to orange in color externally, orange internally. Surface highly ornamented by plates and shallow grooves. Oscula in low abundance and irregularly arranged.

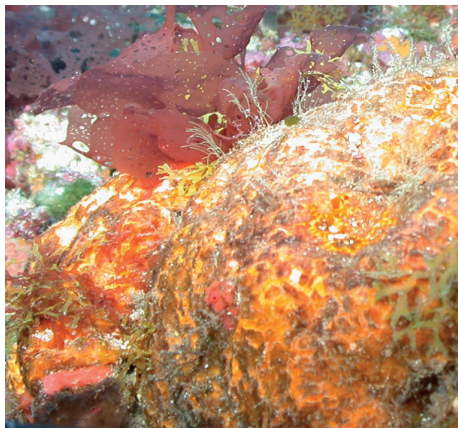


**Figure 7.** *Myrmekioderma gyroderma*. 60–72 m deep. Samples DFH9-11A, DFH9-5B.

**Similar species.** Very similar to *Didiscus oxeatus*, and *Myrmekeiderma rea*; this last species presents a smoother appearance and few thinner grooves. Only a spicule analysis allows to distinguish between them. *Didiscus* spp. have discorhabds as microscleres, *Myrmekeiderma rea* has only straight trichodragmata, while *Myrmekeiderma gyroderma* has twisted long trichodragmata.

**Distribution and abundance.** Shallow and mesophotic reefs, throughout the Caribbean and Gulf of Mexico. At the FGBNMS the species presents low to medium abundance (2–100 individuals) at nine sites.

**Ecology.** Coralline algae reefs, algal nodules, lower mesophotic reefs.

**Identification.** KR, SK, CA, MCD.

**References.** Alcolado 1984; Pomponi et al. 2019.

## Order Axinellida

### Family Raspailiidae

#### *Ectyoplasia ferox* (Duchassaing & Michelotti, 1864)

Fig. 8

**Diagnostic features.** Thickly encrusting to palmate. Brown to reddish externally, orange internally. Rugose to smooth surface. Oscula on tips of chimneys. Pale colored oscular membranes. Compressible, easy to break.

**Similar species.** This species is quite variable in color and level of rugosity. Massive and smooth forms of *Cliona varians* can be confused with it. Spicule composition allows a definitive diagnosis.

**Distribution and abundance.** Throughout the Caribbean, Gulf of Mexico, and SE Brazil, very common in shallow coral reefs. Mesophotic reefs in Cuba. At FGBNMS the species is rare to low in abundance (1–10) at five sites.

**Ecology.** Coralline algae reefs, coral communities, algal nodules, lower mesophotic reefs.

**Identification.** KR, SK, CA, MCD.

**References.** Wiedenmayer 1977; Ugalde et al. 2021



**Figure 8.** *Ectyoplasia ferox*, 60 m deep. Sample DFH9-12C.

***Didiscus oxeatus* Hechtel, 1983**

Fig. 9

**Diagnostic features.** Massive to crustose, brown reddish to orange in color externally, orange internally. Highly ornamented surface consisting of variously shaped plates and vermiform grooves. Few oscula, all with an orange membrane.

**Similar species.** *Myrmekioderma gyroderma* and *Myrmekioderma rea* are very similar externally; the distinction of their microscleres allows their differentiation. *Didiscus* spp. have discorhabds and *Myrmekioderma* spp. have trichodragmata (see Boury Esnault and Rützler 1997).

**Distribution and abundance.** Throughout the Caribbean, SE Brazil, and northern GOM on shallow reefs. Mesophotic reefs at FGBNMS, Lesser and Greater Antilles, Florida, Bahamas, and Brazil (Pomponi et al. 2019). At FGBNMS the species was found once at one site.

**Ecology.** Coralline algae reefs, algal nodules.

**Identification.** KR, SK, CA, MCD.

**Reference.** Alcolado 1984.



**Figure 9.** *Didiscus oxeatus*, 60 m deep. Sample DFH9-11B.

**Order Axinellida****Family Stelligeridae*****Higginsia coralloides* Higgin, 1877**

Fig. 10

**Diagnostic features.** Bushy with several digitate branches diverging from a thicker peduncle. Vermillion red alive. The surface is composed of irregular tubercules, corrugations, or conules with projecting spicules that trap sediment; similar to a cauliflower surface, with interstitial areas where inconspicuous ostia and oscula can be found. Consistency is spongy but firm.



**Figure 10.** *Higginsia coralloides*, specimen partially buried on sediment, 60 m deep. Note fine sediment on sponge. Samples DFH9-7A,7B.

**Similar species.** Younger specimens of *Ptilocaulis marquezii* (with oxeas and styles) and *Ptilocaulis walpersii* (with styles) might be confused with *Higginsia coralloides* (with acanthose micro-oxeas added to large oxeas and styles).

**Distribution and abundance.** Shallow coral reef and hard substrate at Guyana Shelf, Grenada, Bahamas, Florida, Nicaragua, Yucatan, North Carolina, possibly Brazil (van Soest 2017). Mesophotic depths at Brazil, Guyana, Eastern Antilles, Florida, and Bahamas, and northwestern GOM at FGBNMS. At FGBNMS it is rare to low (1–10) in abundance at six sites.

**Ecology.** Lower mesophotic reefs, heavily silted reefs, coralline algae reefs.

**Identification.** KR, SK, CA, MCD.

**Reference.** Wiedenmayer 1977.

## Order Biemnida

### Family Biemnidae

#### *Biemna cribaria* (Alcolado & Gotera, 1986)

Fig. 11

**Diagnostic features.** Massive sub-spherical barrel growth form, with a top central dip. Color dark brown externally, tan internally. Multiple digitate projections on the surface on the top and side areas of the sponge. Oscula are aggregated on the concave upper depression.

**Similar species.** The overall shape is reminiscent of other barrel sponges such as *Ircinia strobilina* or *Sphaciospongia vesparium*, but the digitate projections of *Biemna cribaria*, and the skeleton allow their differentiation.

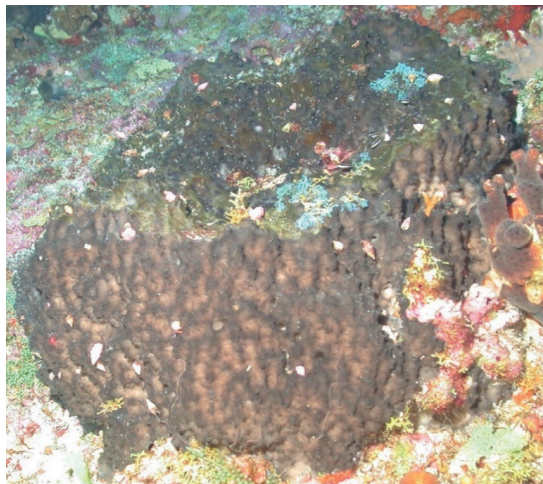


**Figure 11.** *Biemna cribaria*, 36 m deep. Photo code SP22.

**Distribution and abundance.** The sponge is rare in occurrence but reported at 20 m from Cuban and Jamaican reefs (Alcolado 1984; Lehnert and van Soest 1998). This is the first report at mesophotic depths and in the northwestern GOM at FGB-NMS. At FGBNMS it is rare and was observed only once at Bright Bank.

**Ecology.** Coral communities, coralline algae reefs.

**Identification.** MCD.

**Reference.** Lehnert and van Soest 1998.

### *Neofibularia nolitangere* (Duchassaing & Michelotti, 1864)

Fig. 12

**Diagnostic features.** Massive base with thick lobes (10–30 cm high x 10–15 cm wide). Brown to yellowish in color externally, tan internally. The surface is irregularly corrugated to velvety smooth. The oscula are on top of lobes with a thin paler membrane. This species can grow as a thick barrel or massive crusts. The sponge is soft and friable in consistency. It is well known by its tendency to cause skin irritation.

**Similar species.** The massive size and reddish-brown external color reminiscent of some *Neopetrosia* spp. Spicules allow clear differentiation.

**Distribution and abundance.** Coral reefs or rock pavements in shallow depths in southwestern Caribbean (Colombia and Panama), Florida and North Carolina. At FGBNMS it is low to high (2–100+) in abundance at five sites. Thousands of polychaete worms swarmed from the inside of the sponge when it was collected.

**Ecology.** Coralline algae reefs, algal nodules, and lower mesophotic reefs.

**Identification.** KR, SK, CA, MCD.

**Reference.** Wiedenmayer 1977.



**Figure 12.** *Neofibularia nolitangere*, 70 m deep. Sample GFOE3-30 (8-31-19).

## Order Bubarida

### Family Dictyonellidae

#### *Acanthella cubensis* (Alcolado, 1984)

Fig. 13

**Diagnostic features.** Massive digitiform to lobate with lobes 2 cm wide. Orange, spongy. Surface slightly rugose to conulose. Oscula 4–7 mm wide, on top of lobes, with transparent membranes. Soft, compressible.

**Similar species.** *Ptilocaulis walpersii* (with only oxeas), *Ptilocaulis marquezii* (with oxeas and styles), while *Acanthella cubensis* has styles in a wide size range, and sinuous strongyles.

**Distribution and abundance.** *Acanthella cubensis* occurs on shallow coral reefs in Cuba, south Caribbean, Florida, and North Carolina. At FGBNMS the species



**Figure 13.** *Acanthella cubensis*, 68–88 m deep. Samples DFH9-14A DFH9-2A, DFH9-3D.

is from rare to medium (1–100) in abundance at 12 sites. The species occurs also at mesophotic rock pavements in South Carolina, inside proposed Charleston shelf MPA at 54 m (Diaz et al. 2021).

**Ecology.** Coralline algae reefs, algal nodules, lower mesophotic reefs.

**Identification.** CA, MCD.

**Reference.** Alvarez et al. 1998.

***Acanthella* cf. *mastophora* (Schmidt, 1870)**

Fig. 14

**Diagnostic features.** Globular, slightly flattened (4 cm in diameter and 2–4 cm in height). Pale yellow. The surface has ‘woolly’-wart-like appearance due to roundish papillae. Between the papillae there are furrows (1–3 mm deep). The surface is very hairy due to abundant fibrous dense filaments of unknown origin, and projecting spicule brushes. Firm and compressible, with flexible surface projections. The cf. notation is due to predominance of oxea instead of styles. Otherwise, it is very similar to *Acanthella mastophora* in color, surface, and reticulate spicule arrangement.

**Similar species.** Small specimens of *Cinachyrella alloclada* may have similar appearance. Spicules would allow clear distinction.

**Distribution and abundance.** *Acanthella mastophora* is found in south Florida, North Carolina, Azores and Eastern Atlantic (76–394 m deep). Widespread distribution at FGBNMS with rare to low (1–10) abundances at nine localities.

**Ecology.** Coralline algae reefs, algal nodules, lower mesophotic reefs.

**Identification.** MCD, CA.

**Reference.** Alvarez et al. 1998.



**Figure 14.** *Acanthella* cf. *mastophora* 80 m deep. Sample DFH9-13B.

***Auletta tuberosa* (Alvarez et al., 1998)**

Fig. 15

**Diagnostic features.** Clusters of tubes (0.25–1 cm diameter), arborescent, with short and narrow peduncle; tubes anastomose and are crooked, uneven, and bumpy. Orange to yellowish tan in color. The surface is felt-like, smooth visually. Oscula or vents, on top of the tubes (2–4 mm diameter). Soft and compressible in consistency.

**Similar species.** the protuberances of the tubes and ramose thick branches make this a unique species. The spicules include slender oxeas, styles, and wavy strongyles allowing distinction from *Auletta syncinularia*, which contains only styles and wavy strongyles.

**Distribution and abundance.** *Auletta tuberosa* is reported from 60–80 m depth at Guyana, southern Caribbean, eastern Antilles, Florida, Bahamas, and southeast GOM (off Cape Sable) where it was originally described. At FGBNMS it has a wide-spread distribution, occurring at 12 sites, with abundance ranging from rare to common (1–100 individuals).

**Ecology.** Coralline algae reefs, algal nodules, lower mesophotic reefs.

**Identification.** MCD, CA.

**Reference.** Alvarez et al. 1998.



**Figure 15.** *Auletta tuberosa*, 72–78 m deep. Samples DFH9-13A, DFH9-4A.

***Auletta syncinularia* (Schmidt, 1870)**

Fig. 16

**Diagnostic features (young specimen).** Single white tube (1–3 mm wide, 1.6 cm high). Surface rugose. One oscule on top of the tube. As adults this species grows as a cluster of smooth slender tubes (3–10 cm long, 1 cm wide), with a peduncle (2–3 cm long). Spicules are highly conserved (sinuous strongyles and styles present in two or three size classes).

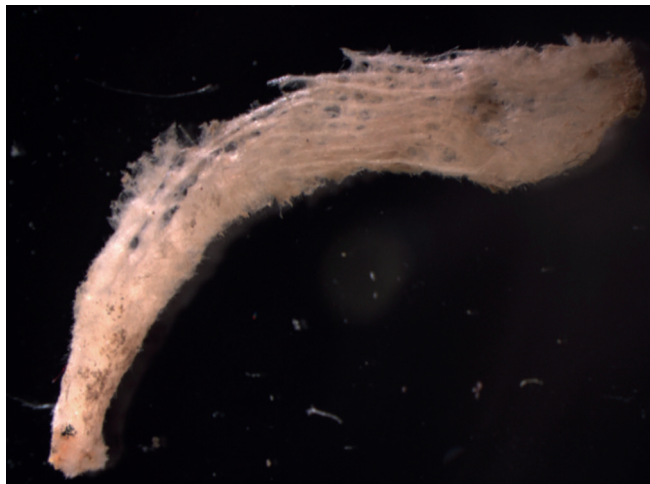


**Figure 16.** *Auletta syncinularia*, young specimen, collected on a rock at 147 m deep. Sample GFOE3-23F.

**Similar species.** The young specimens of *Auletta* sp. nov. 1 (described below).

**Distribution and abundance.** *Auletta syncinularia* is reported from the Gulf of Mexico, Florida, Barbados, and Azores (70–159 m deep); elsewhere, down to 200 m depth (Alvarez et al. 1998). At FGBNMS the species was collected once at Elvers Bank growing on a rock with Hexactinellids and black corals.

**Ecology.** This species was found associated with a rock where a large hexactinellid was growing (DFH3-23).

**Identification.** MCD.

**Reference.** Alvarez et al. 1998.

### *Auletta* sp. nov. 1

Fig. 17

**Diagnostic features.** Single or double slender tubes (0.5–1 cm in diameter), drab orange in color. Adult specimens are 8–13 cm long, and < 5 mm wide (DFH8-15A). A young specimen (GFOE 3-8H) was 2 cm high and 2–4 mm wide. Surface is smooth, microscopically hispid, and porous. Oscula on top of each tube are 4 mm wide. A very thin white membrane surrounds each oscule. Tubes are compressible, but they become harder and thinner towards the base.

**Similar species.** The surface and slender tube shape of *Auletta syncinularia* is similar to this undescribed species of *Auletta*. It differs from *Auletta syncinularia* in having oxeas and anisoxeas (straight and sinuous) and lacking the size categories of styles.

**Distribution and abundance.** Found at mesophotic reefs at FGBNMS. Widespread distribution in the FGBNMS with medium abundances, from low to common (2–100 individuals) at 13 sites.



**Figure 17.** *Auletta* sp. nov. 1, 90–95 m deep. Samples DFH8-15A, GFOE 3-8H.

**Ecology.** Coralline algae reefs, algal nodules, lower mesophotic reefs.

**Identification.** MCD, CA.

**Reference.** Alvarez et al. 1998.

## Order Scopalinida

### Family Scopalinidae

#### *Scopalina ruetzleri* (Wiedenmayer, 1977)

Fig. 18

**Diagnostic features.** Thick encrusting, occasionally lobate, 1–2 cm thick. The color in life is bright orange to pinkish orange. The surface is conulose (1–2 mm high and 1–4 mm apart) with many large contractile ostia (500  $\mu$ m wide). The oscula are 1–3 mm in diameter and have a delicate, transparent membrane. The consistency is very soft, delicate, limp, and easily torn.

**Similar species.** Thicker specimens of *Prosuberites laughlini* (with tylostyles) may be confused in the field with *Scopalina ruetzleri* (with styles). Spicule analysis allows differentiation.



**Figure 18.** *Scopalina ruetzleri*, 50 m deep. Photo code SP23.

**Distribution and abundance.** Common and widespread distribution in shallow water coral reefs and mangroves in the Caribbean, Bermuda, Brazil, and GOM. At FGBNMS it had low abundance (2–10) at two sites.

**Ecology.** Coralline algae reefs, algal nodules.

**Identification.** MCD.

**Reference.** Wiedenmayer 1977.

## Order Clionaida

### Family Clionaidae

#### *Placosphaera antillensis* van Soest, 2009

Fig. 19

**Diagnostic features.** Thick encrusting (1–5 mm thick). Color in life orange, dark orange, brown-orange, or yellowish. The surface consists of elongated plates, separated by meandering ridges and grooves with pores. The system of plates and ridges is irregular in shape. Consistency hard, rough to the touch.

**Similar species.** The plates and canals on the surface are similar to *Placospongia* spp. surface. The intense orange color of *Placosphaera antillensis*, and the spicules allow their differentiation.

**Distribution and abundance.** Usually under coral rubble and in reef caves, 20–23 m depth in Bonaire and Belize. First report at mesophotic depths. At FGBNMS the species has a widespread distribution occurring at 11 sites with rare to medium abundance (1–100).

**Ecology.** Coralline algae reefs, algal nodules, lower mesophotic reefs.

**Identification.** KR, SK, CA.

**References.** van Soest, 2009; Rützler et al. 2014.

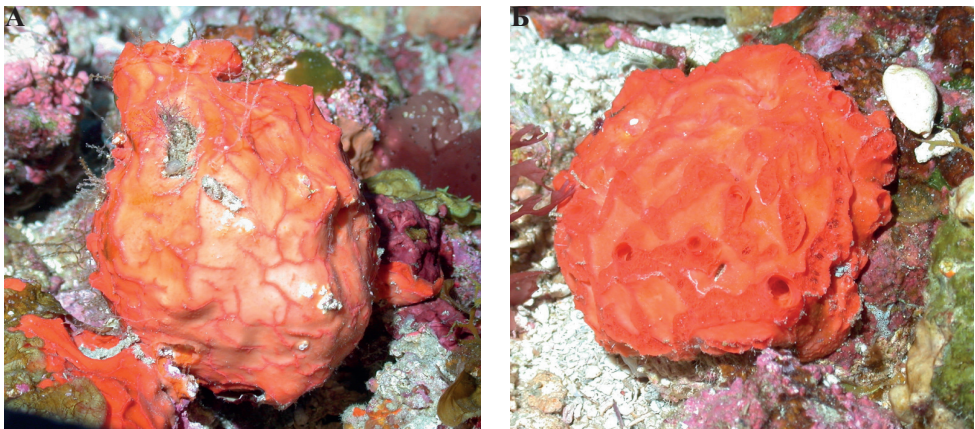


**Figure 19.** **A** *Placosphaera antillensis*, with surface contracted, 60 m deep. Sample DFH9-10C **B** *Placosphaera antillensis* relaxed, showing grooves with ostia (incurrent pores), and oscula (excurrent openings), 60 m deep. Sample DFH9-11C.

**Order Haplosclerida**  
**Family Chalinidae**

***Haliclona* sp. 1**

Fig. 20

**Diagnostic features.** Massive encrusting (1 cm thick), orange in color. Surface smooth with tiny pores. Few oscula 2–3 mm wide. Compressible, soft, and crumbly.

**Similar species.** This species can be confused with smooth specimens of *Pseudaxinella belindae*, which is more red-orange in color and has styles for spicules instead of small oxea.

**Distribution and abundance.** Mesophotic reefs in northwestern GOM at FGB-NMS, and east GOM at Pulley Ridge (MCD, unpublished data). Rare to low abundance at two sites.

**Ecology.** Coralline algae reefs, algal nodules, lower mesophotic reefs. This is probably an undescribed species of *Haliclona*.

**Identification.** CA, MCD.

**Reference.** de Weerd 2000.



**Figure 20.** *Haliclona* (*Reniera*) sp. 1, 69 m deep. Sample DFH9-6E.

**Order Haplosclerida**  
**Family Callyspongiidae**

***Callyspongia* (*Cladochalina*) cf. *armigera* (Duchassaing & Michelotti, 1864)**

Fig. 21

**Diagnostic features.** Short repent branch, gray to cream in color, with thorny conules and a porous surface. Few oscula visible (3–4 mm wide). This species commonly grows as erect branches, although repent specimens are reported in the literature.

**Similar species.** The abundant thorny conules and the stiff consistency of this species allows its morphological differentiation, *Pleraphysilla* sp. 2 (Fig. 56) has similar



**Figure 21.** *Callyspongia* cf. *armigera*, 63 m deep. Photo code SP42. Sample DFH6-39-6.

pronounced but shorter conules and the sponge is quite soft and less porous than this species.

**Distribution and abundance.** An occasional species in shallow coral reefs throughout the Caribbean, south GOM, and Florida. Found at mesophotic reefs in Cuba (52 m) and in northwestern GOM at FGBNMS, occurring in low abundance (2-10) at one site.

**Ecology.** Coralline algae reefs.

**Identification.** KR, SK, CA, MCD.

**Reference.** Wiedenmayer 1977.

## Order Haplosclerida

### Family Petrosiidae

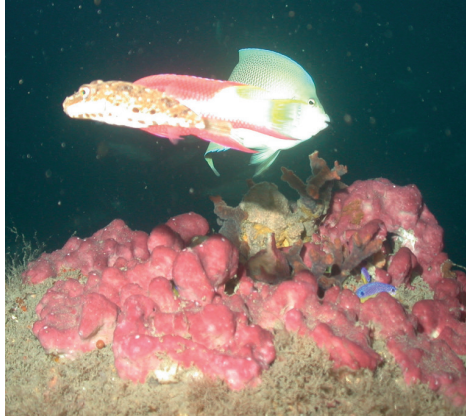
#### *Neopetrosia proxima* (Duchassaing & Michelotti, 1864)

Fig. 22

**Diagnostic features.** Thickly encrusting to massive lobate (2–9 cm in thickness). Pinkish to brown externally, tan internally. The surface is smooth but feels like sandpaper. Abundant oscula, 2–3 mm in diameter, and 1–3 cm apart. Oscula have a thin white membrane that contrasts with the darker surface color. The sponge is very firm to hard.

**Similar species.** This species is similar to other species of *Neopetrosia* described by Vicente et al. (2019). Details of the surface and spicules allow differentiation.

**Distribution and abundance.** A common species on shallow rocky shores and reefs to deeper reef habitats with a variety of wave exposures (Zea et al. 2014), also in caves (Perez et al. 2017). Found at mesophotic reefs on the northwestern GOM at FGBNMS and possibly in Cuba, identified as Petrosiidae CU-17 (Diaz et al. 2018). At FGBNMS the species has been found at three sites with abundances from rare to medium (1–100).



**Figure 22.** *Neopetrosia proxima*, 53–60 m deep. Samples DFH8-37B, DFH9-7D, DFH9-9C.

**Ecology.** Coralline algae reefs, silted lower mesophotic reefs.

**Identification.** KR, SK, CA, MCD.

**Reference.** Vicente et al. 2019.

***Petrosia* sp. nov. 1**

Fig. 23

**Diagnostic features.** Round to flattened branching (branches 1–2 cm wide), occasionally anastomosing, with roundish tips. Branches are erect, horizontal, or creeping along the substrate. Red-brown to purple externally and tan internally in live. The tips are paler in color. The surface is very smooth. White rimmed oscula, 1–2 mm wide, separated by several cm. The sponge is compressible but firm.

**Similar species.** The growth form of this *Petrosia* (*Petrosia*) species is unique.



**Figure 23.** *Petrosia* sp. nov. 1, 73–79 m deep. Sample DFH33-542A.

**Distribution and abundance.** Mesophotic reefs and rocky pavement in the northwestern GOM at FGBNMS, east GOM at Pulley Ridge, and in South Carolina (52–72 m) (Diaz et al. 2021). At FGBNMS the species presents rare to low (1–10) distribution at four sites.

**Ecology.** Coralline algae reefs, algal nodules, lower mesophotic reefs. The purple color probably originates from endosymbiotic cyanobacteria *Synechococcus spongiarium*.

**Identification.** MCD.

**Reference.** van Soest 1980.

### *Petrosia weinbergi* van Soest, 1980

Fig. 24

**Diagnostic features.** Thick crusts (1–2 cm in thickness) to plate-shaped. Dark green to brown in color externally and tan internally, with oscula contrasting by a wide white rim. The surface is smooth to slightly undulating. The oscula are slightly raised from the surface and white, 1–2 mm wide and 2–5 cm apart. Usually, this species forms small patches, and the specimen in Fig. 24 is 8 × 6 × 1.5–2 cm. The sponge is hard, barely compressible.

**Similar species.** The ear-shaped specimens of *Petrosia weinbergi* are similar to *Petrosia pellasarca*. The former is greenish in color and lacks the small toxa. Similar species: include crustose forms of *Cliona varians* and *Cliona aprica* may look similar to crustose forms of *Petrosia weinbergi*.

**Distribution and abundance.** This species is rare in shallow reefs throughout the Caribbean and at mesophotic reefs in the Greater Antilles, Guyana, Brazil and in the northwestern GOM at FGBNMS. At FGBNMS the species is found in rare to low (1–10) abundance at two localities. Depth ranges from 8–500 m.

**Ecology.** Coralline algae reef, algal nodule, lower mesophotic reef.

**Identification.** KR, SK, CA, MCD.

**References.** Pomponi et al. 2019; van Soest 1980, 2017.



**Figure 24.** *Petrosia weinbergi*, 69–71 m deep. Samples DFH9-3C, DFH9-6B.

***Xestospongia muta* (Schmidt, 1870)**

Fig. 25

**Diagnostic features.** Barrel-shaped. with a wide apical vent surrounded by a 2–5-cm wall which thickens towards the sponge base. Smaller specimens may present as a cone-shaped form. Red-brown externally, tan internally. Surface ranges from smooth to irregularly ridged or pitted. Few small openings (2–3 mm in diameter) may be oscula. Inner wall without detachable dermis, rough. The detachable dermis ends on the inside rim of the vent. The atrial cavity extends to ca. half the cup height. Consistency is brittle, easily crumbled.

**Similar species.** *Xestospongia* sp. nov. 1, described below, is shorter, with a flat top, thicker rimmed walls, and much smaller atrium than *X. muta*.

**Distribution and abundance.** An iconic species from shallow reefs in Florida, throughout the Caribbean, to southeastern Brazil, southern GOM, and northwestern GOM at FGBNMS. Mesophotic reefs in Cuba, south Florida, northwestern GOM at FGBNMS, and east GOM at Pulley Ridge. Reed (2022) reports it at three banks in FGBNMS (51–69 m deep).

**Ecology.** Coral reefs, coral communities, coralline algae reefs, algal nodules.

**Identification.** John Reed, MCD.

**Reference.** Diaz et al. 2019; van Soest 1980.



**Figure 25.** *Xestospongia muta* (2 specimens on the right) and *Xestospongia* sp. nov. 1 (2 roundish dark red specimens on the left) at McGrail Bank, 58 m. Photo 202205114-T-161120\_0004 (HBOI-FAU 05-2022).

***Xestospongia* sp. nov. 1**

Fig. 26

**Diagnostic features.** Massive thick barrel sponge, with rounded edges and a small apical oscule or pseudo-oscule (3 cm in diameter). The sponge top is flattened. The

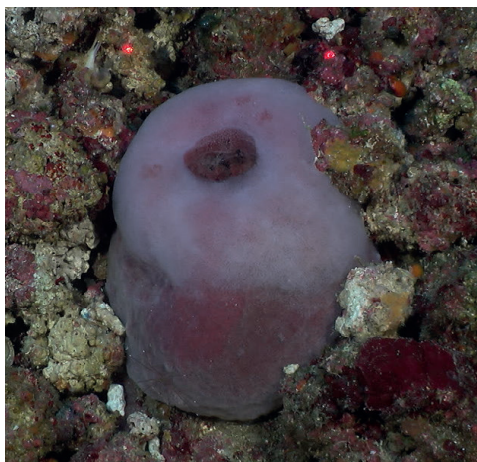


**Figure 26.** *Xestospongia* sp. nov. 1, 56 m deep. Sample GFOE3-27.

color is pink to dark reddish, with whitish spots, tan internally. The surface is smooth to spikey and microscopically porous. A very thin transparent membrane can be distinguished on the oscule rim, and branching thin spicule tracts can be distinguished at high magnification.

**Similar species.** This species is similar to *Xestospongia muta* but it is fat, shorter, with a flat top, thicker walls, and a smaller “atrium” than *Xestospongia muta*.

**Distribution and abundance.** Mesophotic reefs in Cuba, south Florida, northwestern GOM at FGBNMS region, and east GOM at Pulley Ridge. This was the most abundant species at the mesophotic reefs in Cuba, and it is currently being described by a Cuba-USA team. At FGBNMS, it has been recognized once at Geyer Bank; probably confused with *Xestospongia muta* previously.

**Ecology.** Algal nodules.

**Identification.** KR, SK, CA, MCD.

**Reference.** Diaz et al. 2019.

## Order Haplosclerida

### Family Niphatiidae

#### *Niphates erecta* Duchassaing & Michelotti, 1864

Fig. 27

**Diagnostic features.** Single erect branch to multiple branches or arborescent. Pink to gray in color. The surface is porous, microhispid, and rough to the touch. Many oscula dispersed along the branch with a slight elevation compared to the surface. Many oscula had a barnacle inside. The sponge is firm, slightly compressible.

**Similar species.** *Niphates amorpha* with erect branches and *Niphates erecta* can be confused. The possible conspecificity of these two forms remains to be clarified.



**Figure 27.** *Niphates erecta*, 71 m deep. Sample DFH9-6A.

**Distribution and abundance.** Very common species throughout the Caribbean, Bermuda, Florida, and Brazil at shallow (< 50 m) and mesophotic depths (50–100 m). At FGBNMS the species is reported with rare to high abundance (1–100+) at seven localities.

**Ecology.** Coralline algae reef, algal nodule, lower mesophotic reef.

**Identification.** KR, SK, CA, MCD.

**References.** van Soest 1980. Pomponi et al. 2019.

## Order Haplosclerida

### Family Phloeodictyidae

#### *Siphonodictyon* sp. nov. 1

Fig. 28

**Diagnostic features.** Large massive sponge with abundant long yellow brown oscular tubes (3–12 cm long and 1.5–2 cm wide) that project between shorter, amorphous to digitate drab yellow fistules (1–4 cm high and < 10 cm long). Only a soft and smooth oscular tube was collected and had only oxeads as spicules. 18S sequences (738 bp) show that this species is separated phylogenetically from a clade formed by sequences of *Siphonodictyon coralliophagum* and *Siphonodictyon brevitubulatum* available on GenBank (Díaz, Segura, and Pomponi, unpublished data).

**Similar species.** *Oceanapia* spp. may have similar oscular tubes and fistules (Santos Neto et al. 2018). The genetic data was essential to provide the generic assignment to this species.

**Distribution and abundance.** The species was seen once at Geyer Bank at FGBNMS.

**Ecology.** Found in algal nodule beds. This species is a bio-eroding sponge.

**Identification.** Iris Segura, KR, MCD.

**Reference.** Ruetzler 1971; Ruetzler et al. 2014.



**Figure 28.** *Siphonodictyon* sp. nov. 1, 67 m deep. Sample GFOE3-2.

### *Siphonodictyon brevitubulatum* Pang, 1973

Fig. 29

**Diagnostic features.** Small abundant fistules (0.5–1 cm wide, 1–3 cm high) and rare long oscular tubes (1.5 cm in diameter), bright yellow in color. Smooth surface of fistules and oscular tubes.

**Similar species.** *Siphonodictyon coralliophagum* has much larger and thicker bright yellow oscular tubes and fistules.

**Distribution and abundance.** The species is reported from Jamaica, Costa Rica, Colombia, and Martinique, and northwestern GOM in the FGBNMS. At the FGBNMS it was observed once at Geyer Bank, while analyzing the photograph of *Syphonodictyon* sp. nov. 1 (Fig. 28). This is the first report of this species at mesophotic depths.

**Ecology.** Algal nodules. This species is a bio-eroding sponge.

**Identification.** MCD.

**Reference.** Pang 1973.

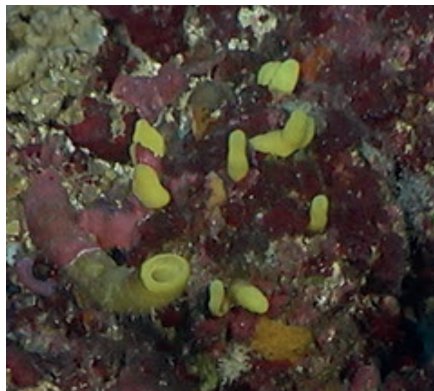


**Figure 29.** *Siphonodictyon brevitubulatum*, 67 m deep. Inset taken from Fig. 28 upper right.

**Order Poecilosclerida**  
**Family Chondropsidae**

***Batzella rubra* (Alcolado, 1984)**

Fig. 30

**Diagnostic features.** Thinly encrusting sponge, growing over dead coral or other sponges. Deep orange to bright red color in live. The surface is smooth and ornamented by paler colored dermal canals that branch away from the oscula, wide close to the oscula and thinner away from it. The consistency is compressible where the sponge is thicker.

**Similar species.** The sponge can be confused with other red encrusting species, but the particular ‘dripping’ morphology of the dermal canals makes them easy to distinguish.

**Distribution and abundance.** This species is reported from shallow reefs in Cuba and Bahamas. This is the first report for the species at mesophotic reefs. At FGBNMS the specimen on the photograph was found at east Flower Garden Bank and the species has rare to moderate abundance at ten other sites.

**Ecology.** Coralline algae reefs, algal nodules, lower mesophotic reefs.

**Identification.** MCD.

**Reference.** Alcolado 1984; Zea et al. 2014.



**Figure 30.** *Batzella rubra*, 90 m deep. Specimen observed on the photo of sample DFH9-13A.

***Batzella cf. rubra* (Alcolado, 1984)**

Fig. 31

**Diagnostic features.** Thinly encrusting sponge (1–10 mm thick) growing over dead coral. Orange to red color in life, black to purple in alcohol. The surface is smooth to bumpy with whitish branching dermal canals, and roundish papillae with two or three clumps



**Figure 31.** *Batzella* cf. *rubra*, 70 m deep. Sample DFH9-6F.

of ostia. The cf. is due to the rounded papillae only described for *Batzella mollis*, a species found at the “Juan Fernandez and Desventuradas islands” off the Chilean Pacific coast.

**Similar species.** Esteves et al. (2018) describe three tropical western Atlantic *Batzella* spp: *Batzella rubra* (deep orange-red, smooth), *Batzella ficus* (dark brown), and *Batzella cataniresis* (yellow). *Monanchora arbuscula* in its orange morphotype can be confused with *Batzella* cf. *rubra*.

**Distribution and abundance.** This is the first record from mesophotic reefs. At FGB-NMS the species has been recorded with rare to low abundance (1–10) in three localities.

**Ecology.** Coralline algae reefs, algal nodules, lower mesophotic reefs.

**Identification.** KR, SK, CA, MCD.

**References.** Alcolado 1984; Esteves et al. 2018.

## Order Poecilosclerida

### Family Microcionidae

#### *Clathria* sp. 1

Fig. 32

**Diagnostic features.** Massive with short, protruding, flattened, digitate branches, forming a roundish bush. Colored red in life. Surface minutely porous and with a translucent veil (dermis). Oscula not visible. This species belongs to the genus *Clathria*; however, species identifications require spicule analysis.

**Similar species.** Several branching bushy *Clathria* species are described by Gomez (2014). Few of those species have been photographed alive, and their appearance changes dramatically once they are taken out of the water.

**Distribution and abundance.** Arborescent *Clathria* species are diverse and well-known from the Gulf of Mexico (Gomez 2014). At the FGBNMS this species has been documented on mesophotic depths at three sites.



**Figure 32.** *Clathria* sp. 1, 63 m deep. Photo code SP03.

**Ecology.** Sandy substrates.

**Identification.** KR, SK, CA, MCD.

**Reference.** Gomez 2014.

## Order Suberitida

### Family Halichondriidae

#### *Halichondria* sp. 1

Fig. 33

**Diagnostic features.** Massive to thick encrusting, or globular to lobate with lobes  $\leq 15$  cm high. Yellow orange sponge alive, tan pinkish in alcohol. The surface is rugose to verrucose, with deep grooves and holes  $< 0.5$  mm wide; the deep grooves, where thin ectosome is absent, have a feathery appearance. Oscula 0.5–2 cm wide, with a yellow membranous collar that is 5–8 mm high when the oscula are fully open. Compressible in consistency.

**Similar species.** *Myrmekeioderma rea* when it grows as a thick massive crust, and massive lobate *Axynissa ambrosia* can be easily confused with this species. Its spicules (oxea in a wide size range) and surface features are unique among the Halichondriidae.

**Distribution and abundance.** The sponge is common at FGBNMS on mesophotic habitats between 55–73 m. This is an undescribed species. The species occurs at four sites with rare to medium abundance (1–100).

**Ecology.** Coralline algae reefs, algal nodules, lower mesophotic reefs.

**Identification.** CA, SWK, MCD.

**References.** Diaz et al. 1993; Zea et al. 2014.



**Figure 33.** *Halichondria* sp. 1, 60–80 m deep. Samples DFH9-11D, DFH9-12D, DFH9-14E, DFH9-3E.

***Topsentia bahamensis* Diaz, van Soest & Pomponi, 1993**

Fig. 34

**Diagnostic features.** Massive, columnar shape with round or blunt tip (10 cm high, 2–4 cm in diameter). The sponge is red-brown externally and tan internally in living sponges. The surface is smooth visually with a sandpaper feel. Five dispersed oscula (1–3 mm in diameter). Very firm in consistency, but crumbly.

**Similar species.** *Topsentia ophirhaphidites*, which has deformed small oxea added to the larger oxea. Petrosiids in general by their reddish brown color and hard brittle consistency. Spicule study needed to distinguish it.

**Distribution and abundance.** Currently reported from shallow reefs in southern GOM in northern Yucatan and Belize, and at mesophotic depths in the Bahamas and northwestern GOM at the FGBNMS.



**Figure 34.** *Topsentia bahamensis*, 60 m deep. Sample DFH9-11F.

**Ecology.** Coralline algae reefs, algal nodules.

**Identification.** CA, SWK, MCD.

**Reference.** Diaz et al. (1993).

## Order Suberitida

### Family Suberitidae

#### *Rhizaxinella clava* (Schmidt, 1870)

Fig. 35

**Diagnostic features.** The “corn dog sponge”. A pale brown, clavate, stipitate sponge (15 cm in total length) with a long thin peduncle (2 mm in diameter at attachment area) and an upper globose soft body (1 cm in diameter at its thickest part). The surface is very smooth and velvety. The apical oscule is slit-shaped and has a collared membrane visible in the *in-situ* photograph. The sponge is firm but slightly compressible.

**Similar species.** The “corn dog sponge” is similar externally to the “lollipop sponge”, *Stylocordyla chupachups* and to other members of the family Stylocordylidae, which are mostly present in cold deep waters.

**Distribution and abundance.** Currently reported at mesophotic depths in the Florida Keys, Guyana, Surinam, and northwestern GOM at the FGBNMS. At FGBNMS the species is widespread, occurring at 15 sites with abundance from rare to very common (1–100+).

**Ecology.** Coralline algae reefs, silted lower mesophotic reefs.

**Identification.** KR, CA, SWK, MCD.

**Reference.** Pomponi et al. 2019; van Soest 2017.



**Figure 35.** *Rhizaxinella clava*, 106 m deep. Samples DFH6-42-4, DFH8-5A.

**Order Tetractinellida**  
**Sub-order Astrophorina**  
**Family Corallistidae**

***Corallistes typus* (Schmidt, 1870)**

Fig. 36

**Diagnostic features.** Small cups or plates, with undulating rims, walls 1–3 cm thick, usually with a thick peduncle. Brown with faintly pink tinges. The surface is smooth, with rims sometimes covered by sediment. Oscula not visible.

**Similar species.** An integrative study of 247 “lithistid” samples from the tropical western Atlantic (Schuster et al. 2021) encounters possibly six different undescribed species of *Corallistes*, similar to *C. typus*. Species of the genus *Neophrissospongia* have a similar appearance to this species.

**Distribution and abundance.** Southern, eastern, and northern Caribbean, Florida, and Bahamas 61–914 m deep (Pomponi et al. 2001). Abundances increase from 150 m to 900 m deep. At FGBNMS the species is widespread at 17 sites with low to medium abundance (2–100).

**Ecology.** Coralline algae reefs, lower mesophotic reefs.

**Identification.** KR, CA, SWK.

**References.** van Soest and Stentoft 1988; Schuster et al. 2021.



**Figure 36.** *In-situ* photo of *Corallistes typus*, 60–108 m deep. Samples GFOE3-23G, DFH8-10B.

***Neophrissospongia cf. nolitangere* Schmidt, 1870**

Fig. 37

**Diagnostic features.** Plate or ear-shaped sponges with 1–2 cm thick walls with rounded margins, and 8–12 cm across. Tan-brown, plate. The *cf.* denomination was given



**Figure 37.** *Neophrissospongia* cf. *nolitangere*, 145 m deep. Sample GFOE3-1.

since minute oscula on inner surface (0.5–1 mm wide) and a pedicel described for *Neophrissospongia nolitangere* were not seen in the image or during voucher analysis.

**Similar species.** *Corallistes typus* and other species from the same genus. *Neophrissospongia* differs from *Corallistes* by the spiny or tuberculate nature of the dichotriaene top in the former, and the smooth nature on the later.

**Distribution and abundance.** *Neophrissospongia nolitangere* is common at deep waters from the eastern Atlantic, Azores and Mediterranean. Schuster et al. (2021) report at least 4 undescribed species of this genus in the tropical western Atlantic. This is the first report of the genus for the northwestern GOM, at FGBNMS seen once at one site.

**Ecology.** Algal nodules.

**Identification.** KR, CA, SWK, MCD.

**References.** Pissera and Levi 2002; Schuster et al. 2021

## Order Tetractinellida

### Sub-order Astrophorina

#### Family Ancorinidae

#### *Stellettinopsis* cf. *megastylifera* (Wintermann-Kilian & Kilian, 1984)

Fig. 38

**Diagnostic features.** Round to massive sponge. Brownish gray to dirty white in color. The surface is prickly, hispid, feels like sandpaper; numerous holes  $\leq 3\text{--}5$  mm in diam-



**Figure 38.** *Stellettinopsis* cf. *megastylifera*, 76 m deep. Samples DFH9-13C.

eter in sponge body. Few larger oscula 1–4 cm wide. Hard and dense in consistency. Species identity requires further analysis and comparative work (Sandes et al. 2020).

**Distribution and abundance.** The species is reported from shallow depths growing on coral reefs, rocks, sand, or mangroves (3–25 m deep) in the Colombian Caribbean, Curacao, Panama, Belize, southern GOM, and Dominican Republic. Rare species. This is the first report of this species for the north GOM mesophotic. At FGBNMS, moderate abundance at three sites.

**Ecology.** Coralline algae reefs, algal nodules.

**Identification.** SWK, CA, KR.

**References.** Sandes et al. 2020; Wintermann-Kilian and Kilian 1984.

## Order Tetractinellida

### Sub-order Astrophorina

#### Family Geodiidae

#### *Erylus alleni* de Laubenfels, 1934

Fig. 39

**Diagnostic features.** Stalks with heart-shaped tops (3–7 cm in height, 1–3 cm wide). Dark brown in color externally, tan internally. Very smooth surface. One or two oscula per stalk located at the tips (1–5 mm wide). The oscula continued by an atrium 1–2 cm deep. Dense in consistency.

**Similar species.** The stalked growth form and certain spicule details (elliptical aspidasters, two categories of oxyasters) allow its differentiation with co-occurring similar species such as *Erylus goffrilleri* and *Erylus trisphaerus*.



**Figure 39.** *Erylus alleni*, 60 m deep. Samples DFH9-12E, DFH9-12F.

**Distribution and abundance.** Mesophotic depths in Puerto Rico and Brazil. Rare species. This is the first report of this species for the GOM, at FGBNMS found with rare to low abundance (1–10) at 7 sites.

**Ecology.** Coralline algae reefs, algal nodules.

**Identification.** KR, CS, SWK, MCD.

**Reference.** Mothes et al. 1999.

***Erylus goffrilleri* Wiedenmayer, 1977**

Fig. 40

**Diagnostic features.** Massive amorphous to lobate. Dark brown color that lightens towards the base of the lobes. Smooth surface, slight wrinkles when out of water. One apical oscule, on top of each lobe (4–8 mm wide), with a paler colored membrane. Compressible but dense in consistency, easily breakable.

**Similar species.** Several species of *Erylus* from the tropical western Atlantic are very similar in external appearance. The calthrop-like triaenes and the tylasters allows its distinction from co-occurring species.

**Distribution and abundance.** Reported in shallow and mesophotic reefs in the Bahamas and Jamaica. First report of this species for the GOM at FGBNMS region, found at low abundance (1–10), at Geyer Bank.

**Ecology.** Algal nodules.

**Identification.** KR, CS, SWK, MCD.

**Reference.** Wiedenmayer 1977.



**Figure 40.** *Erylus goffrilleri* 69 m deep. Sample GFOE3-32.

***Erylus trisphaerus* (de Laubenfels, 1953)**

Fig. 41

**Diagnostic features.** Massive amorphous to lobate, dark to paler brown. The surface is smooth with very small pores. Oscula on top of lobes,  $\leq 1$  cm wide, with a very thin brown membrane. Compressible and dense in consistency.

**Similar species.** The peanut-shaped aspidasters, with two to three swollen areas, allows its distinction from co-occurring species of the genus.



**Figure 41.** *Erylus trisphaerus*, 61 m deep. Sample DFH9-12G.

**Distribution and abundance.** This is a rare species originally described from Apalachee Bay in north Florida at 13 m deep. Since then, it has been reported from shallow reefs in Alacranes Reef (Southern GOM), Cuba, and Curacao. This is the first report from mesophotic reefs and first report from northwestern GOM at FGBNMS where it occurs with rare to low abundance (1–10) at six sites.

**Ecology.** Coralline algal reefs, algal nodules, lower mesophotic reefs.

**Identification.** KR, CA, SWK, MCD.

**Reference.** Ugalde et al. 2015.

### *Geodia cf. curacaoensis* van Soest et al., 2014

Fig. 42

**Diagnostic features.** Spherical, approx. 7 cm in diameter, with a roundish black apical plate (2 cm wide). The sponge color is pale brown with reddish tinges. The surface is mostly smooth, with patches with sediments or turf around the apical plate, and occasionally on body side. Many oscula (2 mm wide) concentrated on the apical plate. Hard as a rock. The cf. is assigned due to the black color of the sieve plate, larger oscula, and the because size of the large category of oxea of *Geodia curacaoensis* is twice the size of oxea from the FGBNMS specimen.

**Similar species.** This specimen is very similar to *Geodia curacaoensis*, in overall external morphology, and spicule composition.

**Distribution and abundance.** *Geodia curacaoensis* was described from mesophotic depths in Curacao and was recorded in shallow reefs at Alacranes Reef, south GOM, and at mesophotic depths in Cuba. This morphotype was found at FGBNMS in low (2–10) abundance at six sites.

**Ecology.** Coralline algae reefs, algal nodules, lower mesophotic reefs.

**Identification.** KR, CA, SWK, MCD.

**Reference.** Ugalde et al. 2015.



**Figure 42.** *Geodia cf. curacaoensis* 81 m deep. Sample GFOE3-21.

**Order Tetractinellida**  
**Sub-order Astrophorina**  
**Family Theonellidae**

***Discodermia* sp. 1**

Fig. 43

**Diagnostic features.** Massive columnar cluster, flattened tops of columns with one apical oscule on each. Smooth to rugose surface. Tan color with pale brown tops. Columns 2–3 cm wide and 10–15 cm tall.

**Similar species.** The image of a *Discodermia dissoluta* specimen (van Soest et al. 2014) shows a columnar growth form for the species. Spicule preparations would be necessary to determine the species identity of this sponge.

**Distribution and abundance.** The genus *Discodermia* is common in deep waters at the tropical western Atlantic. *Discodermia dissoluta* is the most widespread distributed species of the genus in the region from the GOM to Brazil. At FGBNMS, rare to low (1–10) abundance at two sites.

**Ecology.** Lower mesophotic reefs.

**Identification.** KR, CA, SWK, MCD.

**Reference.** van Soest et al. 2014.



**Figure 43.** *In-situ* photograph of *Discodermia* sp. 1, 107 m deep. Photo code SP05.

**Order Tetractinellida**  
**Sub-order Astrophorina**  
**Family Thrombidae**

***Yucatania sphaeroidocladus* (Hartman & Hubbard, 1999)**

Fig. 44

**Diagnostic features.** Encrusting to massive sponge (1–9 cm in thickness). Ochre brown externally in life. The sponge has a vermetid gastropod growing within its body.



**Figure 44.** *In-situ* photograph of *Yucatania sphaeroidocladus* sp. 70–72 m deep. Samples DFH9-5C, DFH9-6D.

Surface microhispid, rough to the touch, oscula numerous and scattered, rounded to oval, 1–4.5 mm wide. Some of the openings at the surface correspond to the vermetids.

**Similar species.** Any massive-amorphous to subglobular species that accumulate debris can be confused with this species. Spicule composition is essential for its identification.

**Distribution and abundance.** Mesophotic depths from eastern Brazil, Guiana, Trinidad, and continental platform of the Yucatan Peninsula. Widely distributed at the mesophotic depths in FGBNMS (12 sites), with rare or medium abundance (1–100).

**Ecology.** Coralline algae reefs, algal nodules, lower mesophotic reefs.

**Identification.** KR, CA, SWK, MCD.

**References.** Gómez 2006; Hartman and Hubbard 1999.

## Order Tetractinellida

### Sub-order Spirophorina

#### Family Tetillidae

#### *Cinachyrella* sp. 1

Fig. 45

**Diagnostic features.** Globular sponge (12 cm wide). Neon yellow in and out, covered by sediment obscuring the sponge color. The surface appears smooth, rough to the touch; microhispid microscopically. Few apical oscula (6–8 mm wide). Dense in consistency. This specimen was initially identified as *Tetilla* sp. However, an 18S barcoding study shows this species is 99.9% *Cinachyrella* sp. (Iris Segura, pers. comm., 2022). The specimen studied lacks protienes and anatrianes found in all *Cinachyrella* species from the region. This specimen has long oxea: 2500–3000 × 10–50 μm, small oxea: 130–170 × 5 μm, and sigma (c-, and s-shaped), 20–30 μm long × < 1 μm wide.



**Figure 45.** *In-situ* photograph of *Cinachyrella* sp. 1, 81 m deep. Sample GFOE3-20.

The determination of this species requires further comparative work and the analyses of other genetic markers.

**Similar species.** Globular yellowish species of the genera *Cinachyrella*, *Cinachyra*, or *Tetilla*.

**Distribution and abundance.** At FGBNMS this species is rare, appearing once at one site.

**Ecology.** Coralline algal reefs.

**Identification.** Iris Segura, MCD.

**Reference.** van Soest and Rützler 2002.

## Order Chondrosida

### Family Chondrosiidae

#### *Chondrosia collectrix* (Schmidt, 1870)

Fig. 46

**Diagnostic features.** Thick encrusting (1–3 cm in thickness) to lobate, brown, black to tan in color externally with darker spotted areas, tan internally. Smooth surface, and round oscula, with elevated membranes. This species has very cartilaginous consistency.

**Similar species.** *Chondrilla caribensis* is very similar in growth form and color but it lacks oscula with a collared membrane and possesses typical and abundant spheraster spicules.

**Distribution and abundance.** The species is distributed at coral reefs, seagrasses, and/or mangroves in Florida, Bermuda, throughout the Caribbean, Brazil, and southern Gulf of Mexico. At FGBNMS is widely distributed with low to high abundance (10–100+) occurring at 12 sites.



**Figure 46.** *Chondrosia collectrix*, 60 m deep. Sample DFH9-9D.

**Ecology.** Inhabits lower mesophotic reef and heavily silted reef, coralline algae reef, algal nodules.

**Identification.** KR, CA, SWK, MCD.

**Reference.** Wiedenmayer 1977.

## Order Verongiida

### Family Aplysinidae

#### *Aiolochoxia crassa* (Hyatt, 1875)

Fig. 47

**Diagnostic features.** Massive/lobate to amorphous. Variable color from yellow to pink and purple. The surface has roundish conules. The oscula are on top of lobe(s), have small flat oscular membranes the same color than the sponge. Compressible and dense in consistency.



**Figure 47.** *Aiolochoxia crassa*, 52 m deep. DFH5 Dive 11269 14 17 20.JPG.

**Similar species.** Some specimens of *Verongula rigida*, with few ridges at the surface, can be confused with this species.

**Distribution and abundance.** This species is very common at shallow coral reefs in Florida, Bermuda, Bahamas, throughout the Caribbean, Brazil, and Gulf of Mexico. At mesophotic depths in FGBNMS it is widely distributed, occurring at ten sites.

**Ecology.** Coral communities.

**Identification.** KR, CA, SWK, MCD.

**Reference.** Wiedenmayer 1977.

### *Aplysina* sp. 1

Fig. 48

**Diagnostic features.** A single white tube (7 cm high, 3–4 cm wide); the sponge turns to medium brown color in alcohol. The surface is verrucose to finely conulose, and firm in consistency. One apical oscule (6 mm wide) with a thin membrane.

**Similar species.** The overall growth form of this species is similar to that of *Aplysina archeri*. However, *Aplysina archeri* tubes are usually much larger, and invariably a pink to violet color at all its depth range of distribution. A similar whitish *Aplysina* with larger dimensions was observed in Cuba at 58 and 81 m deep.

**Distribution and abundance.** This is a unique and rare species of *Aplysina*, found in mesophotic reefs at FGBNMS and Pulley Ridge. At FGBNMS it was found once at the east Flower Gardens bank.

**Ecology.** Found at coralline algal reef, algal nodule, lower mesophotic reef.

**Identification.** KR, CA, SWK, MCD.

**References.** van Soest 1978; Pinheiro et al. 2007.



**Figure 48.** *Aplysina* sp. 1 at 88 m deep. Sample DFH9-2B.

***Aplysina cf. archeri* (Higgin, 1875)**

Fig. 49A, B

**Diagnostic features.** Clusters of short tubes that spread laterally. SP04 was 10–20 cm high, and 3–5 cm in diameter, and SP25 was 3–10 cm high 3–6 cm wide, pink to deep purple in color. Fistulose rods sporadically grow out from the tubes. Surface rugose and microconulose. Roundish tube tops, more pronounced on SP25. The specimens are tentatively identified from the photographs as *Aplysina cf. archeri* due to the predominance of short roundish tubes, and lateral growth; no samples were available for analysis.

**Similar species.** At least three species of *Aplysina* can be a cluster of short tubes, viz. *A. fistularis*, *A. insularis*, and *A. muricyana* but their color is mostly yellow. Collection and genetic data would be very helpful to discern these species.

**Distribution and abundance.** *Aplysina archeri* is common at shallow coral reefs in Florida (Dry Tortugas) and throughout the Caribbean. This species might be a morphological variant of the species or a closely related species which occurs as a single or clumps of elongated purplish tubes.

**Ecology.** Coral communities, sandy substrates.

**Identification.** MCD.

**References.** van Soest 1978; Pinnheiro et al. 2007.

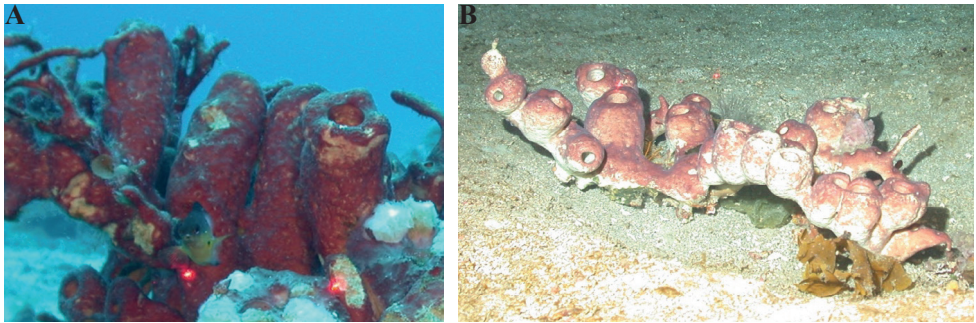


**Figure 49.** *Aplysina cf. archeri*, at 43–76 m deep. Photo code **A** SP04 and **B** SP25.

***Verongula rigida* (Esper, 1794)**

Fig. 50

**Diagnostic features.** Massive lobate to tubular species. This sample had multiple tubes of different lengths (4–20 cm high, 2–4 cm wide). Reddish yellow in color when alive, purple as dry or in alcohol. The surface is rugose to verrucose, ribbed, but smooth to the touch, not like sandpaper. One oscule (0.8–1 cm) on top of each tube, the opening extending the length of sponge. Oscula with a flat diaphragm-like contractile membrane darker in color. The consistency is firm but compressible, fibrous, and tough.

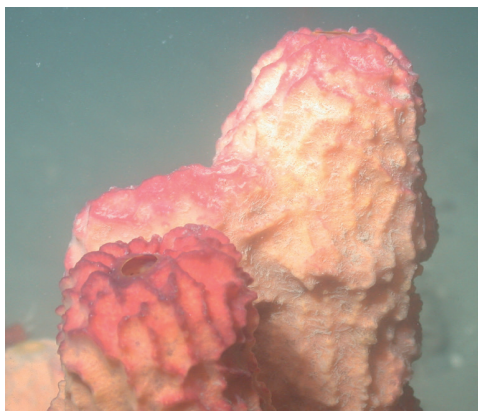


**Figure 50.** *Verongula rigida* at 60 m deep. Samples DFH8-38B, DFH9-9B.

**Similar species.** Specimens of this species with slightly ribbed surface can be confused with *Aiolochoxia crassa*. Some morphotypes of *Smenospongia aurea* can also look like short tubes of *Verongula rigida*.

**Distribution and abundance.** This species is common at shallow coral reefs throughout the Caribbean. At FGBNMS, rare, found only at three sites.

**Ecology.** Heavily silted lower mesophotic reefs.

**Identification.** KR.

**Reference.** Wiedenmayer 1977.

### *Verongula reiswigi* Alcolado, 1984

Fig. 51

**Diagnostic features.** Large tube or vase, wider at the base or at the mid body. The color is yellow with green or pinkish tinges alive, purple when dry or in alcohol. The outer surface is ribbed, forming a regular pattern that covers the whole sponge surface. One large opening (osculum or pseudo-osculum) at top of each “vase” (> 5 cm), with a very thin membrane (1–2 mm) that surrounds the whole rim. The consistency is firm but compressible.

**Similar species.** The overall shape, “osculum” size, and surface of this species makes it unique.

**Distribution and abundance.** This species is rare in occurrence at shallow and mesophotic coral reefs in Florida, Bahamas, Cuba, and eastern Caribbean. Rare at FGBNMS, seen only once at one site,

**Ecology.** Heavily silted lower mesophotic reef.

**Identification.** MCD.

**References.** Alcolado 1984; Perez et al. 2017.



**Figure 51.** *Verongula reiswigi* at 76 m deep. Photo code SP58.

## Order Verongiida

### Family Ianthellidae

#### *Ianthellide* sp. 1.

Fig. 52

**Diagnostic features.** Thin encrusting sponge, < 1 mm thick, bright yellow in life, purple in alcohol (Fig. 52A, red arrow). This thin sponge lacked any type of skeleton and seems to be overgrowing the skeleton of a dictyonal hexactinellid skeletal framework (Fig. 52B). No microscleres could be seen when dissecting and analyzing the skeleton of the hexactinellid, thus it could be dead. The conspecificity of the hexactinellid with *Iphiteon panicea* sample GFOE3-23, to the right of this yellow sample (GFOE3-23A) could not be identified. The thin sponge appears undetachable from the skeletal framework where it grows. Dark cells similar to verongiid spherulous cells (SC), and granular cells (GC), and wide elliptical choanocyte chambers (CC), 30–80  $\mu\text{m}$  in diameter, support the interpretation of this species as a fiber-less species of the family Ianthellidae (Fig. 52B, C). This is the first report of a verongiid overgrowing an hexactinellid.

**Similar species.** Two Ianthellidae genera without fibers have been described, *Hexadella* and *Vansoestia*, which have species with thin bodies, and yellowish color. However, those species have a more detachable leathery body, with surfaces ornamented by dermal canals, and prominent oscula.

**Distribution and abundance.** At FGBNMS the species was collected once at Elvers Bank.

**Ecology.** Coralline algae reefs, lower mesophotic reefs, algal nodules.

**Identification.** MCD.

**Reference.** Díaz et al. 2015.

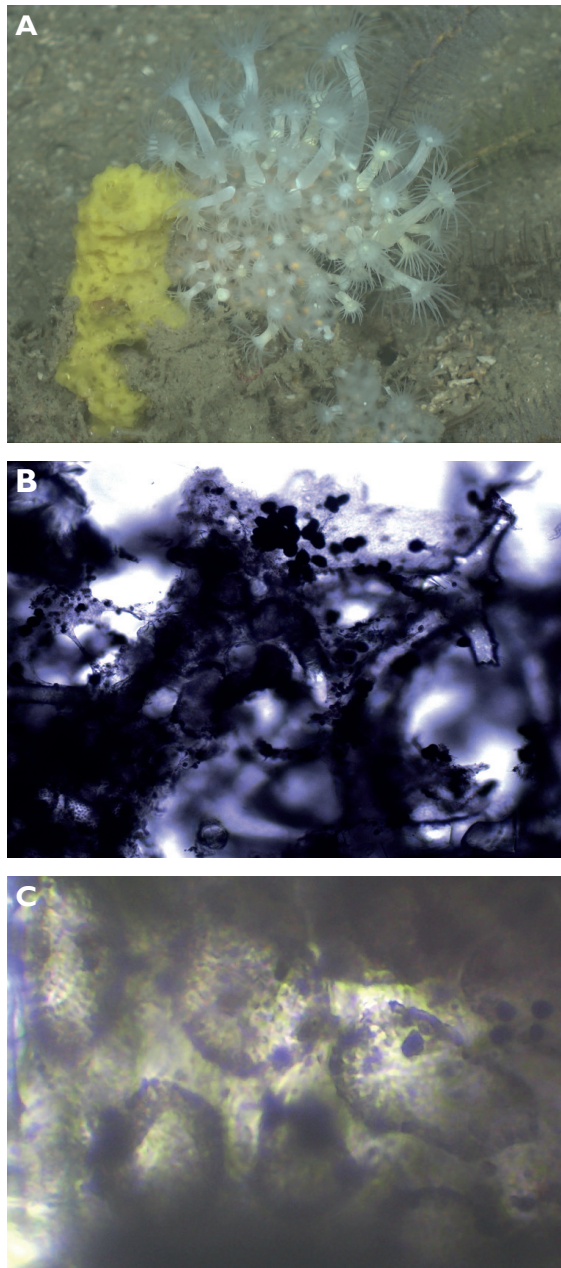


**Figure 52. A** *In-situ* photograph of a thin yellow Verongid growing on an hexactinellid skeletal framework highlighted by the red arrow, 147 m deep. Sample GFOE3-23A **B** fragment of sponge observed under light microscope 100X; arrows show large dark cells potential spherulous cells (SC), and smaller dark cells, potentially granular cells (GC) **C** smear of a sample fragment observed with a light microscope at 400× magnification. Note the large ovoid choanocyte chambers (red arrow).

**Order Dendroceratida**  
**Family Darwinellidae**

*Aplysilla* aff. *sulfurea* Schulze, 1878

Fig. 53

**Diagnostic features.** Thin encrusting sponge, 1–2 mm when preserved in alcohol. Pale yellow/orange in color alive. In alcohol it turns dark purple. In life the surface bears low conules, and oscula a few mm wide.

**Similar species.** The overall growth form, color, and color change in alcohol is similar to those in *Aplysilla sulfurea*.

**Distribution and abundance.** *Aplysilla sulfurea* is the type species for the genus and was described from the Adriatic and Mediterranean seas and eastern Atlantic. The reports from Bermuda, Florida, and southern Africa probably represent different species of similar habit and color. At FGBNMS the species is widely distributed at 14 sites with a range of abundance from rare to medium (2–100).

**Ecology.** Coralline algae reefs, lower mesophotic reefs, algal nodules.

**Identification.** CA, MCD.

**References.** de Laubenfels 1950, 1953.



**Figure 53.** *Aplysilla* aff. *sulfurea*, 78 m deep. Samples DFH9-14B.

**Order Dictyoceratida**  
**Family Dysideidae**

*Dysidea* sp. 1

Fig. 54

**Diagnostic features.** Encrusting to massive (2–4.5 cm in thickness). Pale yellow to orange color in life. The surface is porous and with low conules. Many oscula with transparent membranes. The sponge is compressible.



**Figure 54.** *Dysidea* sp. 1, 76 m deep. Sample DFH9-14F.

**Similar species.** This species is similar to the Mediterranean species *Dysidea fragilis*. There is an inaccurate citation of *Dysidea fragilis* by de Laubenfels (1953) from the GOM, and this is probably an undescribed species.

**Distribution and abundance.** At FGBNMS the species is widely distributed at ten sites with a range of abundance from rare (1 per site) to common (11–100).

**Ecology.** Coralline algae reef, lower mesophotic reef, and algal nodules.

**Identification.** KR, MCD.

**Reference.** de Laubenfels 1953.

### *Pleraplysilla* sp. nov. 1

Fig. 55

**Diagnostic features.** Very thin crust, pale pink color. The surface is smooth with irregularly distributed small conules (< 1 mm high). Oscula with a collar membrane and thick canals that run towards the oscula. The conules are produced by single or branching fibers that depart from a spongin basal plate.

**Similar species.** Very similar in external appearance to *Vansoestia caribensis*, a skeleton-less sponge of the family Ianthellidae, Order Verongiida. This species has abundant single or dendritic fibers, dark in color with an apparent pith, and some foreign spicules inside. This sponge is very similar to the species of *Pleraplysilla* depicted by Zea et al. (2014). It is currently an undescribed species.

**Distribution and abundance.** Reported by Zea et al. (2014) from the Bahamas and possibly Boynton Beach, FL. At FGBNMS the species is found at seven sites with an abundance ranging from rare to low (1–10) at six sites, to common (11–100) at one site.

**Ecology.** Coralline algae reefs, lower mesophotic reefs.

**Identification.** KR, SK, CA, MCD.

**Reference.** Zea et al. 2014.



**Figure 55.** *In-situ* photo of *Pleraplysilla* sp. 1, 79 m deep. Sample DFH9-14C.

***Pleraplysilla* sp. nov. 2**

Fig. 56

**Diagnostic features.** Massive bushy, 5 cm wide, 7 cm high. Tan in color alive. Sharp conules, 2–3 mm high, separated by 3–5 mm. The sponge is compressible but firm. The sponge has dendritic fibers, pale in color, which incorporate broken spicules. This sponge is currently identified as an undescribed species of *Pleraplysilla*. 28S analysis of this specimen clearly places it within the Order Dictyoceratida, but not within the Family Dysideidae. 18S analysis places it as 99.5% similar to *Pleraplysilla spinifera*, the type of the genus; however, that is an eastern Atlantic and Mediterranean species. This result supports the generic assignment of this new species from GOM (Díaz, Segura, and Pomponi, unpublished data).



**Figure 56.** *Pleraplysilla* sp. 2, 47 m deep. Sample GFOE3-19.

**Similar species.** Its massive habit is similar to that of the shallow Caribbean mangrove species *Pleraplysilla stocki*, and to *Pleraplysilla spinifera* from the Mediterranean.

**Distribution and abundance.** The species has been collected once from FGB-NMS, and once from Pulley Ridge, at the southeast GOM (MCD).

**Ecology.** Coralline algal reef.

**Identification.** Iris Segura, MCD.

**Reference.** van Soest 1978.

## Order Dictyoceratida

### Family Irciniidae

#### *Ircinia campana* (Lamarck, 1814)

Fig. 57

**Diagnostic features.** Flabellate to fan- or cup-shaped, sometimes pedunculated. Brown, gray, pinkish, or white color in life. The surface is regularly conulose and rugose. Abundant round oscula (4–8 mm) on the inner wall surface.

**Similar species.** This might be a different species from the shallow reef species, but close genetic and morphological comparison must be carried out to distinguish *Ircinia* species (Kelly and Thacker 2021).

**Distribution and abundance.** Widespread throughout the Caribbean at shallow coral reefs and seagrass meadows. This is the first report of the species for the northwestern GOM and at mesophotic depths in the GOM. At FGBNMS, low (1–10) in abundance and only documented at Stetson Bank. Diaz et al. 2021 report this species' morphotype at mesophotic depths (50–79 m) in various MPA's from North Carolina, South Carolina and Florida.

**Ecology.** Lower mesophotic reefs, coralline algae reefs.

**Identification.** MCD.

**Reference.** Diaz et al. 2019.



**Figure 57.** *Ircinia campana*, 56 m deep. Photo code SP10.

***Ircinia cf. campana* (Lamarck, 1814)**

Fig. 58

**Diagnostic features.** Flabellate to fan. Brown, gray, to pinkish in color. The surface is regularly conulose. Abundant round oscula (2–3 mm) on the upper surface, sometimes clumped. The cf. is to highlight the uncommon plate-shape habitus for the species, indicating that this morphotype could represent either a different species or a variant of *Ircinia campana*. Further genetic and morphologic comparisons are required.

**Distribution and abundance.** Widespread throughout the Caribbean on shallow coral reefs and seagrass meadows. This is the first report of the species for the north-western GOM and at mesophotic depths. Single specimen found at one locality.

**Ecology.** Coralline algal reefs.

**Identification.** MCD.

**References.** van Soest 1978; Diaz et al. 2019.



**Figure 58.** *Ircinia cf. campana*, 55 m deep. Sample DFH9-8A.

***Ircinia strobilina* (Lamarck, 1816)**

Fig. 59

**Diagnostic features.** The sponge is sub-globular to massive and cake-shaped, gray to black color in life. Large specimens show an upper depression where oscula abound. The surface has characteristic large conules (2–15 mm high, 5–15 mm apart). Oscula 4–10 mm in diameter, either single or in groups, with a thin membrane. The specimens are tough in consistency.

**Distribution and abundance.** Widespread throughout the Caribbean, Bermuda, GOM, and Brazil. The species has been previously reported in the northern and southern GOM (de Laubenfels 1936; Green et al. 1986; Gómez 2007). This species is a common inhabitant of coral reefs in the southern GOM (Ugalde et al. 2021). At FGBNMS the species is abundant at Stetson and Sonnier banks.



**Figure 59.** *Ircinia strobilina*, 50 m deep. Photocode SP09.

**Ecology.** Coral communities, coralline algae reefs, lower mesophotic reefs.

**Id.** MCD.

**Reference.** van Soest 1978.

### *Ircinia* sp. 1

Fig. 60

**Diagnostic features.** Single, two, or three tubes connected at the base. Tubes taper towards the tip. Pink to white in life. The tubes in Fig. 60 are 13 cm high. The surface has minute conules homogeneously spaced. One large oscule per tube (~ 2 cm in diameter) with a thin paler membrane.



**Figure 60.** *Ircinia* sp. 1, 54–60 m deep. Samples DFH9-8B, DFH9-7F.

**Similar species.** This is a very unique *Ircinia* species, probably undescribed.

**Distribution and abundance.** This is an undescribed species of *Ircinia*. At FGB-NMS the species was seen once at two localities. MCD has seen this species once in the Bahamas.

**Ecology.** Silted coralline algae reefs, silted lower mesophotic reefs.

**Identification.** CA, KR, SK, MCD.

**Reference.** van Soest 1978.

### *Ircinia* sp. 2

Fig. 61

**Diagnostic features.** Cushion shape to massive (5 cm thick). The surface is finely conulose (< 1 mm high, and 1–2 mm apart). Color alive is pink to reddish brown externally, tan internally. Small oscula 2–4 mm in diameter) with a thin white membrane around their rim, sparsely distributed on the sponge. The sponge is compressible but tough to cut.

**Similar species.** The species appears similar to *Neopetrosia proxima* and its closest species. *Neopetrosia proxima* lacks the conules, has a harder consistency, and a spicular skeleton, while *Ircinia* possess a skeleton of spongin fibers and filaments that may incorporate foreign particles (sand, and broken spicules).

**Distribution and abundance.** At FGBNMS the species was found once at one site.

**Ecology.** Coralline algal reefs.

**Identification.** CA, KR, SK, MCD.

**Reference.** van Soest 1978.



**Figure 61.** *Ircinia* sp. 2, 55 m deep. Sample DFH9-9A.

**Order Dictyoceratida****Family Thorectidae*****Smenospongia cf. echina* (de Laubenfels, 1934)**

Fig. 62

**Diagnostic features.** Globular to cushion shape, dirty yellow to grayish in life, brownish purple in alcohol. The surface has shallow roundish warts ( $\leq 1$  cm wide) but feels smooth to the touch. Oscula from 2 mm to  $> 1$  cm wide, with a slightly elevated membrane.

**Similar species.** Similar to verongiid species, *Smenospongia* spp. tends to turn purplish after collection.

**Distribution and abundance.** *Smenospongia echina* occurs in low abundance at shallow and mesophotic reefs in Puerto Rico (60–72 m), Belize, Florida (Dry Tortugas), Cayman Islands, and Cuba. At FGBNMS the species occurs in rare to low abundance (1–10) at four sites.

**Ecology.** Lower mesophotic reefs, coralline algae reefs.

**Identification.** CA, KR, SK, MCD.

**Reference.** van Soest 1978; Rützler et al. 2014.



**Figure 62.** *Smenospongia cf. echina*, 60–69 m deep. Samples DFH9-10E, DFH9-6C.

**Class Homoscleromorpha****Order Homosclerophorida****Family Plakinidae*****Plakortis cf. zygompha* (de Laubenfels, 1934)**

Fig. 63

**Diagnostic features.** Thick encrusting (5–10 mm thick). Pinkish brown in life. The surface is very smooth, velvety to the touch. Dense consistency. Sponge was overgrowing



**Figure 63.** *Plakortis* cf. *zyggompha*, 88 m deep. Sample DFH9-2B.

the base of an albino *Aplysina* spp. (DFH9-2B). Spicules larger than those of *Plakortis zyggompha* (de Laubenfels, 1934).

**Similar species.** *Plakortis angulospiculatus* and *Plakortis halichondroides*, with the same dark brown color and thick crustose shape; *Plakortis zyggompha* is always much thinner (< 5 mm) and oscula are much smaller. A genetic comparison would clarify the taxonomic status of the FGBNMS material.

**Distribution and abundance.** The species is originally described from mesophotic depths (84–165 m), and it is also reported from Florida (Dry Tortugas), Belize (cryptic habitats), and Jamaica (mangroves). At FGBNMS the species was rare and found at only three sites.

**Ecology.** Algal reef, algal nodule, lower mesophotic reef.

**Identification.** SK, KR, CA.

**References.** de Laubenfels 1934; Rützler et al. 2014.

## Class Hexactinellida

### Order Hexasterosphora

#### Family Dactylocalycidae

#### *Dactylocalyx pumiceus* Stutchbury, 1841

Fig. 64

**Diagnostic features.** Basal funnel expanded distally forming a plate, or a cup, with a wavy rim. Inner cup surface has elongated pits or grooves, several cm long, < 1 cm wide. This sample has not yet been examined but the overall growth form points to this species.

**Distribution and abundance.** This is a species with great latitudinal distribution from Florida and Gulf of Mexico to Brazil, distributed along the western coast of the Atlantic Ocean between 30°N and S, at depth of 91–1996 m. The species is



**Figure 64.** *In-situ* photo of *Dactylocalyx pumiceus*, 147 m deep. Sample GFOE3-24.

also reported off the coast of Portugal. At FGBNMS the species was collected at Elvers Bank where it was found in low (1–10) abundance.

**Ecology.** Lower mesophotic reef.

**Identification.** MCD.

**Reference.** Reiswig 2002.

### ***Iphiteon panicea* Bowerbank, 1869**

Fig. 65

**Diagnostic features.** Massive, flabellate, white, glass sponge, attached to a rock. The white elongated zoanthid, *Vitrumanthus schrieri* Kise et al., 2022, was partially overgrowing its surface. The skeleton study of the white hexactinellid (GFOE- 23) revealed a dictyonal, siliceous, rectangular to triangular framework, and spicules that agree with *Iphiteon panicea* as described by Reiswig (2002: 1299). What appears to be a portion of this specimen with a bright yellow color in life turned dark purple in alcohol, and it was stored as a different sample (GFOE3- 23A). Under a light microscope, the bright yellow hexactinellid appears to be a *Dactylocalycidae* skeletal framework, covered by thin tissue with no fibers or spicules (Fig. 51B, C). The color pattern in life and in alcohol and the type of cells and chambers suggest that this yellow tissue might represent a skeleton-less verongioid of the family *Ianthellidae*. The hexactinellid portion of yellow color area lacked any microscleres; this would suggest that the hexactinellid might have been dead, which would make the yellow species a potential epibiont for this hexactinellid. More study is required to clarify the identity of this apparent yellow hexactinellid. The trabecular surface is evident on the deck photograph (Fig. 65B) with round to elongate pits or grooves (2–10 mm in diameter), possibly exhalant apertures (Reiswig 2002).

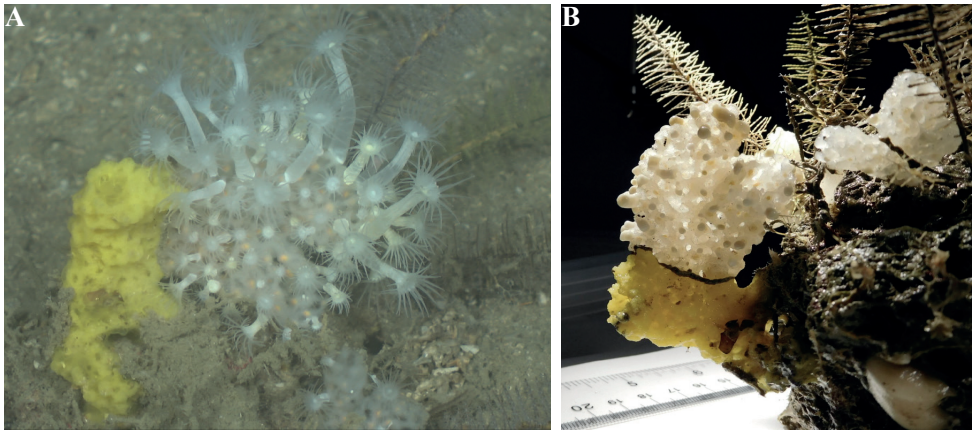


**Figure 65.** **A** *In-situ* photo of 147 m deep. Samples GFOE3-23 (white) and GFOE- 23A (yellow) **B** lab photo of the specimen.

**Similar species.** When zoanthids are extended the species can look like the hexactinellid *Verrucocoeloidea liberatorii* Reiswig & Dohrmann, 2014.

**Distribution and abundance.** This species has a northwestern Caribbean distribution (88–1957 m deep). At FGBNMS the species was collected once at Elvers Bank.

**Ecology.** Lower mesophotic reefs, sandy bottoms. The zoanthid *Vitrumanthus schrieri* (Parazoanthidae) was originally described in association with the glass sponge *Verrucocoeloidea liberatorii*. In this sample, the identity of the zoanthid was obtained by barcoding data (28S gene) (Iris Segura, pers. comm., 2022).

**Identification.** MCD.

**References.** Kise et al. 2022; Reiswig and Dohrmann 2014; Reiswig 2002.

## Discussion and conclusions

This checklist of 64 sponge species represents only a portion of the sponge fauna inhabiting mesophotic depths in the Flower Garden Banks National Marine Sanctuary region. Caribbean coral reefs that have been studied for years, including surveys of both open and sciophilous (shaded) habitats, such as the Belizean barrier reef (Rützler et al. 2014) or the Netherland Antilles (Meesters et al. 1991; van Soest 1978, 1980, 1984; van Soest et al. 2014), describe species richness at more than 200 sponge species. Considering the high diversity of habitats and substrates in the studied region, it is expected that a similar sponge biodiversity potential is possible at the Flower Garden Banks National Marine Sanctuary. Therefore, the 64 species in this study likely represent no more than one-third of the potential sponge biodiversity in the region, and are focused on some of the most conspicuous components in the sanctuary. Even with this partial representation, there are 15 species that could only be identified to genus level,

and one just to family level, demonstrating the high potential to find new species at these mesophotic depths in the northwestern Gulf of Mexico.

Our most recent collection conducted off the Sanctuary boundaries in 2019 contributed specimens of seven potentially new species of the genera *Auleta*, *Petrosia*, *Xestospongia*, *Cinachyrella*, *Siphonodictyon*, and *Pleraplysilla*, and one specimen from the family Ianthellidae. These include species with significant biomass representation and widespread occurrence such as *Petrosia* sp. nov. 1 and *Xestospongia* sp. nov. 1, or species with novel or important ecological features such as the skeletonless Ianthellidae sp. 1 overgrowing an Hexactinellid, and the bioeroding species *Siphonodictyon* sp. nov. 1. Molecular analyses (using 28S and 18S genes) are in progress to complement the morphological characteristics to refine and, in some cases, confirm the identification of these potentially new mesophotic sponge species. Part of the data from this concurrent study was essential for the generic determination of three of the species included in this paper, *Cinachyrella* sp. 1, *Pleraplysilla* sp. nov. 2, and *Siphonodictyon* sp. nov. 1.

The biological role of sponges in coral ecosystems should ignite interest to continue studying this fauna from less studied mesophotic habitats. Sponges are known for their high diversity and high biomass in shallow and mesophotic coral reefs (Diaz and Rützler 2001; Reed et al. 2018). They are important space competitors either by occupying the substrate or by overgrowing other reef organisms (Aerts 1998; Pawlik 2011), and they provide habitats for hundreds of species within or around them (Villamizar and Laughlin 1991). Spongivory is a well-known relationship with a variety of reef fauna ranging from turtles and fish to sea stars (Wulff 1994; Bell 2008; Mah 2020) and sea slugs (Mullins 2021). Sponges, through their high capacity of water filtration and their associated microbes, mediate several microbial metabolic processes such as photosynthesis, nitrification, nitrogen fixation, denitrification, sulfate reduction, and anaerobic ammonium oxidation (anammox) (Fiore et al. 2013). Several species (e.g., *Ircinia*) are known to accumulate phosphorus in granules. Therefore, sponges are known to be major players in the cycles of main nutrients like nitrogen (a major compound for proteins), phosphorous (an element essential for energy transfer) and carbon (the fundamental element of life on Earth). Most species with unicellular endosymbiotic cyanobacteria (*Synechococcus spongiarium* complex) show a red, brown, or purple external coloration in life. Examples in this checklist include *Neofibularia nolitangere*, *Aplysina* spp., *Verongula* spp., *Ircinia* spp., *Geodia* spp., *Erylus* spp., *Neopetrosia* spp., *Petrosia* spp., *Xestospongia* spp., etc. Sponges play a well-known role in reef accretion by gluing the reef framework (Wulff and Buss 1979) or by generating a structurally complex hard substrate, and in bioerosion, coral skeletons, and other calcium carbonate substrates (by species of *Cliona* and *Siphonodictyon*). Few studies have evaluated the dimension, diversity, or dynamics of these sponge roles at mesophotic depths. Therefore, this is an open and exciting horizon to explore, discover, and quantify through the diverse and extensive sponge community in the northwestern Gulf of Mexico and elsewhere.

## Acknowledgements

We would like to recognize the extensive contribution of the people who collected the specimens used in this manuscript including the crew of the R/V ‘Manta’, University of North Carolina at Wilmington Undersea Vehicle Program ROV pilots (Eric Glidden, Lance Horn, Glen Taylor, and Jason White), and the Global Foundation for Ocean Exploration ROV team (Joshua Carlson, Karl McLetchie, Jeff Laning, Todd Gregory, Roland Brian). The scientific results and conclusions, as well as any views or opinions expressed herein, are those of the author(s) and do not necessarily reflect the views of NOAA or the Department of Commerce. We also thank John Reed (Harbor Branch Oceanographic Institute – FAU) for providing photographs from the 2022 NOAA OER expedition to the FGBNMS region), and Dr. Iris Segura (Harbor Branch Oceanographic Institute – FAU) for contributing barcoding data that allowed the generic designation of three sponge and one zoanthid species. Funding for this project was provided in part by Flower Garden Banks National Marine Sanctuary, the NOAA Deep-Sea Coral Program, and the National Marine Sanctuary Foundation.

## References

- Aerts LAM (1998) Sponge/coral interactions in Caribbean reefs: Analysis of overgrowth patterns in relation to species identity and cover. *Marine Ecology Progress Series* 175: 241–249. <https://doi.org/10.3354/meps175241>
- Alcolado PM (1984) Nuevas especies de esponjas encontradas en Cuba. *Poeyana* 271: 1–22. [New species of sponges from Cuba]
- Alvarez B, van Soest RWM, Rützler K (1998) A Revision of Axinellidae (Porifera: Demospongiae) in the Central West Atlantic Region. *Smithsonian Contributions to Zoology* 598(598): 1–47. <https://doi.org/10.5479/si.00810282.598>
- Bell JJ (2008) The functional roles of marine sponges. *Estuarine, Coastal and Shelf Science* 79(3): 341–353. <https://doi.org/10.1016/j.ecss.2008.05.002>
- Boury-Esnault N, Rützler K (1997) Thesaurus of Sponge Morphology. *Smithsonian Contributions to Zoology* 596(596): 1–55. <https://doi.org/10.5479/si.00810282.596>
- de Laubenfels MW (1934) New sponges from the Puerto Rican deep. *Smithsonian Miscellaneous Collections* 91(17): 1–28.
- De Laubenfels MW (1936) A Discussion of the Sponge Fauna of the Dry Tortugas in Particular and the West Indies in General, with Material for a Revision of the Families and Orders of the Porifera. *Carnegie Institute of Washington Publication* 467. *Tortugas Laboratory Paper* (30): 1–225. [pls 1–22]
- de Laubenfels MW (1950) The porifera of the Bermuda archipelago. *Transactions of the Zoological Society of London* 27(1): 1–154. <https://doi.org/10.1111/j.1096-3642.1950.tb00227.x>
- de Laubenfels MW (1953) Sponges from the Gulf of Mexico. *Bulletin of Marine Science of the Gulf and Caribbean* 2(3): 511–557.

- de Weerd WH (2000) A monograph of the shallow-water Chalinidae (Porifera, Haplosclerida) of the Caribbean. *Beaufortia* 50(1): 1–67.
- de Voogd NJ, Alvarez B, Boury-Esnault N, Carballo JL, Cárdenas P, Díaz MC, Dohrmann M, Downey R, Goodwin C, Hajdu E, Hooper JNA, Kelly M, Klautau M, Lim SC, Manconi R, Morrow C, Pinheiro U, Pisera AB, Ríos P, Rützler K, Schönberg C, Vacelet J, van Soest RWM, Xavier J (2023) World Porifera Database. [Accessed on December 20 2022] <https://doi.org/10.14284/359>
- Díaz MC, Pomponi SA (2018) New Poecilosclerida from mesophotic coral reefs and the deep-sea escarpment in the Pulley Ridge region, eastern Gulf of Mexico: *Discorhabdella ruetzleri* n.sp. (Crambeidae) and *Hymedesmia (Hymedesmia) vaceleti* n.sp. (Hymedesmiidae). In: Klautau M, Pérez T, Cárdenas P, de Voogd N (Eds) Deep sea and cave sponges. *Zootaxa* 4466(1): 229–237. <https://doi.org/10.11646/zootaxa.4466.1.17>
- Díaz MC, Rützler K (2001) Sponges: An essential. Component of Caribbean Coral Reefs. *Bulletin of Marine Science* 69(2): 535–546.
- Díaz MC, Pomponi SA, van Soest RWM (1993) A systematic revision of the central West Atlantic Halichondrida (Demospongiae, Porifera). Part III: Description of valid species. In: Uriz MJ, Rützler K (Eds) Recent advances in ecology and systematics of sponges. *Scientia Marina* 57(4): 283–306.
- Díaz MC, Busutil L, García-Hernández MR, Pomponi SA (2019) Cuba's Mesophotic Coral Reefs- Sponge Photo Identification Guide. In: Reed JK, Farrington F (Eds) Cooperative Institute for Ocean Exploration, Research, and Technology (CIOERT) at Harbor Branch Oceanographic Institute, Florida Atlantic University (HBOI-FAU). Harbor Branch Oceanographic Institute Contribution Number 2256. <http://www.cioert.org/wp-content/uploads/2019/06/D%C3%ADaz-et-al-Cubas-Mesophotic-Coral-Reefs-Sponge-Photo-Identification-Guide-Edition-1> [Accessed 10 June 2022]
- Díaz MC, Pomponi SA, Farrington S, Reed JK (2021) Photo Identification Guide of the Sponges inhabiting the Shelf-edge Marine Protected Areas and Deep-water Reefs of the Southeastern USA (1<sup>st</sup> Edn). Harbor Branch Oceanographic Institute Contribution Number, 2294. <http://www.cioert.org/expeditions/mesophotic-reef-ecosystems>
- Esteves EL, de Paula TS, Lerner C, Lôbo-Hajdu G, Hajdu E (2018) Morphological and molecular systematics of the '*Monanchora arbuscula* complex' (Poecilosclerida : Crambeidae), with the description of five new species and a biogeographic discussion of the genus in the Tropical Western Atlantic. *Invertebrate Systematics* 32(2): 457–503. <https://doi.org/10.1071/IS16088>
- Fiore CL, Baker DM, Lesser MP (2013) Nitrogen Biogeochemistry in the Caribbean Sponge, *Xestospongia muta*: A Source or Sink of Dissolved Inorganic Nitrogen? *PLoS ONE* 8(8): e72961. <https://doi.org/10.1371/journal.pone.0072961>
- Gómez P (2006) *Yucatania clavus*, new genus and species of the family Thrombidae (Porifera: Demospongiae: Astrophorida) from the continental shelf off Yucatan, Mexico. *Proceedings of the Biological Society of Washington* 119(3): 339–345. [https://doi.org/10.2988/0006-324X\(2006\)119\[339:YCN GAS\]2.0.CO;2](https://doi.org/10.2988/0006-324X(2006)119[339:YCN GAS]2.0.CO;2)
- Gómez P (2007) Inventario de las esponjas del Parque Nacional Sistema Arrecifal Veracruzano, con nuevos Registros de Especies (Porifera: Demospongiae). In: Jiménez-Hernández MJ,

- Granados-Barba A, Ortiz-Lozano L (Eds) Investigaciones Científicas en el Sistema Arrecifal Veracruzano. Universidad Autónoma de Campeche, Campeche, 51–72.
- Gómez P (2014) The genus *Clathria* from the Gulf of Mexico and Mexican Caribbean, with redescription and resurrection of *Clathria carteri* (Poecilosclerida: Microcionidae). *Zootaxa* 3790(1): 51–085. <https://doi.org/10.11646/zootaxa.3790.1.3>
- Green G, Fuentes L, Gómez P (1986). Nuevos registros de Porifera del arrecife La Blanquilla, Veracruz, México. *Anales del Centro de Ciencias del Mar y Limnología* 13(3): 127–146.
- Hartman WD, Hubbard R (1999) A new species of *Thrombus* (Porifera: Demospongiae: Astrophorida) from Trinidad, West Indies. *Bulletin of Marine Science* 64(1): 1–8.
- Hickerson EL, Schmahl GP (2012) Sponges of Deepwater Communities in the Northwestern Gulf of Mexico. Developed by Flower Garden Banks National Marine Sanctuary. <https://flowergarden.noaa.gov/doc/posters/spongesdeepwaterwngom.pdf>
- Kealoha AK, Doyle SM, Shamberger KEF, Sylvan JB, Hetland RD, DiMarco SF (2020) Localized hypoxia may have caused coral reef mortality at the Flower Garden Banks. *Coral Reefs* 39(1): 119–132. <https://doi.org/10.1007/s00338-019-01883-9>
- Kelly JB, Thacker RW (2021) New shallow water species of Caribbean *Ircinia* Nardo, 1833 (Porifera: Irciniidae). *Zootaxa* 5072(4): 301–323. <https://doi.org/10.11646/zootaxa.5072.4.1>
- Kise H, Montenegro J, Santos MEA, Hoeksema BW, Ekins M, Ise Y, Higashiji T, Fernandez-Silva I, Reimer JD (2022) Evolution and phylogeny of glass-sponge-associated zoantharians, with a description of two new genera and three new species. *Zoological Journal of the Linnean Society* 194(1): 323–347. <https://doi.org/10.1093/zoolinlean/zlab068>
- Lehnert H, van Soest RWM (1998) Shallow water sponges of Jamaica. *Beaufortia* 48(5): 71–103.
- Mah CL (2020) New species, occurrence records and observations of predation by deep-sea Asteroidea (Echinodermata) from the North Atlantic by NOAA ship Okeanos Explorer. *Zootaxa* 4766(2): 201–260. [HTTTPS://DOI.ORG/10.11646/ZOOTAXA.4766.2.1](https://doi.org/10.11646/ZOOTAXA.4766.2.1)
- Meesters E, Knijn R, Willemsen P, Pennartz R, Roebers G, van Soest RWM (1991) Sub-rubble communities of Curaçao and Bonaire coral reefs. *Coral Reefs* 10(4): 189–197. <https://doi.org/10.1007/BF00336773>
- Mothes B, Lerner CB, Silva CMM (1999) Revision of Brazilian *Erylus* (Porifera: Astrophorida: Demospongiae) with description of a new species. In: Hooper JNA (Ed.) *Origin and Outlook*. *Memoirs of the Queensland Museum* 44: 369–380.
- Mullins DA (2021) NudiNotes Column. *Dive Log Australasia Magazine* 387: 34–35.
- Nuttall MF, Hickerson EL, Blakeway RD, Schmahl GP, Sammarco PW (2022) Do oil and gas lease stipulations in the Northwestern gulf of Mexico need expansion to better protect vulnerable coral communities? How low relief habitats support high coral biodiversity. *Frontiers in Marine Science* 8: e780248. <https://doi.org/10.3389/fmars.2021.780248>
- Office of National Marine Sanctuaries (2016) Flower Garden Banks National Marine Sanctuary Expansion Draft Environmental Impact Statement. U.S. Department of Commerce, National Oceanic and Atmospheric Administration, Office of National Marine Sanctuaries, Silver Spring, MD, 156 pp.
- Office of National Marine Sanctuaries (2020) Flower Garden Banks National Marine Sanctuary Expansion Final Environmental Impact Statement. U.S. Department of Commerce, National Oceanic and Atmospheric Administration, Office of National Marine Sanctuaries, Silver Spring, MD, 146 pp.

- Pang RK (1973) The systematics of some Jamaican excavating sponges (Porifera). *Postilla* 161: 1–75. <https://doi.org/10.5962/bhl.part.24559>
- Parra-Velandia FJ, Zea S, van Soest RWM (2014) Reef sponges of the genus *Agelas* (Porifera: Demospongiae) from the Greater Caribbean. *Zootaxa* 3794(3): 301–344. <https://doi.org/10.11646/zootaxa.3794.3.1>
- Pawlik JR (2011) The chemical ecology of sponges on Caribbean reefs: Natural products shape natural systems. *Bioscience* 61(11): 888–898. <https://doi.org/10.1525/bio.2011.61.11.8>
- Pech-Puch D, Pérez-Povedano M, Martínez-Gutián M, Lasarte C, Vázquez Ucha J, Bou G, Rodríguez J, Beceiro A, Jiménez C (2020) In Vitro and In Vivo Assessment of the Efficacy of Bromoageliferin, an Alkaloid Isolated from the Sponge *Agelas dilatata*, against *Pseudomonas aeruginosa*. *Marine Drugs* 18(6): e326. <https://doi.org/10.3390/md18060326>
- Perez T, Diaz MC, Ruiz C, Condor-Lujan B, Klautau M, Hajdu E, Lobo-Hajdu G, Zea S, Pomponi SA, Thacker RW, Carteron S, Tollu G, Pouget-Cuvelier A, Thlamon P, Marechal J-P, Thomas OP, Ereskovsky AV, Vacelet J, Boury-Esnault N (2017) How a collaborative integrated taxonomic effort has trained new spongiologists and improved knowledge of Martinique Island (French Antilles, eastern Caribbean Sea) marine biodiversity. *PLoS ONE* 12(3): e0173859. <https://doi.org/10.1371/journal.pone.0173859>
- Pinheiro US, Hajdu E, Custódio MR (2007) *Aplysina* Nardo (Porifera, Verongida, Aplysinidae) from the Brazilian coast with description of eight new species. *Zootaxa* 1609(1): 1–51. <https://doi.org/10.11646/zootaxa.1610.1.zootaxa.1609.1.1>
- Pomponi SA, Kelly M, Reed JK, Wright AE (2001) Diversity and bathymetric distribution of lithistid sponges in the tropical western Atlantic. *Bulletin of the Biological Society of Washington* 10: 344–353.
- Pomponi SA, Diaz MC, van Soest RWM, Bell LJ, Busutil L, Gochfeld DJ, Kelly M, Slattery M (2019) Sponges. In: Loya Y, Puglise KA, Bridge T (Eds) *Mesophotic Coral Ecosystems of the World*. Springer, New York, 563–588. [https://doi.org/10.1007/978-3-319-92735-0\\_32](https://doi.org/10.1007/978-3-319-92735-0_32)
- Reed J (2022) Dive notes from Mohawk ROV dives on Flower Garden Banks, Wright NOAA OE cruise, May 2022.
- Reed JK, González-Díaz P, Busutil López L, Farrington S, Martínez-Daranas B, Cobián Rojas D, Voss J, Diaz MC, David A, Hanisak MD, González Mendez J, García Rodríguez A, González-Sánchez PM, Viamontes Fernández J, Estrada Pérez D, Studivan M, Drummond F, Pomponi SA (2018) Cuba's mesophotic reefs and associated fish communities. *Revista de Investigaciones Marinas* 38(1): 56–125. [ISSN: 1991-6086] [Harbor Branch Oceanographic Institute Contribution Number 2151] <http://www.cioert.org/wp-content/uploads/2018/09/2018-Reed-et-al-Cubas-Mesophotic-Coral-Reefs-and-Associated-Fish-Communities-RIM-pub.pdf>
- Reed JK, Farrington S, Díaz MC, Pomponi SA, Hanisak D (2021) Photo Identification Guide of the Benthic Taxa Inhabiting the Mesophotic Reefs of the Florida Keys National Marine Sanctuary. Harbor Branch Oceanographic Technical Report Number 197, 220 pp. <http://www.cioert.org/wp-content/uploads/2021/09/2021-Reed-et-al-FKNMS-Mesophotic-Reefs-Photo-Guide.pdf> [accessed 10 June 2022]
- Reiswig HM (2002) Family Dactylocalycidae Gray, 1867. In: Hooper JNA, van Soest RWM (Eds) *Systema Porifera. A guide to the classification of sponges* (2 volumes). Kluwer Academic/Plenum, NY, 1293–1300. [1708 + XLVIII] [ISBN 978-1-4615-0747-5] [https://doi.org/10.1007/978-1-4615-0747-5\\_134](https://doi.org/10.1007/978-1-4615-0747-5_134)

- Reiswig HM, Dohrmann M (2014) Three new species of glass sponges (Porifera: Hexactinellida) from the West Indies, and molecular phylogenetics of Euretidae and Auloplacidae (Sceptrulophora). *Zoological Journal of the Linnean Society* 171(2): 233–253. <https://doi.org/10.1111/zoj.12138>
- Rützler K, Piantoni C, van Soest RWM, Díaz MC (2014) Diversity of sponges (Porifera) from cryptic habitats on the Belize barrier reef near Carrie Bow Cay. *Zootaxa* 3805(1): 1–129. <https://doi.org/10.11646/zootaxa.3805.1.1>
- Sandes J, Lira J, Pinheiro U, Muricy G (2020) Taxonomy of *Melophlus* Thiele, 1899 and *Stellettinopsis* Carter, 1879, with description of two new species from Brazil (Demospongiae: Astrophorina). *Marine Biodiversity* 50(2): 1–24. <https://doi.org/10.1007/s12526-019-01037-8>
- Santos Neto C, Nascimento E, Cavalcanti T, Pinheiro U (2018) Taxonomy of *Oceanapia* Norman, 1869 (Demospongiae: Haplosclerida: Phloeodictyidae) from the Brazilian coast. *Zootaxa* 4455(2): e363. <https://doi.org/10.11646/zootaxa.4455.2.6>
- Schmahl GP, Hickerson EL, Precht WF (2008) Biology and Ecology of Coral Reefs and Coral Communities in the Flower Garden Banks Region, Northwestern Gulf of Mexico. In: Riegl BM, Dodge RE (Eds) *Coral Reefs of the USA*. Springer Netherlands, 221–261. [https://doi.org/10.1007/978-1-4020-6847-8\\_6](https://doi.org/10.1007/978-1-4020-6847-8_6)
- Schmahl GP, Hickerson EL, Nuttall MF (2012) Science-based design of coral protected areas in the Gulf of Mexico. *Proceedings of the 12<sup>th</sup> International Coral Reef Symposium*, Cairns, Australia, 9–13 July 2012.
- Schuster A, Pomponi SA, Pisera A, Cárdenas P, Kelly M, Wörheide G, Erpenbeck D (2021) Systematics of ‘lithistid’ tetractinellid demosponges from the Tropical Western Atlantic—implications for phylodiversity and bathymetric distribution. *PeerJ* 9: e10775. <https://doi.org/10.7717/peerj.10775>
- Semmler R, Hoot WC, Reaka ML (2016) Are mesophotic coral ecosystems distinct communities and can they serve as refugia for shallow reefs? *Coral Reefs* 36(2): 433–444. <https://doi.org/10.1007/s00338-016-1530-0>
- Sigovini M, Keppel E, Tagliapietra D (2016) Open Nomenclature in the biodiversity era. *Methods in Ecology and Evolution* 7(10): 1217–1225. <https://doi.org/10.1111/2041-210X.12594>
- Slattery M, Lesser MP, Gochfeld DJ, et al. (2017) Biogeographic connectivity of Caribbean mesophotic sponge communities. In: Gochfeld, DJ, Wright CA (Eds) *Proceedings of the AAUS 36<sup>th</sup> Scientific Symposium*. American Academy of Underwater Sciences, Dauphin Island, 67–70.
- Ugalde D, Gomez P, Simoes N (2015) Marine sponges (Porifera: Demospongiae) from the Gulf of México, new records and redescription of *Erylus trisphaerus* (de Laubenfels, 1953). *Zootaxa* 3911(2): 151–183. <https://doi.org/10.11646/zootaxa.3911.2.1>
- Ugalde D, Fernandez JCC, Gómez P, Lôbo-Hajdu G, Simões N (2021) An update on the diversity of marine sponges in the southern Gulf of Mexico coral reefs. *Zootaxa* 5031(1): 001–112. <https://doi.org/10.11646/zootaxa.5031.1.1>
- van Soest RWM (1978) Marine sponges from Curaçao and other Caribbean localities. Part I. Keratosa. In: Hummelinck PW, Van der Steen LJ (Eds) *Uitgaven van de Natuurwetenschappelijke Studiekkring voor Suriname en de Nederlandse Antillen*. No. 94. *Studies on the Fauna of Curaçao and other Caribbean Islands* 56(179): 1–94.

- van Soest RWM (1980) Marine sponges from Curaçao and other Caribbean localities. Part II. Haplosclerida. In: Hummelinck PW, Van der Steen LJ (Eds) *Uitgaven van de Natuurwetenschappelijke Studiekring voor Suriname en de Nederlandse Antillen*. No.104. Studies on the Fauna of Curaçao and other Caribbean Islands 62(191): 1–173.
- van Soest RWM (1984) Marine sponges from Curaçao and other Caribbean localities. Part III. Poecilosclerida. In: Hummelinck PW & Van der Steen LJ (Eds) *Uitgaven van de Natuurwetenschappelijke Studiekring voor Suriname en de Nederlandse Antillen*. No. 112. Studies on the Fauna of Curaçao and other Caribbean Islands 66(199): 1–167.
- van Soest RWM (2017) Sponges of the Guyana Shelf. *Zootaxa* 4217(1): 1–225. <https://doi.org/10.11646/zootaxa.4217.1.1>
- van Soest RWM, Rützler K (2002) Family Tetillidae Sollas, 1888. In: Hooper JNA van Soest RWM (Eds) *Systema Porifera: a guide to the classification of sponges*. Kluwer/Plenum, New York, 85–98. [xlviii + 1704 pp.] [https://doi.org/10.1007/978-1-4615-0747-5\\_8](https://doi.org/10.1007/978-1-4615-0747-5_8)
- van Soest RWM, Stentoft N (1988) Barbados Deep-Water Sponges. In: Hummelinck PW, Van der Steen LJ (Eds) *Uitgaven van de Natuurwetenschappelijke Studiekring voor Suriname en de Nederlandse Antillen*. No. 122. Studies on the Fauna of Curaçao and other Caribbean Island 70(215): 1–175.
- Van Soest RWM, Meesters EH, Becking LE (2014) Deep-water sponges (Porifera) from Bonaire and Klein Curaçao, Southern Caribbean. *Zootaxa* 3878(5): 401–443. <https://doi.org/10.11646/zootaxa.3878.5.1>
- Vicente J, Ríos JA, Zea S, Toonen RJ (2019) Molecular and morphological congruence of three new cryptic *Neopetrosia* spp in the Caribbean. *Peer J* 7: e6371. <https://doi.org/10.7717/peerj.6371>
- Villamizar E, Laughlin RA (1991) Fauna Associated with the Sponges *Aplysina archeri* and *Aplysina lacunosa* in a Coral Reef of the Archipiélago de Los Roques, National Park, Venezuela. In: Reitner J, Keupp H (Eds) *Fossil and Recent Sponges*. Springer, Berlin, Heidelberg. [https://doi.org/10.1007/978-3-642-75656-6\\_44](https://doi.org/10.1007/978-3-642-75656-6_44)
- Wagner D, Etnoyer PJ, Schull J, David AW, Nizinski MS, Hickerson EL, Battista TA, Netburn AN, Harter SL, Schmahl GP, Coleman HM, Hourigan TF (2017) Science Plan for the Southeast Deep Coral Initiative (SEDCI): 2016–2019. [NOAA Technical Memorandum NOS NCCOS 230, NOAA National Ocean Service, Charleston, SC, 96 pp.]
- Wiedenmayer F (1977) Shallow-water sponges of the Western Bahamas. *Experientia Supplementum* 28: 1–287. [pls 1–43] <https://doi.org/10.1007/978-3-0348-5797-0>
- Wintermann-Kilian G, Kilian EF (1984) Marine Sponges of the Region of Santa Marta (Colombia). Part II. Homosclerophorida, Choristida, Spirophorida, Hadromerida, Axinellida, Halichondrida, Poecilosclerida. *Studies on Neotropical Fauna and Environment* 19(3): 121–135. <https://doi.org/10.1080/01650528409360650>
- Wulff JL (1994) Sponge feeding by Caribbean angelfishes, trunkfishes, and filefishes. In: van Soest RWM, van Kempen TMG, Brackman JC (Eds) *Sponges Time Space*. Rotterdam, Balkema, 265–271.
- Wulff JL, Buss LW (1979) Do sponges help hold coral reefs together? *Nature* 281(5731): 474–475. <https://doi.org/10.1038/281474a0>
- Zea S, Henkel TP, Pawlik JR (2014) *The Sponge Guide: a picture guide to Caribbean sponges* (3<sup>rd</sup> Edn.). [www.spongeguide.org](http://www.spongeguide.org)

## Supplementary material I

### **Table of localities for mesophotic sponge species in the North Western Gulf of Mexico**

Authors: Maria Cristina Díaz, Marissa Nuttall, Shirley A. Pomponi, Klaus Rützler, Sarah Klontz, Christi Adams, Emma L. Hickerson, G.P. Schmahl

Data type: occurrences, geographic coordinates, habitat type, and localities

Explanation note: The table summarizes distribution data for sponge species collected and observed at 17 localities at the Flower Garden Banks National Marine Sanctuary Region.

Copyright notice: This dataset is made available under the Open Database License (<http://opendatacommons.org/licenses/odbl/1.0/>). The Open Database License (ODbL) is a license agreement intended to allow users to freely share, modify, and use this Dataset while maintaining this same freedom for others, provided that the original source and author(s) are credited.

Link: <https://doi.org/10.3897/zookeys.1161.93754.suppl1>

# On five new species of the genera *Araneus* and *Hypsosinga* (Araneae, Araneidae) from Vietnam

Xiaoqi Mi<sup>1</sup>, Shuqiang Li<sup>2</sup>, Dinh-Sac Pham<sup>3</sup>

**1** College of Agriculture and Forestry Engineering and Planning, Guizhou Provincial Key Laboratory of Biodiversity Conservation and Utilization in the Fanjing Mountain Region, Tongren University, Tongren 554300, Guizhou, China **2** Institute of Zoology, Chinese Academy of Sciences, Beijing 100101, China **3** Vietnam National Museum of Nature (VNMN), Vietnam Academy of Science and Technology (VAST), 18 Hoang Quoc Viet, Cau Giay, Hanoi, Vietnam

Corresponding authors: Shuqiang Li ([lisq@ioz.ac.cn](mailto:lisq@ioz.ac.cn)); Dinh-Sac Pham ([phamdinh sac@vnmn.vast.vn](mailto:phamdinh sac@vnmn.vast.vn))

Academic editor: Zhiyuan Yao | Received 20 February 2023 | Accepted 20 April 2023 | Published 11 May 2023

<https://zoobank.org/AC016DCC-73CF-4D42-ADD0-D030B0FE7D97>

**Citation:** Mi X, Li S, Pham D-S (2023) On five new species of the genera *Araneus* and *Hypsosinga* (Araneae, Araneidae) from Vietnam. ZooKeys 1161: 69–87. <https://doi.org/10.3897/zookeys.1161.102375>

## Abstract

Five new species of the spider family Araneidae Clerck, 1757 from Vietnam are described: *Araneus eugenei* **sp. nov.** (♂♀), *A. ethani* **sp. nov.** (♀), *A. liami* **sp. nov.** (♂♀), *Hypsosinga ryani* **sp. nov.** (♂♀), and *H. zioni* **sp. nov.** (♀). Diagnostic photographs of the habitus and copulatory organs are provided. Types of the new species are deposited in the Institute of Zoology, Chinese Academy of Sciences (IZCAS) in Beijing, China.

## Keywords

Arachnida, biodiversity, diagnosis, morphology, taxonomy

## Introduction

A comprehensive checklist of spiders from Vietnam was first compiled by Pham et al. (2007), who listed 320 spider species in 32 families and 159 genera. The number of spider species in Vietnam was later increased to 456 species of 41 families by Ono et al. (2012), who included 23 genera and 68 species of araneids. Few studies on spiders

of Vietnam were made after 2012 other than Lin et al. (2023) and Wang et al. (2023). However, the true number of Vietnam spider taxa is probably much higher than currently known.

The goal of this paper is to describe five new species collected in three national parks (Cuc Phuong, Cat Ba, and Tam Dao national parks) in northern Vietnam.

## Material and method

All specimens were collected by canopy fogging, leaf-litter sieving, or hand collecting and are preserved in 75% ethanol. Type specimens of new species are deposited in the Institute of Zoology, Chinese Academy of Sciences (IZCAS) in Beijing. The specimens were examined with an Olympus SZX16 stereomicroscope. The epigynes were cleared in lactic acid for examination and imaging. The left male palps were dissected in ethanol for examination, description, and imaging. Photographs of the habitus and copulatory organs were taken with a Kuy Nice digital camera mounted on an Olympus BX43 compound microscope. Compound focus images were generated using Helicon Focus v. 6.7.1.

All measurements are given in millimeters. Leg measurements are given as total length (femur, patella + tibia, metatarsus, tarsus). Abbreviations used in the text and figures are as follows: **ALE** anterior lateral eye; **AME** anterior median eye; **C** conductor; **CD** copulatory duct; **CO** copulatory opening; **E** embolus; **FD** fertilization duct; **MA** median apophysis; **MOA** median ocular area; **PLE** posterior lateral eye; **PME** posterior median eye; **Sc** scape; **Sp** spermatheca; **TA** terminal apophysis.

## Taxonomy

### Family Araneidae Clerck, 1757

### Genus *Araneus* Clerck, 1757

**Type species.** *Araneus angulatus* Clerck, 1757.

**Comments.** Although the three new *Araneus* species in this paper differ greatly from the type species *A. angulatus* in both somatic and copulatory organs, they are placed in *Araneus* provisionally until a phylogenetic analysis is conducted. The three new species, along with *A. bidentatus* Mi & Li, 2022, *A. bidentatoides* Mi & Li, 2022, and *A. semiorbiculatus* Mi & Li, 2022, show some common somatic characters, such as a more or less dark brown carapace, eyes with black bases, an abdomen that is longer than wide, a female abdomen with at least a pair of low humps; these characters indicate these species must be closely related, although their copulatory organs differ.

***Araneus eugenei* sp. nov.**

<https://zoobank.org/128B14DB-E864-4C0C-8DC3-A79F00F21227>

Figs 1, 2, 9A–D

**Type material.** *Holotype* ♂ (IZCAS-Ar44127), VIETNAM: Vinh Phuc Province, Tam Dao National Park (21°31.56'N, 105°33.15'E), 10.V.2005, Dinh-Sac Pham leg.

**Paratypes:** 1♂ (IZCAS-Ar44128), same locality and collector as holotype, 9.V.2005; 1♂ (IZCAS-Ar44129), same locality and collector as holotype, 12.V.2005; 1♀ (IZCAS-Ar44130), Ninh Binh Province, Cuc Phuong National Park (20°15.30'N, 105°42.55'E, ca 250 m), 18.VIII.2007, Dinh-Sac Pham leg.; 1♀ (IZCAS-Ar44131) Hai Phong Province, Cat Ba National Park, acacia plantation (20°47.27'N, 105°59.35'E, ca 40 m), 14.VII.2008, Dinh-Sac Pham leg.

**Etymology.** The species name is a boy's name from Vietnam; noun (name) in genitive case.

**Diagnosis.** The female of the new species resembles that of *A. ethani* sp. nov. in appearance, but it can be distinguished in having 1) a triangular scape (Fig. 1B, D) vs truncated (Fig. 3B–D); 2) the copulatory openings situated on the posterior surface of the epigyne (Fig. 1B, D) vs on the ventral surface (Fig. 3A); and 3) the spermathecae separated by a distance of approximately one radius (Fig. 1C, D) vs one diameter apart (Fig. 3D). The male of the new species resembles that of *A. liami* sp. nov. in appearance, but differs in: 1) lacking heavily sclerotized denticulate protuberances on the palpal tibia (Fig. 2A–C) vs with three heavily sclerotized denticulate protuberances (Fig. 5A, E); 2) having the terminal apophysis distally pointed (Fig. 2A–D) vs bifurcated (Fig. 5C, D); 3) having the embolus tapered (Fig. 2A, D) vs thread-like (Fig. 5A, C, D); and 4) bearing a pair of low humps on the posterior part of abdomen (Fig. 1H, I) vs lacking humps (Fig. 4G, H).

**Description. Male** (holotype, Figs 1H, I, 2, 9A–D). Total length 3.85. Carapace 2.00 long, 1.55 wide. Abdomen 2.45 long, 1.45 wide. Clypeus 0.10 high. Eye sizes and interdistances: AME 0.13, ALE 0.08, PME 0.10, PLE 0.08, AME–AME 0.23, AME–ALE 0.15, PME–PME 0.10, PME–PLE 0.30, MOA length 0.38, anterior width 0.45, posterior width 0.25. Leg measurements: I 6.25 (1.95, 2.20, 1.40, 0.70), II 5.50 (1.75, 1.85, 1.25, 0.65), III 3.70 (1.25, 1.20, 0.70, 0.55), IV 5.20 (1.75, 1.75, 1.05, 0.65). Carapace yellowish brown, with a V-shaped paler patch anteriorly to fovea; cervical groove slightly distinct. Chelicerae yellowish brown with four promarginal and three retromarginal teeth. Endites and labium yellowish brown, with yellow edge. Sternum yellowish brown, with gray setae. Legs yellow, with brown annuli; tibia I with 11 macrosetae; tibia II with seven macrosetae; tibia III with seven macrosetae; tibia IV with six macrosetae. Abdomen elliptical, ~1.7× longer than wide, with two pairs of very low, lateral humps; dorsal abdomen with a longitudinal patch; venter grayish brown medially and with white patches laterally. Spinnerets yellow.

**Palp** (Fig. 2): two patellar bristles; tibia ~2× wider than long; cymbium with projection on prolateral base (see arrow in Fig. 2A); paracymbium finger-like; tegulum

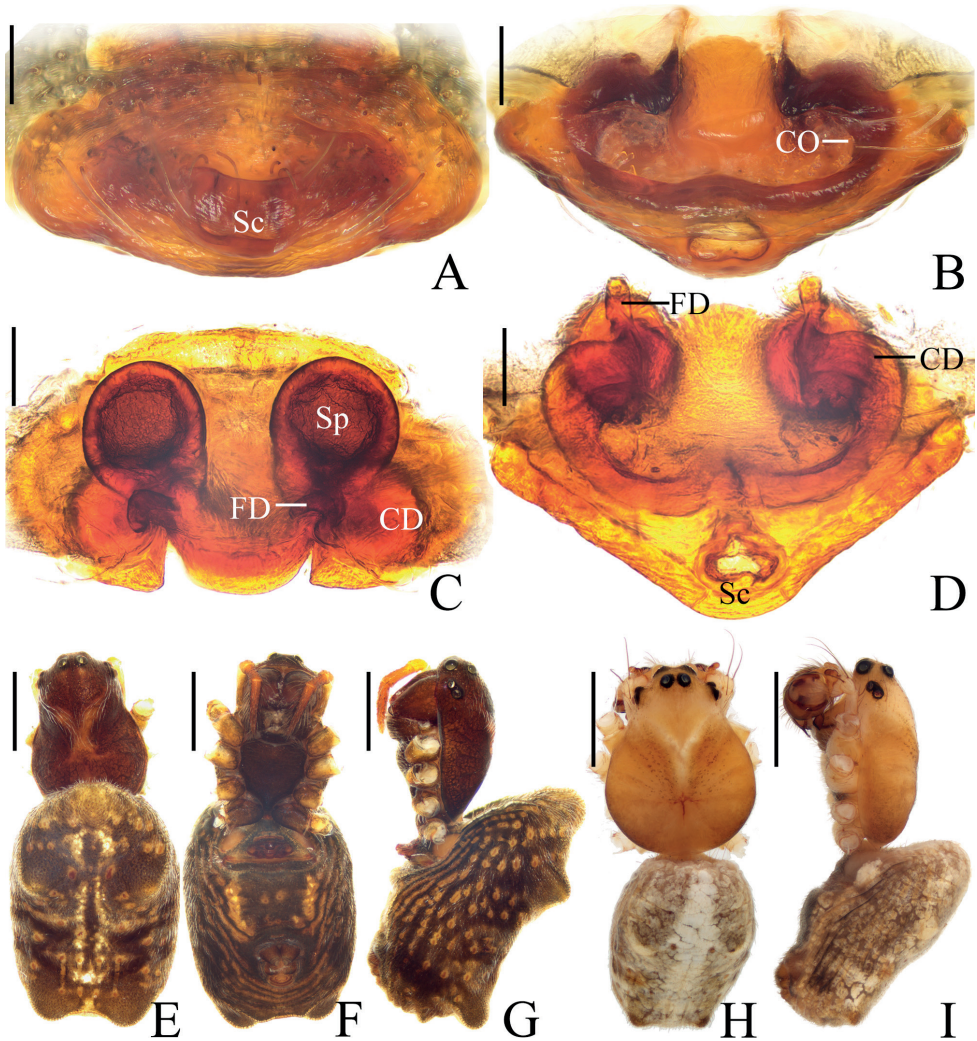


**Figure 1.** *Araneus eugenei* sp. nov. **A–G** female paratype IZCAS-Ar44131 **H, I** male holotype **A** epigyne, ventral view **B** *ibid.*, posterior view **C** vulva, dorsal view **D** *ibid.*, posterior view **E** habitus, dorsal view **F** *ibid.*, ventral view **G** *ibid.*, lateral view **H** *ibid.*, dorsal view **I** *ibid.*, lateral view. Scale bars: 0.1 mm (**A–D**); 1 mm (**E–I**).

smoothly rounded in retrolateral; median apophysis  $\sim 1.4\times$  wider than long, heavily sclerotized, tapered end pointed to tip of cymbium; embolus  $\sim 0.5\times$  length of bulb diameter in prolateral view, tapered distally; conductor membranous, longer than wide; terminal apophysis about half bulb diameter width at base, tapered and curved distally.

**Female** (paratype IZCAS-Ar44131, Fig. 1A–G). Total length 4.75. Carapace 2.25 long, 1.50 wide. Abdomen 3.65 long, 2.25 wide. Clypeus 0.10 high. Eye sizes and inter-distances: AME 0.15, ALE 0.08, PME 0.13, PLE 0.10, AME–AME 0.20, AME–ALE

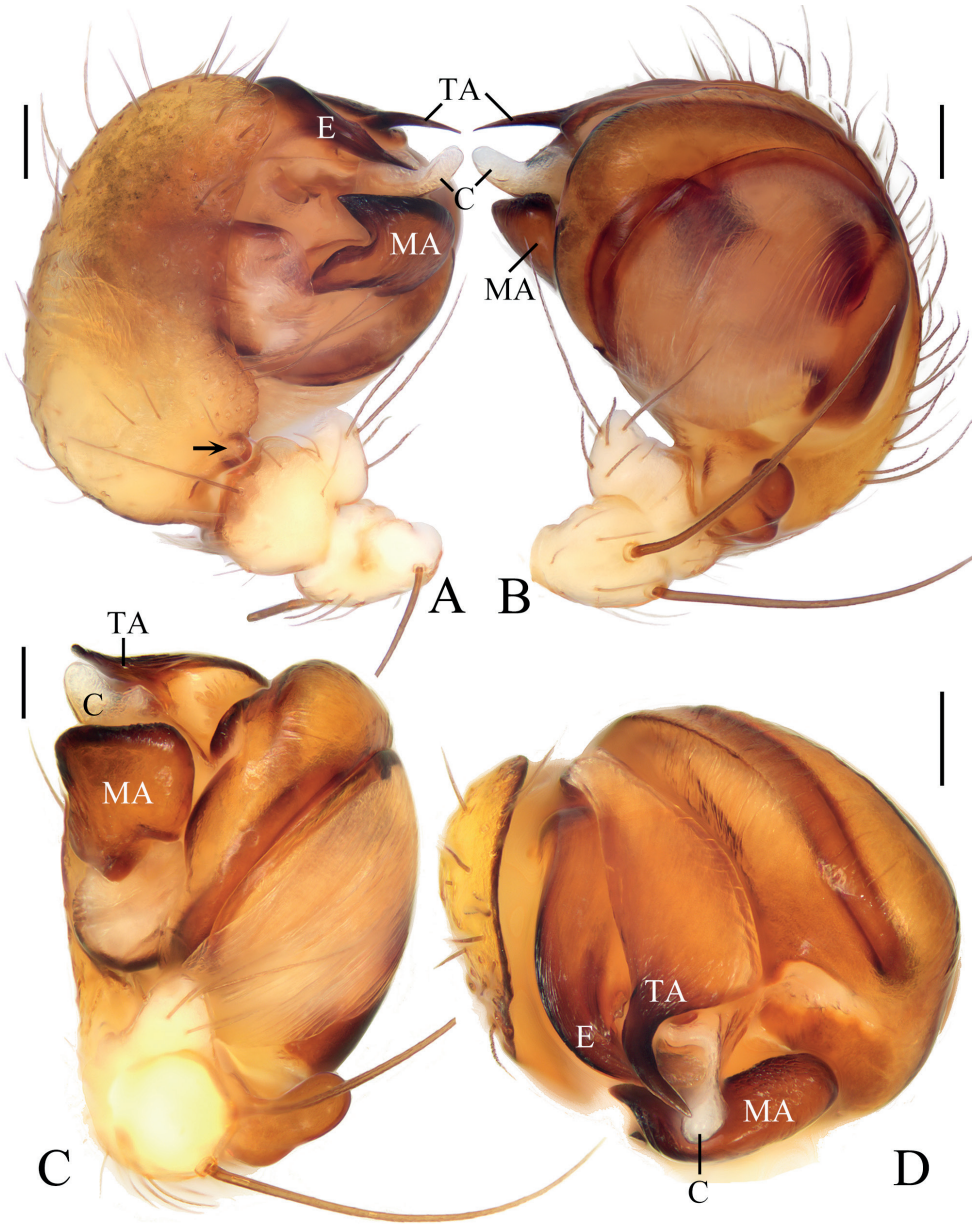


**Figure 2.** *Araneus eugenei* sp. nov., male holotype **A** left palp, prolateral view **B** *ibid.*, retrolateral view **C** *ibid.*, ventral view **D** *ibid.*, apical view. Scale bars: 0.1 mm.

0.18, PME–PME 0.15, PME–PLE 0.38, MOA length 0.43, anterior width 0.48, posterior width 0.38. Leg measurements: I 6.05 (1.85, 2.15, 1.35, 0.70), II 5.40 (1.65, 1.90, 1.20, 0.65), III 3.85 (1.25, 1.30, 0.75, 0.55), IV 5.70 (1.85, 2.00, 1.25, 0.60). Habitus similar to that of male, but much darker, and the two pairs of humps are more obvious.

**Epigyne** (Fig. 1A–D):  $\sim 2.2\times$  wider than long in ventral view, scape triangular,  $\sim 3.0\times$  wider than long in posterior view; copulatory openings arcuated, situated on posterior surface; copulatory ducts also arcuated; spermathecae spherical, spaced by about one radius.

**Variation.** Total length: ♂♂ 3.60–3.85; ♀♀ 4.25–4.75.

**Distribution.** Vietnam (Vinh Phuc, Ninh Binh and Hai Phong Provinces).

***Araneus ethani* sp. nov.**

<https://zoobank.org/E32071BB-3898-4353-B2AD-106D9C2EE312>

Figs 3, 9E–H

**Type material.** **Holotype** ♀ (IZCAS-Ar44132), VIETNAM: Ninh Binh Province, Cuc Phuong National Park, disturbed forest (20°16.38'N, 105°41.10'E, ca 280 m), 3.IV.2007, Dinh-Sac Pham leg. **Paratypes:** 1♀ (IZCAS-Ar44133), same locality and collector as holotype (20°15.30'N, 105°42.55'E, ca 250 m), 4.XII.2007; 1♀ (IZCAS-Ar44134), Hai Phong Province, Cat Ba National Park, disturbed forest (20°48.25'N, 107°00.02'E, ca 80 m), 16.VII.2008, Dinh-Sac Pham leg.

**Etymology.** The species name is a boy's name from Vietnam; noun (name) in genitive case.

**Diagnosis.** The new species resembles *A. eugenei* sp. nov. in appearance but differs in having: 1) the scape truncated (Fig. 3A–D) vs triangular (Fig. 1B, D); 2) the copulatory openings situated on the ventral surface of the epigyne (Fig. 3A, C) vs on the posterior surface (Fig. 1B); and 3) the spermathecae spaced by about one diameter (Fig. 3D) vs about one radius (Fig. 1C).

**Description.** **Female** (holotype, Figs 3, 9E–H). Total length 4.10. Carapace 2.25 long, 1.55 wide. Abdomen 2.60 long, 1.75 wide. Clypeus 0.08 high. Eye sizes and interdistances: AME 0.15, ALE 0.10, PME 0.13, PLE 0.13, AME–AME 0.20, AME–ALE 0.15, PME–PME 0.15, PME–PLE 0.30, MOA length 0.48, anterior width 0.43, posterior width 0.43. Leg measurements: I 5.80 (1.75, 2.15, 1.25, 0.65), II 5.15 (1.55, 1.85, 1.10, 0.65), III 3.90 (1.25, 1.35, 0.70, 0.60), IV 5.35 (1.70, 1.90, 1.10, 0.65). Carapace brown, with yellow anteriorly to fovea and yellow edges in thoracic region, with pale setae. Chelicerae brown with five promarginal and three retromarginal teeth. Endites and labium brown at base, paler distally. Sternum with short, longitudinal, yellow patch. Legs yellow with yellowish-brown annuli. Abdomen elliptical,  $\sim 1.25\times$  longer than wide, pointed anteriorly and with pair of lateral humps posteriorly, covered with pale setae, dorsum grayish brown with white spots; venter brown with yellow patches. Spinnerets yellowish brown.

**Epigyne** (Fig. 3A–D):  $\sim 2.8\times$  wider than long in ventral view; scape truncated,  $\sim 6.0\times$  wider than long in anterior view; copulatory openings slit-like, situated on ventral surface; copulatory ducts longer than spermatheca diameter, curved about 90°; spermathecae globular, about one diameter apart.

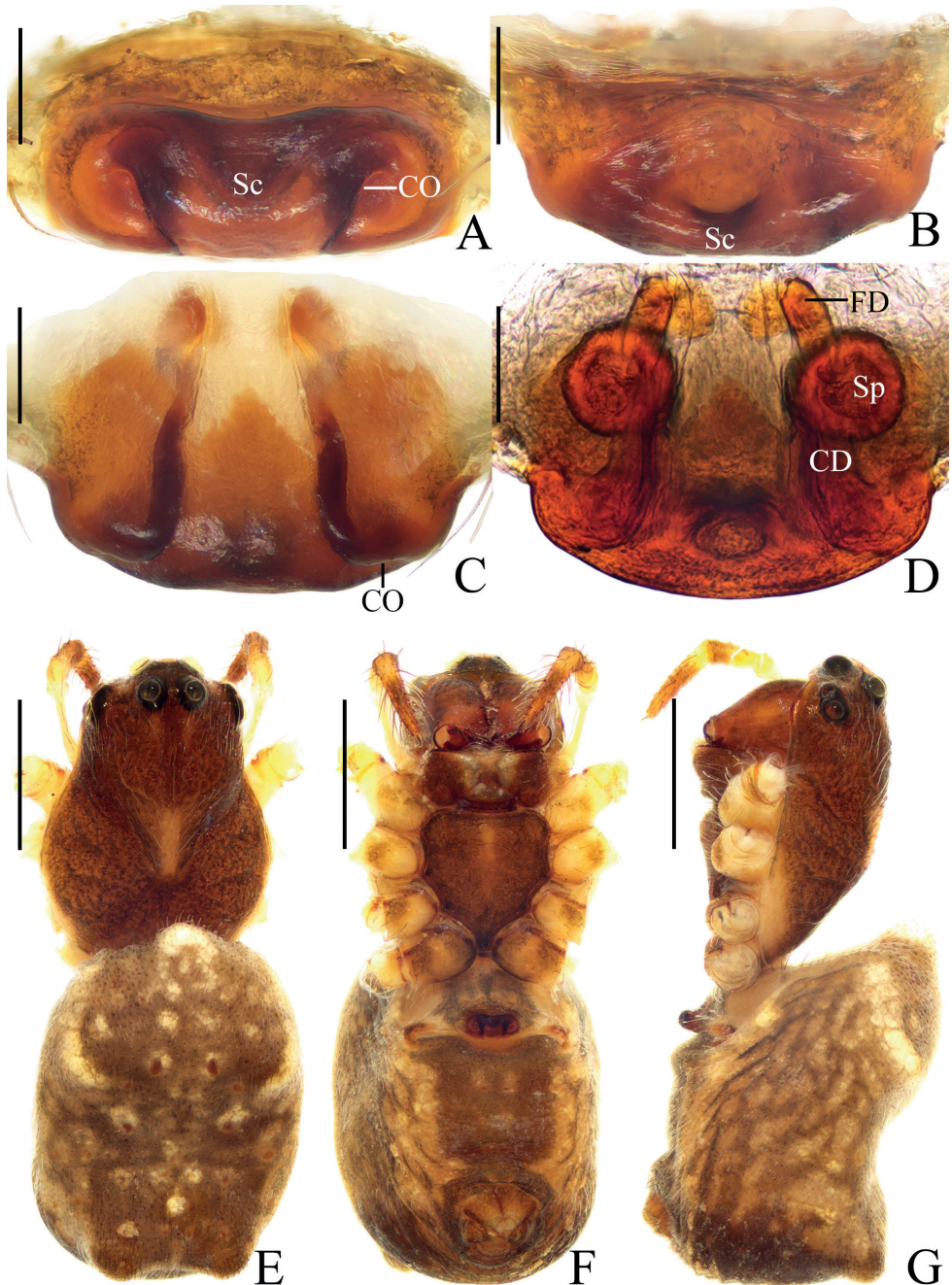


**Figure 3.** *Araneus ethani* sp. nov., female holotype **A** epigyne, ventral view **B** ibid., anterior view **C** ibid., posterior view **D** vulva, posterior view **E** habitus, dorsal view **F** ibid., ventral view **G** ibid., lateral view. Scale bars: 0.1 mm (**A-D**); 1 mm (**E-G**).

**Male.** Unknown.

**Variation.** Total length: ♀♀ 3.9–4.3.

**Distribution.** Vietnam (Ninh Binh and Hai Phong Provinces).

***Araneus liami* sp. nov.**

<https://zoobank.org/AE562B9E-1FE2-42EB-B469-7735C376C98F>

Figs 4, 5, 9I–L

**Type material.** *Holotype* ♂ (IZCAS-Ar44135), VIETNAM: Ninh Binh Province, Cuc Phuong National Park, disturbed forest (20°21.44'N, 105°34.21'E, ca 410 m), 5.II.2008, Dinh-Sac Pham leg. *Paratypes*: 1♀ (IZCAS-Ar44136), same locality and collector as holotype (20°20.23'N, 105°36.28'E, ca 390 m), 2.IV.2007; 1♀ (IZCAS-Ar44137), same locality and collector as holotype (20°20.23'N, 105°36.28'E, ca 390 m), 7.V.2007; 1♀ (IZCAS-Ar44138), same locality and collector as holotype (20°21.22'N, 105°37.03'E, ca 440 m), 5.VI.2007; 1♀ (IZCAS-Ar44139), same locality and collector as holotype, 5.IX.2007; 1♀ (IZCAS-Ar44140), same locality and collector as holotype (20°21.22'N, 105°37.03'E, ca 440 m), 5.IX.2007; 1♀ (IZCAS-Ar44141), same locality and collector as holotype (20°20.23'N, 105°36.28'E, ca 390 m), 3.XII.2007; 1♂ (IZCAS-Ar44142), same locality and collector as holotype (20°20.57'N, 105°36.02'E, ca 410 m), 5.II.2008; 1♀ (IZCAS-Ar44143), Vinh Phuc Province, Tam Dao National Park (21°29.23'N, 105°37.20'E, ca 870 m), 16.V.2007, Dinh-Sac Pham leg.; 1♀ (IZCAS-Ar44144), same locality and collector as IZCAS-Ar44143 (21°29.06'N, 105°37.42'E, ca 1060 m), 16.V.2007; 1♂ (IZCAS-Ar44145), same locality and collector as IZCAS-Ar44143 (21°31.57'N, 105°33.15'E, ca 1010 m), 18.IX.2007; 1♀ (IZCAS-Ar44146), same locality and collector as IZCAS-Ar44143 (21°31.57'N, 105°33.15'E, ca 1010 m), 14.I.2008; 1♀ (IZCAS-Ar44147), same locality and collector as IZCAS-Ar44143 (21°31.50'N, 105°33.43'E, ca 1060 m), 14.I.2008.

**Etymology.** The species name is a boy's name from Vietnam; noun (name) in genitive case.

**Diagnosis.** The new species resembles *A. bidentatus* Mi & Li, 2022 in appearance, but can be distinguished from it in having: 1) the copulatory openings situated on the anterior surface of the epigyne (Fig. 4B, C) vs at the lateral ends of the scape groove (Mi and Li 2022: fig. 3A, B); 2) the scape not grooved (Fig. 4A–D) vs grooved (Mi and Li 2022: fig. 3A, B); 3) the tibia of the male palp with three heavily sclerotized, denticulate protuberances (see arrows in Fig. 5A, E) vs with two protuberances (Mi and Li 2022: fig. 4A, B, E); 4) the median apophysis curved about 90° (Fig. 5A–D) vs curved about 20° (Mi and Li 2022: fig. 4A); and 5) the sternum paler in the middle (Fig. 4F) vs unicolor (Mi and Li 2022: fig. 3H).

**Description.** **Male** (holotype, Figs 4G, H, 5, 9I–L). Total length 2.80. Carapace 1.55 long, 1.20 wide. Abdomen 1.45 long, 1.10 wide. Clypeus 0.10 high. Eye sizes

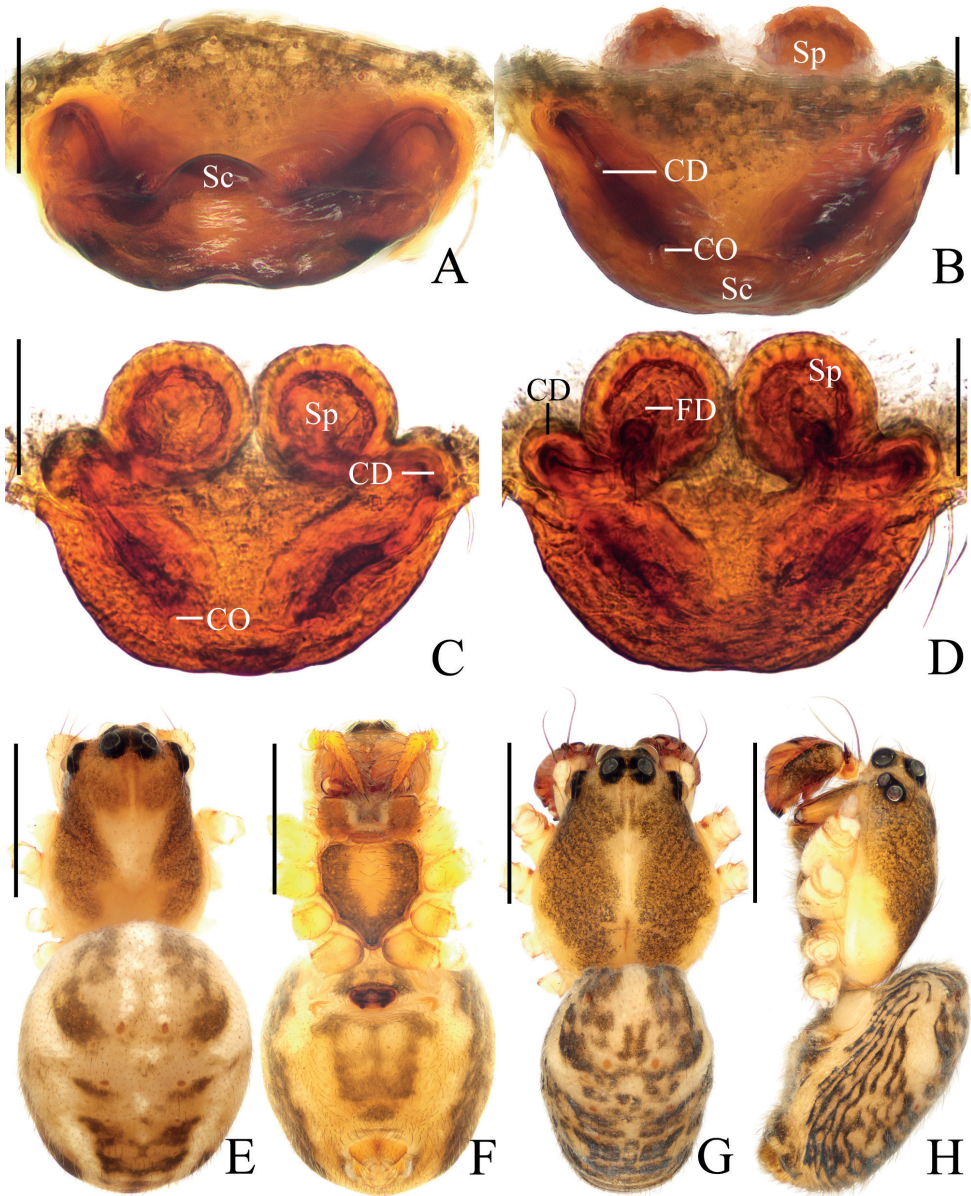


**Figure 4.** *Araneus liami* sp. nov. **A–F** female paratype IZCAS-Ar44147 **G, H** male holotype **A** epigyne, ventral view **B** *ibid.*, anterior view **C** vulva, anterior view **D** *ibid.*, posterior view **E** habitus, dorsal view **F** *ibid.*, ventral view **G** *ibid.*, dorsal view **H** *ibid.*, lateral view. Scale bars: 0.1 mm (**A–D**); 1 mm (**E–H**).

and interdistances: AME 0.13, ALE 0.08, PME 0.10, PLE 0.10, AME–AME 0.15, AME–ALE 0.10, PME–PME 0.10, PME–PLE 0.18, MOA length 0.33, anterior width 0.38, posterior width 0.33. Leg measurements: I 5.30 (1.60, 1.90, 1.15, 0.65),

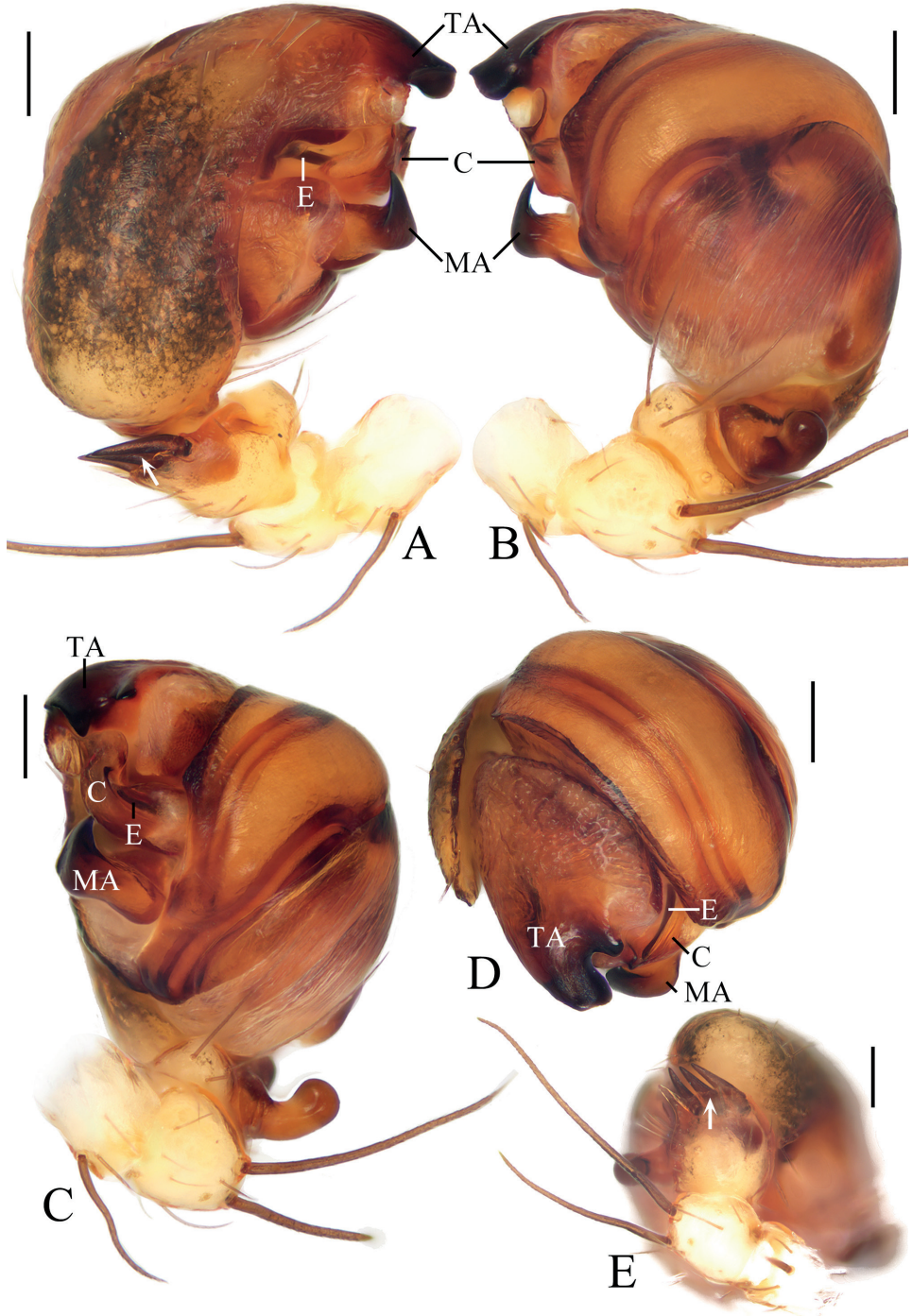


**Figure 5.** *Araneus liami* sp. nov., male holotype **A** left palp, prolateral view **B** ibid., retrolateral view **C** ibid., ventral view **D** ibid., apical view **E** tibia of left palp, dorsal view. Scale bars: 0.1 mm.

II 4.30 (1.40, 1.45, 0.90, 0.55), III 2.90 (0.95, 0.95, 0.55, 0.45), IV 4.00 (1.30, 1.35, 0.85, 0.50). Carapace dark brown, with yellow median patches anterior to and around fovea and on lateral edges of thoracic region; cervical groove inconspicuous. Chelicerae yellowish brown, with five promarginal and three retromarginal teeth. Endites and labium yellowish brown, paler distally. Sternum dark brown with wide yellow band. Legs brown with grayish-brown annuli; tibia I with 13 macrosetae; tibia II with 10 macrosetae; tibia III with six macrosetae; tibia IV with nine macrosetae. Abdomen elliptical,  $\sim 1.3\times$  longer than wide, covered with dark setae; dorsum yellow with grayish brown patches; venter yellow with irregular grayish brown markings. Spinnerets yellowish brown.

**Palp** (Fig. 5): with two patellar bristles; tibia  $\sim 3.0\times$  wider than long in retrolateral view, with three heavily sclerotized, denticulate protuberances and a short ventral projection; paracymbium finger-like; tegulum smoothly rounded in retrolateral view; median apophysis longer than wide, with pointed tip bent about  $90^\circ$ , distal end pointed toward the tip of cymbium in prolateral view; embolus thread-like; conductor curled, covering most of embolus in prolateral view; terminal apophysis about as long as bulb diameter, bifurcated distally.

**Female** (paratype IZCAS-Ar44147, Fig. 4A–F). Total length 3.10. Carapace 1.50 long, 1.10 wide. Abdomen 1.90 long, 1.50 wide. Clypeus 0.05 high. Eye sizes and interdistances: AME 0.13, ALE 0.08, PME 0.13, PLE 0.10, AME–AME 0.13, AME–ALE 0.13, PME–PME 0.13, PME–PLE 0.23, MOA length 0.38, anterior width 0.35, posterior width 0.35. Leg measurements: I 4.40 (1.30, 1.60, 0.95, 0.55), II 3.75 (1.15, 1.30, 0.80, 0.50), III 2.75 (0.90, 0.90, 0.50, 0.45), IV 3.90 (1.30, 1.30, 0.80, 0.50). Habitus similar to that of male, but a bit paler, yellow patches on carapace larger, and cervical groove more obvious.

**Epigyne** (Fig. 4A–D):  $\sim 2.0\times$  wider than long in ventral view; scape short, triangular, directed anteriorly,  $\sim 2.5\times$  wider than long in anterior view; copulatory openings hole-shaped, located on anterior surface; copulatory ducts longer than spermatheca diameter; spermathecae globular, touching each other.

**Variation.** Total length: ♂♂ 2.70–2.90; ♀♀ 2.90–3.45.

**Distribution.** Vietnam (Ninh Binh and Vinh Phuc provinces).

## Genus *Hyposinga* Ausserer, 1871

*Hyposinga* Ausserer, 1871: 823.

**Type species.** *Singa sanguinea* C.L. Koch, 1844.

**Comments.** The two new *Hyposinga* species in this paper differ greatly from the type species, *H. sanguinea*, in their copulatory organs. They are placed in *Hyposinga* provisionally because they show some common somatic characters, such as small total length, reflective carapace, and abdomen.

***Hypsosinga ryani* sp. nov.**

<https://zoobank.org/BD0AF38A-D617-4003-AA6D-37A121C784E6>

Figs 6, 7, 10A–D

**Type material.** *Holotype* ♂ (IZCAS-Ar44148), VIETNAM: Ha Tay Province, Ba Vi District, Tan Linh Village, 23.VII.2000, Dinh-Sac Pham leg. *Paratype*: 1 ♀ (IZCAS-Ar44149), Cao Bang Province, Sac Ha Village, 17.VII.2000, Dinh-Sac Pham leg.

**Etymology.** The species name is a boy's name from Vietnam; noun (name) in genitive case.

**Diagnosis.** The new species resembles *H. alboria* Yin, Wang, Xie & Peng, 1990 in appearance, but can be distinguished from the latter in having: 1) the epigyne lacking a septum (Fig. 6A) vs with a septum (Yin et al. 1990: fig. 182); 2) the spermathecae spaced apart by about one radius (Fig. 6B, C) vs about half of the radius (Yin et al. 1990: fig. 183); 3) the ventral surface of the epigyne smooth (Fig. 6A) vs concave (Yin et al. 1990: fig. 182); 4) the male palpal tibia palmate (Fig. 7A–C) vs not palmate; 5) the median apophysis stout (Fig. 7A, C, D) vs with a long, slender tip (Yin et al. 1990: figs 184–186); 6) the embolus short and straight (Fig. 7A, C, D) vs extremely long and curved (Yin et al. 1990: fig. 184); and 7) the tegular extension lacking (Fig. 7B–D) vs present (Yin et al. 1990: fig. 185).

**Description. Male** (holotype, Figs 6F, G, 7, 10A–D). Total length 2.50. Carapace 1.15 long, 0.95 wide. Abdomen 1.40 long, 0.85 wide. Clypeus 0.20 high. Eye sizes and interdistances: AME 0.06, ALE 0.05, PME 0.10, PLE 0.06, AME–AME 0.08, AME–ALE 0.13, PME–PME 0.08, PME–PLE 0.15, MOA length 0.23, anterior width 0.20, posterior width 0.25. Leg measurements: I 3.80 (1.15, 1.30, 0.85, 0.50), II 3.45 (1.05, 1.20, 0.75, 0.45), III 2.40 (0.80, 0.75, 0.50, 0.35), IV 3.50 (1.15, 1.15, 0.75, 0.45). Carapace reddish brown, with pale stripe before fovea; cervical groove inconspicuous. Chelicerae yellowish brown; four promarginal and two retromarginal teeth. Endites and labium yellowish brown at base, paler distally. Sternum dark brown. Legs yellow to yellowish brown; leg I and II with brown annuli; tibia I with seven macrosetae; tibia II with three macrosetae; tibia III with seven macrosetae; tibia IV with two macrosetae. Abdomen  $\sim 1.6\times$  longer than wide, with a pair of lateral humps posteriorly; dorsum reddish brown, with indistinct longitudinal pale patch and three pairs of pale spots; venter yellow to yellowish brown, with darker patches. Spinnerets yellowish brown.

**Palp** (Fig. 7): with a single patellar bristle; tibia palmate, with bifurcated protuberance and four denticles (see white arrows in Fig. 7A, B, E); cymbium  $\sim 1.25\times$  wider than long and covers most part of bulb in prolateral view, with dorsal protuberance at base (see black arrows in Fig. 7A, B); median apophysis elliptical at base, with two processes in apical view; tegulum smoothly rounded and lacking tegular extension in retrolateral view; embolus tapered, triangular in prolateral view, slightly curved at tip in ventral view; conductor broad at base, tongue-shaped distally in apical view; terminal apophysis membranous, narrow lamellar, about subequal in length to embolus.

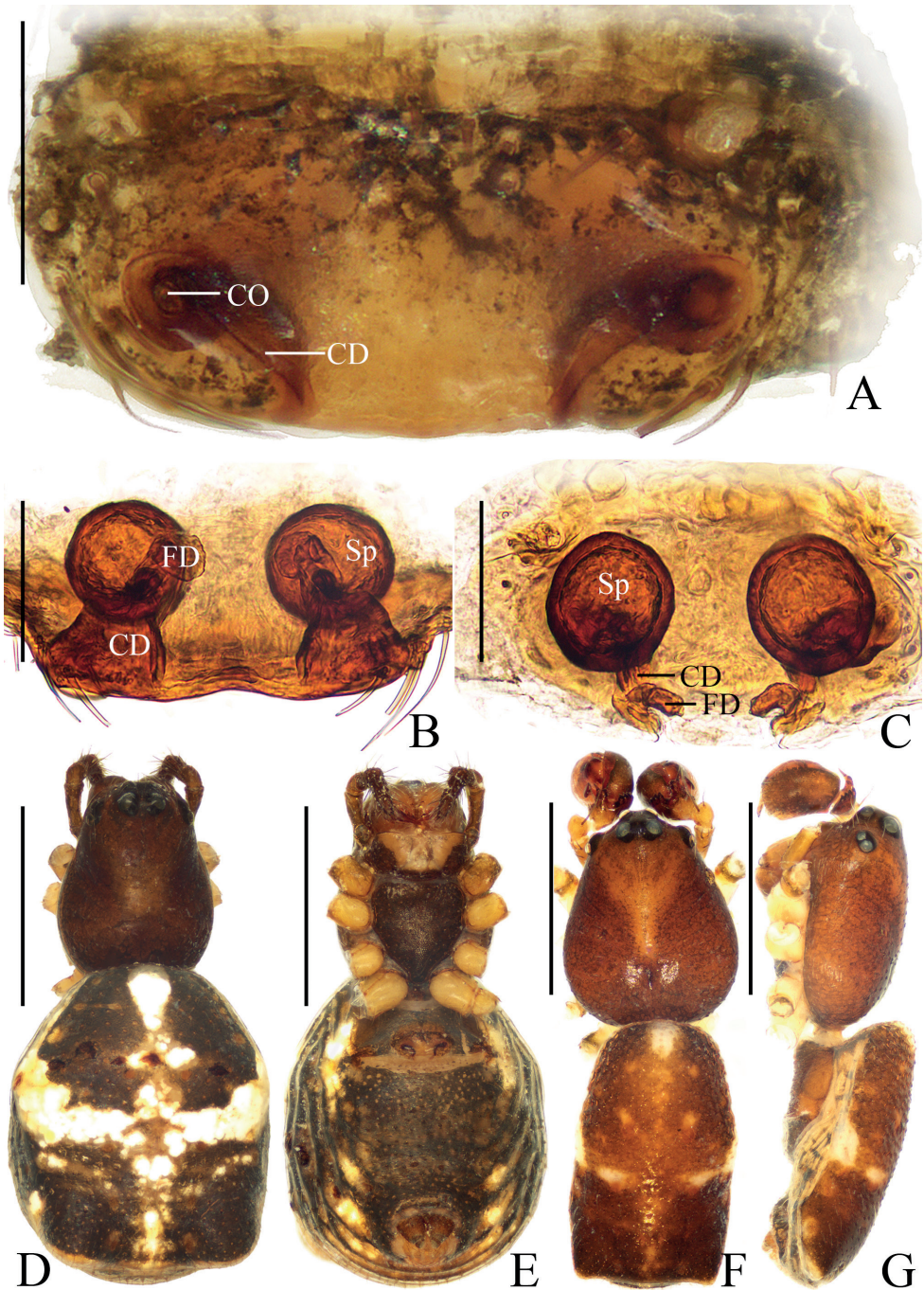


**Figure 6.** *Hyposinga ryani* sp. nov. **A–E** female paratype IZCAS-Ar44149 **F, G** male holotype **A** epigyne, ventral view **B** vulva, posterior view **C** ibid., dorsal view **D** habitus, dorsal view **E** ibid., ventral view **F** ibid., dorsal view **G** ibid., lateral view. Scale bars: 0.1 mm (**A–C**); 1 mm (**D–G**).

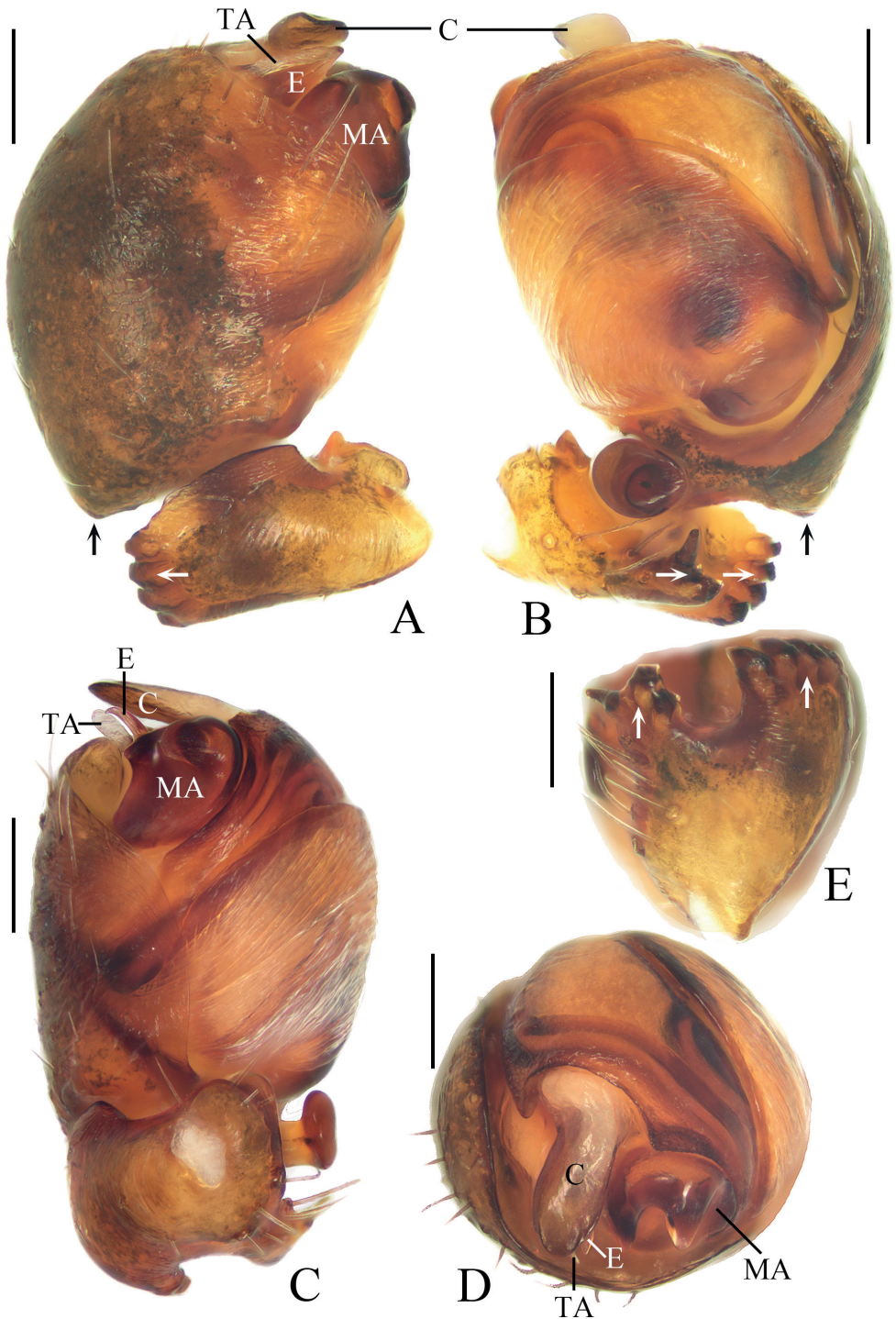


**Figure 7.** *Hyposisinga ryani* sp. nov., male holotype **A** left palp, prolateral view **B** *ibid.*, retrolateral view **C** *ibid.*, ventral view **D** *ibid.*, apical view **E** tibia of left palp, dorsal view. Scale bars: 0.1 mm.

**Female** (paratype IZCAS-Ar44149, Fig. 6A–E). Total length 2.55. Carapace 1.05 long, 0.80 wide. Abdomen 1.65 long, 1.35 wide. Clypeus 0.10 high. Eye sizes and interdistances: AME 0.06, ALE 0.05, PME 0.10, PLE 0.08, AME–AME 0.08, AME–ALE 0.13, PME–PME 0.08, PME–PLE 0.13, MOA length 0.20, anterior width 0.18, posterior width 0.23. Leg measurements: I 2.95 (0.90, 1.05, 0.60, 0.40), II 2.65 (0.85, 0.85, 0.60, 0.35), III 1.80 (0.60, 0.60, 0.35, 0.25), IV 2.90 (0.95, 1.00, 0.60, 0.35). Habitus similar to that of male but darker, and pale patches on dorsum of abdomen more distinct.

**Epigyne** (Fig. 6A–C):  $\sim 2.3\times$  wider than long in ventral view, lacking scape; copulatory openings rounded, situated at the lateral side of ventral surface; copulatory ducts about of equal length to spermatheca diameter; spermathecae globular, about one radius apart.

**Distribution.** Vietnam (Ha Tay and Cao Bang provinces).

***Hypsosinga zioni* sp. nov.**

<https://zoobank.org/456B12BF-5FE9-4061-B02A-14F973EB17AE>

Figs 8, 10E–H

**Type material.** *Holotype* ♀ (IZCAS-Ar44150), VIETNAM: Cao Bang Province, Sac Ha Village, 17.VII.2000, Dinh-Sac Pham leg. *Paratypes*: 1 ♀ (IZCAS-Ar44151), Ha Giang Province, Gao Bao Village, 9.XII.2000, Dinh-Sac Pham leg.; 1 ♀ (IZCAS-Ar44152), Cao Bang Province, Sac Ha Village, 17.VII.2000, Dinh-Sac Pham leg.

**Etymology.** The species name is a boy's name from Vietnam; noun (name) in genitive case.

**Diagnosis.** The new species resembles the female of *H. ryani* sp. nov. in appearance, but it can be distinguished from the latter in having: 1) the epigyne with scape (Fig. 8A–D) vs scape lacking (Fig. 6A); 2) the copulatory openings situated on the posterior surface of the epigyne (Fig. 8C, D) vs on the ventral surface (Fig. 6A); 3) the spermathecae touching each other (Fig. 8D) vs apart (Fig. 6B, C); and 4) dorsum of abdomen with three transverse bands (Fig. 8E) vs only one band (Fig. 6D).

**Description. Female** (holotype, Figs 8, 10E–H). Total length 2.65. Carapace 1.10 long, 0.80 wide. Abdomen 1.70 long, 1.40 wide. Clypeus 0.13 high. Eye sizes and interdistances: AME 0.06, ALE 0.06, PME 0.10, PLE 0.08, AME–AME 0.10, AME–ALE 0.13, PME–PME 0.10, PME–PLE 0.15, MOA length 0.23, anterior width 0.20, posterior width 0.25. Leg measurements: I 3.05 (0.95, 1.05, 0.65, 0.40), II 2.70 (0.85, 0.90, 0.55, 0.40), III 1.95 (0.65, 0.65, 0.35, 0.30), IV 3.00 (1.00, 1.00, 0.60, 0.40). Carapace reddish brown; cervical groove distinct; foeva depressed. Chelicerae yellowish brown; four promarginal and two retromarginal teeth. Endites and labium dark brown at base, and paler distally. Sternum dark brown, with dark setae. Legs yellowish brown; leg III and IV with grayish brown annuli. Abdomen oval, rounded anteriorly, with a pair of lateral humps posteriorly; dorsum yellowish brown with a longitudinal median white band and three transverse white bands; also with a pair of lateral white patches; venter dark brown, with lateral pale patches. Spinnerets yellow.

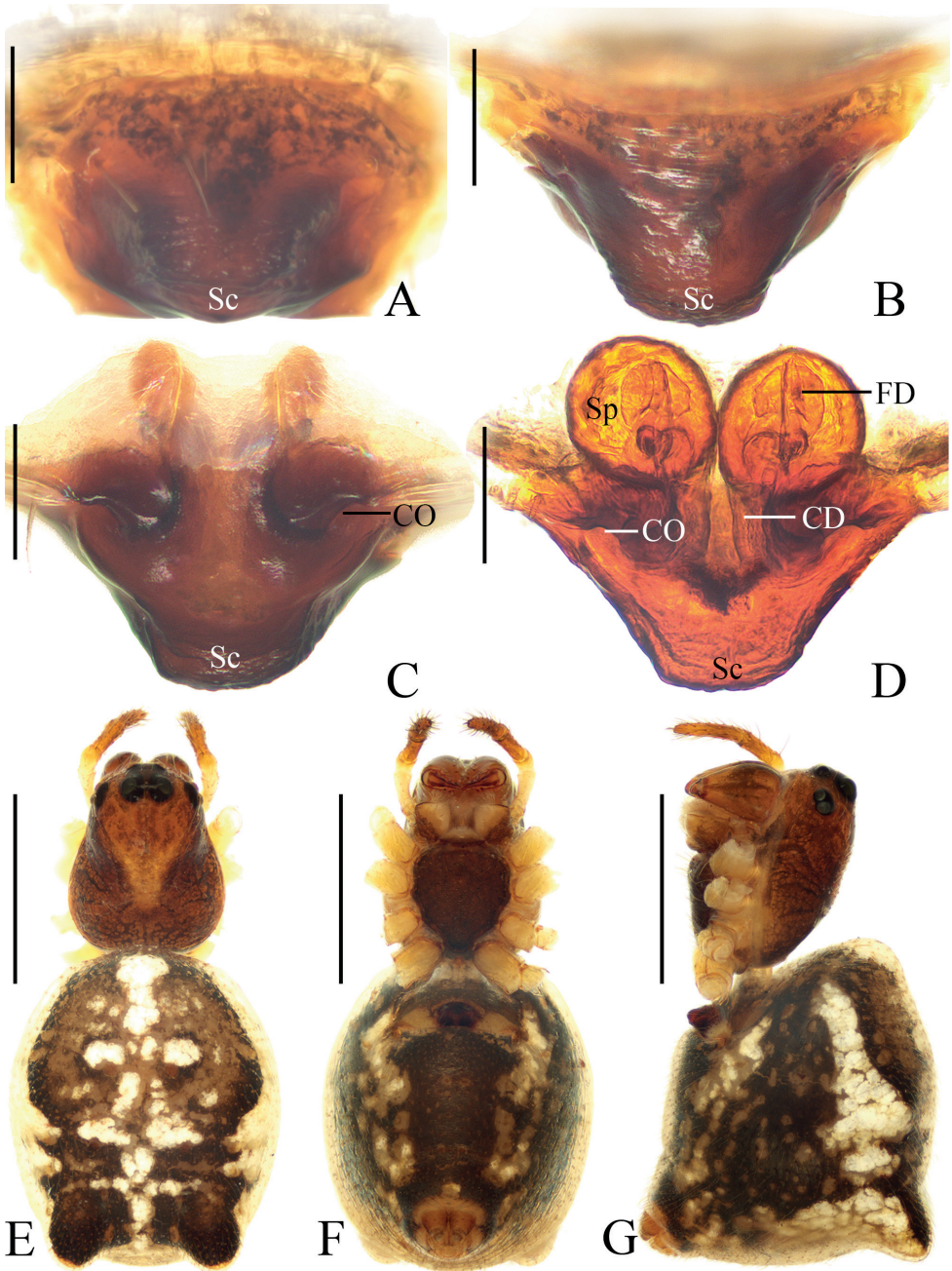


**Figure 8.** *Hypsozinga zioni* sp. nov., female holotype **A** epigyne, ventral view **B** ibid., anterior view **C** ibid., posterior view **D** vulva, posterior view **E** habitus, dorsal view **F** ibid., ventral view **G** ibid., lateral view. Scale bars: 0.1 mm (A–D); 1 mm (E–G).

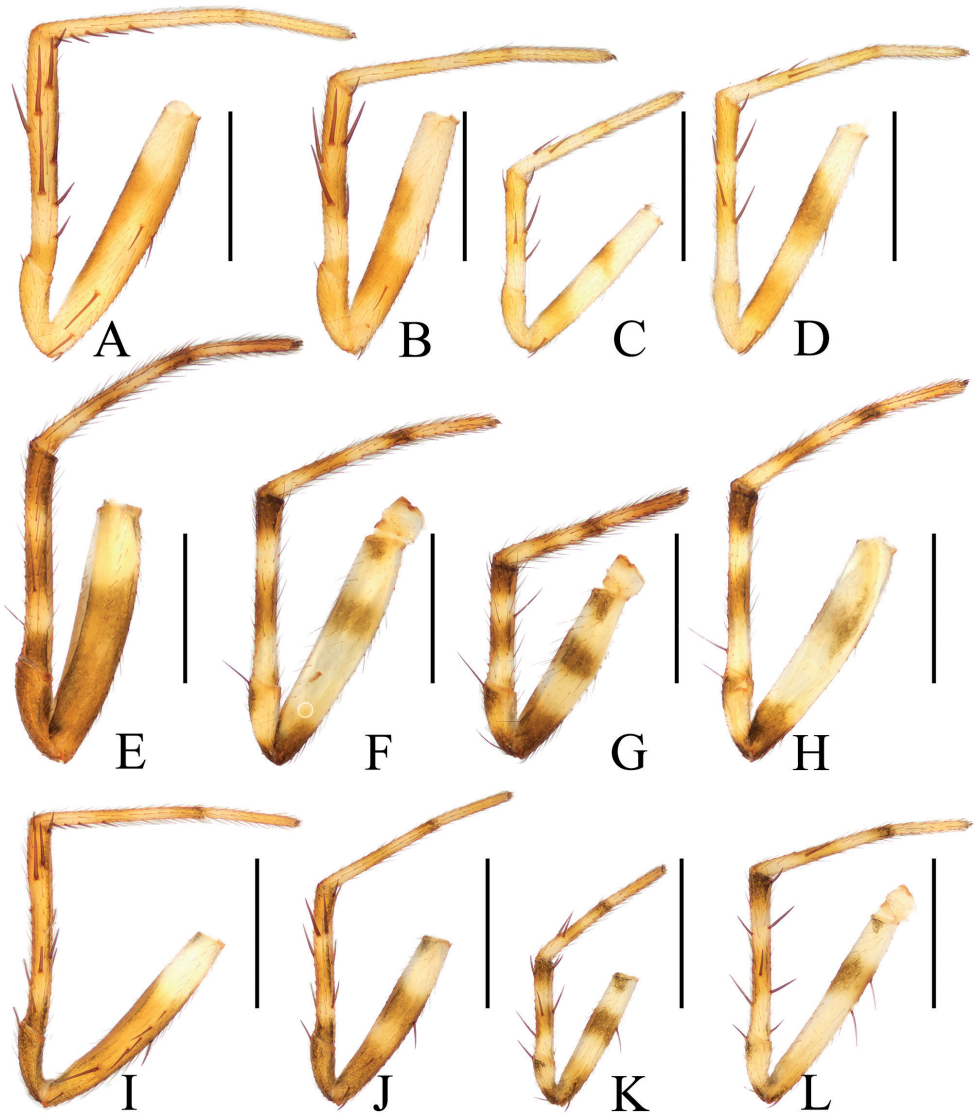


**Figure 9.** Legs of the new species, holotypes, prolateral view **A–D** *Araneus eugenei* sp. nov. **E–H** *Araneus ethani* sp. nov. **I–L** *Araneus liami* sp. nov. **A, E, I** legs I **B, F, J** legs II **C, G, K** legs III **D, H, L** legs IV. Scale bars: 1 mm.

*Epigyne* (Fig. 8A–D): scape short thick,  $\sim 2.0\times$  wider than long in posterior view; copulatory openings elliptical, situated on lateral edge of posterior surface; copulatory ducts slightly longer than spermatheca diameter, curved about  $90^\circ$ ; spermathecae globular, touching each other.

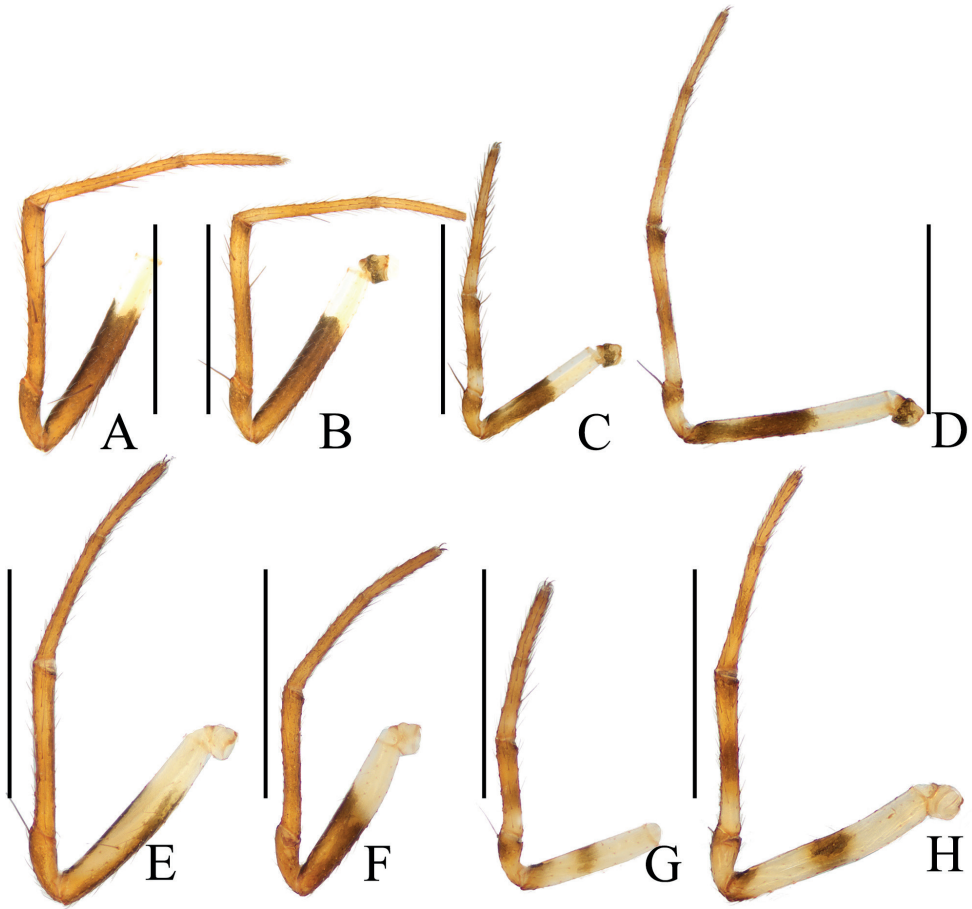


**Figure 10.** Legs of the new species, holotypes, prolateral view **A–D** *Hyposisinga ryani* sp. nov. **E–F** *Hyposisinga zioni* sp. nov. **A, E** legs I **B, F** legs II **C, G** legs III **D, H** legs IV. Scale bars: 1 mm.

**Male.** Unknown.

**Variation.** Total length: ♀♀ 2.60–2.75.

**Distribution.** Vietnam (Cao Bang and Ha Giang provinces).

## Acknowledgements

The manuscript benefitted greatly from comments by Zhiyuan Yao (Shenyang, China), Yuri M. Marusik (Magadan, Russia), Mikhail M. Omelko (Vladivostok, Russia), and an anonymous referee. Danni Sherwood (London, UK) and Robert Forsyth (Kamloops, Canada) checked the English. This research was supported by the Science and Technology Project Foundation of Guizhou Province ([2020]1Z014), the National Natural Science Foundation of China (NSFC-31660609, 32200369), and the Key Laboratory Project of Guizhou Province ([2020]2003).

## References

- Ausserer A (1871) Neue Radspinnen. Verhandlungen der Kaiserlich-Königlichen Zoologisch-Botanischen Gesellschaft in Wien 21: 815–832. [pl. 5.]
- Clerck C (1757) Aranei Svecici. Svenska Spindlar, uti Sina Hufvud-Slägter Indelte Samt Under Några och Sextio Särskildte Arter Beskrefne och med Illuminerade Figurer Uplyste. Laurentius Salvius, Stockholmiae, 154 pp. <https://doi.org/10.5962/bhl.title.119890>
- Lin Y, Li S, Pham D-S (2023) Taxonomic notes on some spider species (Arachnida: Araneae) from China and Vietnam. *Zoological Systematics* 48(1): 1–99. <https://doi.org/10.1186/zs.2023101>
- Mi X, Li S (2022) On eleven new species of the orb-weaver spider genus *Araneus* Clerck, 1757 (Araneae, Araneidae) from Xishuangbanna, Yunnan, China. *ZooKeys* 1137: 75–108. <https://doi.org/10.3897/zookeys.1137.96306>
- Ono H, Thinh TH, Pham D-S (2012) Spiders (Arachnida, Araneae) recorded from Vietnam, 1837–2011. *Memoirs of the National Museum of Nature and Science Tokyo* 48: 1–37.
- Pham D-S, Xu X, Li S (2007) A preliminary note on spider fauna of Vietnam (Arachnida: Araneae). *Acta Arachnologica Sinica* 16: 121–128.
- Wang C, Li S, Pham D-S (2023) Thirteen species of jumping spiders from northern Vietnam (Araneae, Salticidae). *ZooKeys* 1148: 119–165. <https://doi.org/10.3897/zookeys.1148.98271>
- Yin C, Wang J, Xie L, Peng X (1990) New and newly recorded species of the spiders of family Araneidae from China (Arachnida, Araneae). *Spiders in China: One Hundred New and Newly Recorded Species of the Families Araneidae and Agelenidae*. Hunan Normal University Press, Changsha, 171 pp.



# Three new species of *Atkinsoniella* (Arthropoda, Insecta, Hemiptera, Cicadellidae, Cicadellinae) from China, with an updated checklist to the known species worldwide

Yan Jiang<sup>1</sup>, Xiao-fei Yu<sup>1,2</sup>, Mao-fa Yang<sup>1,2</sup>

**1** Institute of Entomology, Guizhou Provincial Key Laboratory for Agricultural Pest Management of the Mountainous Region, Guizhou University, Guiyang 550025, China **2** College of Tobacco Sciences, Guizhou University, Guiyang 550025, China

Corresponding author: Mao-Fa Yang ([gdgdly@126.com](mailto:gdgdly@126.com))

Academic editor: J. Adilson Pinedo-Escatel | Received 28 January 2023 | Accepted 14 April 2023 | Published 11 May 2023

<https://zoobank.org/844E6494-F722-4F3C-B363-61931F91CBCD>

**Citation:** Jiang Y, Yu X-f, Yang M-f (2023) Three new species of *Atkinsoniella* (Arthropoda, Insecta, Hemiptera, Cicadellidae, Cicadellinae) from China, with an updated checklist to the known species worldwide. ZooKeys 1161: 89–115. <https://doi.org/10.3897/zookeys.1161.101062>

## Abstract

The sharpshooter genus *Atkinsoniella* Distant, 1908 includes 99 valid species worldwide. Here, three new species from China are described and illustrated: *Atkinsoniella stenopyga*, *A. wangi*, and *A. yingjiangensis* spp. nov. An updated checklist of the known *Atkinsoniella* species worldwide based on the data of previous literature and studied materials is also provided. All the type specimens of three new species are deposited at the Institute of Entomology, Guizhou University, Guiyang, China.

## Keywords

Auchenorrhyncha, leafhopper, morphology, taxonomy, Tibet, Yunnan

## Introduction

The genus *Atkinsoniella* is a relatively large genus of the subfamily Cicadellinae. It was established by Distant (1908) with two new species: *A. decisa* (type species) and *A. maculata*. Young (1986) systematically revised *Atkinsoniella*, proposed 15 new combinations and 13 synonyms, described 10 new species, and confirmed 26 valid species of this genus. Thereafter, new species were described successively.

Feng and Zhang (2015) provided a checklist of 75 known species worldwide and described two new species. Yang et al. (2017) conducted a systematic morphological study of 88 *Atkinsoniella* species from China, including 33 new species, two Chinese new records, 12 new synonyms, and proposed *Curvufacies* Kuoh, 1993 as a new synonym of *Atkinsoniella*. Subsequently, 2 new species from China and Pakistan were described (Naveed and Zhang 2018; Jiang et al. 2022).

To date, 99 valid species were described worldwide, of which 89 species occurred in China, and a few were scattered in Bay of Bengal, Bhutan, India, Indonesia, Kingdom of Bhutan, Laos, Malay Islands, Malaysia, Myanmar, Nepal, Pakistan, Philippines, Thailand, and Vietnam (Feng and Zhang 2015; Yang et al. 2017; Naveed and Zhang 2018; Jiang et al. 2022). In this study, the description, male genitalia and habitus photos of three new species, *A. stenopyga*, *A. wangi*, and *A. yingjiangensis* spp. nov. from Qinghai–Tibet Plateau (Tibet Autonomous Region) and Yunnan-Guizhou Plateau (Yunnan Province) of China are provided. The checklist of all known *Atkinsoniella* species worldwide and the three new species is updated.

## Material and methods

### Morphology

The specimens were collected by sweeping (27–35 sweeps per collecting event) on shrubs and weeds using 2.5 m insect sweep nets on day-light and off-set sun by using a 500W high-pressure mercury lamps; all materials were preserved in absolute ethanol and stored at -20 °C in the laboratory. The abdomens of specimens were detached and soaked in 10% NaOH solution, boiled for 1–3 min, rinsed with water to remove traces of NaOH, and transferred to glycerol for further dissection, photography and preservation. The habitus and male genitalia were photographed using a KEYENCE VHX-6000 digital camera and a Nikon Eclipse Ni-E microscope, respectively. Adobe Photoshop 2020 was used to edit compiled photos. The length of the body was measured from the vertex to the rear of the forewings using a KEYENCE VHX-6000 digital camera. The morphological terminology is adapted from Young (1968, 1986) and Yang et al. (2017). The holotype and paratypes were deposited at the Institute of Entomology, Guizhou University, Guiyang, China (GUGC).

## Results

### *Atkinsoniella* Distant, 1908

*Atkinsoniella* Distant, 1908: 235.

*Soibanga* Distant, 1908: 236.

*Curvufacies* Kuoh, 1993: 38.

**Type species.** *Atkinsoniella decisa* Distant, 1908.

**Distribution.** Palaearctic, Oriental.

***Atkinsoniella stenopyga* Jiang & Yang, sp. nov.**

<https://zoobank.org/325305A3-840F-480C-B5CF-1F5FC86957C5>

Figs 1A–D, 2A–F

**Description.** Crown and thorax canary yellow and greyish white in dorsal view; a small subcircular black spot at apex of head and basal margin medially, and interocular width 2× wider than long; eyes fuscus; ocelli greyish white with narrow black border; forewing light orange; face off-white, frontoclypeus median with a broad yellowish white longitudinal; thorax and abdomen yellowish white in ventral view; legs orangish with pretarsi black or dark brown.

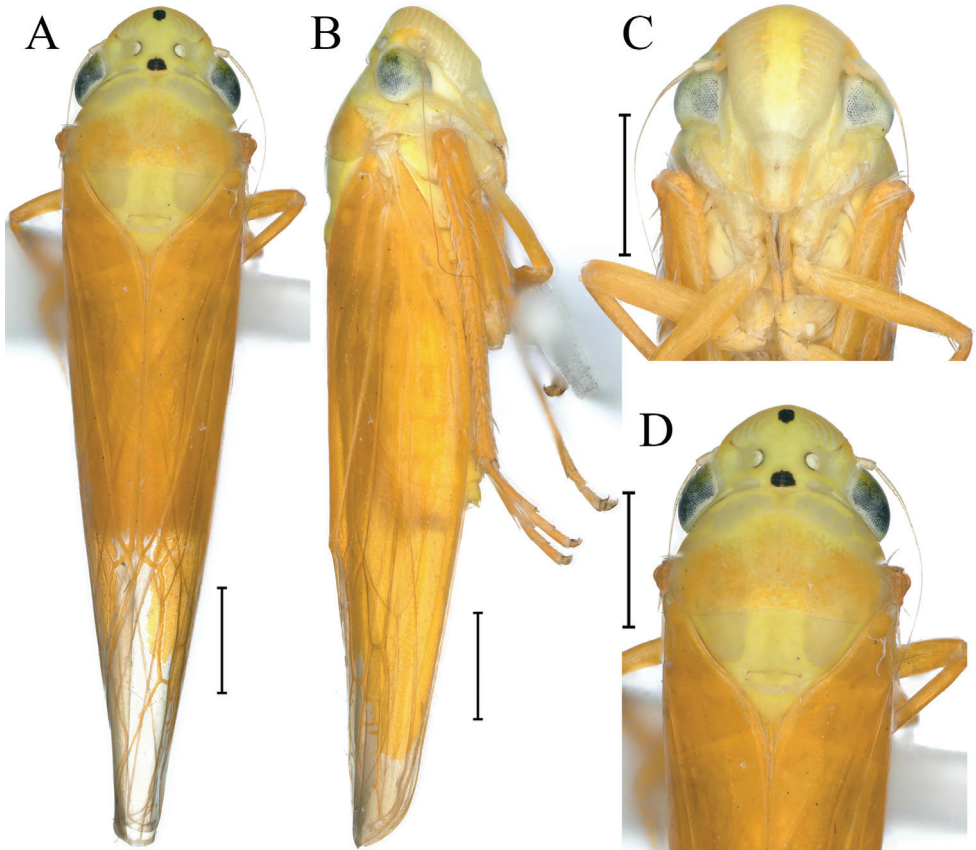


**Figure 1.** External features of *Atkinsoniella stenopyga* Jiang & Yang, sp. nov., male holotype **A** habitus, dorsal view **B** habitus, lateral view **C** face, anterior view **D** head and pronotum, dorsal view. Scale bars: 1000  $\mu\text{m}$ .

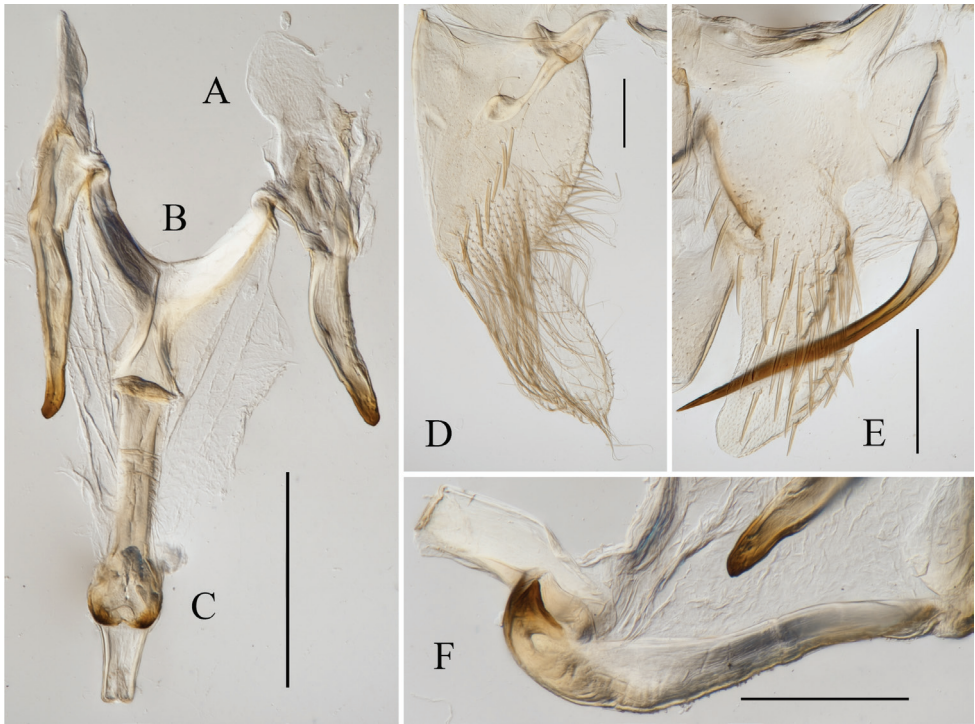


**Figure 2.** Male genitalia of *Atkinsoniella stenopyga* Jiang & Yang, sp. nov. **A** style **B** connective **C** aedeagus and paraphysis, ventral view **D** subgenital plate, ventral view **E** pygofer, lateral view **F** aedeagus and paraphysis, lateral view. Scale bars: 200  $\mu$ m.

Anterior margin of crown broadly rounded and convex, and median length of crown shorter than interocular width. Ocelli nearest to midline and posterior margin than eyes, lateral area concave, each ocellus further from the other than to the adjacent eye. Face with frontoclypeus flat medially; muscle impressions distinct and extend to the tip of crown; clypeal sulcus blurred in the median; anteclypeus longitudinally gibbous. Pronotum wider than head, anterior margin arcuately convex, posterior margin with medially concave. Scutellum with medial transverse depression. Forewings with distinct apical membranous area, base of second cells more proximal than third cells transversely.

Male pygofer narrowly rounded posteriorly and convex dorsally, posterior half long scoop-shaped with macrosetae; pygofer processes slender and strongly sclerosed, base broad with microsetae; bending dorsad from basal one-third and then extending straightly, tip acute and exceeding dorsal margin posteriorly of pygofer. Subgenital plates in ventral view convex and short with one row of macrosetae uniseriate obliquely, long dense mid microsetae, and posterior half with long and short microsetae dispersedly with apex rounded. Aedeagus stubby and straight, with posterior margin truncate and dorsal margin concave subbasally, one protuberance at base ventrally articulating with paraphysis, and concave at the articulation with paraphysis apically; paraphysis

long and thick, apical portion intumescent, apex bifurcated and articulating with aedeagus. Connective Y-shaped; style slender, with tip tapered and curved.

**Etymology.** The specific epithet is the combined noun of *stenos* and *tail* from Greek, *stenopyga*, referring a narrow pygofer shape.

**Measurement.** Length of male 7.8–8.0 mm.

**Material examined.** *Holotype*: ♂, Motuo, Tibet, CHINA, 18 August 2020, coll. Xian-Yi Wang. *Paratype*, 1♂, same data as holotype.

**Remarks.** This species is similar to *A. thaloidea* Young, 1986, *A. flavipenna* Li & Wang, 1992, *A. uniguttata* Li, 1993, and *A. bowa* Yang, Meng & Li, 2017 in appearance, but can be easily differentiated from these species by the following characteristics: (1) pygofer slender; (2) aedeagus stubby with posterior margin truncate; and (3) two pointed dentate protrusions at the apex of the paraphysis incurred dorsally and embracing.

**Distribution.** China (Tibet).

***Atkinsoniella wangi* Jiang & Yang, sp. nov.**

<https://zoobank.org/89195CDF-6EDC-4BF0-AEDB-A7508F9A9795>

Figs 3A–D, 4A–F

**Description.** Crown, thorax and forewings orange in dorsal view; crown with a black spot at anterior margin medially and a smaller black spot at posterior margin medially; eyes off-white or dark brown; ocelli off-white with black border; forewings orange, with apical membranous area darker; face, thorax and abdomen in ventral view, legs orange.

Crown with anterior margin rounded prominently, and interocular width 2× wider than long. Ocelli nearest to midline and posterior margin than eyes, lateral area concave, each ocellus slightly further from the other one than to the adjacent eye. Face with a nodular protrusion in the center, frontoclypeus flat medially, muscle impressions distinct and extending to the tip of crown, clypeal sulcus distinct medially. Pronotum broader than head, anterior margin protruding roundly, posterior margin with medially concave. Scutellum convex anterior and posterior to transverse depression, with transverse depression arcuate, a large black spot near each basal angle in some specimens. Forewings with four apical cells, the base of the second cells more basal than third cells transversely, apical membranous area distinct.

Male pygofer slender, posterior portion tilted dorsad and posterior margin round, posterior half with macrosetae; pygofer process lamellate, base with several macrosetae, bending dorsad from basal one-third, posterior one-third portion lamellate broadly and tortile backward and apex acute. Subgenital plates broad at base, posterior half narrow and bent dorsally, one row of macrosetae uniseriate obliquely in the median, lateral area with long dense microsetae, apical half with short microsetae dispersedly. Aedeagus broad at base, posterior half constricted and tilted dorsad, tip swordlike, ventral margin protuberant at the articulation with the tip of paraphysis and concave subbasally; paraphysis dilated apically and constricted subapically, apex bifurcated and articulating with aedeagus. Connective V-shaped. Style wide at base and tapered at tip, apex acute.

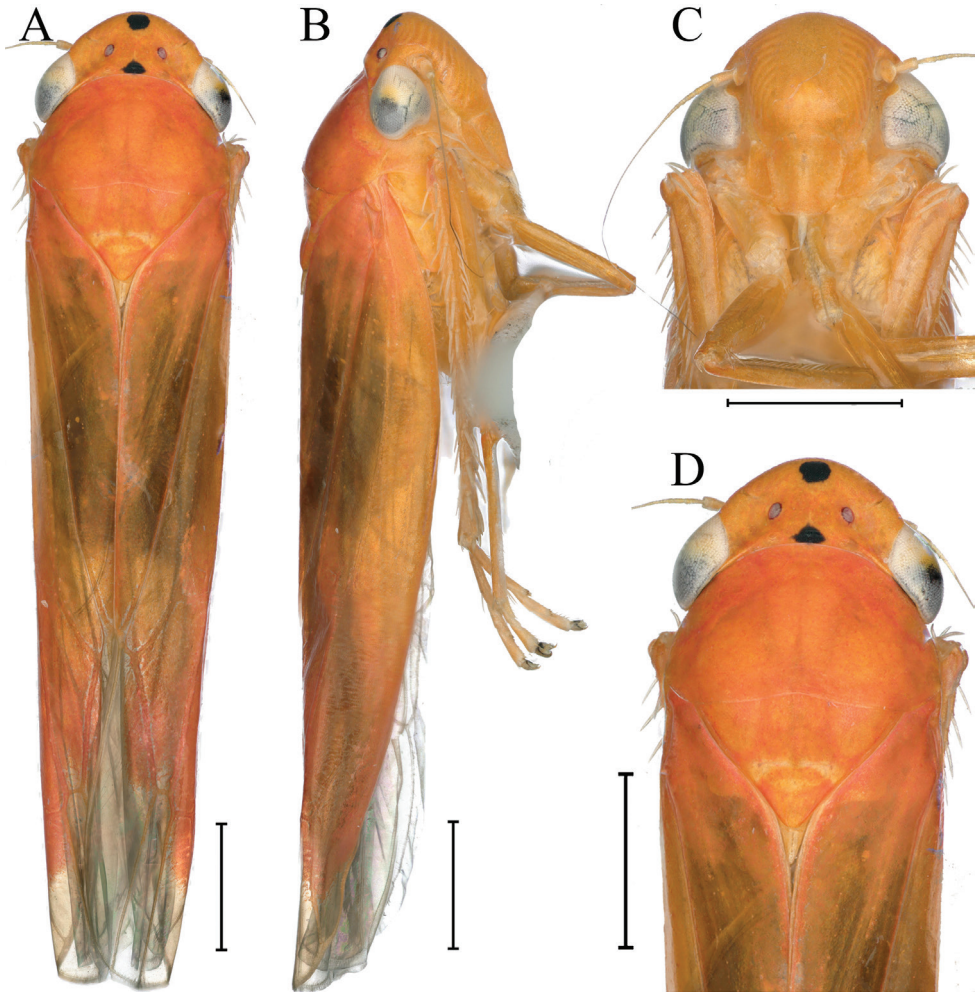


**Figure 3.** External features of *Atkinsoniella wangi* Jiang & Yang, sp. nov., male holotype **A** habitus, dorsal view **B** habitus, lateral view **C** face, anterior view **D** head and pronotum, dorsal view. Scale bars: 1000  $\mu$ m.

**Etymology.** The new species is named after the family name of collector Xian-Yi Wang.

**Measurement.** Length of male 7.9–8.0 mm.

**Material examined.** *Holotype*: ♂, Tongmai, Tibet, CHINA, 18 August 2020, coll. Xian-Yi Wang. *Paratypes*, 1♂ (light trapped) + 11♂♂, same data as holotype; 1♂, Tongmai, Tibet, China, 19 August 2020, light trapped, coll. Xian-Yi Wang.

**Remarks.** This species is similar to *A. curvata* Zhang & Kuoh in appearance and male genitalia, but can be distinguished from the latter by the following characteristics: (1) crown with a black spot in the median of the anterior margin, and the smaller black spot at the basal margin medially narrower than the width between the ocelli, but the latter only with a large V-shaped black spot below the ocelli; (2) pygofer of the

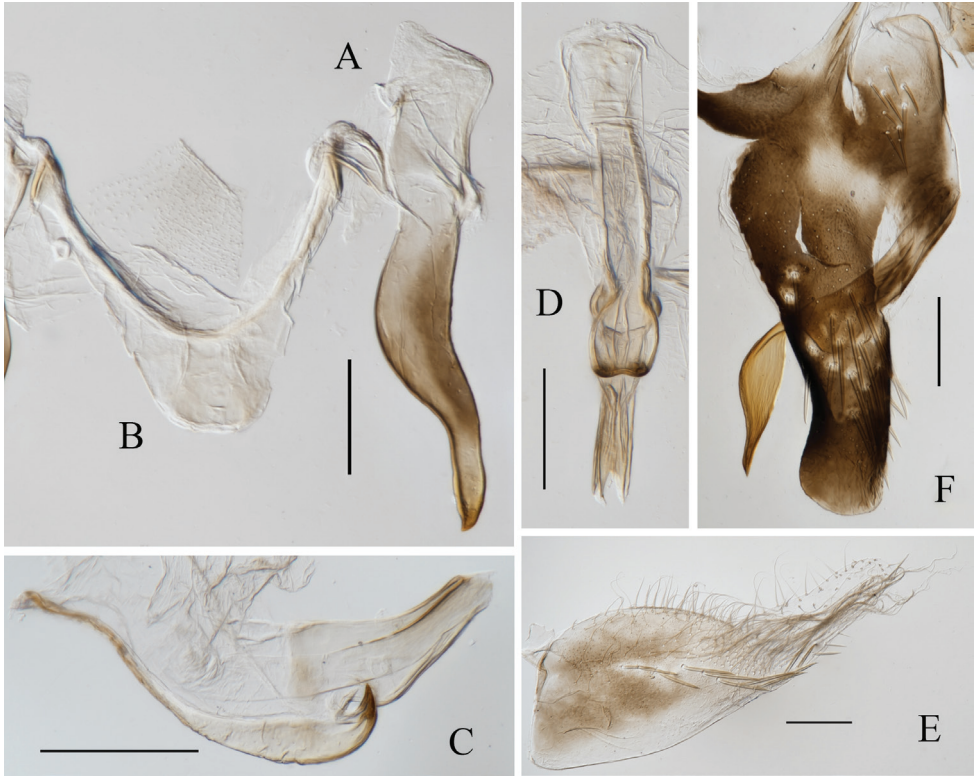


**Figure 4.** Male genitalia of *Atkinsoniella wangi* Jiang & Yang, sp. nov. **A** style **B** connective **C** aedeagus and paraphysis, lateral view **D** aedeagus and paraphysis, ventral view **E** subgenital plate, ventral view **F** pygofer, lateral view. Scale bars: 200  $\mu$ m.

new species slender overall, with posterior margin rounded, while pygofer of the latter slender at apical one-third, with the posterior margin truncate; (3) aedeagus of the new species tilted dorsally at the posterior half, while aedeagus of the latter straight overall; and (4) connective of the new species V-shaped, but connective of the latter Y-shaped.

**Distribution.** China (Tibet).

***Atkinsoniella yingjiangensis* Jiang & Yang, sp. nov.**

<https://zoobank.org/6FD2EA20-B2DA-442B-B50E-A35F91051243>

Figs 5A–D, 6A–G

**Description.** Head and thorax dark orange in dorsal view; crown with a black spot at the anterior margin medially, basal margin with a black spot below each ocellus, and lateral margin with a black spot anterior to each antennal ledge; eyes dark brown; ocelli gray; pronotum with two small black spots abreast in the center, and posterior area with two large black spots transversely; scutellum with a large triangular black spot at

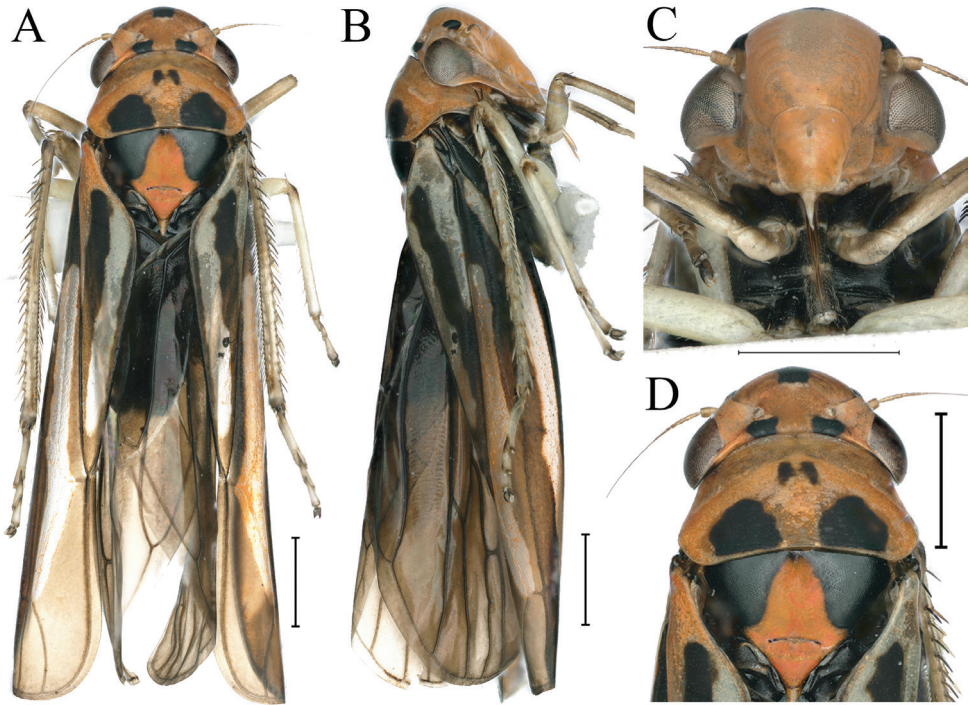


**Figure 5.** External features of *Atkinsoniella yingjiangensis* Jiang & Yang, sp. nov., male holotype **A** habitus, dorsal view **B** habitus, lateral view **C** face, anterior view **D** head and pronotum, dorsal view. Scale bars: 1000  $\mu\text{m}$ .

each basal, and the base of the two spots linked; forewings black, with three longitudinal grayish white stripes, apical membranous area dark brown; face dark orange; thorax black in ventral view; legs grayish white.

Crown with anterior margin convex roundly, median length of crown approximately equal to half of interocular width, concave lateral area of ocelli. Ocelli located at the line of anterior eyes, each ocellus slightly further from the other one than to the adjacent eye. Face with frontoclypeus flat in the median, muscle impressions and clypeal sulcus distinct. Pronotum wider than head, anterior margin convex roundly and posterior margin concave. Scutellum with transverse depression slightly posterior to the median. Forewings with apical membranous area not obvious, base of the second and third cells almost aligned transversely.

Male pygofer narrowly rounded posteriorly, tip oblique dorsally, dorsal margin with lamellar prominence at basal one-third, with macrosetae in posterior half and microsetae in the median dispersedly; pygofer processes with microsetae at base, arising basiventrally on each side and extending dorsolateral posteriorly of pygofer, apex acute and exceeding posterior margin of pygofer. Subgenital plates broad at base and constrictive at tip, with one row of macrosetae uniseriate obliquely, long microsetae on lateral area, short microsetae on posterior half. Aedeagus slender, bent dorsally at tip and curved ventral, ventral margin with a horned protuberance basically articulating with paraphysis; paraphysis wide subapically,



**Figure 6.** Male genitalia of *Atkinsoniella yingjiangensis* Jiang & Yang, sp. nov. **A** style **B** connective **C** aedeagus and paraphysis, ventral view **D** aedeagus and paraphysis, lateral view **E** pygofer, lateral view **F** pygofer process, lateral view **G** subgenital plate, ventral view; Scale bars: 200  $\mu$ m.

with two lamellate bulges at tip, apex uncinata and articulating with aedeagus. Connective Y-shaped. Style narrow at posterior portion, apex curved and exceeding the tip of connective.

**Etymology.** The name of the new species is derived from Yingjiang where the type specimens were collected.

**Measurement.** Length of male 8.0–8.1 mm.

**Material examined.** *Holotype*: ♂, Yingjiang, Yunnan, CHINA, 25 June 2019, coll. Tie-Long Xu. *Paratypes*, 2♂♂, same data as holotype.

**Remarks.** This species is similar to *A. limba* Kuoh, 1991 in male genitalia, but markedly differ in the following characteristics: (1) pronotum with two small black spots abreast in the center and two large black spots transversely at posterior area; (2) apex of the pygofer process exceeding the posterior margin of the pygofer; (3) aedeagus concave obviously at the ventral margin basally; and (4) paraphysis inflated subapically and posterior margin  $\Lambda$ -shaped in ventral view.

**Distribution.** China (Yunnan).

Checklist of the genus *Atkinsoniella* worldwide (updated from Yang et al. 2017)

***Atkinsoniella albimacula* Yang & Li, 2002**

*Atkinsoniella albimacula* Yang & Li, 2002a: 556.

**Distribution.** China (Yunnan).

***Atkinsoniella albipenna* Yang, Meng & Li, 2017**

*Atkinsoniella albipenna* Yang, Meng & Li, 2017: 219.

**Distribution.** China (Guangxi, Yunnan).

***Atkinsoniella alcmena* (Distant, 1908)**

*Tettigoniella alcmena* Distant, 1908: 219.

*Atkinsoniella alcmena* (Distant): Young, 1986: 96.

**Distribution.** China (Tibet), India.

***Atkinsoniella alternata* Young, 1986**

*Atkinsoniella alternata* Young, 1986: 100.

**Distribution.** China (Guizhou, Taiwan, Yunnan).

***Atkinsoniella angula* Kuoh, 1992**

*Atkinsoniella angula* Kuoh, 1992: 126.

**Distribution.** China (Gansu, Yunnan).

***Atkinsoniella anabella* Young, 1986**

*Atkinsoniella anabella* Young, 1986: 107.

**Distribution.** Bhutan, India, Nepal.

***Atkinsoniella atrata* Yang, Meng & Li, 2017**

*Atkinsoniella atrata* Yang, Meng & Li, 2017: 207.

**Distribution.** China (Yunnan).

***Atkinsoniella atronotata* (Distant, 1918)**

*Kolla atronotata* Distant, 1918: 10.

*Atkinsoniella atronotata* (Distant): Young, 1986: 96.

**Distribution.** India.

***Atkinsoniella aurantiaca* Cai & Kuoh, 1995**

*Atkinsoniella aurantiaca* Cai & Kuoh, 1995: 89.

**Distribution.** China (Guizhou, Hubei, Jiangxi, Yunnan, Zhejiang).

***Atkinsoniella beaka* Yang, Meng & Li, 2017**

*Atkinsoniella beaka* Yang, Meng & Li, 2017: 218.

**Distribution.** China (Yunnan).

***Atkinsoniella bella* (Walker, 1851)**

*Tettigonia bella* Walker, 1851: 778.

*Atkinsoniella bella* (Walker): Young, 1986: 96.

**Distribution.** India, Nepal.

***Atkinsoniella biundulata* Meng, Yang & Ni, 2010**

*Atkinsoniella biundulata* Meng, Yang & Ni, 2010: 42.

**Distribution.** China (Yunnan).

***Atkinsoniella bowa* Yang, Meng & Li, 2017**

*Atkinsoniella bowa* Yang, Meng & Li, 2017: 206.

**Distribution.** China (Yunnan).

***Atkinsoniella brevistyla* Yang & Li, 2004**

*Atkinsoniella brevistyla* Yang & Li, 2004: 757.

**Distribution.** China (Tibet, Yunnan).

***Atkinsoniella changae* Yang, Meng & Li, 2017**

*Atkinsoniella changae* Yang, Meng & Li, 2017: 240.

**Distribution.** China (Yunnan).

***Atkinsoniella contrariuscula* (Jacobi, 1944)**

*Cicadella contrariuscula* Jacobi, 1944: 44.

*Atkinsoniella contrariuscula* (Jacobi): Young, 1986: 97.

*Atkinsoniella furcata* Zhang & Kuoh, 1993: 15.

**Distribution.** China (Anhui, Fujian, Guangdong, Guangxi, Guizhou, Sichuan).

***Atkinsoniella curvata* Zhang & Kuoh, 1993**

*Atkinsoniella curvata* Zhang & Kuoh, 1993: 13.

**Distribution.** China (Tibet, Yunnan).

***Atkinsoniella cuspidata* Meng, Yang & Ni, 2010**

*Atkinsoniella cuspidata* Meng, Yang & Ni, 2010: 45.

**Distribution.** China (Yunnan).

***Atkinsoniella cyclops* (Melichar, 1914)**

*Tettigoniella cyclops* Melichar, 1914: 127.

*Atkinsoniella cyclops* (Melichar): Young, 1986: 97.

**Distribution.** China (Hainan, Yunnan), Indonesia, Nepal.

***Atkinsoniella dactylia* Yang & Li, 2000**

*Atkinsoniella dactylia* Yang & Li, 2000: 410.

*Atkinsoniella trinotata* Cai & He, 2002: 147.

**Distribution.** China (Fujian, Guangdong, Guangxi, Guizhou, Hainan, Jiangxi, Yunnan).

***Atkinsoniella decisa* Distant, 1908**

*Atkinsoniella decisa* Distant, 1908: 236.

**Distribution.** India.

***Atkinsoniella divaricata* Yang, Meng & Li, 2017**

*Atkinsoniella divaricata* Yang, Meng & Li, 2017: 205.

**Distribution.** China (Guangdong, Guangxi, Guizhou).

***Atkinsoniella dormana* Li, 1992**

*Atkinsoniella dormana* Li, 1992: 345.

**Distribution.** China (Chongqing, Fujian, Guizhou, Hubei, Jiangxi, Sichuan, Shaanxi, Yunnan).

***Atkinsoniella dubia* Young, 1986**

*Atkinsoniella dubia* Young, 1986: 104.

**Distribution.** China (Tibet), Bhutan.

***Atkinsoniella duna* Yang, Meng & Li, 2017**

*Atkinsoniella duna* Yang, Meng & Li, 2017: 236.

**Distribution.** China (Guizhou, Yunnan).

***Atkinsoniella expanda* Yang, Meng & Li, 2017**

*Atkinsoniella expanda* Yang, Meng & Li, 2017: 214.

**Distribution.** China (Yunnan).

***Atkinsoniella fishtaila* Yang, Meng & Li, 2017**

*Atkinsoniella fishtaila* Yang, Meng & Li, 2017: 221.

**Distribution.** China (Hubei).

***Atkinsoniella fistular* Naveed & Zhang, 2018**

*Atkinsoniella fistular* Naveed & Zhang, 2018: 286.

**Distribution.** Pakistan.

***Atkinsoniella flavilega* Yang, Meng & Li, 2017**

*Atkinsoniella flavilega* Yang, Meng & Li, 2017: 242.

**Distribution.** China (Yunnan).

***Atkinsoniella flavipenna* Li & Wang, 1992**

*Atkinsoniella flavipenna* Li & Wang, 1992: 95.

**Distribution.** China (Fujian, Hubei, Hunan, Guangdong, Guangxi, Guizhou, Sichuan).

***Atkinsoniella flexa* Kuoh, 1992**

*Atkinsoniella flexa* Kuoh, 1992: 127.

**Distribution.** China (Yunnan).

***Atkinsoniella furipygofera* Yang & Meng, 2011**

*Atkinsoniella furipygofera* Yang & Meng in Yang, Meng & Li, 2011: 765.

**Distribution.** China (Yunnan).

***Atkinsoniella fuscopenna* Yang & Li, 2004**

*Atkinsoniella fuscopenna* Yang & Li, 2004: 756.

**Distribution.** China (Tibet).

***Atkinsoniella goosenecka* Yang, Meng & Li, 2017**

*Atkinsoniella goosenecka* Yang, Meng & Li, 2017: 222.

**Distribution.** China (Chongqing, Sichuan).

***Atkinsoniella grahami* Young, 1986**

*Atkinsoniella grahami* Young, 1986: 105.

*Atkinsoniella nigroscuta* Zhang & Kuoh, 1993: 11.

*Atkinsoniella furcula* Yang & Li, 2002b: 40.

**Distribution.** China (Chongqing, Gansu, Guangdong, Guizhou, Hainan, Henan, Hubei, Hunan, Shaanxi, Sichuan, Yunnan).

***Atkinsoniella gregalis* (Distant, 1908)**

*Kolla gregalis* Distant, 1908: 226.

*Atkinsoniella gregalis* (Distant): Young, 1986: 97.

**Distribution.** India, Myanmar.

***Atkinsoniella guttata* Kuoh, 1992**

*Atkinsoniella guttata* Kuoh, 1992: 125.

**Distribution.** China (Yunnan, Tibet).

***Atkinsoniella heae* Yang, Meng & Li, 2017**

*Atkinsoniella heae* Yang, Meng & Li, 2017: 238.

**Distribution.** China (Tibet).

***Atkinsoniella heiyuana* Li, 1992**

*Atkinsoniella heiyuana* Li, 1992: 348.

*Atkinsoniella rubra* Kuoh & Cai in Cai & Kuoh, 1994: 14.

**Distribution.** China (Chongqing, Gansu, Fujian, Guangdong, Guangxi, Guizhou, Hainan, Hubei, Hunan, Jiangxi, Shaanxi, Sichuan, Tibet, Yunnan), Vietnam.

***Atkinsoniella huangi* Yang & Zhang, 2000**

*Atkinsoniella huangi* Yang & Zhang, 2000: 187.

**Distribution.** China (Guizhou, Sichuan, Yunnan).

***Atkinsoniella hupehna* Young, 1986**

*Atkinsoniella hupehna* Young, 1986: 118.

*Atkinsoniella obliqua* Zhang & Kuoh, 1993: 14.

**Distribution.** China (Chongqing, Fujian, Guangxi, Guizhou, Hubei, Jiangxi, Shaanxi, Zhejiang).

***Atkinsoniella insignata* (Haupt, 1924)**

*Tettigonia trilineata* Melichar, 1902: 132.

*Tettigoniella trilineata insignata* Haupt, 1924: 306.

*Tettigella chinensis* Metcalf, 1955: 264.

*Atkinsoniella insignata* (Haupt): Young, 1986: 97.

*Atkinsoniella longinotata* Kuoh, 1992: 124.

**Distribution.** China (Hubei, Qinghai, Sichuan, Yunnan).

***Atkinsoniella javana* (Melichar, 1914)**

*Kolla javana* Melichar, 1914: 124.

*Atkinsoniella javana* (Melichar): Young, 1986: 97.

**Distribution.** Indonesia.

***Atkinsoniella jini* Yang, Meng & Li, 2017**

*Atkinsoniella jini* Yang, Meng & Li, 2017: 199.

**Distribution.** China (Tibet).

***Atkinsoniella latior* Young, 1986**

*Atkinsoniella latior* Young, 1986: 113.

**Distribution.** China (Guangdong, Guangxi, Hubei, Jiangxi).

***Atkinsoniella lii* Yang & Zhang, 2000**

*Atkinsoniella lii* Yang & Zhang, 2000: 186.

**Distribution.** China (Yunnan).

***Atkinsoniella limba* Kuoh, 1991**

*Atkinsoniella limba* Kuoh, 1991: 20.

**Distribution.** China (Fujian).

***Atkinsoniella liui* Yang, Meng & Li, 2017**

*Atkinsoniella liui* Yang, Meng & Li, 2017: 241.

**Distribution.** China (Tibet).

***Atkinsoniella longa* Yang, Meng & Li, 2017**

*Atkinsoniella longa* Yang, Meng & Li, 2017: 212.

**Distribution.** China (Yunnan).

***Atkinsoniella longiaurita* Yang, Meng & Li, 2017**

*Atkinsoniella longiaurita* Yang, Meng & Li, 2017: 202.

**Distribution.** China (Yunnan).

***Atkinsoniella longiuscula* Feng & Zhang, 2015**

*Atkinsoniella longiuscula* Feng & Zhang, 2015: 281.

**Distribution.** China (Sichuan, Yunnan).

***Atkinsoniella malaisei* Young, 1986**

*Atkinsoniella malaisei* Young, 1986: 102.

**Distribution.** China (Yunnan), Myanmar.

***Atkinsoniella mediofasciola* Yang & Li, 2002**

*Atkinsoniella mediofasciola* Yang & Li, 2002b: 40.

**Distribution.** China (Chongqing, Fujian, Guangxi, Sichuan).

***Atkinsoniella membrana* Yang, Meng & Li, 2017**

*Atkinsoniella membrana* Yang, Meng & Li, 2017: 213.

**Distribution.** China (Yunnan).

***Atkinsoniella motuoensis* Meng, Yang & Ni, 2010**

*Atkinsoniella motuoensis* Meng, Yang & Ni, 2010: 47.

**Distribution.** China (Tibet).

***Atkinsoniella multiseta* Yang, Meng & Li, 2017**

*Atkinsoniella multiseta* Yang, Meng & Li, 2017: 226.

**Distribution.** China (Yunnan).

***Atkinsoniella mungphuensis* (Distant, 1908)**

*Kolla mungphuensis* Distant, 1908: 225.

*Atkinsoniella mungphuensis* (Distant): Young, 1986: 97.

**Distribution.** India, Myanmar.

***Atkinsoniella stenopyga* Jiang & Yang, sp. nov.**

**Distribution.** China (Tibet).

***Atkinsoniella nigra* Kuoh & Cai, 1994**

*Atkinsoniella nigra* Kuoh & Cai in Cai & Kuoh, 1994: 13.

**Distribution.** China (Yunnan).

***Atkinsoniella nigricephala* Li, 1992**

*Atkinsoniella nigricephala* Li, 1992: 349.

**Distribution.** China (Guizhou, Hubei, Zhejiang).

***Atkinsoniella nigradorsum* Kuoh & Zhuo, 1996**

*Atkinsoniella nigradorsum* Kuoh & Zhuo, 1996: 2.

**Distribution.** China (Chongqing, Fujian, Guizhou, Hubei, Sichuan, Zhejiang).

***Atkinsoniella nigripennis* Yang & Li, 1999**

*Atkinsoniella nigripennis* Yang & Li, 1999: 2.

**Distribution.** China (Yunnan).

***Atkinsoniella nigriscens* Yang & Li, 2004**

*Atkinsoniella nigriscens* Yang & Li, 2004: 756.

**Distribution.** China (Yunnan, Tibet).

***Atkinsoniella nigrisigna* Li, 1992**

*Atkinsoniella nigrisigna* Li, 1992: 344.

*Atkinsoniella chloritta* Yang & Li, 2002a: 558.

**Distribution.** China (Chongqing, Guangxi, Guizhou, Hubei, Sichuan, Yunnan).

***Atkinsoniella nigrita* Zhang & Kuoh, 1993**

*Atkinsoniella nigrita* Zhang & Kuoh, 1993: 12.

*Atkinsoniella bimanculata* Cai & Shen, 1998: 43.

**Distribution.** China (Chongqing, Gansu, Henan, Hubei, Sichuan, Shaanxi, Zhejiang).

***Atkinsoniella nigrominiatula* (Jacobi, 1944)**

*Cicadella nigrominiatula* Jacobi, 1944: 44.

*Atkinsoniella nigrominiatula* (Jacobi): Young, 1986: 97.

**Distribution.** China (Chongqing, Fujian, Gansu, Guangxi, Guizhou, Hubei, Jiangxi, Sichuan, Zhejiang).

***Atkinsoniella nigrosteaka* Li & Wang, 1994**

*Atkinsoniella nigrosteaka* Li & Wang, 1994: 27.

**Distribution.** China (Tibet).

***Atkinsoniella opponens* (Walker, 1851)**

- Tettigonia opponens* Walker, 1851: 757.  
*Tettigoniella bellona* Distant, 1908: 212.  
*Tettigoniella marpessa* Distant, 1908: 215.  
*Kolla canidia* Distant, 1908: 226.  
*Kolla maculifrons* Schmidt, 1911: 295.  
*Kolla maculifrons similis* Schmidt, 1911: 296.  
*Kolla trimaculata* Schmidt, 1911: 297.  
*Tettigoniella cuprea* Melichar, 1914: 128.  
*Kolla tigrina* Distant, 1918: 9.  
*Kolla melichari* China, 1935: 305.  
*Atkinsoniella opponens* (Walker): Young, 1986: 97.  
*Atkinsoniella triguttata* Zhang & Kuoh, 1993: 9.

**Distribution.** China (Chongqing, Fujian, Guangdong, Guangxi, Guizhou, Hainan, Jiangxi, Sichuan, Yunnan), India, Indonesia, Laos, Malay Islands, Malaysia, Myanmar, Nepal, Pakistan, Philippines, Thailand, Vietnam.

***Atkinsoniella peaka* Yang, Meng & Li, 2017**

- Atkinsoniella peaka* Yang, Meng & Li, 2017: 237.

**Distribution.** China (Jiangxi).

***Atkinsoniella punica* Yang & Li, 2002**

- Atkinsoniella punica* Yang & Li, 2002a: 556.

**Distribution.** China (Yunnan).

***Atkinsoniella recta* Yang, Meng & Li, 2017**

- Atkinsoniella recta* Yang, Meng & Li, 2017: 209.

**Distribution.** China (Yunnan).

***Atkinsoniella rectangulata* Yang, Meng & Li, 2017**

- Atkinsoniella rectangulata* Yang, Meng & Li, 2017: 210.

**Distribution.** China (Yunnan).

***Atkinsoniella rhomboida* Yang, Meng & Li, 2017**

*Atkinsoniella rhomboida* Yang, Meng & Li, 2017: 216.

**Distribution.** China (Yunnan).

***Atkinsoniella rinkihonis* (Matsumura, 1912)**

*Tettigonia rinkihonis* Matsumura, 1912: 36.

*Atkinsoniella rinkihonis* (Matsumura): Young, 1986: 97.

*Curvufacies sordidula* Kuoh, 1993: 39.

*Atkinsoniella tylata* Yang & Li, 1999: 1.

**Distribution.** China (Fujian, Guangxi, Guizhou, Jiangxi, Sichuan, Taiwan).

***Atkinsoniella rubrostriata* Kuoh, 1992**

*Atkinsoniella rubrostriata* Kuoh, 1992: 123.

**Distribution.** China (Yunnan).

***Atkinsoniella rufistigma* Yang, Meng & Li, 2017**

*Atkinsoniella rufistigma* Yang, Meng & Li, 2017: 233.

**Distribution.** China (Yunnan).

***Atkinsoniella steelei* Young, 1986**

*Atkinsoniella steelei* Young, 1986: 109.

**Distribution.** India.

***Atkinsoniella sulphurata* (Distant, 1908)**

*Tettigoniella sulphurata* Distant, 1908: 216.

*Atkinsoniella maculata* Distant, 1908: 236.

*Bhandara tetraspila* Jacobi, 1944: 41.

*Atkinsoniella sulphurata* (Distant): Young, 1986: 97.

*Atkinsoniella tetramaculata* Zhang & Kuoh, 1993: 7.

*Atkinsoniella stigma* Zhang & Kuoh, 1993: 8.

**Distribution.** China (Chongqing, Fujian, Guangxi, Guizhou, Hubei, Hunan, Sichuan, Yunnan, Zhejiang), India, Indonesia, Myanmar.

***Atkinsoniella thalia* (Distant, 1918)**

*Tettigoniella thalia* Distant, 1918: 2.

*Atkinsoniella thalia* (Distant): Young, 1986: 97.

*Atkinsoniella rubrivenosa* Kuoh & Zhuo, 1996: 3.

**Distribution.** China (Anhui, Chongqing, Fujian, Gansu, Guangdong, Guangxi, Guizhou, Hainan, Hebei, Henan, Hubei, Hunan, Jiangxi, Shaanxi, Sichuan, Tibet, Yunnan, Zhejiang), Bay of Bengal, India, Myanmar, Pakistan, Thailand.

***Atkinsoniella thaloidea* Young, 1986**

*Atkinsoniella thaloidea* Young, 1986: 117.

**Distribution.** China (Guangdong, Guangxi, Guizhou, Hainan, Tibet, Yunnan), Myanmar.

***Atkinsoniella tiani* Yang, Meng & Li, 2017**

*Atkinsoniella tiani* Yang, Meng & Li, 2017: 230.

**Distribution.** China (Yunnan).

***Atkinsoniella transifasciata* Yang, Meng & Li, 2017**

*Atkinsoniella transifasciata* Yang, Meng & Li, 2017: 215.

**Distribution.** China (Yunnan).

***Atkinsoniella tridentata* Yang & Li, 2011**

*Atkinsoniella tridentata* Yang & Li in Yang, Meng & Li, 2011: 766.

**Distribution.** China (Yunnan).

***Atkinsoniella tripunctata* Dmitriev, 2020**

= *Atkinsoniella trimaculata* Li, 1992: 347.

*Atkinsoniella tripunctata* Dmitriev, 2020: 7.

**Distribution.** China (Guizhou, Sichuan, Yunnan).

***Atkinsoniella tuberostyla* Yang, Meng & Li, 2017**

*Atkinsoniella tuberostyla* Yang, Meng & Li, 2017: 225.

**Distribution.** China (Yunnan).

***Atkinsoniella uniguttata* Li, 1993**

*Atkinsoniella uniguttata* Li, 1993: 40.

*Atkinsoniella valida* Feng & Zhang, 2015: 283.

**Distribution.** China (Fujian, Guangxi, Guizhou, Hainan, Yunnan).

***Atkinsoniella variata* Young, 1986**

*Atkinsoniella variata* Young, 1986: 110.

**Distribution.** China (Guizhou, Sichuan, Tibet, Yunnan), Nepal.

***Atkinsoniella vesta* (Distant, 1908)**

*Kolla vesta* Distant, 1908: 224.

*Atkinsoniella vesta* (Distant): Young, 1986: 97.

**Distribution.** India, Pakistan.

***Atkinsoniella wangi* Jiang & Yang, sp. nov.**

**Distribution.** China (Tibet).

***Atkinsoniella warpa* Yang, Meng & Li, 2017**

*Atkinsoniella warpa* Yang, Meng & Li, 2017: 203.

**Distribution.** China (Tibet, Yunnan).

***Atkinsoniella wui* Yang, Meng & Li, 2017**

*Atkinsoniella wui* Yang, Meng & Li, 2017: 200.

**Distribution.** China (Tibet, Yunnan).

***Atkinsoniella xanthoabdomena* Yang, Meng & Li, 2017**

*Atkinsoniella xanthoabdomena* Yang, Meng & Li, 2017: 232.

**Distribution.** China (Yunnan).

***Atkinsoniella xanthonota* Kuoh, 1994**

*Atkinsoniella xanthonota* Kuoh in Cai & Kuoh, 1994: 12.

**Distribution.** China (Yunnan).

***Atkinsoniella xanthovena* Yang & Li, 2002**

*Atkinsoniella xanthovena* Yang & Li, 2002c: 176.

**Distribution.** China (Jiangxi, Fujian, Hainan, Guangxi, Guizhou, Yunnan).

***Atkinsoniella xanthovitta* Kuoh, 1994**

*Atkinsoniella xanthovitta* Kuoh in Cai & Kuoh, 1994: 11.

**Distribution.** China (Yunnan).

***Atkinsoniella xinfengi* Yang, Meng & Li, 2017**

*Atkinsoniella xinfengi* Yang, Meng & Li, 2017: 223.

**Distribution.** China (Yunnan).

***Atkinsoniella yani* Yang, Meng & Li, 2017**

*Atkinsoniella yani* Yang, Meng & Li, 2017: 235.

**Distribution.** China (Yunnan).

***Atkinsoniella yingjiangensis* Jiang & Yang, sp. nov.**

**Distribution.** China (Yunnan).

***Atkinsoniella yunnanana* Yang, Meng & Li, 2017**

*Atkinsoniella yunnanana* Yang, Meng & Li, 2017: 229.

**Distribution.** China (Yunnan).

***Atkinsoniella zaihuai* Yang & Meng, 2011**

*Atkinsoniella zaihuai* Yang & Meng in Yang, Meng & Li, 2011: 766.

**Distribution.** China (Yunnan).

***Atkinsoniella zhangmuensis* Yang, Meng & Li, 2017**

*Atkinsoniella zhangmuensis* Yang, Meng & Li, 2017: 227.

**Distribution.** China (Tibet).

***Atkinsoniella zizhong* Jiang & Yang, 2022**

*Atkinsoniella zizhong* Jiang & Yang in Jiang, Li, Yu & Yang, 2022: 5

**Distribution.** China (Hubei, Guizhou, Zhejiang).

## Acknowledgements

We are grateful to Xian-Yi Wang and Tie-Long Xu (Institute of Entomology, Guizhou University) for collecting specimens. This study is supported by the Guizhou Province Science and Technology Innovation Talent Team Project (Qian Ke He Pingtai Rencai – CXTD [2021] 004), and the Program of Excellent Innovation Talents, Guizhou Province, China ([2016]-4022).

## References

- Cai P, He JH (2002) Homoptera: Cicadelloidea: Cicadellidae. In: Huang FS (Ed.) Forestry Insects from Hainan. Science Press, Beijing, 134–157. [In Chinese]
- Cai P, Kuoh CL (1994) Five new species and a new record of the genus *Atkinsoniella* from Yunnan, China (Homoptera: Cicadelloidea: Cicadellidae). Zoological Research 15(4): 11–19. [In Chinese]
- Cai P, Kuoh CL (1995) Homoptera: Ledridae, Cicadellidae, Iassidae and Coelidiidae. In: Wu H (Ed.) Insects of Baishanzu Mountain, Eastern China. Series of the Bioresources Expedition to the Baishanzu Mountain Nature Reserve. China Forestry Publishing House, Beijing, 86–94. [In Chinese]
- Cai P, Shen XC (1998) New species of family Cicadellidae from Mt. Funiu in Henan (Homoptera: Cicadelloidea). Fauna and Taxonomy of Insects in Henan 2: 37–52. [In Chinese]

- China WE (1935) The terrestrial Hemiptera of the German Limnological Sunda-Expedition. *Tropische Binnengewasser* 6: 295–307.
- Distant WL (1908) The Fauna of British India Including Ceylon and Burma: Rhynchota. Vol. IV. Homoptera and Appendix (Pt.). Taylor and Francis, London, 501 pp.
- Distant WL (1918) Rhynchota. Homoptera: Appendix. Heteroptera: addenda. The Fauna of British India. Including Ceylon and Burma 7: 1–210. [Published under the authority of the Secretary of State for India in Council]
- Dmitriev DA (2020) Nomenclatural changes in the suborders Auchenorrhyncha (Hemiptera) and Paleorrhyncha (Palaeohemiptera). *Zootaxa* 4881(1): 25–53. <https://doi.org/10.11646/zootaxa.4881.1.2>
- Feng L, Zhang Y (2015) The leafhopper genus *Atkinsoniella* Distant (Hemiptera: Cicadellidae: Cicadellinae) with descriptions of two new species from China. *Zootaxa* 4028: 274–286. <https://doi.org/10.11646/zootaxa.4028.2.7>
- Haupt H (1924) Die Homoptera der Tibetreise W. Stötzners. *Deutsche Entomologische Zeitschrift* 1923: 295–306. <https://doi.org/10.1002/mmnd.48019230313>
- Jacobi A (1944) Die Zikadenfauna der Provinz Fukien in Südchina und ihre tiergeographischen Beziehungen. *Mitteilungen der Münchener Entomologischen Gesellschaft* 34: 5–66.
- Jiang Y, Li HX, Yu XF, Yang MF (2022) Description and complete mitochondrial genome of *Atkinsoniella zizhongii* sp. nov. (Hemiptera: Cicadellidae: Cicadellinae) from China and its phylogenetic implications. *PeerJ* 10: e14026. <https://doi.org/10.7717/peerj.14026>
- Kuoh CL (1991) Five new species of Cicadellidae from Fujian (Homoptera: Cicadelloidea). *Wuyi Science Journal* 8: 15–22. [In Chinese]
- Kuoh CL (1992) Five new species of *Atkinsoniella* Distant from China (Homoptera: Cicadellidae). *Journal of Anhui Agricultural College* 19(2): 123–129. [In Chinese]
- Kuoh CL (1993) A new genus and a new species of Cicadellidae (Homoptera: Cicadelloidea). *Acta Zoologica Sinica* 39(1): 38–40. [In Chinese]
- Kuoh CL, Zhuo WX (1996) A new record genus and three new species of Cicadellidae from Fujian of China (Homoptera: Cicadelloidea). *Entomological Journal of East China* 5(1): 1–5. [In Chinese]
- Li ZZ (1992) Five new species of the genus *Atkinsoniella* from China (Homoptera: Tettigellidae). *Acta Zootaxonomica Sinica* 17(3): 344–351. [In Chinese]
- Li ZZ (1993) A new species of *Atkinsoniella* from Yunnan (Homoptera: Tettigellinae). *Journal of Guizhou Agricultural College* 12(Supplement): 40–41. [In Chinese]
- Li ZZ, Wang LM (1992) Agriculture and Forestry Insect Fauna of Guizhou (Homoptera: Cicadellidae) Vol. 4. Guizhou Science and Technology Publishing House, Guiyang, 304 pp.
- Li ZZ, Wang BH (1994) A new species of *Atkinsoniella* from Xizang (Homoptera: Tettigellinae). *Journal of Guizhou Agricultural College* 13(3): 27–28. [In Chinese]
- Matsumura S (1912) Die Cicadinen Japans II. *Annotationes Zoologicae Japonenses* 8: 15–51.
- Melichar L (1902) Homoptera aus West China, Persien, und dem Süd-Ussuri-Gebiete. *Annuaire du Musée Zoologique de l'Académie Impériale des Sciences de St.-Petersbourg* 7: 76–146.
- Melichar L (1914) Homopteren von Java, gesammelt von Herrn Ewd Jacobson. *Leyden Museum Notes* 36: 91–147.

- Meng ZH, Yang MF, Ni JQ (2010) Three new species of *Atkinsoniella* from China (Hemiptera: Cicadellidae: Cicadellini). *Zootaxa* 2654(1): 41–51. <https://doi.org/10.11646/zootaxa.2654.1.4>
- Naveed H, Zhang YL (2018) Newly recorded leafhoppers of the subfamily Cicadellinae (Hemiptera: Cicadellidae) with description of a new species from Pakistan. *Zootaxa* 4504(2): 285–295. <https://doi.org/10.11646/zootaxa.4504.2.9>
- Yang MF, Meng ZH, Li ZZ (2011) Three new species of the genus *Atkinsoniella* (Homoptera, Cicadellidae, Cicadellinae). *Acta Zootaxonomica Sinica* 36(3): 765–771. [In Chinese]
- Yang MF, Meng ZH, Li ZZ (2017) Hemiptera: Cicadellidae (II): Cicadellinae. *Fauna Sinica: Insecta*. Vol. 67. Science Press, Beijing, China, 637 pp. [In Chinese]
- Young DA (1968) Taxonomic study of the Cicadellinae (Homoptera: Cicadellidae), Part 1, Proconiini. *Bulletin - United States National Museum* 261: 1–287. <https://doi.org/10.5962/bhl.part.20869>
- Young DA (1986) Taxonomic study of the Cicadellinae (Homoptera: Cicadellidae), Part 3, Old World Cicadellini. *Bulletin of the North Carolina Agricultural Experimental Station* 281: 1–639.
- Zhang ZM, Kuoh CL (1993) Eight new species and a new record species of the genus *Atkinsoniella* from China (Homoptera: Cicadellidae). *Journal of Anhui Agricultural University* 20(1): 7–17. [In Chinese]



# A remarkable new species of the genus *Psammoecus* Latreille (Coleoptera, Silvanidae) from Lord Howe Island, Australia

Takahiro Yoshida<sup>1</sup>, Chris A. M. Reid<sup>2</sup>

**1** Systematic Zoology Laboratory, Department of Biological Sciences, Graduate School of Science, Tokyo Metropolitan University, 1-1 Minami-osawa, Hachioji, Tokyo, 192-0397 Japan **2** Entomology, Australian Museum Research Institute, Australian Museum, 1 William Street, Sydney NSW 2010, Australia

Corresponding author: Takahiro Yoshida ([yoshida\\_toritoma@yahoo.co.jp](mailto:yoshida_toritoma@yahoo.co.jp))

---

Academic editor: Patrice Bouchard | Received 21 January 2023 | Accepted 17 April 2023 | Published 11 May 2023

---

<https://zoobank.org/165D7A94-95E0-4556-B4CC-58AE0F24D366>

---

**Citation:** Yoshida T, Reid CAM (2023) A remarkable new species of the genus *Psammoecus* Latreille (Coleoptera, Silvanidae) from Lord Howe Island, Australia. ZooKeys 1161: 117–127. <https://doi.org/10.3897/zookeys.1161.100872>

---

## Abstract

A new species, *Psammoecus lordhowensis* **sp. nov.**, is described from Lord Howe Island, Australia. The new species is brachypterous and most likely endemic to the island. This species is distinct and can be distinguished by the following morphological characters: body rounded and convex; eyes small; temples well developed; lateral pronotal teeth absent; and hind wing strongly reduced.

## Keywords

Brachyptery, endemism, southwest Pacific, taxonomy, Telephanini

## Introduction

Lord Howe Island is a small volcanic island (1455 ha) situated in the temperate zone of the Tasman Sea, about 600 km from the east sea coast of Australia (Hutton et al. 2007). It was formed about 6.9 million years ago (McDougall et al. 1981). The native biota of this island is diverse with a high degree of endemism (Hutton et al. 2007). Several endemic genera are present on the island, for example the palms *Howea* Becc., *Hedyscepe*

H. Wendl. & Drude and *Lepidorrhachis* (H. Wendl. & Drude) O. F. Cook, a woody composite *Lordhowea* B. Nord., the tree *Negria* F. Muell., the leech *Quantenobdella* Richardson, three annelid genera (*Paraplutellus* Jamieson, *Pericryptodrilus* Jamieson and *Eastoniella* Jamieson), an isopod *Stigmops* Lillemetts & Wilson, a hemipteran bug *Howeria* Evans and a cricket *Howeta* Otte & Rentz (Hutton et al. 2007). The native flora includes 241 species, of which 43.6% are endemic (Green 1994). Although over 50% of the terrestrial invertebrates of Lord Howe are probably endemic species (Recher and Ponder 1981), many species still have not been described or recorded (Hutton et al. 2007).

Silvanidae are generally small, cryptic, detritivores, feeding on dead plant material and fungi in closed forests (Lawrence and Ślipiński 2013). The Australian fauna has not been revised, but is known to include about 75 species, many of which are undescribed (Lawrence and Ślipiński 2013). Two Silvanidae are recorded from Lord Howe, *Australodendrophagus australis* (Erichson) and the cosmopolitan species *Cryptamorpha desjardinsii* (Guérin-Ménéville) (Olliff 1889). Here we describe a third, new species, in *Psammoecus* Latreille. *Psammoecus* includes 84 species and is characterized by the securiform distal maxillary palpomere, the simple scutellary shield, lack of a scutellary striole, and the bilobed third tarsomere (Thomas 1984; Thomas and Nearn 2008; McElrath et al. 2023). Although the distribution of most species is restricted to the Old World, two Old World *Psammoecus* species have been found in the New World: *P. trimaculatus* Motschulsky from Brazil and *P. simonis* Grouvelle from the airport of Minnesota, United States (Thomas and Yamamoto 2007; Ouellette 2018). Some *Psammoecus* species show an extremely wide distribution, which seems to be sometimes caused by human activity (Karner 2020) and several intercepted records at ports or airports with imported materials have been published (e.g., Lu and Han 2006; Ouellette 2018; Yoshida 2020). Seven *Psammoecus* species are known from Australia, three of which are endemic, but the others may be accidental introductions (Karner 2020). The distinctive new species described here is flightless and almost certainly endemic to Lord Howe Island.

## Material and methods

### Observation, dissection and photographic techniques

Observations and dissections were performed under a stereomicroscope (Olympus SZX10 or Nikon SMZ1270). Male genital structures were placed on a cavity slide glass with Euparal for observation under an optical microscope (Nikon Eclipse E400). Measurements were made using a digital microscope (Olympus DSX110) with an integrated measuring function and read up to three decimal places in millimeters.

The abdomens of some specimens were removed and soaked in a 10% potassium hydroxide solution at room temperature overnight. After rinsing in water, the soaked abdomen was dissected under a stereomicroscope (Nikon SMZ1270) using fine insect pins, and the genital organs were detached for observation. After observations were completed, the dissected parts were mounted in Euparal on cover glasses

which were glued to a piece of cardboard, and pinned with the relevant specimen (Maruyama 2004).

Photographs were taken with a digital camera (Canon EOS 7D) fitted with a macro lens (Canon MP-E 65 mm). Composite images were produced using Affinity Photo version 1.10.6 (Serif Europe Ltd.). Images were retouched using the same software.

### Terminology, abbreviations and specimen deposition

Morphological terminology follows Lawrence et al. (2010) and Lawrence et al. (2011). Abbreviations and measurements are as follows:

<b>BL</b>	HL + PL + EL;
<b>HL</b>	length from anterior margin of clypeus to imaginary line between posterior margins of temples in dorsal view measured along the median line;
<b>HW</b>	greatest width of head across eyes;
<b>IE</b>	narrowest width of interspace between eyes;
<b>PL</b>	length of pronotum measured along the median line;
<b>PW</b>	greatest width of pronotum, excluding teeth;
<b>EL</b>	length of elytra measured along suture plus length of scutellar shield;
<b>EW</b>	greatest combined width of elytra.

Depositories of the examined specimens are as follows:

<b>ANIC</b>	Australian National Insect Collection, CSIRO, Canberra, Australia;
<b>AM</b>	Australian Museum, Sydney, Australia.

## Results

### Taxonomy

**Family Silvanidae Kirby, 1837**

**Subfamily Brontinae Erichson, 1845**

**Tribe Telephanini LeConte, 1861**

**Genus *Psammoecus* Latreille, 1829**

***Psammoecus lordhowensis* Yoshida & Reid, sp. nov.**

<https://zoobank.org/F0ABF9A7-2F5D-4BC1-9506-9B19DEC19489>

Figs 1, 2

**Diagnosis.** This new species is distinguished from other *Psammoecus* species by the rounded and convex body shape, small eyes, well-developed temples, the pronotum with irregular crenulation of obtuse tubercles (shorter than wide) not forming obvious teeth, and the extremely reduced hindwing and the male genital morphology.

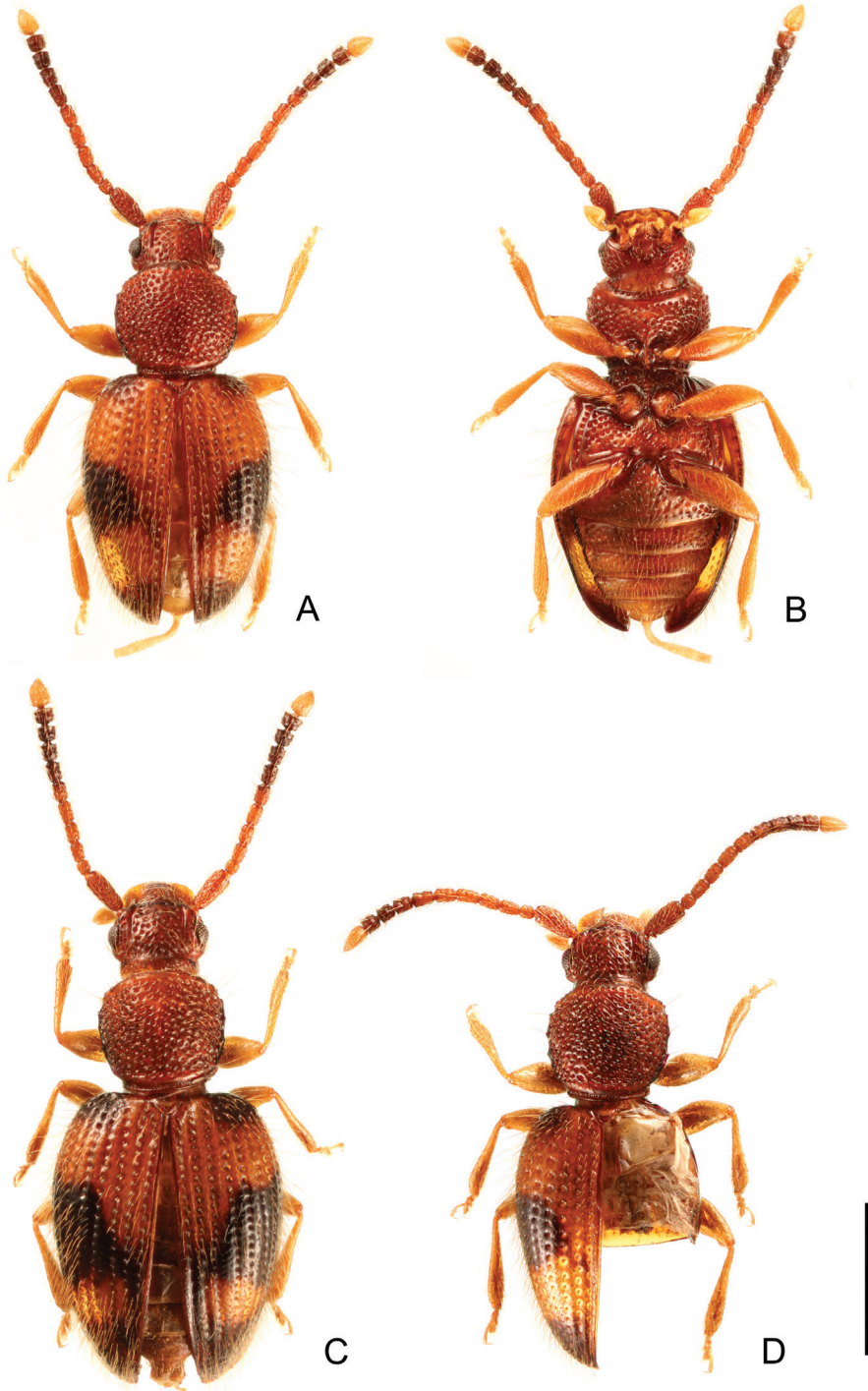


**Figure 1.** Habitus of *Psammoecus lordhowensis* sp. nov. **A, B** holotype (male), dorsal (**A**) and ventral views (**B**) **C** darker colored specimen, dorsal view **D** specimen of which right elytron and abdomen were removed, dorsal view. Scale bar: 1.0 mm.

**Description.** BL: 2.79–3.50 mm ( $n = 20$ ).

**Coloration** (Fig. 1). Head and pronotum reddish brown. Elytra reddish brown or somewhat lighter colored, with a quadrate or triangular black macula on each elytron at middle, narrowly darkened around humeri and apex of elytra; middle macula and apical darkened area connected by darkened area along lateral margin, also connected by darkened area along suture in darker colored specimens (Fig. 1C). Mouthparts and legs yellowish brown. Antennae reddish brown or somewhat lighter colored, 7<sup>th</sup> antennomere dark brown, 8<sup>th</sup> to 10<sup>th</sup> black, 11<sup>th</sup> white; setae golden.

**Head** (Fig. 1). Subquadrate, longer than wide, HL: 0.47–0.61 mm, HW: 0.58–0.71 mm, HW/HL: 1.14–1.31; IE/HL 0.89–1.02 ( $n = 20$ ); Temples well developed, narrowed immediately at base. Eyes small, round, laterally prominent. Punctuation strong, moderately dense, without microsculpture on the interstices. Antennae very long; antennomeres with pubescence of moderate to large length; distal portion of 7<sup>th</sup> to 10<sup>th</sup> and entire 11<sup>th</sup> antennomeres with short pubescence, denser on 9<sup>th</sup> to 11<sup>th</sup> antennomeres; with reticulate microsculpture on 2<sup>nd</sup> to 10<sup>th</sup> antennomeres; antennal total length and antennomere approximate length ratios from base to apex, both for the holotype, 1.68 mm; 3.6: 1.0: 1.5: 1.5: 1.5: 1.5: 1.6: 1.4: 1.3: 1.2: 2.2.

**Pronotum** (Fig. 1). Subquadrate, widest near middle, with slightly enlarged margins, PL: 0.70–0.90 mm, PW: 0.56–0.86 mm, PL/PW: 0.91–1.29 ( $n = 20$ ), without obvious lateral teeth. Punctuation on pronotal disk as on vertex. Pubescence composed of setae of moderate length, very long setae on tubercles on lateral margins and anterior and posterior angles. Anterior angle with a few tiny setiferous tubercles; lateral margin with 2–4 obtuse setiferous tubercles (shorter than wide) of similar size, not acute teeth; distances between setiferous tubercles on lateral margins irregular; posterior angle with a long seta.

**Legs** (Fig. 1) moderate length, without microsculpture; femora thick; tibiae somewhat thick, gradually widening distally; tarsi moderate length.

**Elytra** (Fig. 1). Oval, EL: 1.60–2.02 mm, EW: 1.08–1.47 mm (greatest width at anterior 1/3), EW/BL: 0.38–0.44, EW/EL: 0.67–0.74 ( $n = 20$ ), convex, with poorly developed humeri, with moderately rounded apices. Strial punctures moderate depth, mostly same width of the interstices. Pubescence composed of numerous semi-erect setae of medium length, erect long setae along margins and humeri, gradually shorter toward apices.

**Scutellary shield** triangular, with several short setae.

**Hindwing** (Fig. 1D) strongly reduced (brachypterous), about 1/4× as long as elytron, lacking venation.

**Male genitalia** (Fig. 2). Spiculum gastrale (Fig. 2A) with elongate strut, moderately diverging around posterior 2/9; posterior half of branches slightly narrowed, curved inwards near apices, connected by a membrane; lateral sclerites membranous, elongate, curved inwards. Parameres (Fig. 2B, D) stick-shaped, elongate, sub-parallel, slightly curved inwards, dorsally with a few punctures near bases, ventrally with setae of various lengths on posterior 3/4 (Fig. 2D), dorsally without setae, with two very long setae on each apex. Phallobase (Fig. 2B) elongate, sub-parallel; tegminal strut longer than basal piece; basal piece slightly narrowed toward posterior, with anterior margin widely incised at anterior 1/3. Penis (Fig. 2C) elongate, sub-parallel, apical 1/6

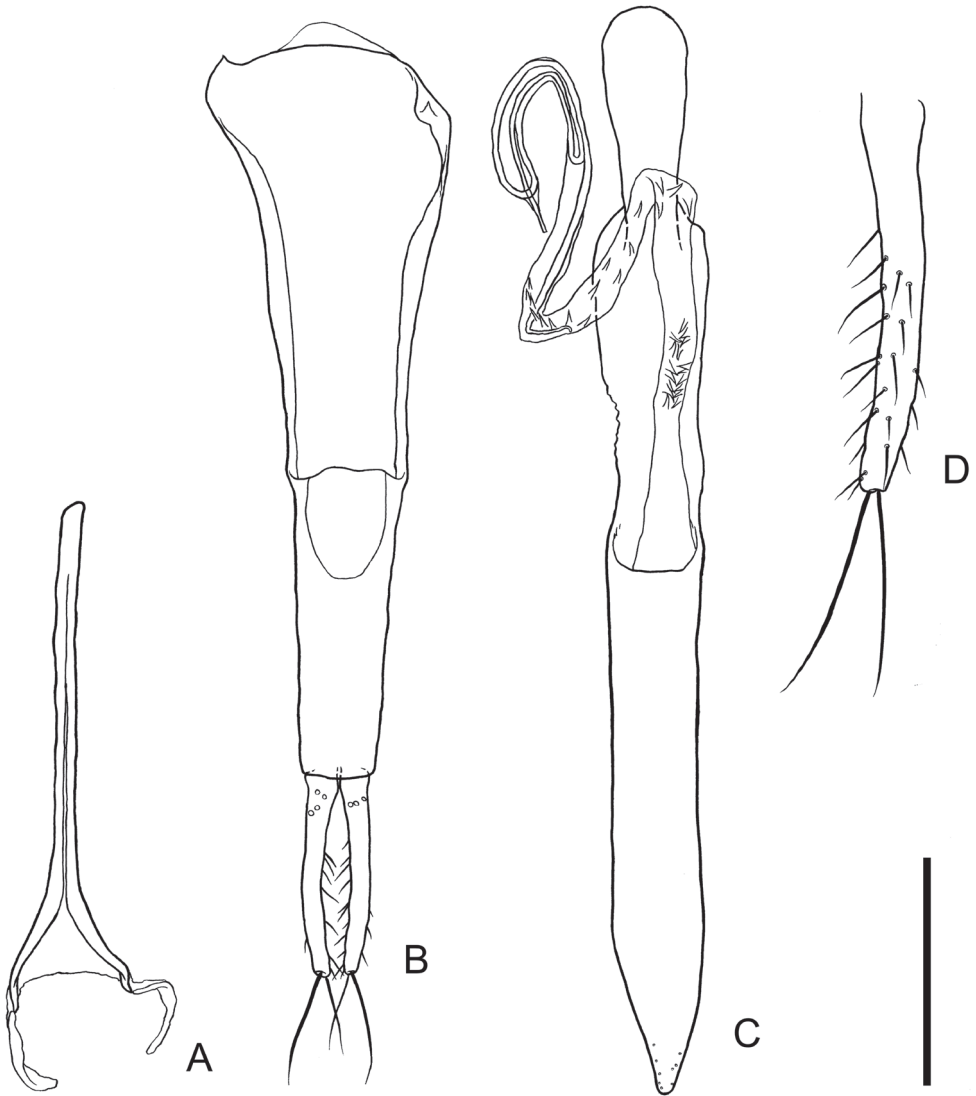


**Figure 2.** Male genital organs of *Psammoecus lordhowensis* sp. nov. **A** spiculum gastrale, ventral view **B** phallobase, ventral view **C** penis, dorsal view **D** right paramere, dorsal view. Scale bars: 0.1 mm (**A–C**); 0.2 mm (**D**).

narrowed, roundly protruded at apex, with some fine punctures near apex. Internal sac moderate length, recurved around apex, apically with a thin ringed structure and a thin long apical strut, sparsely armed with some spines on middle area, densely with spines near basal piece.

**Type series. Holotype:** male, 'NSW; On walking track to Erskine | Valley, adjacent to Salmon Beach, Lord | Howe Island; -31:33:39; 159:4:31; 10- | Dec-2000; G. Cassis; LHI/GC/L18 leaf | litter ex collected at night', '+3 in vial', 'K188166' (AM).

**Paratypes** (33 specimens): [Lord Howe Island] • 1 male; Anderson Road, south end; 40 m; 16 Nov. 1979; G. B. Monteith; Calcareous soil, sieved litter; Q. M. Berlesate No. 149, Pickard Veg: DaCt [*Drypetes austrasica*-*Cryptocarya triplinervis*] (ANIC: male genital structures illustrated and photo presenting brachyptery, Figs 1D and 2) • 1 male; same label data (ANIC) • 1 female; summit of Dawson Point Ridge; 150 m; 5 Nov. 1979; G. B. Monteith.; volcanic soil, sieved litter; Q. M. Berlesate No. 120; Pickard Veg: DaCt; voucher Specimen 81–106 (ANIC) • 1 ex.; same locality; 7 Nov. 1979; G. B. Monteith; same microhabitat and collecting method; Q. M. Berlesate No. 128, Pickard Veg: DaCt (ANIC) • 1 ex.; eastern slope of Dawsons Point Ridge above old settlement; 31°31'15"S, 159°3'7"E; 1 Dec. 2000; CBCR, Australian Museum; Leaf litter ex Closed Rain Forest *Drypetes*/*Cryptocarya* (exposed) habitat; LHIS014L, K188156 (+5) (AM) • 1 ex.; Intermediate Hill, near summit; 250 m; 6 Nov. 1979; G. B. Monteith; volcanic soil, sieved litter; Q. M. Berlesate No. 123, Pickard Veg: DaCt (ANIC) • 1 ex.; 100 m into Intermediate Hill from Kings Beach side; 31°33'S, 159°05'E; 8 Dec. 2000; C. Reid; palm leaf litter; K188160 (AM) • 1 male; Malabar Ridge saddle; 120 m; 25 Nov. 1979; G. B. Monteith; volcanic soil, sieved litter; Q. M. Berlesate No. 167, Pickard Veg: DaCt (ANIC) • 1 ex.; western slope of Malabar Ridge S of Kims Lookout trail; 31°30'57"S, 159°3'31"E; 24 Nov. 2000; CBCR, Australian Museum; leaf litter ex Broad Megaphyllous Closed Sclerophyll Forest – *Howea belmoryana* habitat; LHIS007L, K188158 (+1 in vial) (AM) • 1 ex.; on walking track to Erskine Valley, adjacent to Salmon Beach; 31°33'39"S, 159°4'31"E; 10 Dec. 2000; G. Cassis; leaf litter ex collected at night; LHI/GC/L18, K188157 (+1 in vial) (AM) • 1 female: North Bay trail, 50 m from junction with Kims Lookout trail; 31°31'4"S, 159°3'0"E; 11 Dec. 2000; G. Cassis; leaf litter ex; LHI/GC/L22, K188165 (AM) • 2 exs; Stevens Reserve; 10 m; 13 Nov. 1979; G. B. Monteith; calcareous soil, sieved litter; Q. M. Berlesate No. 144, Pickard Veg: DaCt (ANIC) • 1 ex.; Stephens Reserve; 31°31'15"S, 159°03'53"E; 13 Dec. 2000; CBCR; leaf litter; LHIS059L, K188155 (AM) • 1 female and 1 ex.; Stephens Reserve, c. 10 m; 31°31'33"S, 159°03'53"E; 9 Dec. 2000; C. Reid; Palm frond leaf litter; K188161(188162) (AM) • 1 ex.; junction of Kims Lookout trail and North Beach trail; 31°31'8"S, 159°3'0"E; 18–27 Feb. 2001; Australian Museum; pit trap; LHIS010/05, K188163 (AM) • 1 female; "Little Slope"; 31°35'12"S, 159°4'3"E; 30 Nov. 2000; CBCR, Australian Museum; leaf litter ex Broad Megaphyllous Closed Sclerophyll Forest – *Howea belmoryana* habitat; LHIS051L, K188154 (+1) (AM) • 1 ex.; "Get Up Place", trail to Mt. Gower; 31°34'58"S, 159°4'52"E; 2 Dec. 2000; CBCR, Australian Museum; Leaf litter ex Broad Closed Sclerophyll Scrub, *Dracophyllum*/*Metrosideros* habitat; LHIS048L, K188159 (AM) • 1 ex.; Mt Gower tk [track]; 31°34'43"S, 159°05'6"E; 330 m; 10–17 May 2004; N. Velez; Site G13 litter *Chion. quadristamineus* forest; Australian Museum K517792 (AM) • 1 ex.; same locality, geo-coordinate and altitude; 1–12 Nov. 2005; N. Velez; same microhabitat; Australian Museum K517794 (AM) • 1 ex.; Mt Gower tk; 31°34'44"S, 159°05'7"E; 360 m; 10–17 May 2004; N. Velez; Site G14 litter *Chion. quadristamineus* forest; Australian Museum K517793 (AM) • 1 ex.; Mt Gower tk; 31°34'22"S, 159°04'42"E; 160 m; 10–17 May 2004; N. Velez; Site G6

litter *Syzigium fullagarii* forest; Australian Museum K517791 (AM) • 1 ex.; Mt Gower tk; 31°34'41"S, 159°05'3"E; 260 m; 1–12 Nov. 2005; N. Velez; Site G10 litter *Chion. quadristamineus* forest; Australian Museum K517795 (AM) • 1 ex.; Mt Gower tk; 31°34'49"S, 159°05'9"E; 460 m; 10–17 May 2004; N. Velez; Site G18 litter *Chion. quadristamineus* forest; Australian Museum K517796 (AM) • 1 male; Mt Gower tk; 31°34'45"S, 159°05'7"E; 390 m; 10–17 May 2004; N. Velez; Site G15 litter *Chion. quadristamineus* forest; Australian Museum K517797 (AM) • 1 female; Mt Gower tk; 31°34'52"S, 159°05'8"E; 530 m; 1–12 Nov. 2005; N. Velez; Site G21 litter *Draco Metrosideros nervulosa* scrub; Australian Museum K517798 (AM: habitus image taken, Fig. 1C) • 1 ex.; Mt Gower tk; 31°34'43"S, 159°05'4"E; 290 m; 1–14 Apr. 2006; N. Velez; Site G11 litter *Chion. quadristamineus* forest; Australian Museum K517799 (AM) • 1 female; Forest behind Salmon Beach; 31°33'96.2"S, 159°04'33.3"E; 29 m; 10 Feb. 2017; Jenkins Shaw & Jensen; under bark, fallen tree; LHI2017Feb10-J23, Australian Museum K517790 (AM) • 1 female; SEern [southeastern] face of Mt Lidgberg, at base of summit tabletop; 31°34'26"S, 159°4'54"E; 2–12 Dec. 2000; CBCR, Australian Museum; Pit trap; LHI031/05; K188164 (AM) • 2 exs; Mt Lidgbird E shelf; 31°33'82.6"S, 159°05'27.1"E; 486 m; 9 Feb. 2017; Jenkins Shaw & Jensen; shifting leaf litter; LHI2017Feb9-J20a, Australian Museum K517801 (517802) (AM) • 1 ex.; Mt Lidgbird tk; 31°33'44"S, 159°05'38"E; 390 m; 10–27 May 2004; N. Velez; Site L12 litter *Drypetes/Cryptocarya*; Australian Museum K517800 (AM).

**Distribution.** Lord Howe Island (New South Wales, Australia).

**Habitat.** *Psammoecus lordhowensis* is endemic to the Lord Howe main island, where it is widespread in closed temperate rainforest, from the northern (Malabar Ridge) to the southern (Little Slope) end of the island, and from sea level to 530 m elevation. It does not appear to occur in the cloud forest on the summit of Mount Gower (above 700 m). This species is mostly collected by sieving leaf litter, but one specimen was collected in a pitfall trap and another under bark.

**Etymology.** The specific name of this new species is derived from the type locality, as a noun in genitive case.

## Discussion

### Hindwing reduction in the tribe Telephanini

The hindwing of this new species is extremely reduced (brachypterous), which means that it cannot fly. In *Psammoecus*, brachypterous or apterous species have not been recorded previously. In related genera, four apterous species are known in *Telephanus* from Jamaica (2 spp.), Reunion Island (1 sp.) and Mexico (1 sp.), and one brachypterous species is known in *Cryptamorpha* (*C. triregia*) from the Three Kings Islands, New Zealand (Thomas 1984, 1992, 2011; Brown et al. 2012). Additionally, several flightless species of Telephanini are known from rainforests on the Australian mainland (Lawrence and Ślipiński 2013). The loss of the ability to fly among animals is

characteristic of the well-known “island syndrome” (Carlquist 1974; Baeckens and Van Damme 2020). Although, in general, many species of *Psammoecus* have high-flight activity (Karner 2020), this new species has likely reduced its flight activity and lost its functional hindwing in Lord Howe Island.

### Which species is most closely related to this new species?

In *Psammoecus*, the male genital structures (including the spiculum gastrale and the internal sac, which are sometimes overlooked in descriptions) are similar to each other between closely related species (e.g., *P. trimaculatus*, *P. triguttatus* Reitter and *P. labyrinthicus* Yoshida & Hirowatari; *P. fasciatus* Reitter and *P. hiranoi* Yoshida & Hirowatari) (Yoshida and Hirowatari 2013, 2014; Yoshida et al. 2018; Karner 2020). For identification of these species, it is often necessary to examine male genital morphology. The male genital structure of this new species is similar to those of some *Psammoecus* species (e.g., *P. venustus* Karner, *P. taiwanensis* Yoshida, Karner & Hirowatari). However, due to its distinctive morphology (see Diagnosis), this new species can be distinguished from other congeneric species without examination of its male genital structure. In addition, information on the whole male genital morphology of other *Psammoecus* species is significantly lacking. Although some species have similar male genitalia to those of this new species, it is difficult to conclude which species is closely related to this new species. To determine the species most closely related to this new species, further studies on the male genital morphology of this genus and the phylogenetic relationships among this genus are required.

### Acknowledgements

We wish to express our cordial thanks to Adam Ślipiński and Cate Lemann (ANIC) and Derek Smith (AM) for their generous loan of materials. TY received valuable information from the ABS (Nagoya Protocol on Access and Benefit-sharing) Advisory Team of Tokyo Metropolitan University, a subproject of the National BioResource Project supported by the Ministry of Education, Culture, Sports, Science and Technology, Japan. CAMR is grateful to the Lord Howe Island Board for past and present permissions to collect Coleoptera.

### References

- Baeckens S, Van Damme R (2020) The island syndrome. *Current Biology* 30(8): R338–R339. <https://doi.org/10.1016/j.cub.2020.03.029>
- Brown STJ, Marris JWM, Leschen RAB (2012) Review of New Zealand *Cryptamorpha* (Coleoptera: Silvanidae), with a description of a new species from the three kings islands. *New Zealand Entomologist* 35(1): 29–38. <https://doi.org/10.1080/00779962.2012.649706>

- Carlquist S (1974) *Island biology*. Columbia University Press, New York, 660 pp. <https://doi.org/10.5962/bhl.title.63768>
- Green PS (1994) Norfolk Island and Lord Howe Island. *Flora Australia* 49: 1–42.
- Hutton I, Parkes JP, Sinclair ARE (2007) Reassembling island ecosystems: The case of Lord Howe Island. *Animal Conservation* 10(1): 22–29. <https://doi.org/10.1111/j.1469-1795.2006.00077.x>
- Karner M (2020) Taxonomic Studies on Australian *Psammoecus* Latreille (Coleoptera, Silvanidae, Brontinae). *European Journal of Taxonomy* 723: 135–158. <https://doi.org/10.5852/ejt.2020.723.1149>
- Lawrence JF, Ślipiński A (2013) *Australian beetles. Volume 1: morphology, classification and keys*. CSIRO Publishing, Collingwood, 561 pp. <https://doi.org/10.1071/9780643097292>
- Lawrence JF, Beutel RG, Leschen RAB, Ślipiński A (2010) Glossary of morphological terms. In: Leschen RAB, Beutel RG, Lawrence JF (Eds) *Handbook of Zoology, Coleoptera, Beetles, Vol. 2: Morphology and Systematics (Elateroidea, Bostrichiformia, Cucujiformia partim)*. Walter de Gruyter, Berlin New York, 9–20. <https://doi.org/10.1515/9783110911213.9>
- Lawrence JF, Ślipiński A, Seago AE, Thayer MK, Newton AF, Marvaldi AE (2011) Phylogeny of the Coleoptera based on morphological characters of adults and larvae. *Annales Zoologici (Warszawa)* 61(1): 1–217. <https://doi.org/10.3161/000345411X576725>
- Lu Y, Han Z (2006) Five narrowly distributed species of Silvanidae from Yangzhou captured in wet blue leather and packages. *Chinese Bulletin of Entomology* 43: 398–400. [In Chinese, with English title]
- Maruyama M (2004) A permanent slide under a specimen. *Elytra* 32(2): 276.
- McDougall I, Embleton BJJ, Stone DB (1981) Origin and evolution of Lord Howe Island, southwest Pacific Ocean. *Journal of the Geological Society of Australia* 28(1–2): 155–176. <https://doi.org/10.1080/00167618108729154>
- McElrath TC, Thomas MC, Yoshida T (2023) Nomenclature of family Silvanidae extracted from Cucujoidea World Catalog curated in TaxonWorks [software]. <https://sfg.taxonworks.org/api/v1/> [Retrieved March 11, 2023]
- Olliff AS (1889) The insect fauna of Lord Howe Island. *Australian Museum Memoir* 2(4): 75–98[plate vi]. <https://doi.org/10.3853/j.0067-1967.2.1889.482>
- Ouellette GD (2018) Intercepted Silvanidae (Insecta: Coleoptera) from the International Falls, MN (U.S.A.) Port of Entry. *Great Lakes Entomologist* 51: 5–9.
- Recher HF, Ponder WF [Eds] (1981) *Lord Howe Island. A summary of current and projected scientific and environmental activities. Occasional Reports of the Australian Museum No. 1*. Australian Museum, Sydney, 72 pp. <https://doi.org/10.3853/isbn.0-7240-2060-8>
- Thomas MC (1984) A new species of apterous *Telephanus* (Coleoptera: Silvanidae) with a discussion of phylogenetic relationships of the Silvanidae. *Coleopterists Bulletin* 38: 43–55.
- Thomas MC (1992) Review of the species of *Telephanus* Erichson from the Malagasy Region, with description of a new species (Coleoptera: Silvanidae). *Journal of the New York Entomological Society* 100: 142–154.
- Thomas MC (2011) Two new Neotropical species of *Telephanus* Erichson near *T. serratus* Nevermann (Coleoptera: Silvanidae). *Insecta Mundi* 0197: 1–11. <http://digitalcommons.unl.edu/insectamundi/705>

- Thomas MC, Nearn EH (2008) A new genus of telephanine Silvanidae (Coleoptera: Cucujoidea), with a diagnosis of the tribe and key to genera. *Insecta Mundi* 0048: 1–14. <http://digitalcommons.unl.edu/insectamundi/576>
- Thomas MC, Yamamoto PT (2007) New records of Old World Silvanidae in the New World (Coleoptera: Cucujoidea). *Coleopterists Bulletin* 61(4): 612–613. [https://doi.org/10.1649/0010-065X\(2007\)61\[612:NROOWS\]2.0.CO;2](https://doi.org/10.1649/0010-065X(2007)61[612:NROOWS]2.0.CO;2)
- Yoshida T (2020) Identification of Silvanidae (Coleoptera) intercepted from ports and airports in Japan. *Urban Pest Management* 10(2): 51–66. [In Japanese, with English title and abstract]
- Yoshida T, Hirowatari T (2013) A new species of the genus *Psammoecus* (Coleoptera, Silvanidae) from the Nansei Islands, Japan. *Japanese Journal of Systematic Entomology* 19: 85–90.
- Yoshida T, Hirowatari T (2014) A revision of Japanese species of the genus *Psammoecus* Latreille (Coleoptera, Silvanidae). *ZooKeys* 403: 15–45. <https://doi.org/10.3897/zookeys.403.7145>
- Yoshida T, Karner M, Hirowatari T (2018) A revision of Taiwanese species in the genus *Psammoecus* Latreille (Coleoptera, Silvanidae). *Zoological Studies (Taipei, Taiwan)* 57: 1–18. <https://doi.org/10.6620/ZS.2018.57-18>



# Confirmation of the existence of Himalayan long-eared bats, *Plecotus homochrous* (Chiroptera, Vespertilionidae), in China

Pengfei Luo<sup>1,2\*</sup>, Xiangyang He<sup>1\*</sup>, Yuzhi Zhang<sup>1</sup>, Jianping Ye<sup>3</sup>, Min Guo<sup>1</sup>, Jin Deng<sup>1</sup>, Chunhui Zhou<sup>1</sup>, Jiang Zhou<sup>2</sup>, Libiao Zhang<sup>1</sup>

**1** Guangdong Key Laboratory of Animal Conservation and Resource Utilization, Guangdong Public Laboratory of Wild Animal Conservation and Utilization, Institute of Zoology, Guangdong Academy of Sciences, Guangzhou 510260, China **2** School of Karst Science, State Engineering Technology Institute for Karst Desertification Control, Guizhou Normal University, Guiyang 550001, China **3** Guangxi Guilin Maershan National Nature Reserve Administration, Guilin 541000, China

Corresponding authors: Jiang Zhou ([zhoujiang@ioz.ac.cn](mailto:zhoujiang@ioz.ac.cn)); Libiao Zhang ([zhanglb@giz.gd.cn](mailto:zhanglb@giz.gd.cn))

Academic editor: Wieslaw Bogdanowicz | Received 2 January 2023 | Accepted 6 April 2023 | Published 11 May 2023

<https://zoobank.org/C0D34672-5AC0-4AA8-8F6C-8D9AC3972F15>

**Citation:** Luo P, He X, Zhang Y, Ye J, Guo M, Deng J, Zhou C, Zhou J, Zhang L (2023) Confirmation of the existence of Himalayan long-eared bats, *Plecotus homochrous* (Chiroptera, Vespertilionidae), in China. ZooKeys 1161: 129–141. <https://doi.org/10.3897/zookeys.1161.99487>

## Abstract

The existence of Himalayan long-eared bats, *Plecotus homochrous* (Chiroptera, Vespertilionidae), in China has not been previously confirmed. In this study, four bats captured with harp traps from two sites in the Maershan National Nature Reserve in Guangxi, China were investigated. These bats have long, wide auricles, each with a prominent tragus. The length of each auricle is about the same as that of a forearm. Hairs on the ventral fur have a dark base with mixed grey and yellowish tips; those on the dorsal fur also have a dark base and are bicolored with brown tips. The thumbs are very short. A concavity is present in the front of the dorsal side of the cranium. Based on morphological characteristics and phylogeny using Cyt *b* gene sequences, these bats were identified as *P. homochrous*, thus confirming the existence of Himalayan long-eared bats in China.

## Keywords

cyt *b* gene, morphology, echolocation calls

\* These authors contributed equally to this study.

## Introduction

As bats of various species of the genus *Plecotus* E. Geoffroy, 1818 are morphologically very similar (Spitzenberger et al. 2006), taxonomic classification of them is very difficult. In 1847, Hodgson described the bats that he found in Nepal as Himalayan Long-eared bats (*Plecotus homochrous* Hodgson, 1847). However, this taxon was later considered a subspecies of *P. auritus* (Linnaeus, 1758) (Ellerman and Morrison-Scott 1951; Hanák 1966; Corbet 1978; Koopman 1993; Wang 2003; Simmons 2005). Horáček et al. (2000) proposed that *P. homochrous* should be considered an independent species based on its biogeographical characteristics. Later, Spitzenberger et al. (2006) revised the taxonomic status of all species in the genus based on results of morphological and molecular analyses and classified *P. homochrous* as a distinct species.

The first evidence for the existence of *P. homochrous* in China was reported by Wang (2003) who identified the bats he found in Xiping County, Yunnan Province, China as *P. auritus homochrous*. However, this record was not acknowledged by Simmons (2005), Wilson and Mittermeier (2019), Jiang et al. (2021), and Wei et al. (2021). Therefore, the existence of *P. homochrous* in China remained uncertain, and *P. homochrous* were believed to occur only in the southern Himalayas and Southeast Asia, including northern Pakistan, northwestern India, Nepal, and Vietnam (Wilson and Mittermeier 2019; Dai et al. 2020). In this study, we confirm the existence of *P. homochrous* in China and report on their morphological characteristics, phylogenetic relationships, and echolocation call patterns.

## Materials and methods

### Sample collection

Bats examined in this study were captured from the Maershan National Nature Reserve (25°48'N–25°58'N, 110°20'E–110°35'E), which covers an area of 170.09 km<sup>2</sup> of mountains with varied vegetation types. Although some areas at lower elevations have been transformed into bamboo forests, most of the reserve is undisturbed with primary forests, especially at higher elevations (Huang and Jiang 2002). Four *Plecotus* bats were captured from two sites (Fig. 1; 25°26'20"N, 110°53'32"E, 2002 m a.s.l. and 25°54'42"N, 110°27'14"E, 1708 m a.s.l.) with harp traps during a bat survey along an elevational gradient in June 2022. These bat specimens, designated GD-221656, GD-221657, GD-221658, and GD-221659, were preserved in anhydrous ethanol after all examinations were completed. These specimens are stored at the Guangdong Institute of Zoology.

### Morphological measurements and recording of echolocation calls

Morphological measurements of bats were performed with electronic digital calipers according to Dai et al. (2020). Definitions of the measurements are as

follows: FA, forearm length; T, tail length; HB, head and body length; Thsu, thumb length excluding claws; Thcu, thumb length including claws; Tib, tibia length; Hfsu, hindfoot length excluding claws; Hfcu, hindfoot length including claws; Trag, tragus length; E, ear length; STOTL, total length of the skull; CBL, condylobasal length; CCL, condylo-canine length; MAW, mastoid width;  $CM^3L$ , maxillary toothrow length; CCW, width across upper canines;  $M^3M^3W$ , width across upper molars;  $CM_3L$ , mandibular tooth row length; ML, mandible length; UJH, lower jaw height; BCW, braincase width; BCH, braincase height; ZYW, zygomatic width; RL, rostral length; Bulla, diameter of tympanic bulla; IOW, interorbital width. The wing shape of each bat was recorded by tracing on paper, followed by a determination of wing loading and wingspan ratio using IMAGE J according to the method of Norberg and Rayner (1987). The criteria of Bininda-Emonds and Russell (1994) and Aldridge and Rautenbach (1987) were used for

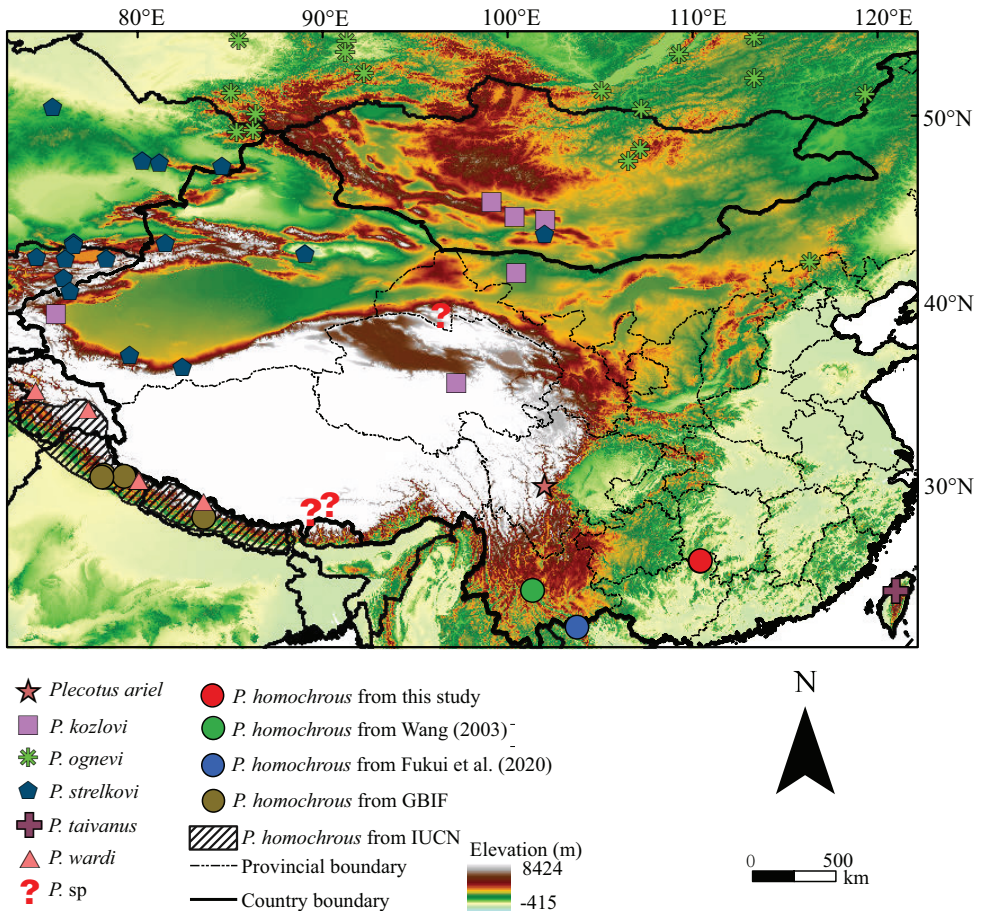


**Figure 1.** Distribution of *Plecotus* bats in China and other regions. The map shows the southernmost regions, not the entire China, where *Plecotus* bats have been found.

classification of wingspan ratio and wing loading as follows: wingspan ratio: low, 6.1–7.3; high,  $\geq 7.3$ ; wing loading: very low,  $\leq 6.45$  N/m<sup>2</sup>; low, 6.45–10.3 N/m<sup>2</sup>; high,  $\geq 10.3$  N/m<sup>2</sup>.

Morphological measurements of six *Plecotus* species (Suppl. material 1: table S1) were used for the principal component analysis (PCA) using ‘prcomp’ function of the R package ‘stats’ (R Core Team 2021). The following 10 craniodental measurements were assessed by PCA: STOTL, CBL, MAW, CM<sup>3</sup>L, M<sup>3</sup>M<sup>3</sup>W, CM<sub>3</sub>L, BCW, BCH, Bulla, and IOW (Suppl. material 1: table S2).

Echolocation calls of four bats were recorded using a handheld ultrasound detector (UltraSoundGate 116Hm, Avisoft Bioacoustics, Germany) when they were allowed to fly in a room of 5 × 5 × 2.5 m<sup>3</sup> in size. Ultrasound spectrograms were generated using the 512-point Fast Fourier Transform (FFT) algorithm with 96.87% of the frequency overlapped with a Hanning window. A total of 30 pulses were arbitrarily selected from each bat for determination of start frequency, end frequency, frequency of maximum energy, and pulse duration using the Batsound software (Pettersson Elektronik AB, Uppsala, Sweden). The values were determined based on the second (highest energy) harmonic and statistically compared with those of the study from Vietnam (Dai et al. 2020) using ‘kruskal.test’ function of the R package ‘stats’ (R Core Team 2021) as the data were non-normally distributed as determined by the Shapiro-Wilk and normal Q-Q plot.

## Phylogenetic analyses

To further identify the bats, DNA was extracted from a small piece of the wing membrane of each bat, and polymerase chain reaction was performed to amplify a portion of the mitochondrial cytochrome *b* gene (Cyt *b*) using primers Cyt *b*-F (5'-TAG AAT ATC AGC TTT GGG TG-3') and Cyt *b*-R (5'-AAA TCA CCG TTG TAC TTC AAC-3') (Li et al. 2006). Each PCR was conducted in a volume of 50 µl containing 8 µl of genomic DNA, 2 µl each of primer F and R (10 mM each), 13 µl of water, and 25 µl of HiFi DNA polymerase master mix. PCR conditions were as follows: 5 min at 94 °C, followed by 10 cycles of 60 s at 94 °C, 30 s at 46 °C, and 62 s at 72 °C; 25 cycles of 60 s at 94 °C, 40 s at 50 °C (+0.3 °C/cycle), and 60 s at 72 °C; 35 cycles of 60 s at 94 °C, 40 s at 54 °C, 60 s at 72 °C, and final elongation for 10 min at 72 °C.

The obtained sequences were deposited in GenBank under the following accession numbers: OP425735 (GD-221657), OP425736 (GD-221659), and OP425737 (GD-221656). No sequences were obtained from bat GD-221658 because of a failure in DNA isolation. The sequences were aligned with those of 30 Cyt *b* genes (Table 4) from GenBank for phylogenetic analysis using MAFFT software (Katoh and Standley 2013). Selection of the best-fit nucleotide substitution model was performed by MODELINDER (Kalyaanamoorthy et al. 2017), and the phylogenetic tree was constructed using the maximum-likelihood (ML) method in IQ-TREE with 5,000 ultrafast bootstraps (Nguyen et al. 2015).

## Results

### Morphological characteristics

In PCA, the percentages of explained variance of the first two principal components (PC1 and PC2) were 65.8% and 12.3%, respectively, with a cumulative percentage of 78.1% (Suppl. material 1: table S2). PC1 results were derived from all measurements except those of tympanic bullae (Bulla) and interorbital width (IOW), whereas results of PC2 were from analysis of Bulla and IOW (Table 1). PCA plots revealed that the four investigated bats were clustered with *P. homochrous* from Vietnam but were widely separated from other bats including *P. ariel* (Thomas, 1911), *P. kozlovi* (Bobrinski, 1926), *P. ognevi* (Kishida, 1927), *P. strelkovi* (Spitzenberger, 2006), and *P. wardi* (Thomas, 1911). This result suggests that these four bats are *P. homochrous*.

Morphologically, the bats have long, wide auricles, each with a prominent tragus (Fig. 3B). The length of each auricle is about the same as that of a forearm

**Table 1.** External and cranial measurements (in mm) of *Plecotus homochrous* bats.

	Guangxi, China	Lao Cai, Vietnam
	This study	Dai et al. 2020
Body sites measured	GD-221656(♂) / GD-221657(♂) / GD-221658(♂) / GD-221659(♀)	IEBR-M-5469(♀) / IEBR-M-5472(♀) / IEBR-M-5483(♂) / HNHM202011(♀)
FA	37.30 / 37.28 / 37.36 / 38.49	38.09 / 37.36 / 37.75 / 37.58
T	39.63 / 42.01 / 44.15 / 43.12	49.00 / 45.00 / 44.00 / 47.00
HB	50.49 / 50.75 / 46.92 / 45.77	45.00 / 42.50 / 37.50 / 42.50
Thsu	3.82 / 3.28 / 3.84 / 4.46	5.34 / 4.78 / 5.11 / 4.89
Thcu	4.86 / 4.14 / 4.73 / 5.61	6.22 / 5.89 / 5.71 / 5.64
Tib	17.84 / 17.02 / 17.07 / 18.49	17.40 / 18.00 / 16.80 / 17.00
Hfsu	7.96 / 8.18 / 8.56 / 8.38	7.98 / 7.64 / 7.96 / 7.99
Hfcu	8.68 / 8.70 / 9.03 / 9.11	9.18 / 8.32 / 8.85 / 8.86
Trag	17.29 / 14.54 / 15.76 / 15.88	18.00 / 17.00 / 18.00 / 18.00
E	36.43 / 38.85 / 38.12 / 39.12	38.00 / 39.00 / 37.00 / 39.50
STOTL	16.02 / 16.34 / 16.43 / 16.37	16.03 / 16.00 / 15.35 / 15.61
CBL	14.92 / 14.94 / 15.21 / 14.98	14.79 / 14.88 / 14.28 / 14.45
CCL	14.13 / 14.20 / 14.45 / 14.23	14.38 / 14.33 / 13.74 / 14.05
MAW	8.70 / 8.81 / 8.69 / 8.79	8.95 / 8.94 / 8.41 / 8.70
CM <sup>3</sup> L	5.12 / 5.13 / 5.19 / 5.08	5.33 / 5.02 / 5.05 / 5.23
CCW	3.51 / 3.35 / 3.27 / 3.53	3.65 / 3.59 / 3.56 / 3.52
M <sup>3</sup> -M <sup>3</sup>	5.77 / 5.72 / 5.71 / 5.69	6.00 / 5.50 / 5.56 / 5.63
CM <sub>3</sub> L	5.74 / 5.60 / 5.75 / 5.65	5.70 / 6.00 / 5.27 / 5.27
ML	9.67 / 9.69 / 9.95 / 9.71	10.38 / 10.54 / 9.90 / 9.96
UJH	2.78 / 2.88 / 2.90 / 2.91	3.01 / 3.16 / 2.86 / 3.01
BCW	7.30 / 7.34 / 7.17 / 7.30	7.76 / 7.53 / 7.75 / 7.83
BCH	5.67 / 5.29 / 5.25 / 5.07	5.89 / 5.99 / 5.83 / 5.86
ZYW	8.13 / 8.27 / — / 8.22	8.32 / — / — / 8.12
RL	3.32 / 3.21 / 3.47 / 3.25	4.02 / 3.97 / 3.64 / 4.05
Bulla	4.32 / 4.22 / 4.20 / 4.43	4.41 / 4.25 / 4.18 / 4.47
IOW	3.68 / 3.43 / 3.31 / 3.56	3.63 / 3.76 / 3.63 / 3.69

(Table 1). The bases of the two ears intersect at the forehead (Fig. 2A). Hairs on the ventral fur have a dark base with mixed grey and yellowish tips; those on the dorsal fur also have a dark base and are bicolored with brown tips (Fig. 2A, C). The facial fur is dark, and the skin is pink (Fig. 2B). The thumbs are very short (Fig. 2C). The wing membrane is attached to the base of toes, and there is a small, triangular protrusion at the base of the tail membrane near the heel (keeled calcar) (Fig. 2A). The dental formula is I 2/3, C 1/1, P 2/3, and M3/3. The first upper incisor is double pointed and higher than the second upper incisor. The second upper premolar is absent (Fig. 3B). The cranium is 16.02–16.43 mm in length and 8.13–8.27 mm in zygomatic width (Table 1), with a slight sagittal crest, which is the smallest among all *Plecotus* species. The bullae are medium-sized (diameter 4.20–4.43 mm). A concavity is present in the front of the dorsal side of the cranium (Fig. 3C). The orbital ridge is in the anterior part of the eye socket (Fig. 3A). All these morphological characteristics are identical to those of *P. homochoerus* from Vietnam (Dai et al. 2020).

### Echolocation calls and wing characteristics

Echolocation calls of the four bats are of frequency-modulation (FM) with multiple harmonics. The maximum energy of calls is mostly in the second harmonic (Fig. 4). Sound parameters of echolocation calls vary among the four individuals. Start frequency, end frequency, frequency of maximum energy, and pulse durations are 74.0

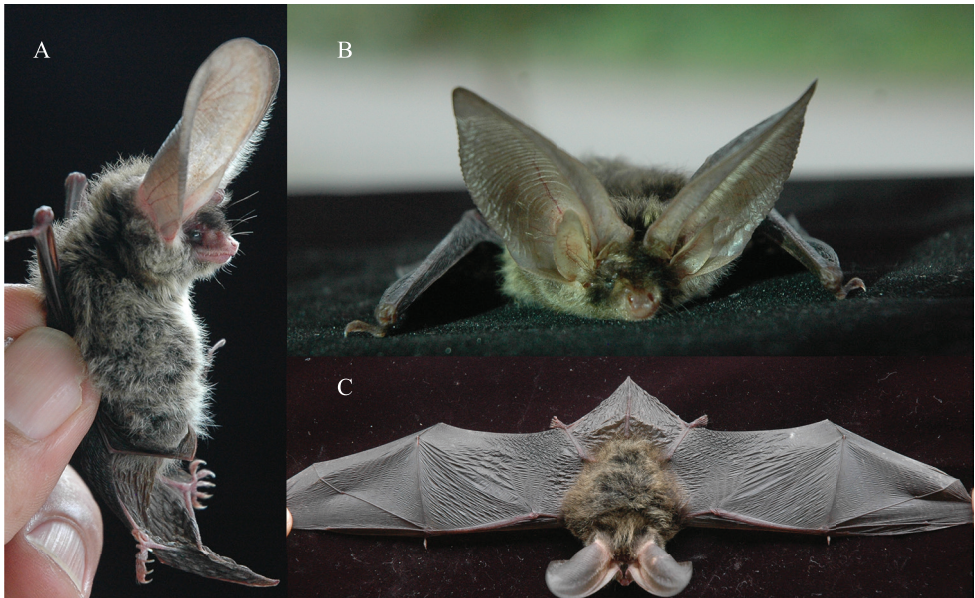


**Figure 2.** Pictures of *Plecotus homochoerus* (GD-221656) examined in this study **A** left side **B** face **C** dorsal side.

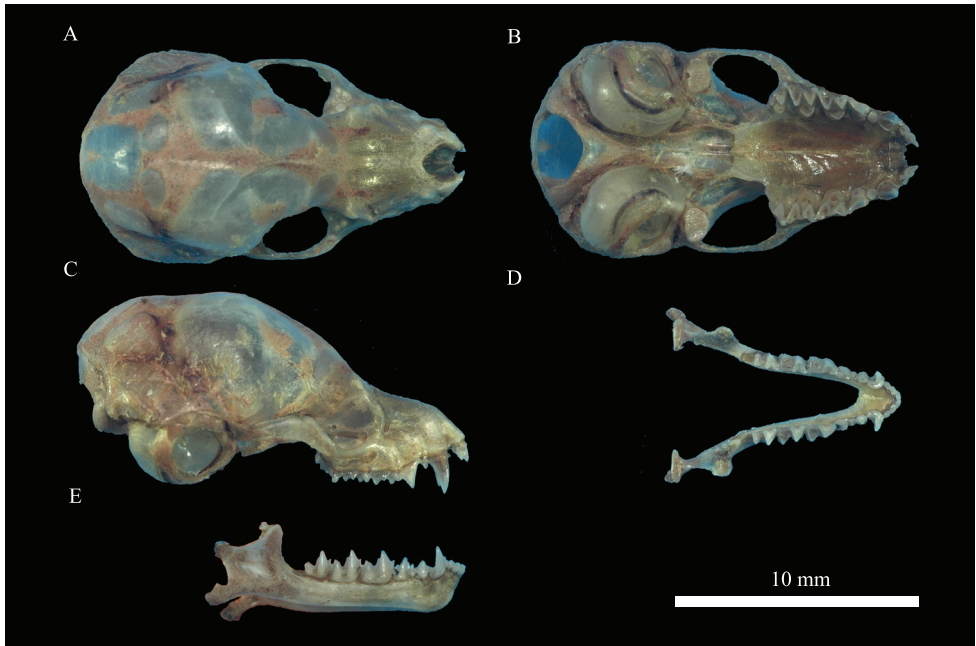


**Figure 3.** Cranial morphology of *Plecotus homochrous* (GD-221656) **A** cranium in dorsal view **B** cranium in ventral view **C** cranium in left side view **D** mandible in dorsal view **E** mandible left side view.

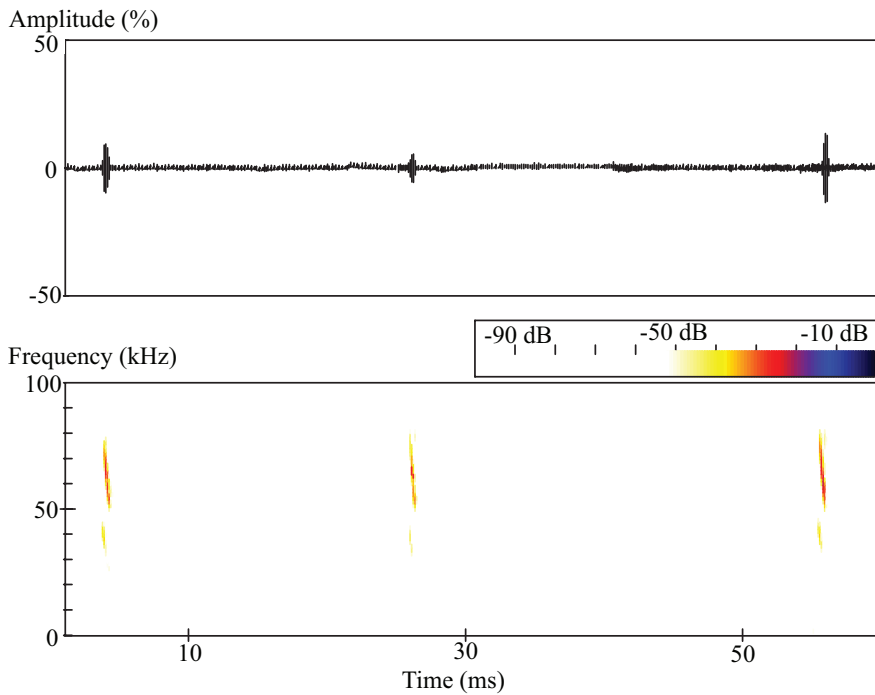


**Figure 4.** Amplitude and spectrogram of echolocation calls of bats examined in this study.

$\pm 2.8$  kHz,  $52.2 \pm 1.9$  kHz,  $58.7 \pm 0.6$  kHz, and  $1.5 \pm 0.2$  ms (Mean  $\pm$  SD), respectively. There is no significant difference in start frequency, end frequency, and frequency of maximum energy between the *P. homochrous* bats from Vietnam and the four bats examined in this study (*P* values 0.16, 0.53, and 0.26) (Table 2). However, there is a significant difference in pulse duration (*P* value 0.01). The four bats also have a very low wing loading ( $5.68 \pm 0.29$  N/m<sup>2</sup>) and a low wingspan ratio ( $6.82 \pm 0.70$ ) (Table 3), indicative of slow and flexible flights.

**Table 2.** Sound parameters of *Plecotus homochrous* echolocation calls.

Specimens	Country	Start frequency (kHz)	End frequency (kHz)	Frequency of maximum energy (kHz)	Duration (ms)
GD-221656	China	70.8	53.6	57.8	1.4
GD-221657	China	72.9	53.6	59.1	1.4
GD-221658	China	73.8	52.6	59.2	1.9
GD-221659	China	78.5	49.0	58.5	1.3
Mean $\pm$ SD		$74.0 \pm 2.8$	$52.2 \pm 1.9$	$58.7 \pm 0.6$	$1.5 \pm 0.2$
IEBR-M-5469	Vietnam	69.6	51.6	59.3	1.1
IEBR-M-5483	Vietnam	71.8	53.3	62.6	1.1
HNHM202011	Vietnam	71.2	55.3	59.3	1.1
Mean $\pm$ SD		$70.9 \pm 0.9$	$53.4 \pm 1.5$	$60.4 \pm 1.6$	$1.1 \pm 0.0$
Kruskal–Wallis test		ns	ns	ns	<i>P</i> = 0.01

**Table 3.** Wing characteristics of *Plecotus homochrous* from China.

Specimens	Wingspan ratio (N/m <sup>2</sup> )	Wingload
GD-221656	8.01	5.42
GD-221657	6.44	5.41
GD-221658	6.57	6.09
GD-221659	6.26	5.81
Mean $\pm$ SD	$6.82 \pm 0.70$	$5.68 \pm 0.29$

## Phylogenetic analysis

The phylogenetic tree reveals two major clades. The first clade contains *P. auritus*, *P. homochrous*, *P. kozlovi*, *P. macrobullaris*, *P. ognevi*, and *P. sacrimontis* (i.e. *P. auritus* group). The second one includes *P. austriacus*, *P. balensis*, *P. kolombatovici*, and *P. teneriffae* (i.e. the *P. austriacus* group). Bats GD-221656, GD-221657, and GD-221659 are clustered with *P. homochrous* from Vietnam (Fig. 5).

## Discussion

In this study, we identified four bats captured from Guangxi, China as *P. homochrous* based on their morphological characteristics and phylogenetic relationship. In addition to these individuals of *P. homochrous*, bats of six other *Plecotus* species have been

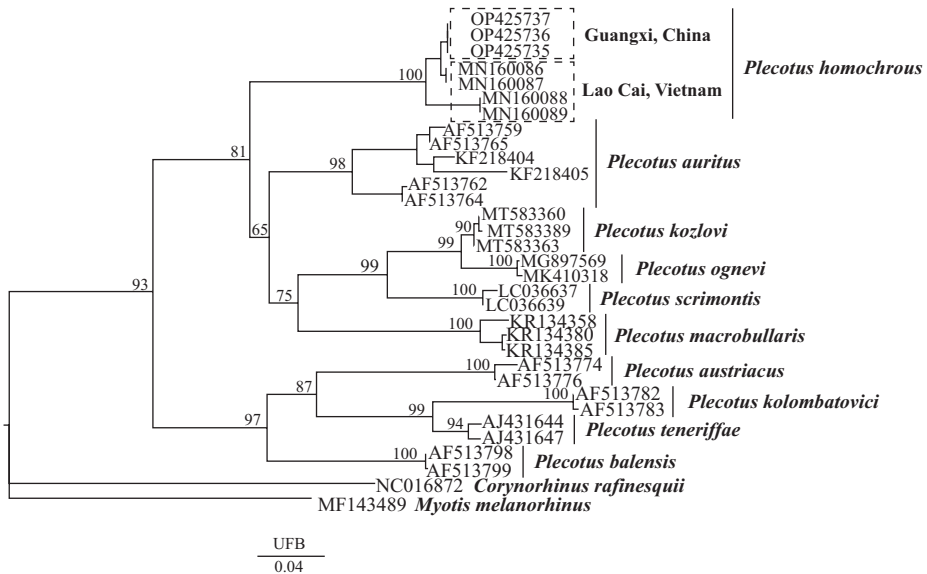


**Figure 5.** Phylogenetic tree of bats constructed based on results from the maximum-likelihood (ML) analysis of *Cyt b* gene sequences. Numbers on ML tree nodes are ultrafast bootstrap (UFB) support values.

found in China, including *P. ariel*, *P. kozlovi*, *P. ognevi*, *P. strelkovi*, *P. taivanus* (Yoshiyuki, 1991), and *P. wardi* (Wilson and Mittermeier 2019; Wei 2022). Among these, *P. homochrous* has the smallest skull and body size and thus are readily distinguishable from the others (Fig. 6). Other major differences include fur color and thumb length. Both ventral and dorsal fur of the four bats are bicolored (ventral fur dark to mixed grey and yellowish; dorsal fur dark to brown), but the fur of other species varies in color pattern as follows: *P. ariel*: ventral, slightly pale; dorsal, grizzled dark brown; *P. kozlovi*: ventral, pale or whitish; *P. ognevi*: ventral, bicolored (with pale brown base and white tips); *P. strelkovi*: dorsal, tricolored (black base, straw-colored middle shaft, and pale tips). Thumb lengths, excluding claws, of the four bats are 3.28–4.46 mm, but those of other bat species are longer (*P. kozlovi*, 7.20–7.60 mm; *P. ognevi*, 7.50–8.30 mm). The major difference between the four *P. homochrous* bats and *P. wardi* is that they have a smaller second upper incisor. Compared to *P. taivanus*, the four bats have a longer forearm (FA) and shorter head body (HB) and tail (T) length than *P. taivanus* [(FA)/(HB+T), 41.5% vs 39.0%]. In addition, the four bats have a keel, but *P. taivanus* lacks such structure.

Although the four bats are morphologically and phylogenetically identical to *P. homochrous* from Vietnam, the pulse duration of their echolocation calls is significantly longer than in *P. homochrous* from Vietnam; such differences may be due to the complexity in recording echolocation calls, as bats tend to send more pulses to obtain sufficient information when they fly in complex environments (Siemers et al. 2001; Dietrich et al. 2006; Peng et al. 2019). The relatively high frequency of maximum energy and low wing loading and wingspan ratio of the bats suggest that they forage

**Table 4.** List of bat species used in phylogenetic analyses.

Species	Locality	Cyt <i>b</i>
<i>Corynorhinus rafinesquii</i>	United States	NC016872
<i>Myotis melanorhinus</i>	United States	MF143489
<i>Plecotus auritus</i>	Guadalajara, Spain	AF513762
	La Rioja, Spain	AF513764
<i>P. auritus</i>	Valais, Switzerland	AF513759
	Navarra, Spain	AF513765
	Kırklareli, Turkey	KF218404
	Rize, Turkey	KF218405
<i>P. austriacus</i>	Mainz, Germany	AF513774
	Granada, Spain	AF513776
<i>P. balensis</i>	Abune Yusef, Ethiopia	AF513798
	Abune Yusef, Ethiopia	AF513799
<i>P. homochrous</i>	Guangxi, China	OP425735
	Guangxi, China	OP425736
	Guangxi, China	OP425737
	Lao Cai, Vietnam	MN160086
	Lao Cai, Vietnam	MN160087
	Lao Cai, Vietnam	MN160088
	Lao Cai, Vietnam	MN160089
<i>P. kolombatovici</i>	Cyrenaica, Libya	AF513782
	Cyrenaica, Libya	AF513783
<i>P. kozlovi</i>	Mongolian	MT583360
	Mongolian	MT583363
	Mongolian	MT583369
<i>P. macrobullaris</i>	Italy	KR134358
	Greece	KR134380
	Montenegro	KR134385
<i>P. ognevi</i>	Hovsgol National Park, Mongolia	MK410318
	Baikal, Russian	MG897569
<i>P. sacrimontis</i>	Oita, Japan	LC036637
	Hokkaido, Japan	LC036639
<i>P. teneriffae</i>	La Palma, Spain	AJ431644
	El Hierro, Spain	AJ431647

in relatively dense and complex environment using gleaning strategy and are montane forest dweller.

Although many *Plecotus* species have been found in China, detailed information on their geographical distribution is not available (Yu et al. 2021), and the identity of two of these species (*P. ariel* and *P. taiwanus*) remains uncertain because of the lack of molecular evidence. There are also two *Plecotus* species found in Xizang and Gansu, China that have yet to be named (Fig. 1; Spitzenberger et al. 2006). A well-defined list of species diversity can provide important information for the designation of protected areas for ecological conservation of various bat species. As such list is currently lacking, further efforts to identify novel bat species and investigate their distribution ranges in China are warranted.

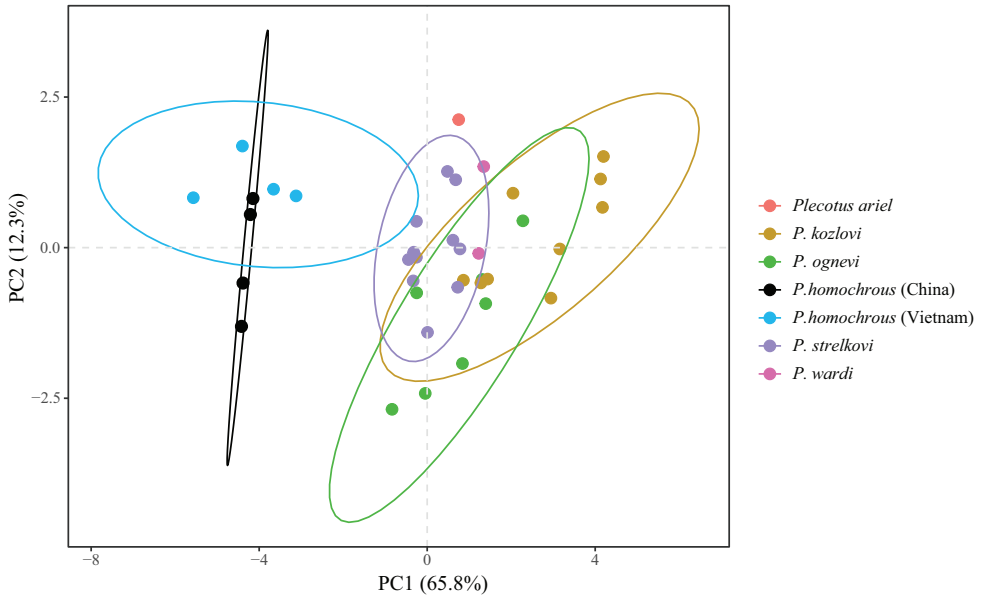


**Figure 6.** Plots of the first (PC1) versus the second (PC2) principal component for *Plecotus ariel*, *P. kozlovi*, *P. ognevi*, *P. homochrous* (examined in this study and those from Vietnam), *P. strelkovi*, and *P. wardi*.

## Acknowledgements

This work was funded by the Special Foundation for National Science and Technology Basic Research Program of China (2021FY100303) and Guangdong Provincial Science and Technology Program (2021B1212110003, 2021B1212050021).

## References

- Aldridge HDJN, Rautenbach IL (1987) Morphology, echolocation and resource partitioning in insectivorous bats. *Journal of Animal Ecology* 56(3): 763–778. <https://doi.org/10.2307/4947>
- Bininda-Emonds ORP, Russell AP (1994) Flight style in bats as predicted from wing morphometry: The effects of specimen preservation. *Journal of Zoology* 234(2): 275–287. <https://doi.org/10.1111/j.1469-7998.1994.tb06075.x>
- Corbet G (1978) *The Mammals of the Palearctic Region: a Taxonomic Review*. British Museum (Natural History), London and Cornell University Press, Ithaca.
- Dai F, Tu VT, Thanh HT, Arai S, Harada M, Csorba G, Son NW (2020) First record of the genus *Plecotus* from Southeast Asia with notes on the taxonomy, karyology and echolocation call of *P. homochrous* from Vietnam. *Acta Chiropterologica* 22(1): 57–74. <https://doi.org/10.3161/15081109ACC2020.22.1.006>

- Dietrich S, Diana PS, Andreas K, Hans US, Annette D (2006) Echolocation signals of the plecotine bat, *Plecotus macrobullaris* Kuzyakin, 1965. *Acta Chiropterologica* 8(2): 465–475. [https://doi.org/10.3161/1733-5329\(2006\)8\[465:ESOTPB\]2.0.CO;2](https://doi.org/10.3161/1733-5329(2006)8[465:ESOTPB]2.0.CO;2)
- Ellerman JR, Morrison-Scott TCS (1951) Checklist of Palaearctic and Indian Mammals 1758 to 1946. British Museum (Natural History), London, 810 pp.
- Hanák V (1966) Zur Systematik und Verbreitung der Gattung *Plecotus* Geoffroy, 1818 (Mammalia, Chiroptera). *Lynx* (n.s.) 6: 57–66.
- Horáček I, Hanák V, Gaisler J (2000) Bats of the Palaearctic region: a taxonomic and biogeographic review. *Proceedings of the VIII<sup>th</sup> European Bat Research Symposium* 1: 11–157. <https://doi.org/10.13140/2.1.4099.2643>
- Huang JL, Jiang DB (2002) Comprehensive Scientific Investigation of Maershan Nature Reserve in Guangxi. Hunan Science and Technology Press, Changsha.
- Jiang Z, Wu Y, Liu S, Jiang X, Zhou K, Hu H (2021) China's Red List of Biodiversity: Vertebrates, Volume I, Mammals (II). Science Press, Beijing, 886–887.
- Kalyaanamoorthy S, Minh BQ, Wong TKF, von Haeseler A, Jermiin LS (2017) ModelFinder: Fast model selection for accurate phylogenetic estimates. *Nature Methods* 14(6): 587–589. <https://doi.org/10.1038/nmeth.4285>
- Katoh K, Standley DM (2013) MAFFT multiple sequence alignment software version 7: Improvements in performance and usability. *Molecular Biology and Evolution* 30(4): 772–780. <https://doi.org/10.1093/molbev/mst010>
- Koopman K (1993) Order Chiroptera. In: Wilson DE, Reeder DM (Eds) *Mammal Species of the World*, 2<sup>nd</sup> Edn. Smithsonian Institution Press, Washington DC, 137–241.
- Li G, Jones G, Rossiter SJ, Chen SF, Parsons S, Zhang S (2006) Phylogenetics of small horseshoe bats from East Asia based on mitochondrial DNA sequence variation. *Journal of Mammalogy* 87(6): 1234–1240. <https://doi.org/10.1644/05-MAMM-A-395R2.1>
- Nguyen LT, Schmidt HA, Haeseler AV, Minh BQ (2015) IQ-TREE: A fast and effective stochastic algorithm for estimating maximum-likelihood phylogenies. *Molecular Biology and Evolution* 32(1): 268–274. <https://doi.org/10.1093/molbev/msu300>
- Norberg UM, Rayner JMV (1987) Ecological morphology and flight in bats (Mammalia; Chiroptera): Wing adaptations, flight performance, foraging strategy and echolocation. *Biological Sciences* 316(1179): 335–427. <https://doi.org/10.1098/rstb.1987.0030>
- Peng L, Ye J, Zhu G, Liu Z, Zhang L (2019) Vocal plasticity of two sympatric hipposiderid bats in different space openness. *Acta Theriologica Sinica* 39(3): 252–257. <https://doi.org/10.16829/j.slxb.150235>
- R Core Team (2021) R: a Language and Environment for Statistical Computing. R Foundation for Statistical Computing, Vienna.
- Siemers BM, Kalko EK, Schnitzler HU (2001) Echolocation behavior and signal plasticity in the Neotropical bat *Myotis nigricans* (Schina, 1982) (Vespertilionidae): A convergent case with European species of *Pipistrellus*. *Behavioral Ecology and Sociobiology* 50(4): 317–328. <https://doi.org/10.1007/s002650100379>
- Simmons NB (2005) Order Chiroptera. In: Wilson DE, Reeder DM (Eds) *Mammal Species of the World: a Taxonomic and Geographic Reference*. 3<sup>rd</sup> edn. Johns Hopkins University Press, Baltimore, 886–887.

- Spitzenberger F, Strelkov P, Winkler H, Haring E (2006) A preliminary revision of the genus *Plecotus* (Chiroptera, Vespertilionidae) based on genetic and morphological results. *Zoologica Scripta* 35(3): 187–230. <https://doi.org/10.1111/j.1463-6409.2006.00224.x>
- Wang YX (2003) A complete checklist of mammal species and subspecies in China, a taxonomic and geographic reference. China Forestry Publishing House, Beijing, 55 pp.
- Wei F (2022) Taxonomy and Distribution of Mammals in China. Science Press, Beijing, 622 pp.
- Wei F, Yang Q, Wu Y, Jiang X, Liu S, Li B, Yang G, Li M, Zhou J, Li S, Hu Y, Ge D, Li S, Yu W, Chen B, Zhang Z, Zhou C, Wu S, Zhang L, Chen Z, Chen S, Deng H, Jiang T, Zhang L, Shi H, Lu X, Liu Z, Cui Y, Li Y (2021) Catalogue of mammals in China. *Acta Theriologica Sinica* 41(5): 487–501.
- Wilson DE, Mittermeier RA (2019) Handbook of the Mammals of the World, Vol. 9. Bats. Lynx Edicions, Barcelona, 868 pp.
- Yu W, He K, Fan P, Chen B, Li S, Liu S, Zhou J, Yang Q, Li M, Jiang X, Yang G, Wu S, Lu X, Hu Y, Li B, Li Y, Jiang T, Wei F, Wu Y (2021) Taxonomic and systematic research progress of mammals in China. *Acta Theriologica Sinica* 41(5): 502–524. <https://doi.org/10.16829/j.slx.150535>

## Supplementary material I

### Additional information

Authors: Pengfei Luo

Data type: tables (docx. file)

Explanation note: table S1: references of *Plecotus* species investigated; table S2: Factor loading scores of characteristics used for the PCA of six bat species from China and other regions.

Copyright notice: This dataset is made available under the Open Database License (<http://opendatacommons.org/licenses/odbl/1.0/>). The Open Database License (ODbL) is a license agreement intended to allow users to freely share, modify, and use this Dataset while maintaining this same freedom for others, provided that the original source and author(s) are credited.

Link: <https://doi.org/10.3897/zookeys.1161.99487.suppl1>



# Revision of the genus *Colasia* Koch, 1965 (= *Belousovia* Medvedev, 2007, **syn. nov.**) (Coleoptera, Tenebrionidae, Blaptini)

Xing-Long Bai<sup>1</sup>, Jing-Ze Liu<sup>1</sup>, Guo-Dong Ren<sup>2</sup>

**1** Hebei Key Laboratory of Animal Physiology, Biochemistry and Molecular Biology, College of Life Sciences, Hebei Normal University, Shijiazhuang, Hebei 050024, China **2** The Key Laboratory of Zoological Systematics and Application, School of Life Sciences, Institute of Life Science and Green Development, Hebei University, Baoding, Hebei 071002, China

Corresponding authors: Jing-Ze Liu ([liujingze@hebtu.edu.cn](mailto:liujingze@hebtu.edu.cn)); Guo-Dong Ren ([gdren@hbu.edu.cn](mailto:gdren@hbu.edu.cn))

Academic editor: Patrice Bouchard | Received 11 November 2022 | Accepted 17 April 2023 | Published 11 May 2023

<https://zoobank.org/1684F7A5-31BC-4396-AB1A-7444208EA958>

**Citation:** Bai X-L, Liu J-Z, Ren G-D (2023) Revision of the genus *Colasia* Koch, 1965 (= *Belousovia* Medvedev, 2007, **syn. nov.**) (Coleoptera, Tenebrionidae, Blaptini). ZooKeys 1161: 143–167. <https://doi.org/10.3897/zookeys.1161.97440>

## Abstract

The relationship between the genera *Colasia* Koch, 1965 and *Belousovia* Medvedev, 2007 within the tribe Blaptini is discussed, and a new synonymy is proposed: *Belousovia* Medvedev, 2007, **syn. nov.** of *Colasia* Koch, 1965. As a result, three new combinations are established: *Colasia helenae* (Medvedev, 2007), **comb. nov.**, *C. kabaki intermedia* (Medvedev, 2007), **comb. nov.**, and *C. kabaki kabaki* (Medvedev, 2007), **comb. nov.** *Colasia akisoides* Koch, 1965 is redescribed, and a lectotype is designated. Three new species of the genus *Colasia* are described and illustrated from China: *C. bijica* **sp. nov.** (Guizhou), *C. medvedevi* **sp. nov.** (Yunnan), and *C. pilosa* **sp. nov.** (Yunnan). A distribution map and a key to species of the revised genus *Colasia* are presented.

## Keywords

Blaptinae, lectotype, new combinations, new species, new synonymy

## Introduction

The genera *Colasia* Koch, 1965 and *Belousovia* Medvedev, 2007 belong to the tribe Blaptini Leach, 1815 (Tenebrionidae, Blaptinae) (Koch 1965; Medvedev 2007; Kamiński et al. 2021). The genus *Colasia*, dedicated to M.G. Colas (Mr. Guy Colas 1902–1993; Dr.

Christophe Hervé, pers. comm., March 2023), is represented only by the type species *C. akisoides* Koch, 1965 described from Chongqing, China. According to the original description, *Colasia* is similar to *Tagonoides* Fairmaire, 1886 as both have granulated elytra. Moreover, to a certain extent, *Colasia akisoides* is also somewhat similar to *Asidoblaps glyptoptera* Fairmaire, 1886, also by the granules on the elytra (Koch 1965).

A new genus *Montagona* Medvedev, 1998 was established and compared with *Colasia* and the three other genera. The tribe Blaptini was subdivided into two subtribes by Skopin (1960) but later into five subtribes by Medvedev (2001), and *Colasia* and another ten genera were classified within the subtribe Gnaptorinina Medvedev, 2001. Based on the ovipositor structure, this subtribe Gnaptorinina was further divided into three subgroups (Medvedev and Merkl 2003):

(1) *Gnaptorina* Reitter, 1887, *Itagonia* Reitter, 1887, *Montagona*, and *Tagonoides*, characterized by apically cuneate and narrowed ovipositorial lobes;

(2) *Agnaptoria* Reitter, 1887, *Asidoblaps* Fairmaire, 1886, *Nepalindia* Medvedev, 1998, and probably also *Sintagona* Medvedev, 1998 (female unknown), characterized by apical margin of ovipositorial lobes obliquely truncate;

(3) *Colasia*, and *Viettagona*, characterized by apically rounded ovipositorial lobes.

The genus *Belousovia*, named for Igor Alexandrowich Belousov, is represented by one species and two subspecies described from western Yunnan, China: *B. helenae* Medvedev, 2007, *B. kabaki intermedia* Medvedev, 2007, and *B. kabaki kabaki* Medvedev, 2007. According to the original description (Medvedev 2007), *Belousovia* closely resembles *Colasia* (based on the examination of *C. medvedevi* sp. nov., erroneously determined by N. Skopin and G. Medvedev as *C. akisoides*) in the structure of aedeagus, spiculum gastrale, ovipositor, and elytra, but clearly differs from *Colasia* by the structure of legs, female genital tubes, and head capsule. The first and the most specific character, male legs: in *Belousovia* species, the ventral surface of pro- and mesotarsomeres I–IV, and metatarsomeres I–III with long and dense hairy tuft, the apical part of the metatibiae with a row of dense setae on the inner side (e.g., *B. kabaki kabaki* Medvedev, 2007: figs 116, 117); in *Colasia* species, the ventral surface of tarsal segments without hairy brush or tuft (from Koch 1965), only very short and strong setae present, metatibiae without a row of setae on the inner side. The second character, head capsule: the labrum and apical maxillary palpomere are covered with long setae in *Belousovia* species, but are short in *Colasia* species; eyes short and distinctly arcuately projecting outwards in *Belousovia* species, but absolutely flat in *Colasia* species. The third character, appearance: the pronotum is obviously heart-shaped in *Colasia* species, which never occurs in *Belousovia* species; the body is coal-black in *Colasia* species, but appears reddish in strong illumination in *Belousovia* species, especially on the humeral carinae and declivity of the elytra. The last character, female genital tubes: in *Colasia* species, bases of first and second reservoirs and base of spermathecal sphincter diverge from one point; in *Belousovia* species, the base of the first reservoir is separated from the place of divergence of the bases of the second reservoir and spermathecal sphincter

by a very long duct. However, the boundary between the genera *Belousovia* and *Colasia* becomes blurred with the examination of additional materials from western Guizhou, and eastern, central and western Yunnan, China.

This study aims to investigate the taxonomic status of the genera *Colasia* and *Belousovia*. Additionally, a redescription of *C. akisoides* and descriptions of three new Chinese species are provided.

## Material and method

The specimens were examined and dissected under a Nikon SMZ800 microscope, and photographs were taken using Canon EOS 5DSR camera and processed by Adobe Photoshop 2021. The distribution map was made by QGIS and processed by Adobe Photoshop 2021. Aedeagi was detached from the body with insect pins, then glued to separate cards and pinned under the specimens. A single slash (/) separates data of different lines on a label, a double slash (//) separates data of different labels, authors' remarks are enclosed in brackets “[ ]”.

Specimens examined in this study are deposited at the following institutes and collections:

- CTLH** private collection of Tian-Long HE, Huainan, China;  
**HBUM** Hebei University Museum, Baoding, China;  
**HNHM** Hungarian Natural History Museum, Budapest, Hungary;  
**MYNU** Invertebrate Collection of Mianyang Normal University, Sichuan, China;  
**ZIN** Zoological Institute of Russian Academy of Sciences, St.-Petersburg, Russia.

## Taxonomic accounts

### Genus *Colasia* Koch, 1965

*Colasia* Koch, 1965: 131; Medvedev 2001: 95; Löbl et al. 2008: 231; Ren et al. 2016: 333; Nabozhenko and Chigray 2020: 285; Bouchard et al. 2021: 44. Type species: *Colasia akisoides* Koch, 1965, by monotypy.

*Belousovia* Medvedev, 2007: 157; Ren et al. 2016: 328; Nabozhenko and Chigray 2020: 285; Bouchard et al. 2021: 44. Syn. nov. Type species: *Belousovia helenae* Medvedev, 2007, by original designation.

**Remarks.** After the examination of types of the genera *Belousovia* and *Colasia*, and also additional materials, we propose the genus *Belousovia* Medvedev, 2007 as a junior synonym of the genus *Colasia* Koch, 1965.

Firstly, in male legs: after the re-examination of the types of *Colasia akisoides*, apical part of metatibiae with a row of setae on the inner side (Fig. 5G, G'; not mentioned

in the original description by Koch 1965), although less dense than *Belousovia* species (Fig. 19G, G'), but dense enough compared to materials from Western Guizhou, and Western Yunnan (Figs 6G, G', 20; a few setae present only); ventral surface of tarsal segments with hairy tuft at apex (Fig. 5E, F, H). As emphasized by Medvedev (2007), the degree of development of the setae on ventral surface of pro- and mesotarsomeres of the male, and the setae on the inner side of tibiae steadily characterizes morphological distinctiveness of separate genera in the subtribe Gnaptorinina. However, Medvedev is sometimes a little over-dependent on the degree of development of the setae (Medvedev 2009), and this has been questioned by the molecular evidence (Li et al. 2021). Moreover, acquired activities can also damage setae. Thus, the first and the most important evidence presented by Medvedev (2007) is untenable. Secondly, in head capsule, and in appearance: setae on labrum and maxillary palpi, size and shape of eyes, shape of pronotum, and coloration of body are common characters, they may be distinct in separate genera, but are also variable between different species within a genus. Besides, the author is a bit exaggerates the differences between the genera *Belousovia* and *Colasia*, as the pictures presented in the publication (Medvedev 2007). Lastly, the female genital tubes can indeed be used to separate genera, as the author used in the diagnosis (Medvedev 2007), but is not a decisive character. Therefore, the last three distinctions observed by Medvedev are perhaps not enough to distinguish the genera *Belousovia* and *Colasia*.

### ***Colasia akisoides* Koch, 1965**

Figs 1–5, 28, 29, 33

*Colasia akisoides* Koch, 1965: 131; Medvedev 2001: 95; Löbl et al. 2008: 231; Ren et al. 2016: 333; Nabozhenko and Chigray 2020: 285.

**Type material. Lectotype, designated here:** ♂ (HNHM), Giufu-Shan / Szechuan / Em. Reitter // *depressa* // Paratypus 1965 / *Colasia akisoides* / C.Koch // *Colasia akisoides* C.Koch / Dr Z. Kaszab det., 1974 // LECTOTYPE / *Colasia akisoides* / Koch, 1965 / design. Bai, Liu, Ren, 2022 (Figs 1–4). **Paralectotypes:** 1♀ (HNHM), ♀ // Giufu-Shan / Szechuan / Em. Reitter // *depressa* // Paratypus 1965 / *Colasia akisoides* / C.Koch // Paralectotype / *Colasia akisoides* / Koch, 1965 / design. Bai, Liu, Ren, 2022; 1♀ (HNHM), ♀ // Kinfushan / Prov. Szechuan / West-China IV/V 29 / Coll.,H. Becker // *depressa* // Paratypus 1965 / *Colasia akisoides* / C.Koch // Paralectotype / *Colasia akisoides* / Koch, 1965 / design. Bai, Liu, Ren, 2022.

**Additional material. CHINA:** 1♂ (HBUM), 2015.VII.10 / 1665 m / North Slope of Jinfo Shan, Nanchuan District, Chongqing / 29°02'34"N / leaf litter / 107°11'10"E / Ri-Xin JIANG leg. / Mianyang Normal University, MYNU; 2♀ (HBUM), 2022. VI.30-VII.3 / Shangding, North Slope of Jinfo Shan, Chongqing / 2000 m / Tian-Xuan GU leg. / Hebei University Museum.

**Distribution.** China: Chongqing.



**Figures 1–4.** Habitus and type labels of *Colasia akisoides* Koch 1–3 lectotype, male in 1 dorsal 2 lateral, and 3 ventral views 4 type labels. Scale bar: 3.5 mm.



**Figure 5.** Characters of *Colasia akisoides* Koch, male, lectotype **A** head **B** antenna **C** pronotum **D** protibia **E** protarsus **F** mesotarsus (mesotarsomeres III–V are missing) **G** metatibia **G'** distal part of metatibia **H** metatarsus **I, J** aedeagus in dorsal and lateral view, respectively. Scale bars: 1.0 mm.

**Remarks.** This species was described based on the collection of Muséum national d’Histoire naturelle, Paris, France (Koch 1965), including ten specimens from China in the original description: “2♂♂ 2♀♀ <<Giufu-Shan, Szechuan>>! leg. REITTER; 1♂ 4♀♀, Kintushan, Prov. Szechuan, West-China>>! leg. BECKER; 1 ♀ <<Junan, Junan-fu>>!”.

In January 2017, the first author had a chance to visit the Muséum national d’Histoire naturelle, but no types of this species have been found. In May 2022, XB

asked Dr. Antoine Mantilleri (curator for Coleoptera at the MNHN) for help in searching for the types of this species. No such specimens were identified. Fortunately, three syntypes (1♂, 2♀) of this species were founded in HNHM and lent us to study by late Dr. Ottó Merkl. Therefore, the male type deposited in HNHM is designated as the lectotype in this paper, and the remaining types becoming paralectotypes.

The identification of the female paralectotype from Junan-fu (most likely Kunming City), Junan (Yunnan) is in doubt. On the one hand, according to the distribution of all the species of the revised genus *Colasia*, it is unlikely to be *C. akisoides*. On the other hand, it was once identified as *Asidoblaps glyptoptera* by Gebien (Koch 1965). Recently, we have obtained some specimens from Kunming, Yunnan, and they were confirmed to be *Asidoblaps* sp. after the identification. These specimens superficially resembled representatives of *Colasia*, but were obviously different by aedeagal morphology. Thus, we speculate that the female paralectotype from Yunnan belongs to the *Asidoblaps* species.

Giufu-Shan and Kinfushan (sometimes erroneously spelled Kintushan) both refer to the current Jinfo Shan (Bezdek et al. 2015; Kataev and Liang 2015; Ge et al. 2021). Jinfo Shan is located in southern Chongqing, Chongqing once belonged to Sichuan Province, and now it is a municipality directly under the Central Government. Thus, the type locality of this species is Jinfo Shan, and the distribution of this species should be changed from Sichuan and Yunnan (Löbl et al. 2008; Ren et al. 2016; Nabozhenko and Chigray 2020) to Chongqing.

**Redescription.** Body black, weakly shiny; legs shiny.

**Male. Head.** Apical maxillary palpomere triangular, covered with moderately dense and long setae. Anterior margin of labrum emarginate, lateral margins weakly arcuate. Anterior margin of epistoma emarginate; surface flat, matte, inconspicuous punctate. Frontoepistomal suture shallow and arcuate. Dorsal surface of head flat, matte, sparsely and finely granulated. Genal margins arcuately converging forwards, densely and shallowly punctures merged into short wrinkles. Emargination of outer margins of head above antennal base straight. Eyes transverse, not protruding beyond contour of head, distance between outer margins of eyes represent the widest of head; height 0.53 mm, width 0.17 mm from lateral view, respectively (height 3.1× width; 2.5× if the height and width rounded to one decimal place). Temples arcuately narrowing backwards, weakly granulated. Antennae slender and long, with the last segment reaching beyond pronotal base; basal part of antennomere I invisible in dorsal view; II–VII cylindrical, thicker at apex, II very short, III very long, V–VI equal in length, longer than IV and shorter than VII; VIII–X nearly spherical; XI sharpened-oval.

**Prothorax.** Pronotum cordiform, widest at middle, 1.5× wide as long, 1.8× wide as head, ratio of width at anterior margin to middle and base 7: 11: 8; anterior margin deeply emarginate, beaded laterally; lateral margins weakly “S” curved, entirely beaded and smooth; posterior margin straight at middle, beaded laterally; anterior angles rectangular and protruding forwards, posterior angles rectangular; surface matte, central convex, lateral sides weakly depressed along lateral margins, with shallowly and rounded depressions in sides of central, moderately depressed near posterior angles in sides

of base, longitudinal median line (median depression in Medvedev 2007) smooth and inconspicuous; shallowly, sparsely and finely punctate in central part, near posterior margin, lateral margins, and lateral sides of anterior margin with wrinkly punctures, sparsely and finely granulated. Prothoracic hypomera depressed, densely and shallowly wrinkled in longitudinal, with sparse and tiny granules. Prosternal process sharply sloping downwards behind procoxae, apex blunt in lateral view.

**Pterothorax.** Elytra oval, widest at middle, 1.3× long as wide, 1.3× wide as pronotum; base nearly as wide as pronotal base; dorsal surface matte, weakly convex, declivity sharply sloping downwards; humeral carinae smooth, with very sparse, smooth and large tubercles, sparse and fine granules, sparse, coarse and shallow wrinkles between humeral carinae; each elytron with two carinae (sensu Medvedev 2007) between suture and humeral carina, the second carina inconspicuous; declivity with sparse and short setae, slightly convex along suture; surface of epipleuron (sensu Kamiński et al. 2019) matte, edge relatively wide; pseudopleuron (outer part of elytra in Medvedev 2007) much wider than epipleuron, surface matte, with sparse and inconspicuous granules, edge thin and elevated, reaching sutural angle. Scutellum triangular, covered by pronotum.

**Abdomen.** Apex of ventrite 1, and base of ventrite 2 flat in middle; ventrites 1, 2, and anterior part of ventrite 3 rough, with moderately dense and long setae, and inconspicuous granules, densely, shallowly, and finely wrinkled at sides; posterior part of ventrite 3 smooth, shallowly punctate; ventrite 4 smooth, shallowly and finely punctate; last ventrite smooth, with sparse, fine punctures and short setae, apical margin widely rounded.

**Legs.** Slender and long. Femora claviform, mesofemora slightly longer than profemora, and shorter than metafemora. Protibiae weakly curved, distal part distinctly thick; mesotibiae and metatibiae straight, both gradually widened toward apex; distal part of metatibiae with a row of golden yellow hairy row on inner side. Ventral surface of pro- and mesotarsomeres I–IV, and metatarsomeres I–III with undeveloped hairy tuft at apex.

**Aedeagus.** Length 1.8 mm, width 0.5 mm. Parameres length 0.5 mm, width 0.4 mm. Parameres relatively wide and short, widest at base, basal 1/4 parallel, and then narrowing toward apex nearly straight, distal part weakly curved to ventral side in lateral view.

**Female.** Antennae not reaching pronotal base; elytra wider and more convex; abdominal ventrites 1 and 2 convex; inner side of metatibiae without golden yellow setae; other characters similar to male.

**Measurements.** Body length: 11.5–13.5 mm; width: ♂ 5.5–6.0 mm, ♀ 6.5–7.0 mm.

### ***Colasia bijica* sp. nov.**

<https://zoobank.org/08015B8B-836B-4E4E-9BF0-A4EC716F786F>

Figs 6, 22, 33

**Type material. Holotype:** ♂ (HBUM), 2011-IV-24 / JiUCAIPING, [Hezhang County, Bijie City], Guizhou / Wen-Bin JU leg.

**Diagnosis.** This new species closely resembles *C. akisoides* based on the pronotum cordiform, but can be distinguished from the latter by the following characters

(based on male): (1) emargination of outer margins of head above antennal base widely obtuse-angular (straight in *C. akisoides*); (2) distal part of metatibiae with a few golden yellow spines on inner side (with a row of golden yellow hairy row in *C. akisoides*); (3) parameres relatively narrow and long (wide and short in *C. akisoides*), widest at base, and narrowing toward apex nearly straight (basal 1/4 parallel, and then narrowing toward apex nearly straight in *C. akisoides*), distal part nearly straight in lateral view (weakly curved to ventral side in *C. akisoides*). This new species is also somewhat similar to *C. medvedevi* sp. nov. based on the distal part of metatibiae with a few golden yellow setae on inner side in male, it differs from the later by the following characters (based on male): (1) eyes not protruding beyond contour of head (slightly protruding beyond contour of head in *C. medvedevi* sp. nov.); (2) pronotum cordiform (transverse, subcordiform in *C. medvedevi* sp. nov.), anterior and posterior angles rectangular (nearly rectangular in *C. medvedevi* sp. nov.); (3) distal part of protibiae distinctly thick (protibiae gradually widened toward apex in *C. medvedevi* sp. nov.); (4) parameres relatively narrow and long (wide and short in *C. medvedevi* sp. nov.), widest at base, and narrowing toward apex nearly straight (basal 1/3 parallel, and then narrowing toward apex nearly straight in *C. medvedevi* sp. nov.), distal part nearly straight in lateral view (weakly curved to ventral side in *C. medvedevi* sp. nov.).

**Distribution.** China: Guizhou.

**Etymology.** The species name is derived from the type locality Bijie.

**Description.** Body black, weakly shiny; legs shiny.

**Male. Head.** Apical maxillary palpomere triangular, covered with moderately dense and long setae. Anterior margin of labrum emarginate, lateral margins parallel. Anterior margin of epistoma emarginate, nearly straight at middle; surface flat, matte, inconspicuous punctured. Frontoepistomal suture shallow and arcuate. Dorsal surface of head flat, matte, sparsely and finely granulated. Genal margins arcuately converging forwards, densely and shallowly punctures merging into shallow wrinkles. Emargination of outer margins of head above antennal base widely obtuse-angular. Eyes transverse, not protruding beyond contour of head, distance between outer margins of eyes represent the widest of head; height 0.53 mm, width 0.17 mm from lateral view, respectively (height 3.1× width; 2.5× if the height and width rounded to one decimal place). Temples arcuately narrowing backwards, weakly granulated. Antennae slender and long, with the last segment reaching beyond pronotal base; basal part of antennomere I invisible in dorsal view; antennomeres II–VII cylindrical, thicker at apex, II shortest, III longest, V–VI equal in length, longer than IV and shorter than VII; antennomeres VIII–X nearly spherical; antennomere XI sharp-edged-oval.

**Prothorax.** Pronotum cordiform, widest at middle, 1.4× wide as long, 1.8× wide as head, ratio of width at anterior margin to middle and base 8: 12: 10; anterior margin deeply emarginate, beaded laterally; lateral margins weakly “S” curved, entirely beaded and smooth; posterior margin bisinuate, beaded laterally; anterior angles rectangular and protruding forwards, posterior angles rectangular; surface matte, central convex, lateral sides weakly depressed along lateral margins, with shallowly and rounded depressions in sides of central, moderately depressed near posterior angles in sides of base, longitudinal median line smooth and inconspicuous; shallowly, sparsely, and finely punctate in cen-



**Figure 6.** Characters of *Colasia bijica* sp. nov., male, holotype **A** head **B** antenna **C** pronotum **D** protibia **E** protarsus **F** mesotarsus **G** metatibia **G'** distal part of metatibia **H** metatarsus **I, J** aedeagus in dorsal and lateral view, respectively. Scale bars: 1.0 mm.

tral part, near posterior margin, lateral margins, and lateral sides of anterior margin with wrinkly punctures, sparsely and finely granulated. Prothoracic hypomera depressed, densely and shallowly wrinkled in longitudinal, with sparse and tiny granules. Prosternal process sharply sloping downwards behind procoxae, apex blunt in lateral view.

**Pterothorax.** Elytra oval, widest near middle,  $1.3\times$  long as wide,  $1.4\times$  wide as pronotum; base nearly as wide as pronotal base; dorsal surface matte, weakly convex, declivity sharply sloping downwards; humeral carinae smooth, with very sparse, smooth and large tubercles, sparse and fine granules, sparse, coarse and shallow wrinkles between

humeral carinae; each elytron with two carinae between suture and humeral carina, the second carina inconspicuous; declivity with sparse and short setae, slightly convex along suture; surface of epipleuron matte, edge relatively wide; pseudopleuron much wider than epipleuron, surface matte, with sparse and inconspicuous granules, edge thin and elevated, reaching sutural angle. Scutellum triangular, covered by pronotum.

**Abdomen.** Apex of ventrite 1 flat in middle; ventrites 1, 2, and anterior part of ventrite 3 rough, with moderately dense and long setae, and inconspicuous granules, densely, shallowly, and finely wrinkled at sides; posterior part of ventrite 3 smooth, shallowly punctate; ventrite 4 smooth, shallowly and finely punctate; last ventrite smooth, apex with sparse, fine punctures and short setae, apical margin widely rounded.

**Legs.** Slender and long. Femora claviform, mesofemora slightly longer than profemora, and shorter than metafemora. Protibiae weakly curved, distal part distinctly thick; mesotibiae nearly straight, metatibiae straight, both gradually widened toward apex; distal part of metatibiae with a few golden yellow setae on inner side. Ventral surface of pro- and mesotarsomeres I–IV, and metatarsomeres I–III with undeveloped hairy tuft at apex.

**Aedeagus.** Length 1.7 mm, width 0.5 mm. Parameres length 0.6 mm, width 0.4 mm. Parameres relatively narrow and long, widest at base, and narrowing toward apex nearly straight, distal part nearly straight in lateral view.

**Female.** Unknown.

**Measurements.** Body length: ♂ 11.1 mm, width: ♂ 5.9 mm.

***Colasia helenae* (Medvedev, 2007), comb. nov.**

Figs 7–10, 33

*Belousovia helenae* Medvedev, 2007: 159; Ren et al. 2016: 328; Nabozhenko and Chigray 2020: 285.

**Type material (studied).** **Holotype:** ♂ (ZIN), CH, W Yunnan, SSW Liuku / 25 41 31 N / 98 47 16 E / H = 3000 m, 21.05.2006 / *Belousov & Kabak* leg. // Holotypus / *Belousovia helenae* G.Medvedev // ZOOLOGICAL / INSTITUTE RAS / ST. PETERSBURG.

**Additional material.** CHINA: 4♂, 7♀ (HBUM), 2008-VII-25 / Liuku Town, [Lushui City], Yunnan / Ji-Shan XU leg. / Hebei University Museum.

**Distribution.** China: Yunnan.

***Colasia kabaki intermedia* (Medvedev, 2007), comb. nov.**

Figs 11–14, 33

*Belousovia kabaki intermedia* Medvedev, 2007: 164; Ren et al. 2016: 331; Nabozhenko and Chigray 2020: 285.

**Type material (studied).** **Holotype:** ♂ (ZIN), CH, Yunnan, N Baoshan / 25 29 28 N / 99 05 35 E / 25 29 38 N / 99 04 51 E / 2790–3370 m, 09.05.2006 / *Belousov & Kabak*

leg. // Holotypus / *Belousovia kabaki* / *intermedia* G. Medvedev // ZOOLOGICAL / INSTITUTE RAS / ST. PETERSBURG.

**Distribution.** China: Yunnan.

***Colasia kabaki kabaki* (Medvedev, 2007), comb. nov.**

Figs 15–19, 23, 33

*Belousovia kabaki kabaki* Medvedev, 2007: 162; Ren et al. 2016: 330; Nabozhenko and Chigray 2020: 285.

**Type material (studied).** *Holotype*: ♂ (ZIN), CH, Yunnan, N Baoshan / 25 28 54 N / 99 05 05 E / H = 3200 m, 10.05.2006 / *Belousov & Kabak* leg. // Holotypus / *Belousovia* / *kabaki* G. Medvedev // ZOOLOGICAL / INSTITUTE RAS / ST. PETERSBURG.

**Additional material.** CHINA: 5♂, 3♀ (HBUM), 2008-VII-19 / Baoshan City, Yunnan / Ji-Shan XU et al. leg. / Hebei University Museum; 4♂, 1♀ (HBUM), 2009-IV-18 / Dapoqing, [Xieyangfeng Peak], Cang Shan, [Dali City], Yunnan, 2400 m / Zi-Zhong YANG leg. / Museum of China West Normal University; 1♀ (HBUM), 2009-VIII-22 / Dapoqing, Cang Shan, Yunnan, 2400 m / Ye ZHAO & Kui-Chang ZHANG leg. / Museum of China West Normal University; 3♂, 3♀ (HBUM), 2011-VI-20 / Dapoqing, Cang Shan, Yunnan / 2700 m, Wu-Bang WANG leg. / Biological Science Museum, Dali University; 8♂, 7♀ (HBUM), 2009-V-6 / 1986 Huoshaodi [Burned Blank of forest fires in 1986, refers to Dapoqing], Cang Shan, 2700 m / Ye ZHAO & Kui-Chang ZHANG leg. / Museum of China West Normal University; 1♂ (HBUM), 2009-VIII-7-9 / Ailao Shan, Jingdong County, Yunnan / Ji-Shan XU & Li-Xiang ZHANG leg. / Hebei University Museum // 24°32'30.3"N / 101°01'35.9"E / 2450 m / Hebei University Museum.

**Distribution.** China: Yunnan.

**Remarks.** Eye height 0.52 mm, width 0.17 mm from lateral view (height 3.1× width; 2.5× if the height and width are rounded to one decimal place).

***Colasia medvedevi* sp. nov.**

<https://zoobank.org/56F2B086-3BB0-4597-B8B5-D06614111873>

Figs 20, 24, 25, 33

*Colasia akisioides* sensu Medvedev, 2001: 110, 123, 145, 220, 243, 328, figs 68, 144, 254, 255, 873, 990, 1323.

**Type material.** *Holotype*: ♂ (HBUM), 2006-VII-14 / Junzi Shan, Shizong County, Yunnan / Ben-Yong MAO et al. leg. / Hebei University Museum. *Paratypes*: 2♂, 3♀ (HBUM), 2006-VII-14 / Junzi Shan, Shizong County, Yunnan / Ben-Yong MAO et al. leg. / Hebei University Museum; 1♂ (ZIN), China. Prov. Yunnan. Vallis flumin. Soling-ho. [Longchuan River, Yuanmou County (Wang 2022: 4)] // Coll. N. Skopin // Coll. G. Hauser // *Colasia akisioides* Koch. Det. N. Skopin, 1977.



**Figures 7–18.** Habitus and type labels of **7–10** *Colasia helenae* (Medvedev) male, holotype **11–14** *C. kabaki intermedia* (Medvedev) male, holotype, and **15–18** *C. kabaki kabaki* (Medvedev) male, holotype **7, 11, 15** dorsal views **8, 12, 16** lateral views **9, 13, 17** ventral views (photographs by Ivan Chigray).

**Diagnosis.** This new species closely resembles *C. helenae*, *C. kabaki intermedia*, and *C. kabaki kabaki* based on the pronotum transverse, subcordiform, but can be distinguished from the last three taxa by the following characters (based on male): (1)

distal part of metatibiae with a few golden yellow spines and setae on inner side (with a row of golden yellow hairy brush in *C. helenae*, *C. kabaki intermedia*, and *C. kabaki kabaki*); (2) elytral surface more wrinkled; (3) lateral margins of pronotum distinctly arcuate from middle to base (nearly straight in *C. helenae*, and *C. kabaki intermedia*); (4) basal 1/3 of parameres parallel, and then narrowing toward apex nearly straight (parameres widest at base, and narrowing toward apex nearly straight in *C. helenae*, and *C. kabaki kabaki*). This new species is also similar to *C. bijica* sp. nov. based on the distal part of metatibiae with a few golden yellow setae on inner side in male, the differences between them see diagnosis of *C. bijica* sp. nov.

**Distribution.** China: Yunnan.

**Etymology.** The species name is derived from the name of Prof. Gleb Sergeevich Medvedev, in memory of his outstanding contribution to the knowledge of the tribe Blaptini of the tenebrionid beetles.

**Description.** Body black, weakly shiny; legs shiny.

**Male. Head.** Apical maxillary palpomere triangular, covered with moderately dense and long setae. Anterior margin of labrum slightly emarginate, lateral margins parallel. Anterior margin of epistoma slightly emarginate; surface flat, matte, shallowly punctate. Frontoepistomal suture shallow and arcuate. Dorsal surface of head flat, matte, sparsely and finely granulated. Genal margins arcuately converging forwards, densely and shallowly punctures merged into short wrinkles. Emargination of outer margins of head above antennal base widely obtuse-angular. Eyes transverse, slightly protruding beyond contour of head, distance between outer margins of eyes represent the widest of head; height 0.52 mm, width 0.19 mm from lateral view, respectively (height 2.7× width; 2.5× if the height and width are rounded to one decimal place). Temples arcuately narrowing backwards, sparsely granulated. Antennae slender and long, with the last segment reaching beyond pronotal base; basal part of antennomere I invisible in dorsal view; antennomeres II–VII cylindrical, thicker at apex, II very short, III very long, V–VI equal in length, slightly longer than IV and shorter than VII; VIII–X nearly spherical; XI sharpened-oval.

**Prothorax.** Pronotum transverse, subcordiform, widest at middle, 1.5× wide as long, 1.9× wide as head, ratio of width at anterior margin to middle and base 7: 11: 8; anterior margin deeply emarginate, beaded laterally; lateral margins weakly “S” curved, entirely beaded and smooth; posterior margin straight at middle, beaded laterally; anterior angles nearly rectangular and protruding forwards, posterior angles nearly rectangular; surface matte, central convex, lateral sides weakly depressed along lateral margins, with shallowly and rounded depressions in sides of central, moderately depressed near posterior angles in sides of base, longitudinal median line smooth and weak; shallowly, sparsely, and finely punctate in central part, near posterior margin, lateral margins, and lateral sides of anterior margin with wrinkly punctures, sparsely and finely granulated. Prothoracic hypomera depressed, densely and shallowly wrinkled in longitudinal, with sparse and tiny granules. Prosternal process sharply sloping downwards behind procoxae, apex blunt in lateral view.



**Figure 19.** Characters of *Colasia kabaki kabaki* (Medvedev) (male) **A** head **B** antenna **C** pronotum **D** protibia **E** protarsus **F** mesotarsus **G** metatibia **G'** distal part of metatibia **H** metatarsus **I, J** aedeagus in dorsal and lateral view, respectively. Scale bars: 1.0 mm.

***Pterothorax.*** Elytra oval, widest at middle, 1.3× long as wide, 1.3× wide as pronotum; base nearly as wide as pronotal base; dorsal surface matte, relatively flat, declivity sharply sloping downwards; humeral carinae smooth, with very sparse, smooth and large tubercles, sparse and fine granules, sparse, coarse and shallow wrinkles between



**Figure 20.** Characters of *Colasia medvedevi* sp. nov., male, holotype **A** head **B** antenna **C** pronotum **D** protibia **E** protarsus **F** mesotarsus **G** metatibia **G'** distal part of metatibia **H** metatarsus **I, J** aedeagus in dorsal and lateral view, respectively. Scale bars: 1.0 mm.

humeral carinae; each elytron with two carinae between suture and humeral carina, the second carina inconspicuous; declivity with sparse and short setae; surface of epipleuron matte, edge relatively wide; pseudopleuron much wider than epipleuron, surface matte, with sparse and inconspicuous granules, edge thin and elevated, reaching sutural angle. Scutellum triangular, covered by pronotum.

**Abdomen.** Apex of ventrite 1, and base of ventrite 2 flat in middle; ventrites 1, 2, and anterior part of ventrite 3 rough, with moderately dense and long setae, and inconspicuous granules, densely, shallowly, and finely wrinkled at sides; posterior part of ventrite 3 smooth, shallowly punctate; ventrite 4 smooth, shallowly and finely punctate; last ventrite smooth, with sparse, fine punctures and short setae, apical margin widely rounded.

**Legs.** Slender and long. Femora claviform, mesofemora slightly longer than profemora, and shorter than metafemora. Protibiae weakly curved, mesotibiae nearly straight, metatibiae straight, both gradually widened toward apex; distal part of metatibiae with a few golden yellow setae on inner side. Ventral surface of pro- and mesotarsomeres I–IV, and metatarsomeres I–III with undeveloped hairy tuft at apex.

**Aedeagus.** Length 1.3 mm, width 0.6 mm. Parameres length 0.7 mm, width 0.5 mm. Parameres relatively wide and short, widest at base, basal 1/3 parallel, and then narrowing toward apex nearly straight, distal part weakly curved to ventral side in lateral view.

**Female.** Antennae not reaching pronotal base; elytra wider and convex; abdominal ventrites 1 and 2 convex; inner side of metatibiae without golden yellow setae; other characters similar to male.

**Measurements.** Body length: ♂ 12.8–13.5 mm, ♀ 13.0–14.0 mm; width: ♂ 6.2–6.5 mm, ♀ 7.2–7.5 mm.

***Colasia pilosa* sp. nov.**

<https://zoobank.org/DD8788CB-7E54-428F-9835-C0D1C1376B55>

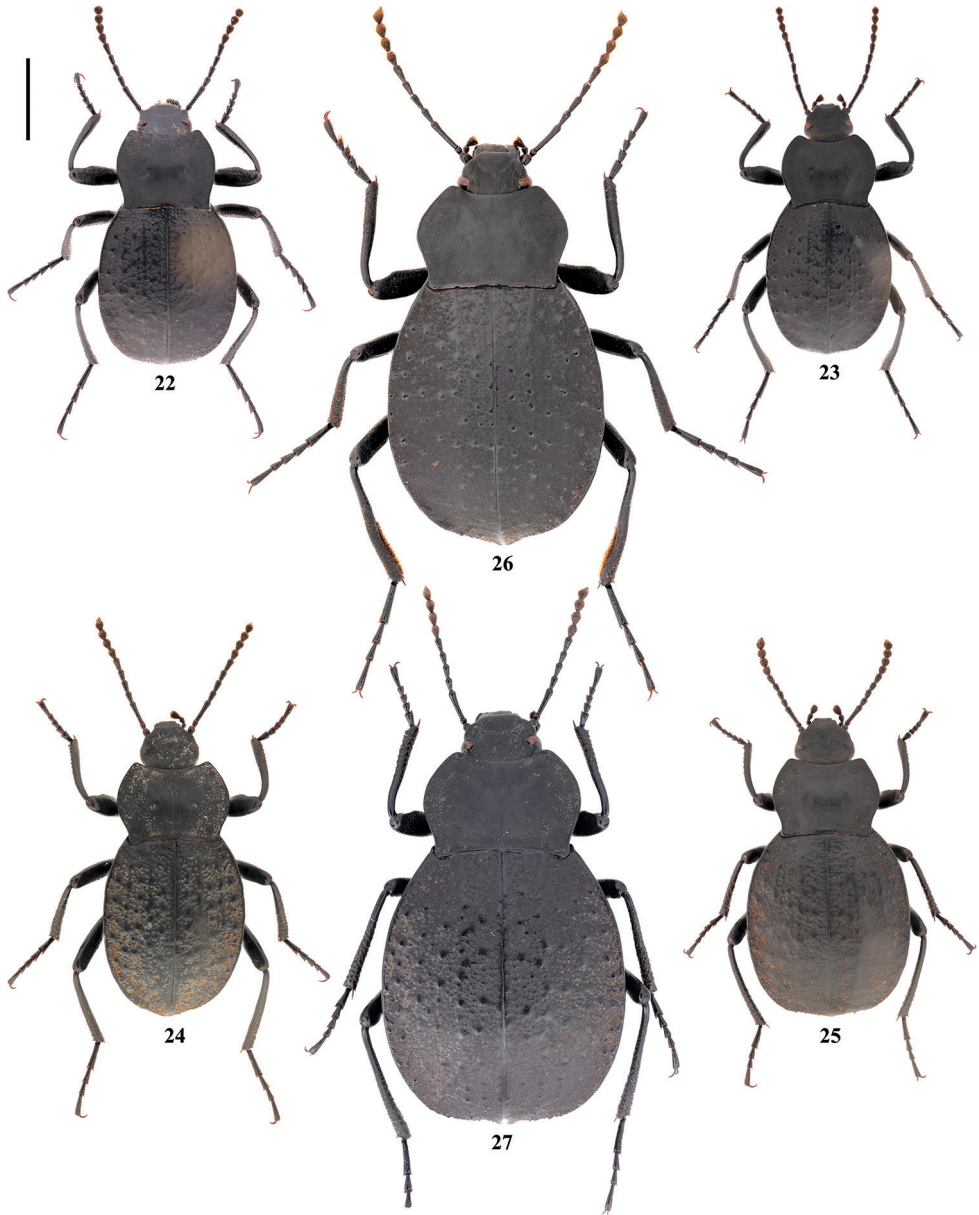
Figs 21, 26, 27, 30–33

**Type material. Holotype:** ♂ (HBUM), 2016.V.6 / Dajian Shan, Dawei Shan Nature Reserve, Pingbian County, Yunnan, 2100 m / Lu QIU leg. / Mianyang Normal University, MYNU. **Paratypes:** 1♀ (HBUM), 2016.V.6 / Dajian Shan, Dawei Shan Nature Reserve, Pingbian County, Yunnan, 2100 m / Lu QIU leg. / Mianyang Normal University, MYNU; 1♀ (MYNU), 2015.V.20 / Dajian Shan, Dawei Shan Nature Reserve, Pingbian County, Yunnan, 2100 m / Jian-Yue QIU leg. / Mianyang Normal University, MYNU; 1♀ (MYNU), 2016.X.27 / Dajian Shan, Dawei Shan Nature Reserve, Pingbian County, Yunnan, 2100 m / Gui-Qiang HUANG & Yan-Chao WANG leg. / Mianyang Normal University, MYNU; 1♂, 2♀ (MYNU), 2018.V.25–27 / Dajian Shan, Dawei Shan Nature Reserve, Pingbian County, Yunnan, 2100 m / Hao XU & Jian-Yue QIU leg. / Mianyang Normal University, MYNU; 1♂ (MYNU), 2021.V.29–VI.3 / Dajian Shan, Dawei Shan Nature Reserve, Pingbian County, Yunnan, 2050 m / Hao XU, Xin-Yuan ZHANG & Rui-Ying LIU leg. / Mianyang Normal University, MYNU; 3♂ (CTLH), 2022.V.28 / Dawei Shan Yakou, Pingbian County, Honghe Zhou [equivalent to City], Yunnan, 2050 m / Tian-Long HE & Zi-Dan XU leg.; 1♀ (CTLH), 2022.V.29 / Dawei Shan Yakou, Pingbian County, Honghe



**Figure 21.** Characters of *Colasia pilosa* sp. nov., male, holotype **A** head **B** antenna **C** pronotum **D** prothoracic tibia **E** protarsus **F** mesotarsus **G** metatibia **G'** distal part of metatibia **H** metatarsi **I, J** aedeagus in dorsal and lateral view, respectively. Scale bars: 1.0 mm.

Zhou [equivalent to City], Yunnan, 2050 m / Tian-Long HE & Zi-Dan XU leg.; 1♂ (HBUM), 2022-V-28 / Dawei Shan Yakou, Pingbian County, Yunnan / 2050 m, Tian-Long HE & Zi-Dan XU leg. / Hebei University Museum; 1♀ (HBUM), 2022-V-29 / Dawei Shan Yakou, Pingbian County, Yunnan / 2050 m, Tian-Long HE & Zi-Dan XU leg. / Hebei University Museum; 2♂, 3♀ (HBUM), 2010-V-22 /



**Figures 22–27.** Habitus of **22** *Colasia bijica* sp. nov. male, holotype **23** *C. kabaki kabaki* (Medvedev) male **24, 25** *C. medvedevi* sp. nov. **24** male, holotype **25** female, paratype, and **26, 27** *C. pilosa* sp. nov. **26** male, holotype **27** female, paratype. Scale bar: 3.5 mm.

Dawei Shan, Pingbian County, Yunnan / Chang-Chin CHEN leg. / Hebei University Museum; 1♀ (HBUM), 2010-V-20 / Dawei Shan, Pingbian County, Yunnan / 2100 m, Chang-Chin CHEN leg. / Hebei University Museum; 1♀ (HBUM), 2014-V-9-

10 / Dawei Shan, Pingbian County, Yunnan / Xiao-Yu ZHU leg. / Hebei University Museum; 1♂, 1♀ (HBUM), 2015-VI-20-21 / Dawei Shan, Pingbian County, Yunnan / Zi-Zhong YANG leg. / Institute of Entomocetics Research, Dali University; 2♂, 4♀ (HBUM), 2005-IV-25 / Pingbian County, Yunnan / Ben-Yong MAO leg. / Hebei University Museum.

**Diagnosis.** This new species is obviously different from other species in the following characters (based on male): body large size, length 15.5–17.5 mm (vs. 11.1–13.8 mm in other species); inner side of metatibiae with a row of well-developed densely hairy brush from middle to apex; ventral surface of pro- and mesotarsomeres I–IV, and metatarsomeres I–III with well-developed hairy brush from middle to apex; parameres laminar in dorsal view.

**Distribution.** China: Yunnan.

**Etymology.** The species name is derived from the dense hairy brush of male metatibiae.

**Description.** Body black, weakly shiny.

**Male. Head.** Apical maxillary palpomere triangular, covered with moderately dense and long setae. Anterior margin of labrum slightly emarginate, lateral margins weakly arcuate. Anterior margin of epistoma slightly emarginate; surface flat, matte, shallowly punctate. Frontoepistomal suture shallow and arcuate. Dorsal surface of head flat, matte, sparsely granulated at sides. Genal margins arcuately converging forwards, densely and shallowly punctate. Emargination of outer margins of head above antennal base widely obtuse-angular. Eyes transverse, protruding beyond contour of head, distance between outer margins of eyes represent the widest of head; height 0.80 mm, width 0.26 mm from lateral view, respectively (height 3.1× width; 2.7× if the height and width are rounded to one decimal place). Temples arcuately narrowing backwards, sparsely granulated. Antennae slender and long, with the last segment reaching beyond pronotal base; basal part of antennomere I invisible in dorsal view; antennomeres II–VII cylindrical, thicker at apex, II very short, III very long, IV and VI subequal in length, V and VII subequal in length; VIII–X nearly spherical; XI sharpened-oval.

**Prothorax.** Pronotum transverse, subcordiform, widest at middle, 1.5× wide as long, 1.9× wide as head, ratio of width at anterior margin to middle and base 6: 10: 8; anterior margin deeply emarginate, beaded laterally; lateral margins weakly “S” curved, entirely beaded and smooth; posterior margin straight at middle, beaded laterally; anterior angles nearly rectangular and protruding forwards, posterior angles nearly rectangular; surface matte, central convex, lateral sides weakly depressed along lateral margins, with moderately depressions in middle of sides and near posterior angles in sides of base, sometimes shallowly and transversely depressed before posterior margin in middle, longitudinal median line inconspicuous; shallowly, sparsely, and finely punctate in central part, near posterior margin, lateral margins, and anterior margin with wrinkly punctures, sparsely and finely granulated. Prothoracic hypomera depressed, densely and shallowly wrinkled in longitudinal, with sparse and tiny granules. Prosternal process sharply sloping downwards behind procoxae, apex blunt in lateral view.

**Pterothorax.** Elytra oval, widest at middle, 1.2× long as wide, 1.4× wide as pronotum; base wider than pronotal base; dorsal surface matte, relatively flat, declivity



**Figures 28–32.** Habitats of *Colasia akisoides* Koch **28** photograph by Ri-Xin Jiang **29** photograph by Tian-Xuan Gu. *C. pilosa* sp. nov. **30** female, photograph by Lu Qiu **31** male, photograph by Tian-Long He **32** photograph by Tian-Long He.

sharply sloping downwards; humeral carinae smooth, with very sparse, smooth and large tubercles, sparse and fine granules, sparse, coarse and shallow wrinkles between humeral carinae; each elytron with two carinae between suture and humeral carina, the second carina inconspicuous; declivity with sparse and short setae, slightly convex along suture; surface of epipleuron matte, edge relatively wide; pseudopleuron much

wider than epipleuron, surface matte, sparsely granulated, edge thin, reaching sutural angle. Scutellum triangular, covered by pronotum.

**Abdomen.** Apex of ventrites 1 and 2 weakly depressed or flat in middle; ventrites 1,2, and anterior part of ventrite 3 rough, with moderately dense and long setae, and inconspicuous granules, densely, shallowly, and finely wrinkled at sides; posterior part of ventrite 3 smooth, shallowly punctate; ventrite 4 smooth, shallowly and finely punctate; last ventrite smooth, with sparse, fine punctures and short setae, apical margin widely rounded.

**Legs.** Slender and long. Femora claviform, mesofemora slightly longer than profemora, and shorter than metafemora. Protibiae and metatibiae weakly curved, mesotibiae straight, both gradually widened toward apex; inner side of metatibiae with a row of densely golden yellow hairy row from middle to apex. Ventral surface of pro- and mesotarsomeres I–IV, and metatarsomeres I–III with dense hairy brush from middle to apex.

**Aedeagus.** Length 2.8 mm, width 0.9 mm. Parameres length 1.0 mm, width 0.7 mm. Parameres relatively wide and short, widest at base, and narrowing toward apex nearly straight, distal part straight in lateral view.

**Female.** Antennae not reaching pronotal base; elytra wider and more convex; abdominal ventrites 1 and 2 convex; inner side of metatibiae without golden yellow hairy row; ventral surface of tarsi without hairy brush; other characters similar to male.

**Measurements.** Body length: ♂ 15.5–17.5 mm, ♀ 16.0–18.0 mm; width: ♂ 8.5–9.5 mm, ♀ 9.5–10.6 mm.

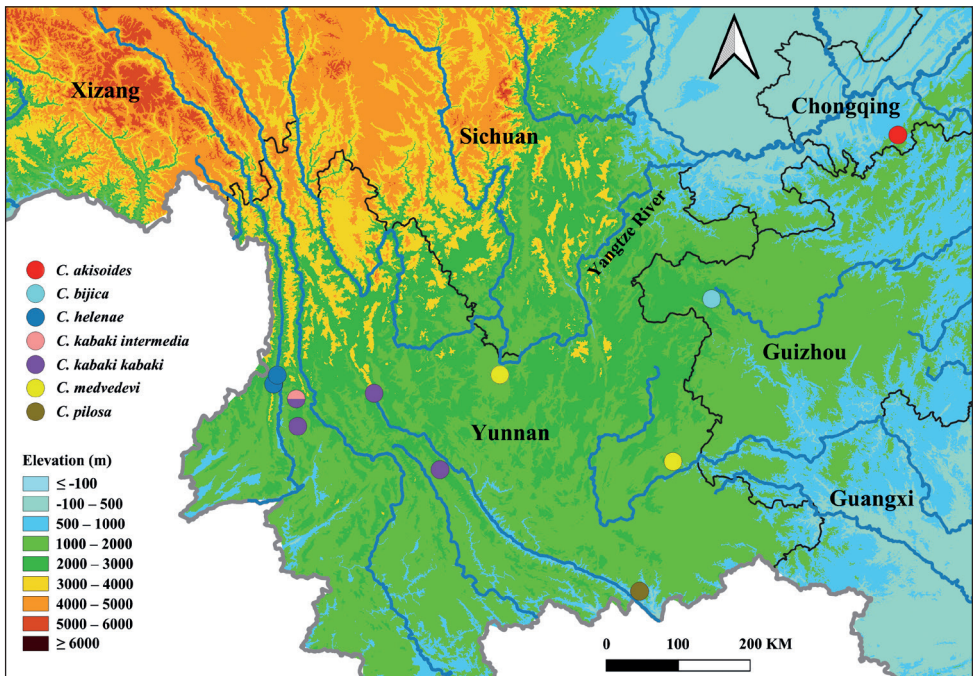


**Figure 33.** Distribution of the species of the revised genus *Colasia* (known to occur only in the south of the Yangtze River).

Key to species of the revised genus *Colasia* Koch, 1965 (based on males)

- 1 Body length 15.5–17.5 mm; inner side of metatibiae with a row of well-developed densely hairy brush from middle to apex (Fig. 21G’); ventral surface of pro- and mesotarsomeres I–IV, and metatarsomeres I–III with well-developed hairy brush from middle to apex (Fig. 21E, F, H) ..... ***C. pilosa* sp. nov.**
- Body length 11.1–13.8 mm; inner side of metatibiae with or without a row of hairy brush (Figs 5G’, 6G’); ventral surface of pro- and mesotarsomeres I–IV, and metatarsomeres I–III with less-developed hairy brush from middle to apex (Fig. 19E, F, H; Medvedev 2007: fig. 116) or with undeveloped hairy tuft at apex (Fig. 6E, F, H)..... **2**
- 2 Eyes not protruding beyond contour of head (Fig. 6A); pronotum strongly cordiform, anterior and posterior angles rectangular (Fig. 6C) ..... **3**
- Eyes slightly protruding beyond contour of head (Fig. 20A); pronotum transverse, weakly cordiform, anterior and posterior angles weakly obtuse or subrectangular (Fig. 20C) ..... **4**
- 3 Lateral margins of head straight above antennal base (Fig. 5A); distal part of metatibiae with a row of setae on inner side (Fig. 5G’); parameres relatively wide and short, basal 1/3 parallel, and then narrowing toward apex nearly straight, distal part weakly curved to ventral side in lateral view (Fig. 5I, J)..... ***C. akisoides* Koch, 1965**
- Lateral margins of head widely obtuse-angled above antennal base (Fig. 6A); distal part of metatibiae with a few setae on inner side (Fig. 6G’); parameres relatively narrow and long, widest at base, and narrowing toward apex nearly straight, distal part nearly straight in lateral view (Fig. 6I, J) ..... ***C. bijica* sp. nov.**
- 4 Distal part of metatibiae with a few setae on inner side (Fig. 20G’); lateral margins of pronotum distinctly arcuate from middle to base (Fig. 20C); basal 1/3 of parameres parallel, and then narrowing toward apex nearly straight (Fig. 20I, J)..... ***C. medvedevi* sp. nov.**
- Distal part of metatibiae with a row of setae on inner side (Fig. 19G’); lateral margins of pronotum distinctly arcuate (Fig. 20C) or nearly straight from middle to base (Medvedev 2007: fig. 125); parameres widest at base, and narrowing toward apex nearly straight; or basal 1/3 of parameres parallel, and then narrowing toward apex nearly straight (Fig. 19I, J; Medvedev 2007: figs 103, 119, 128)..... **5**
- 5 Basal 1/3 of parameres parallel, and then narrowing toward apex nearly straight (Medvedev 2007: fig. 128)..... ***C. kabaki intermedia* (Medvedev, 2007)**
- Parameres widest at base, and narrowing toward apex nearly straight (Fig. 19I, J; Medvedev 2007: figs 103, 119)..... **6**
- 6 Lateral margins of pronotum nearly straight from middle to base (Medvedev 2007: fig. 101) ..... ***C. helenae* (Medvedev, 2007)**
- Lateral margins of pronotum distinctly arcuate from middle to base (Fig. 19C)..... ***C. kabaki kabaki* (Medvedev, 2007)**

## Acknowledgements

We express heartfelt thanks to the late Dr. Ottó Merkl (Hungarian Natural History Museum, Budapest, Hungary) for the loan of type material of *Colasia akisoides*, to Prof. Ai-Min Shi (China West Normal University, Nanchong, China), Prof. Zi-Zhong Yang, and Dr. Ji-Shan Xu (both Dali University, Dali, China), Dr. Hao Xu and Dr. Lu Qiu (both Mianyang Normal University, Sichuan, China), Dr. Ri-Xin Jiang (Guizhou University, Guiyang, China), Mr. Tian-Long He (Huainan, China), and Mr. Tian-Xuan Gu (Sichuan Fine Arts Institute, Chongqing, China) for the specimens donated; and to the collectors for their hard work on the field trip. Dr. Ri-Xin Jiang, Dr. Lu Qiu, Mr. Tian-Long He, and Mr. Tian-Xuan Gu also shared their photographs of the habitats of two species with us. We sincerely thank Mr. Ivan Chigray (Zoological Institute of Russian Academy of Sciences, St. Petersburg, Russia) for his help in taking photographs of three holotypes, to Dr. Antoine Mantilleri (Muséum national d'Histoire naturelle, Paris, France) for his help in searching for the types of *Colasia akisoides*, to Dr. Christophe Hervé (Muséum national d'Histoire naturelle, Paris, France) and Dr. Sun-Bin Huang (South China Agricultural University, Guangzhou, China) for their information on M.G. Colas. Our thanks are also due to Prof. Patrice Bouchard (Agriculture and Agri-Food Canada, Ottawa, Canada), Prof. Maxim Nabozhenko (Daghestan Federal Research Centre of the Russian Academy of Sciences, Makhachkala, Russia), Prof. Marcin Jan Kamiński (Zoological Museum, Museum and Institute of Zoology, Polish Academy of Sciences, Warsaw, Poland), and Dr. Nathalie Yonow (Department of Biosciences, Swansea University, Wales, UK) for their valuable comments and improvements of our manuscript. Special thanks to Mr. Quan-Yu Ji (School of Life Sciences, Hebei University) for his help taking photographs. This work was supported by the National Natural Science Foundation of China (No. 31970452), and Postdoctoral Foundation of Hebei Normal University (No. 13505254).

## References

- Bezděk A, Král D, Sládeček FXJ (2015) *Oniticellus (Liatongus) boucomonti* Balthasar, 1932 (Coleoptera: Scarabaeidae: Scarabaeinae: Oniticellini)—clarification of its taxonomic status by lectotype designation. *Zootaxa* 3974(1): 145–147. <https://doi.org/10.11646/zootaxa.3974.1.13>
- Bouchard P, Bousquet Y, Aalbu RL, Alonso-Zarazaga MA, Merkl O, Davie AE (2021) Review of genus-group names in the family Tenebrionidae (Insecta, Coleoptera). *ZooKeys* 1050: 1–633. <https://doi.org/10.3897/zookeys.1050.64217>
- Ge SX, Hu SJ, Shi HL, Han FY, Li MJ, Ren LL (2021) The first record of the genus *Belenois* (Lepidoptera: Pieridae) from China. *Biodiversity Data Journal* 9: e61332. <https://doi.org/10.3897/BDJ.9.e61332>
- Kamiński MJ, Kanda K, Lumen R, Smith AD, Iwan D (2019) Molecular phylogeny of Pedini (Coleoptera, Tenebrionidae) and its implications for higher-level classification. *Zoological Journal of the Linnean Society* 185: 77–97. <https://doi.org/10.1093/zoolinnean/zly033>
- Kamiński MJ, Lumen R, Kanda K, Iwan D, Johnston MA, Kergoat GJ, Bouchard P, Bai XL, Li XM, Ren GD, Smith AD (2021) Reevaluation of Blapimorpha and Opatrinae: address-

- ing a major phylogeny-classification gap in darkling beetles (Coleoptera: Tenebrionidae: Blaptinae). *Systematic Entomology* 46(1): 140–156. <https://doi.org/10.1111/syen.12453>
- Kataev BM, Liang HB (2015) Taxonomic review of Chinese species of ground beetles of the subgenus *Pseudoophonus* (genus *Harpalus*) (Coleoptera: Carabidae). *Zootaxa* 3920(1): 1–39. <https://doi.org/10.11646/zootaxa.3920.1.1>
- Koch C (1965) Sur les types de Fairmaire des tribus Blaptini et Platyscelini conservés au Muséum de Paris (Col. Tenebrionidae). *Annales de la Société Entomologique de France* 1: 125–135. [Nouvelle Série]
- Leach WE (1815) Entomology: 57–172. In: Brewster D (Ed.) *Brewster's Edinburgh Encyclopedia* (Vol. IX) [part I]. W. Blackwood, J. Waugh, etc., Edinburgh, 764 pp.
- Li XM, Bai XL, Kergoat GJ, Pan Z, Ren GD (2021) Phylogenetics, historical biogeography and molecular species delimitation of *Gnaptorina* Reitter (Coleoptera: Tenebrionidae: Blaptini). *Systematic Entomology* 46(1): 239–251. <https://doi.org/10.1111/syen.12459>
- Löbl I, Nabozhenko M, Merkl O (2008) Tribe Blaptini Leach, 1815: 219–238. In: Löbl I, Smetana A (Eds) *Catalogue of Palaearctic Coleoptera* (Vol. 5). Tenebrionoidea. Apollo Books, Stenstrup, 670 pp.
- Medvedev GS (1998) To the knowledge of the tenebrionid beetles of the tribe Blaptini (Coleoptera, Tenebrionidae) of eastern part of the Tibet plateau. *Entomological Review* 78: 79–111. [in Russian, *Entomologicheskoe Obozrenie* 77: 171–208]
- Medvedev GS (2001) Evolution and system of darkling beetles of the tribe Blaptini (Coleoptera, Tenebrionidae). *Meetings in memory of N.A. Kholodkovsky. Iss. 53. Russian Entomological Society Press, St.-Petersburg*, 332 pp. [In Russian]
- Medvedev GS (2007) A contribution to the taxonomy and morphology of the tribe Blaptini (Coleoptera, Tenebrionidae). *Entomological Review* 87(2): 181–214. [In Russian, *Entomologicheskoe Obozrenie* 86(1): 132–170] <https://doi.org/10.1134/S0013873807020078>
- Medvedev GS (2009) Composition of the genera *Gnaptorina* Reitter and *Pseudognaptorina* Kaszab of the tribe Blaptini (Coleoptera, Tenebrionidae). *Entomological Review* 89(4): 451–461. [In Russian, *Entomologicheskoe Obozrenie* 88(2): 416–429] <https://doi.org/10.1134/S0013873809040095>
- Medvedev GS, Merkl O (2003) *Viettagona vietnamensis* gen. et sp. n. from Vietnam (Coleoptera, Tenebrionidae: Blaptini). *Acta Zoologica Academiae Scientiarum Hungaricae* 48[2002]: 317–332.
- Nabozhenko M, Chigray I (2020) Tribe Blaptini Leach, 1815: 268–296. In: Iwan D, Löbl I (Eds) *Catalogue of Palaearctic Coleoptera* (Vol. 5). Tenebrionoidea. Revised and Updated Second Edition. Koninklijke Brill NV, Leiden-Boston, 945 pp. <https://doi.org/10.1163/9789004434998>
- Ren GD, Ba YB, Liu HY, Niu YP, Zhu XC, Li Z, Shi AM (2016) *Fauna Sinica. Insecta* (Vol. 63). Coleoptera. Tenebrionidae (I). Science Press, Beijing, 532 pp. [In Chinese, with English abstract]
- Skopin NG (1960) Material on the morphology and ecology of larvae of the tribe Blaptini (Coleoptera, Tenebrionidae). *Trudy instituta zoologii Akademii nauk Kazakhskoy SSR* 11: 36–71. [In Russian]
- Wang FL (2022) Three new species of genus *Anomala* Samouelle from Yunnan, China (Coleoptera: Scarabaeidae, Rutelinae). *Faunitaxys* 10(56): 1–9. [https://doi.org/10.57800/faunitaxys-10\(56\)](https://doi.org/10.57800/faunitaxys-10(56))



# Evidence using morphology, molecules, and biogeography clarifies the taxonomic status of mole crabs of the genus *Emerita* Scopoli, 1777 (Anomura, Hippidae) and reveals a new species from the western Atlantic

Fernando L. Mantelatto<sup>1</sup>, Juliana M. Paixão<sup>1</sup>, Rafael Robles<sup>2</sup>,  
Jeniffer N. Teles<sup>1</sup>, Felipe C. Balbino<sup>1</sup>

**1** Laboratory of Bioecology and Crustacean Systematics (LBSC), Faculty of Philosophy, Sciences and Letters at Ribeirão Preto (FFCLRP), University of São Paulo (USP), Av. Bandeirantes 3900, 14040-901, Ribeirão Preto, SP, Brazil **2** Facultad de Ciencias Químico-Biológicas, Universidad Autónoma de Campeche, Campus V. Predio s/n – Avenida Ing. Humberto Lanz Cárdenas y Fracc. Ecológico Ambiental Siglo XXIII, Colonia Ex Hacienda Kalá, San Francisco de Campeche, Camp., 24085, Mexico

Corresponding author: Fernando L. Mantelatto ([flmantel@usp.br](mailto:flmantel@usp.br))

Academic editor: I. S. Wehrtmann | Received 30 December 2022 | Accepted 10 April 2023 | Published 12 May 2023

<https://zoobank.org/1F8B2202-F33C-4036-B30E-FC4BF141A414>

**Citation:** Mantelatto FL, Paixão JM, Robles R, Teles JN, Balbino FC (2023) Evidence using morphology, molecules, and biogeography clarifies the taxonomic status of mole crabs of the genus *Emerita* Scopoli, 1777 (Anomura, Hippidae) and reveals a new species from the western Atlantic. ZooKeys 1161: 169–202. <https://doi.org/10.3897/zookeys.1161.99432>

## Abstract

Uncertainties regarding the taxonomic status and biogeographical distribution of some species of the genus *Emerita* from the western Atlantic led to thorough examination of the subtle morphological differences between two coexistent species (*E. brasiliensis* Schmitt, 1935 and *E. portoricensis* Schmitt, 1935) along the Brazilian coast and compare them using two genetic markers. The molecular phylogenetic analysis based on sequences of the 16S rRNA and COI genes showed that individuals identified as *E. portoricensis* were clustered into two clades: one containing representatives from the Brazilian coast and another containing specimens distributed in Central America. Our molecular-based phylogeny, combined with a detailed morphological analysis, revealed the Brazilian population as a new species, which is described here as *Emerita almeidai* Mantelatto & Balbino, **sp. nov.** The number of species in the genus *Emerita* is now raised to 12, with five of them occurring in the western Atlantic, five in the Indo-Pacific, and two in the eastern Pacific.

## Keywords

16S rRNA, COI, Cryptic diversity, distribution, molecular data, phylogeny

## Introduction

The superfamily Hippoidea Latreille, 1825 is one of the seven superfamilies that belong to the highly diverse infraorder Anomura Macleay, 1838 (Boyko and McLaughlin 2010). It is represented by three families of sand/mole crabs: Albuneidae Stimpson, 1858 (nine genera and 53 recognized species), Blepharipodidae Boyko, 2002 (two genera and six species) and Hippidae Latreille, 1825 (three genera and 28 species) (Boyko 2002; WoRMS 2023). Representatives of all these families are well known due to their presence in intertidal sandy beaches of temperate, tropical, and subtropical areas. Their ability to bury themselves in this environment of constant hydrodynamics is one of the most outstanding characteristics of this group.

The genus *Emerita* Scopoli, 1777 (family Hippidae) contains eleven species that are widely distributed around the globe, living in intertidal and upper subtidal sandy marine regions. Their filter feeding habit is an ecologically essential activity in sandy beach environments (Rodgers 1987; Lercari and Defeo 1999; Hubbard and Dugan 2003). These sand crabs are also considered as bioindicators of environment quality (Pérez 2003; Petracco et al. 2003). Five species are reported in the Indo-Pacific [*Emerita emeritus* (Linnaeus, 1767), *E. austroafricana* Schmitt, 1937, *E. holthuisi* Sankolli, 1965, *E. karachiensis* Niazi & Haque, 1974, and *Emerita taiwanensis* Hsueh, 2015], two in the eastern Pacific [*Emerita analoga* (Stimpson, 1857) and *Emerita rathbunae* Schmitt, 1935], and four in the western Atlantic [*Emerita talpoida* Say, 1817, *E. benedicti* Schmitt, 1935, *E. brasiliensis* Schmitt, 1935, and *E. portoricensis* Schmitt, 1935].

Most of the studies that established the current taxonomic status of species in *Emerita* were based on morphology (see Calado 1990 and Melo 1999 for revisions). Molecular data has been used to test for genetic flow between distant populations of conspecifics of *E. analoga* and *E. talpoida* from the eastern Pacific and western Atlantic populations, respectively (Tam et al. 1996). Later, a molecular phylogeny, using two genetic markers, rejected the hypothesis that species of *Emerita* from the New World form a monophyletic group (Haye et al. 2002). Recently, specimens of *Emerita* from Indonesia were evaluated using DNA barcoding and morphology to identify, but not describe a new species (Bhagawati et al. 2020, 2022). More recently, the inaccurate identity of some specimens and the distribution of *E. portoricensis* was clarified (Felder et al. 2023).

The two species of *Emerita* reported from the Brazilian coast are *E. brasiliensis* and *E. portoricensis*. The former species can be found in Venezuela, Trinidad and Tobago, Brazil (Espírito Santo, Rio de Janeiro, São Paulo, Paraná, Santa Catarina, Rio Grande do Sul), Uruguay, and Argentina (Efford 1976; Calado 1998; Melo 1999; Veloso and Cardoso 1999; Spivak et al. 2019; Mantelatto et al. 2021), with a gap of records from Venezuela to Bahia (Brazil), the species is abundant from Espírito Santo to southern Brazil (Mantelatto et al. 2021; present work). *Emerita portoricensis* occurs in Central American mainland shorelines of the Caribbean Sea, confirmed to include, but not limited to Puerto Rico, Dominican Republic, Virgin Islands, Jamaica, Belize, Costa Rica, Panama, Colombia, St. Lucia, St. Thomas, Venezuela, and Trinidad and Tobago (Felder et al. 2023); Brazilian records (from Maranhão to

Sergipe) have been treated as *E. portoricensis* by several authors (Schmitt 1935; Efford 1976; Calado 1990; Melo 1999).

These patterns of geographical distribution and uncertain records in the western Atlantic raise questions about whether these gaps are due to a lack of faunal surveys and/or a misidentification of specimens that are morphologically similar. Thus, we were motivated to perform a reassessment of the specimens assigned as *E. portoricensis* and *E. brasiliensis* along the Brazilian coast, using both morphological and molecular tools to evaluate the phylogenetic relationships between species of *Emerita*. We also examined the possible existence of cryptic taxa, which resulted in the new species described herein.

## Materials and methods

### Sample collection and morphological data

Almost all specimens of *Emerita* analyzed herein were obtained by us and are deposited in the Crustacean Collection of the Department of Biology (CCDB) at the Faculty of Philosophy, Sciences and Letters at Ribeirão Preto (FFCLRP), University of São Paulo (USP), Brazil. Additional species of *Emerita* and other genera of Albuneidae (see Boyko 2002) were obtained and used in order to root the phylogenetic analyses. Individuals were collected by hand during low tide at different sandy beaches along the geographic distribution of the species (see references in Introduction). We also studied specimens obtained by means of loans or donations from University of Louisiana at Lafayette Zoological Collection, LA, United States (ULLZ – recently transferred to the National Museum of Natural History, Smithsonian Institution, Washington, D.C. USNM; old catalog numbers are used in the text).

Specimens were identified according to previous morphological characters established in the literature (Calado 1990; Melo 1999; Felder et al. 2023). All data along with new characters/variation were also considered for the comparative analysis along the species' geographic distribution. When secondary sexual characters (presence of the gonopores on the coxae of the fifth pair of pereopods and absence of mature pleopods for males – ♂s, and the presence of the gonopores on the coxae of the third pair of pereopods and presence of mature pleopods or eggs for females – ♀s) were not conspicuously observed, specimens were classified as juveniles (Delgado and Defeo 2006). Most of the morphological characters followed the references cited above and are designated in Fig. 1. Analyses were made and photographs were taken under a LEICA M205C stereomicroscope equipped with a LEICA DFC 295 camera, and measurements (mm) of structures were taken using the software Leica Application Suite.

### Abbreviations

- coll(s).** collector(s),
- cl.** carapace length,
- cw.** carapace width,

- dl.** dactylus length,  
**dw.** dactylus width,  
**tl.** telson length,  
**tw.** telson width.

### Brazilian states

- BA** Bahia,  
**CE** Ceará,  
**ES** Espírito Santo,  
**PE** Pernambuco,  
**RJ** Rio de Janeiro,  
**RN** Rio Grande do Norte,  
**SC** Santa Catarina,  
**SP** São Paulo.

### Molecular data

The molecular markers 16S rRNA and cytochrome c oxidase subunit I (COI) were chosen because these mitochondrial genes are effective in studies that contribute to our comprehension of decapod diversity (see Schubart et al. 2000 and Timm and Bracken-Grissom 2015 for references), including anomuran members (Mantelatto et al. 2006, 2009; Miranda et al. 2020) and the target genus (Bhagawati et al. 2020, 2022). In this study, we used four different primers (see below).

We used muscle tissue from the telson or 3<sup>rd</sup> pereopods for DNA extraction according to the protocols proposed by Mantelatto et al. (2007) and Robles et al. (2007), and some

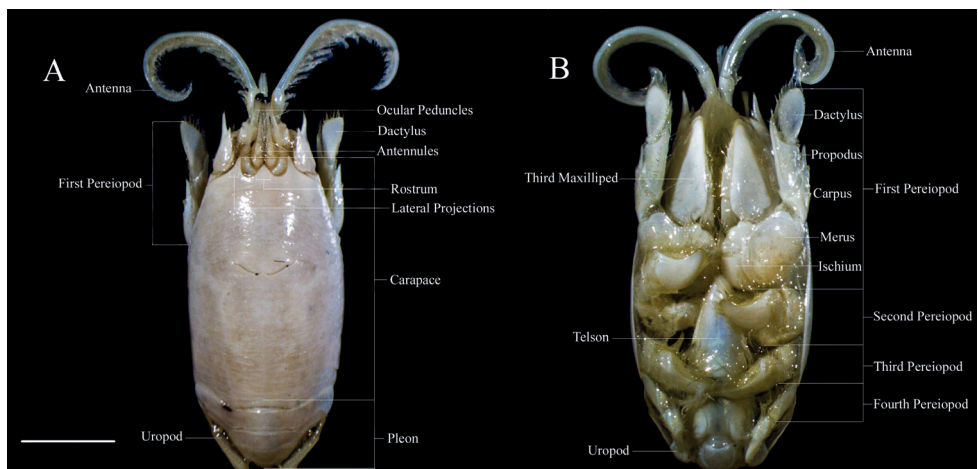


**Figure 1.** **A** dorsal view of adult ♀ of *Emerita almeidai* sp. nov. (CCDB 3369) **B** ventral view of adult ♀ of *Emerita brasiliensis* (CCDB 2552). The main characters used for external morphology analysis are labeled. Scale bar: 5 mm.

adaptations were made to suit our material using the manufacturer's protocol of the salt-out method (Miller et al. 1988). The extracted DNA's final concentration was measured using a spectrophotometer (NanoDrop 2000/2000c). Approximately 658 base pairs (bp) of the COI and 316 bp of the 16S rRNA genes were amplified using polymerase chain reactions (PCR) by thermal cycler (Veriti 96 Well Thermal Cycler Applied Biosystems). Fragments were amplified using the following thermal profiles: 16S rRNA – initial denaturing for 2 min at 94 °C; annealing for 40 cycles, 45 s at 94 °C, 45 sec at 46 °C and 1 min at 72 °C; final extension for 10 min at 72 °C; COI – initial denaturing for 2 min at 94 °C; annealing for 35 cycles, 30 sec at 94 °C, 30 sec at 50 °C, and 1 min at 72 °C; final extension for 7 min at 72 °C. We used the following primers: 16S-1472 (5'–AGA TAG AAA CCA ACC TGG – 3') (Crandall and Fitzpatrick 1996) and 16SL (5'–CGC CTG TTT ATC AAA AAC AT – 3') (Palumbi and Benzie 1991), HCO1-2198 (5'–TAA ACT TCA GGG TGA CCA AAA AAT CA – 3') and LCO1-1490 (5'–GGT CAA CAA ATC ATA AAG ATA TTG – 3') (Folmer et al. 1994). PCR products were observed in electrophoresis with 1.0% agarose gel and photographed with digital camera Olympus C-7070 on a UV transilluminators M20 UVP. Successful PCR products were purified using the SureClean Plus kit, following the manufacturer's protocol. Purified samples were sent to the Department of Technology at the College of Agricultural and Veterinary Sciences (FCAV, Jaboticabal) at São Paulo State University (UNESP) for sequencing.

A consensus was reached between the forward and reverse sequences of each specimen in BioEdit v. 7.0.5 (Hall 2005), and unspecific readings were manually corrected when required. Primer regions and non-readable parts at the beginning of the sequences were omitted. All consensus sequences were deposited in GenBank (<http://www.ncbi.nlm.nih.gov/genbank/>).

The alignment of the consensus of all sequences used in the phylogeny was performed with MAFFT (Kato and Standley 2006) in the software Geneious 2022.1 (Kearse et al. 2012). Three maximum likelihood (ML) phylogenetic analyses were performed using the IQ-TREE program (Miller et al. 2010), one with the COI gene, one with the 16S rRNA gene, and one using a concatenated alignment. The evolutionary model that best fit the data was determined by IQ-TREE according to the Bayesian Information Criterion (BIC) (Luo et al. 2010) and used for tree inference. The branch support was evaluated by ultra-fast bootstrap with 2000 pseudoreplicates.

## Results

### Molecular data

We generated new sequences for 38 individuals from different localities: for 16S rRNA – 1 of *Emerita analoga*, 10 of *Emerita almeidai* sp. nov., 1 of *Emerita benedicti*, 11 of *Emerita brasiliensis*, 1 of *Emerita portoricensis*, 3 of *Emerita rathbunae*, and 3 of *Emerita talpoida*; for COI – 9 of *E. almeidai* sp. nov., 1 of *E. analoga*, 1 of *E. benedicti*, 15 of *Emerita brasiliensis*, 2 of *E. portoricensis*, 2 of *E. rathbunae*, and 2 of *E. talpoida*. Additional sequences from GenBank were used to build a robust reconstruction (Table 1).

**Table 1.** Species of *Emerita* and *Lepidopa* used in the molecular analyses. CCDB: Coleção de Crustáceos do Departamento de Biologia, FFCLRP, USP, Brazil; ULLZ: University of Louisiana at Lafayette Zoological Collection, USA (recently transferred to National Museum of Natural History, Smithsonian Institution, Washington, D.C. (USNM)); (-) = data not available.

Species	Locality	Catalogue number	GenBank accession number	
			COI	16S
<i>E. analoga</i>	California, USA	–	–	AF246153
	California, USA	–	–	L43107
	California, USA	–	–	L43108
	California, USA	–	–	AF425322
	Oregon, USA	–	GU443297	–
	–	–	HQ341148	–
	–	–	HQ340917	–
	Calfuco, Chile	CCDB 4870	OQ679992	KP091505
Algaborro, Chile	–	–	AF246154	
	–	–	–	
<i>E. almeidai</i> sp. nov.	Rio Grande Norte, Brazil	CCDB 3369	KP091512	KP091493
	Rio Grande Norte, Brazil	CCDB 3376	KP091509	KP091491
	Rio Grande Norte, Brazil	CCDB 3380	KP091507	KP091489
	Rio Grande Norte, Brazil	CCDB 3393	KP091514	KP091496
	Pernambuco, Brazil	CCDB 4937	KP091515	KP091498
	Alagoas, Brazil	CCDB 4869	KP091516	KP091497
	Bahia, Brazil	CCDB 2606	–	KP091495
	Bahia, Brazil	CCDB 3026	KP091508	KP091490
	Bahia, Brazil	CCDB 4262	KP091513	KP091494
	Espírito Santo, Brazil	CCDB 3992	KP091510	KP091488
Rio de Janeiro, Brazil	CCDB 4376	KP091511	KP091492	
<i>E. benedicti</i>	Los Tuxtlas, Mexico	CCDB 4674	KP091525	KP091501
	Texas, USA	–	–	AF256155
	Texas, USA	–	–	L43109
<i>E. brasiliensis</i>	Espírito Santo, Brazil	CCDB 3990	KP091533	KP091477
	Espírito Santo, Brazil	CCDB 3994	KP091536	KP091481
	Rio de Janeiro, Brazil	CCDB 4119	KP091537	KP091482
	Rio de Janeiro, Brazil	CCDB 4935	KP091527	–
	São Paulo, Brazil	CCDB 1442	KP091530	KP091475
	São Paulo, Brazil	CCDB 1443	KP091531	–
	São Paulo, Brazil	CCDB 2552	–	KP091478
	São Paulo, Brazil	CCDB 2751	–	KP091483
	São Paulo, Brazil	CCDB 3923	KP091529	–
	São Paulo, Brazil	CCDB 3924	KP091532	KP091476
	São Paulo, Brazil	CCDB 4617	KP091538	KP091484
	Santa Catarina, Brazil	CCDB 4407	KP091534	KP091479
	Santa Catarina, Brazil	CCDB 4409	KP091535	KP091480
	Rio Grande Sul, Brazil	CCDB 4985	KP091526	–
	Rio Grande Sul, Brazil	CCDB 4986	KP091528	–
	Rio Grande Sul, Brazil	CCDB 3921	KP091539	–
	Fortaleza de Santa Teresa, Uruguay	–	–	L43110
	–	–	–	DQ079712
	<i>E. emeritus</i>	Pondichvory, India	–	–
–		–	–	–
<i>E. holthuisi</i>	Dubai, United Arab Emirates	–	–	AF246157
<i>E. portoricensis</i>	Mayaguez, Puerto Rico	–	–	L43111
	Boca del Drago, Panama	CCDB 3525	KP091517	KP091486
	Boca del Drago, Panama	USNM 1546871 (= ULLZ 13325)	KP091519	–
<i>E. rathbunae</i>	–	–	–	JN800539
	Acapulco, Mexico	CCDB 1029	KP091523	KP091499

Species	Locality	Catalogue number	GenBank accession number	
			COI	16S
<i>E. talpoida</i>	Los Tuxtlas, Mexico	CCDB 4675	KP091521	KP091502
	South Carolina, USA	–	–	AF246150
	Massachusetts, USA	–	–	AF246151
	Massachusetts, USA	–	–	L43112
	Massachusetts, USA	–	–	L43113
	Florida, USA	ULLZ 13055	KP091522	KP091503
	Florida, USA	ULLZ 10144	–	KP091504
	Florida, USA	–	–	L43114
	Florida, USA	–	–	AF246152
<i>Lepidopa richmondi</i>	São Paulo, Brazil	CCDB 3920	KP091540	KP091506

### 16S rRNA reconstruction

The automated alignment of 16S rRNA with 316 bp included 50 sequences of *Emerita* species. The phylogenetic tree, generated by ML analyses, indicated a clear separation of each species of *Emerita* (Fig. 2). *Emerita brasiliensis* consisted of a single clade, with all specimens assigned to this species, which was supported by bootstrap values of 96%. In this analysis, the closest relative of *E. brasiliensis* was *E. rathbunae*, although with low support (31%).

All specimens of *E. almeidai* sp. nov. were clustered in a strongly supported clade (bootstrap values of 91%), which was the sister group of *E. portoricensis* s.s. from Central America (bootstrap values of 99%). Specimens of *Emerita talpoida* were split into two groups, one of them containing individuals from Florida (USA) and Mexico and the second one containing individuals from Massachusetts and South Carolina (USA). The positioning of a supposed “*E. analoga*” (AF425322) in this second group indicated a misidentification that should be fixed in the GenBank database. The phylogram positioned *E. benedicti* as a sister species of the clade composed by *E. almeidai* sp. nov., *E. portoricensis*, and *E. talpoida*, although with low support (60%). This major group, including *E. almeidai* sp. nov., *E. portoricensis*, *E. talpoida*, and *E. benedicti*, is the sister group of the clade composed of *E. brasiliensis* and *E. rathbunae*.

The clade containing *E. holthuisi* and *E. emeritus*, species from the Indo-Pacific, was positioned as a sister group of the major American clade mentioned above.

*Emerita analoga*, with reservations on the above-mentioned misidentified specimen, formed a single well-defined clade, with individuals from California (USA) and Chile, and was positioned as the sister species of all other species of *Emerita* used in the reconstruction, including members from the Americas as well as the Old World (*E. emeritus* and *E. holthuisi*).

### Cytochrome Oxidase I (COI) reconstruction

The automated alignment of COI sequences with 658 bp included some sequences of *Emerita* species from GenBank. The phylogram also confirmed the clear separation of every species of *Emerita* (Fig. 3), including the strongly supported position of *Emerita almeidai*

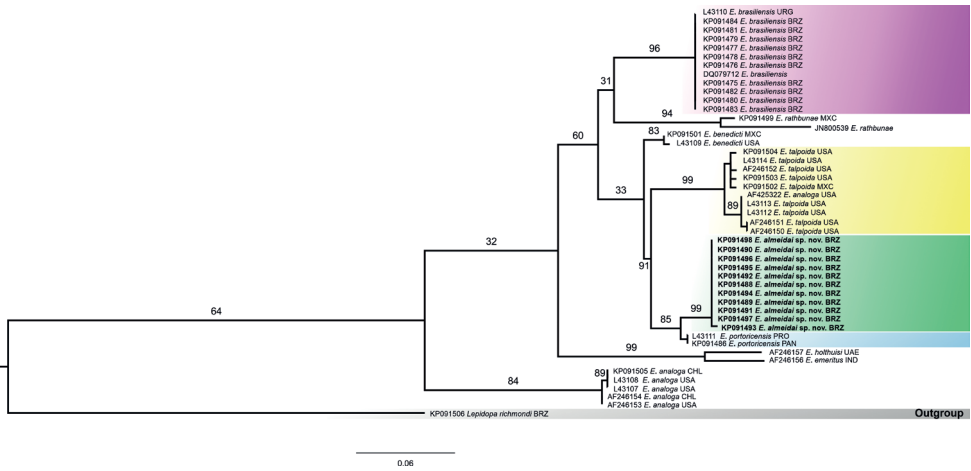


**Figure 2.** Maximum likelihood phylogram obtained for 16S rRNA sequences of *Emerita* specimens. Numbers represent bootstrap values (2000 pseudoreplicates). GenBank code is shown before the species name. Abbreviations: BRZ: Brazil; URG: Uruguay; MXC: Mexico; USA: United States of America; PAN: Panama; PRO: Puerto Rico; UAE: United Arab Emirates; IND: India; CHL: Chile.

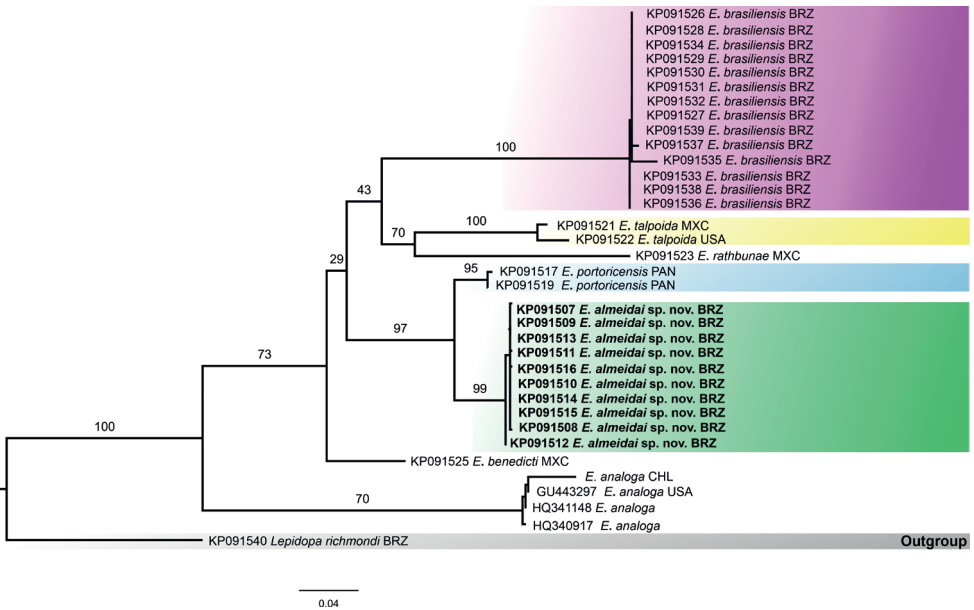


**Figure 3.** Maximum likelihood phylogram obtained for COI (HCO1/LCO1) sequences of *Emerita* specimens. Numbers represent bootstrap values (2000 pseudoreplicates). GenBank code is shown before the species name. Abbreviations: BRZ: Brazil; MXC: Mexico; USA: United States of America; PAN: Panama; CHL: Chile.

sp. nov. Some differences were observed in the phylogenetic position of some of the species included in this alignment compared to that of the 16S rRNA alignment. For instance, *E. rathbunae* was recovered as the closest relative of *E. talpoida* instead of *E. brasiliensis*.

The clade composed of *E. talpoida* and *E. rathbunae* was recovered as the sister group of *E. brasiliensis*. Furthermore, this clade [*E. brasiliensis* + (*E. rathbunae* + *E. talpoida*)] was recovered as the sister group of the clade composed of *E. portoricensis* and *E. almeidai* sp. nov. In this analysis, *E. benedicti* was found to be the sister species of the clade comprising *E. brasiliensis*, *E. talpoida*, *E. rathbunae*, *E. portoricensis*, and *E. almeidai* sp. nov.

Once again, despite the low number of specimens of *E. talpoida*, a clear division into two groups was recovered, with a few differences in relation to the 16S rRNA topology (the individual from Mexico was separated from the Florida one). The phylogenetic positioning of *E. analoga* was maintained as sister to all other species of *Emerita* included in this analysis.

### Concatenated phylogram

The concatenated topology obtained for the 16S rRNA and COI genes (Fig. 4) recovered the main groups that were observed in the two separate analyses carried out for each gene. All specimens of *Emerita almeidai* sp. nov. were clustered together in a well-supported clade. The only specimen of *E. portoricensis* included in the analysis was well separated from other species. These two groups were recovered as sister species in a larger clade, as can be observed in the 16S rRNA and COI phylograms. *Emerita rathbunae* was recovered as the sister species of *E. brasiliensis*, and *E. talpoida* was recovered as the sister species of the clade composed by *E. rathbunae* and *E. brasiliensis*. The division of *E. talpoida* in two subclades was not observed because there were only two specimens of this species. However, subtle differences could be inferred by the long branches connecting the two specimens within this clade. *Emerita benedicti* was recovered as the sister species of all other species of *Emerita* in the analysis.

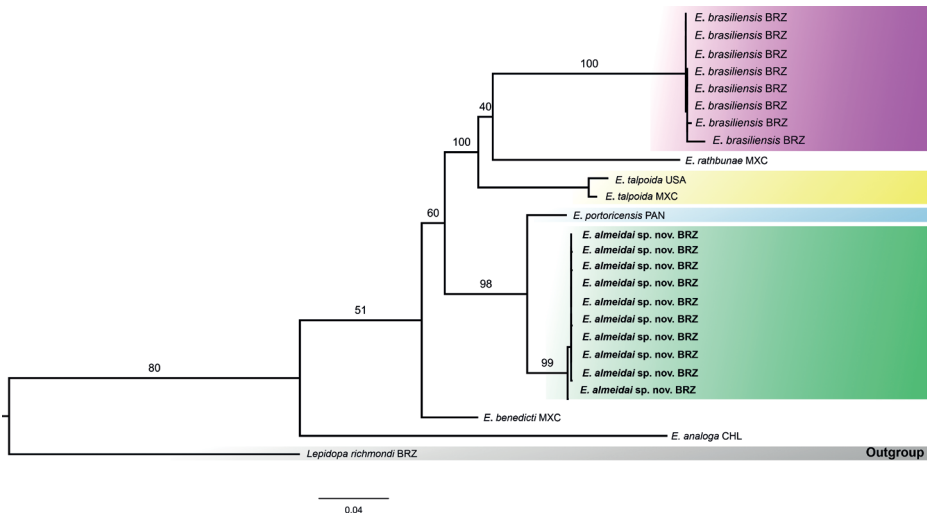


**Figure 4.** Concatenated tree molecular data set (16S rRNA and HCO1/LCO1) of maximum likelihood for *Emerita* specimens. Numbers represent bootstrap values (2000 replicates). GenBank code is shown before the species name. Abbreviations: BRZ: Brazil; MXC: Mexico; USA: United States of America; PAN: Panama; CHL: Chile.

## Taxonomy

Below we present the list of examined material and the description of the new species. A comparative image shows details about the general morphology of the seven species of *Emerita* from the Americas (Fig. 5) and a detailed comparison between *E. brasiliensis* and *E. almeidai* sp. nov. (Fig. 6) is furnished to complement the information. The updated distribution (Fig. 7) and a comparative analysis of the main characters of these two species and *E. portoricensis* was presented in Table 2.

### Superfamily Hippoidea Latreille, 1825

### Family Hippidae Latreille, 1825

### *Emerita* Scopoli, 1777

#### *Emerita almeidai* Mantelatto & Balbino, sp. nov.

<https://zoobank.org/6A094FCB-F019-4853-B561-E427D0963CA8>

Figs 1, 5, 6, 8–12

*Emerita portoricensis* – Efford, 1976: 178, 179; Calado 1990: 266, 268, 271; Tam et al. 1996: 490; Haye et al. 2002: 904 (non *Emerita portoricensis* Schmitt, 1935).

**Type material. Holotype:** ovigerous ♀ (cl. 13.52 mm), CCDB 7233, Praia do Paiva (lower intertidal, quartzite, coarse sand off wave-washed beach), Ilha do Amor, Cabo de Santo Agostinho, PE, Brazil, 08°13'48"S, 34°55'22"W, 27 August 2022, colls. Mantelatto, F.L., Bochini, G.L., Balbino, F.C., Rios, A. **Paratypes:** 3 ovigerous ♀s (cl. 17.31 mm, 17.93 mm, 15.90 mm), 1 ♀ (cl. 14.67mm) (1 ovigerous ♀ cl. 17.31 mm dissected – left antennule, antennae, mouthparts, maxillipeds, pereopods, uropods and telson), CCDB 5855, Praia de Serrambi, Município de Serrambi, Ipojuca, PE, Brazil, 08°33'39.91"S, 35°00'45.15"W, 20 July 2015, colls. Mantelatto, F.L., Mantelatto, F.B., Biagi, R.; 3 ovigerous ♀s (cl. 15.01 mm, 15.93 mm, 9.94 mm), 4 ♀s (cl. 9.66 mm, 9.64 mm, 9.24 mm, 9.02 mm), 1 juvenile (cl. 4.72 mm), "1 ovigerous ♀ (cl. 15.01 mm dissected – mouthparts, maxillipeds, pereopods, uropods and telson), CCDB 4937, Praia de Boa Viagem, Recife, PE, Brazil, 08°08'12.96"S, 34°54'05.84"W, 28 January 2014, colls. Mantelatto, F.L., Mantelatto, F.B., Biagi, R.; 1 ♀ (cl. 10.49 mm), MOUFPE 20112, Praia do Paiva, Ilha do Amor, Cabo de Santo Agostinho, PE, Brazil, 08°13'48"S, 34°55'22"W, 27 August 2022, colls. Mantelatto, F.L., Bochini, G.L., Balbino, F.C., Rios, A.; 1 ♂ (cl. 7.29 mm), MZUSP 43536, Praia do Forte Orange, Vila Velha, Ilha de Itamaracá, PE, Brazil, 07°50'40"S, 34°50'33"W, 30 August 2022, colls. Mantelatto, F.L., Bochini, G.L., Balbino, F.C., Rios, A., Almeida, A.O."

**Additional material.** 1 ♀, CCDB 4526, Morro Branco (CE), 25 March 1989; 1 ♀, 1 ovigerous ♀, CCDB 3369, Praia de Perobas, Touros (RN), 10 June 2011, colls. Robles, R., Pileggi, L.G.; 5 ovigerous ♀s, CCDB 3376, Praia de Maracajaú, Maxaranguape (RN), 10 June 2011, colls. Robles, R., Pileggi, L.G.; 2 ♀s, 1 ovigerous ♀, CCDB 3393, Morro do Careca, Ponta Negra, Natal (RN), 06 June 2011, coll. Robles,

**Table 2.** Diagnostic characters (Calado 1990; Melo 1999; Felder et al. 2023; present study) used for comparison between three studied species.

Characters	<i>E. brasiliensis</i>	<i>E. portoricensis</i>	<i>E. almeidai</i> sp. nov.
Antennal flagellum	103–134 articles	76–86 articles	74–104 articles
Ocular peduncle	Not exceeding the spines of the second antennal article	Usually extending beyond the spines of the second antennal article	Usually extending beyond the spines of the second antennal article
Front (rostrum + lateral projections)	Anterior margin with two triangular projections with rounded distal ends that are ca. the same size as the rostrum	Anterior margin with two triangular projections that extend beyond the level of the rostrum	Anterior margin with two triangular projections that extend beyond the level of the rostrum
Dactylus of first pereopod	Wide, oval shaped, inferior margin not serrated	Narrow, visibly longer than wide, inferior margin slightly, irregularly, or inconspicuously serrated	Narrow, visibly longer than wide, inferior margin conspicuously and regularly serrated
Carapace	Proportionally wider than that of <i>E. portoricensis</i> and <i>E. almeidai</i> sp. nov.	Proportionally longer than that of <i>E. brasiliensis</i> and <i>E. almeidai</i> sp. nov.	Proportionally longer than that of <i>E. brasiliensis</i> ; proportionally wider than that of <i>E. portoricensis</i>
Carapace rugae	Broken into cusps	Dense and non-broken	Dense and non-broken
Telson	Distal end reaching the proximal region of the coxa of the first pereopod	Tends to be longer than wide in relation to the telson of <i>E. brasiliensis</i>	Tends to be longer than wide in relation to the telson of <i>E. brasiliensis</i>
Coloration	Brownish white or olive brown throughout	Olive brown carapace with wide white lines and markings, a white line marking posterior 1/4 of carapace, most rugae the same color as carapace, pleon with alternating olive brown and white bars	Olive brown carapace with slim white lines and markings, line marking posterior 1/4 of carapace usually absent, rugae white in color contrasting with carapace, pleon with alternating olive brown and white bars

R.; 1 ♀, 4 ovigerous ♀s, CCDB 3380, Morro do Careca, Ponta Negra, Natal (RN), 07 June 2011, coll. Robles, R.; 2 ♀s, 10 ovigerous ♀s, CCDB 4869, Praia de Maragogi, Maragogi (AL), 05 October 2013, colls. Mantelatto, F.L., Mantelatto F.B.; 2 ♀s, 2 ovigerous ♀s, CCDB 6127, Praia de Imbassá, Mata de São João (BA), 25 January 2017, colls. Mantelatto, F.L., Mantelatto, F.B.; 1 ovigerous ♀, CCDB 2606, Praia do Pé da Serra, Uruçuca (BA), 31 March 2009, colls. Mantelatto, F.L., Almeida, A.O.; 1 ovigerous ♀, CCDB 2605, Praia do Sul, Km 01, Hotel Praia do Sol, Ilhéus (BA), 30 March 2009, colls. Mantelatto, F.L., Almeida, A.O.; 2 ovigerous ♀s, CCDB 3026, Praia do Sul, Km 01, Hotel Praia do Sol, Ilhéus (BA), 10 November 2010, colls. Mantelatto, F.L., Peiró, D.F.; 1 ♀, 1 ♂, CCDB 4262, Praia da Lagoa Pequena, Prado (BA), 12 August 2012, colls. Carvalho, F.L., Souza-Carvalho, E.A.; 1 ♂, 3 ♀s, 1 ovigerous ♀, CCDB 3992, Praia de Iriri, Iriri (ES), 19 June 2012, colls. Carvalho, F.L., Robles, R., Peiró, D.F.; 2 ovigerous ♀s, CCDB 4376, Pedra do Sal (RJ), 19 November 2009, coll. Arresda, E.

**Comparative material.** *Emerita analoga*: 4 ovigerous ♀s, CCDB 4870, Calfuco, XIV Región, Chile, 20 August 2013, coll. Fuentes, J.P.; *Emerita benedicti*: 5 ♀s, 4 juveniles, CCDB 4674, Playa Escondida, Los Tuxtlas, México, 07 February 2013, coll. Robles, R.; *Emerita brasiliensis*: 7 ♀s, 6 ♂s, CCDB 3990, Laguna Marginal, Guarapari (ES), Brazil, 18 June 2012, colls. Carvalho, F.L., Robles, R., Peiró, D.; 7 ♂s, 12 ♀s, 1 ovigerous ♀, 5 juveniles, CCDB 7226, Praia de Iriri, Anchieta (ES), Brazil, 19 June 2012, colls. Carvalho, F.L., Peiró, D., Robles, R.; 3 ♀s, CCDB 1030, Ubatuba (SP),

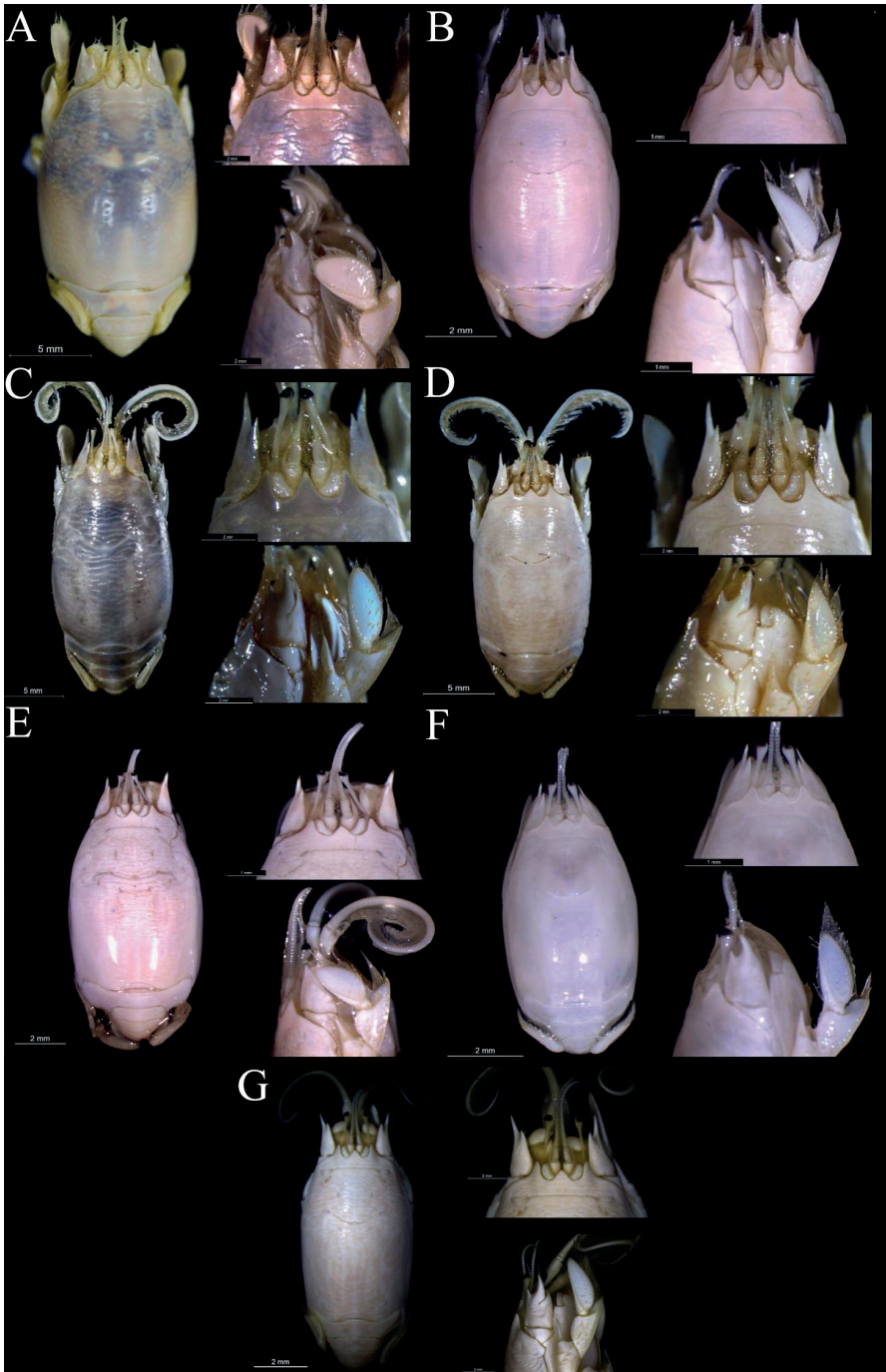


**Figure 5.** Dorsal view of carapace and rostrum/front, and lateral view of antenna/first pereopod of adult ♀s of *Emerita* species from the Americas **A** *Emerita analoga* (CCDB 4870) **B** *Emerita benedicti* (CCDB 4674) **C** *Emerita brasiliensis* (CCDB 4615) **D** *Emerita almeidai* sp. nov. (CCDB 3369) **E** *Emerita rathbunae* (CCDB 1029) **F** *Emerita talpoida* (CCDB 4675) **G** *E. portoricensis* (CCDB 3525).

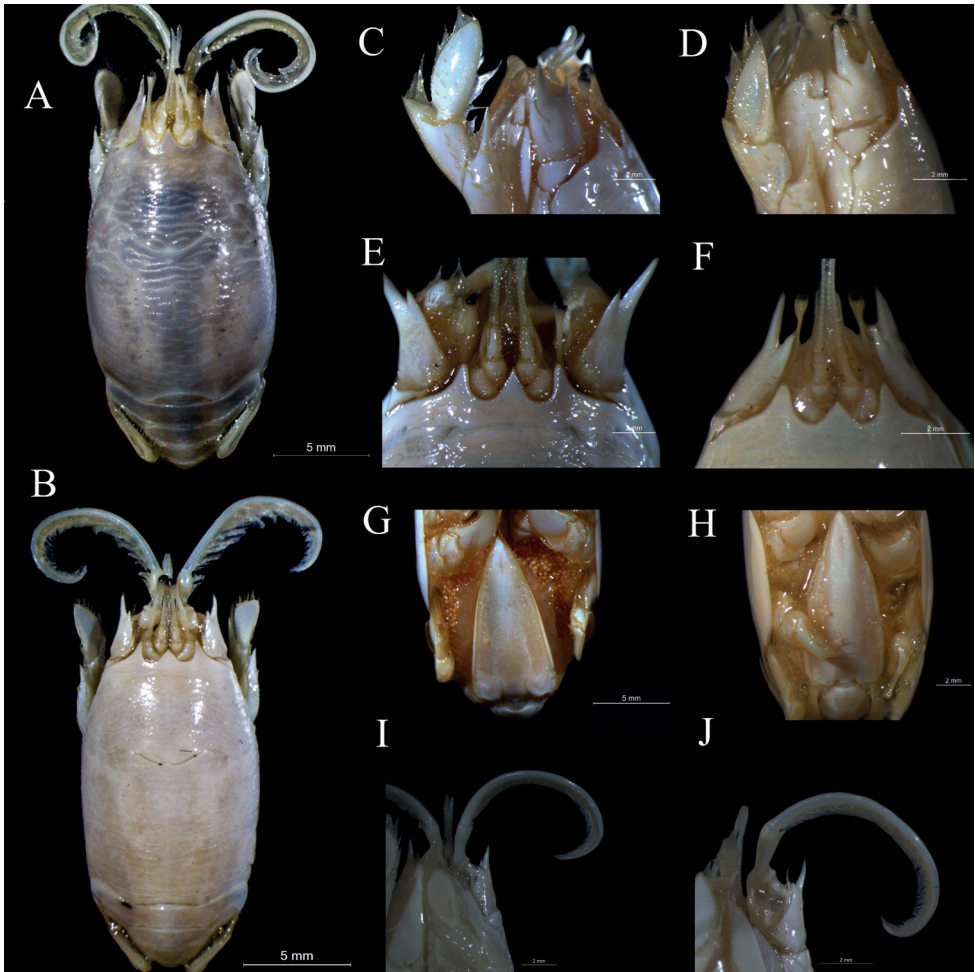


**Figure 6.** Comparative morphological characters observed in adult ♀s of similar sizes between *Emerita brasiliensis* (CCDB 2552) and *E. almeidai* sp. nov. (CCDB 3026). Carapace shape: Dorsal view of **A** *E. brasiliensis* and **B** *E. almeidai* sp. nov.; Dactylus of first pereopod: Lateral view of **C** *E. brasiliensis* and **D** *E. almeidai* sp. nov.; Anterior region with rostrum, lateral spines, and ocular peduncle: Dorsal view of **E** *E. brasiliensis* and **F** *E. almeidai* sp. nov.; Posterior region/telson: Ventral view of **G** *E. brasiliensis* and **H** *E. almeidai* sp. nov.; Left ventral view of antenna **I** *E. brasiliensis* and **J** *E. almeidai* sp. nov.

Brazil, 20 November 2002, colls. Mantelatto, F.L., Scelzo, M.A.; 1 ♀, 1 ovigerous ♀, CCDB 2552, Praia Jaquehy, São Sebastião (SP), Brazil, 26 December 2008, colls. Mantelatto, F.L., Mantelatto, F.B., Biagi, R.; 1 ♀, CCDB 7301, Praia de Guaratuba, Bertioga (SP), Brazil, 07 January 2023, colls. Mantelatto, F.L., Mantelatto, F.B., Mantelatto, H.B.; 2 ♂s, 6 ♀s, 2 ovigerous ♀s, CCDB 3924, Praia Guaiuba, Guarujá (SP), 22 October 2011, colls. Rossi, N.; Leone, I., Carvalho, F.L., Costa, A.; 5 ♀s, CCDB 1443, Praia Itararé, São Vicente (SP), Brazil, 23 October 2011, colls. Rossi, N., Leone, I., Carvalho, F.L., Costa, A.; 3 ♂s, 1 ♀, 7 ovigerous ♀s, CCDB 4409, Praia de Bal-

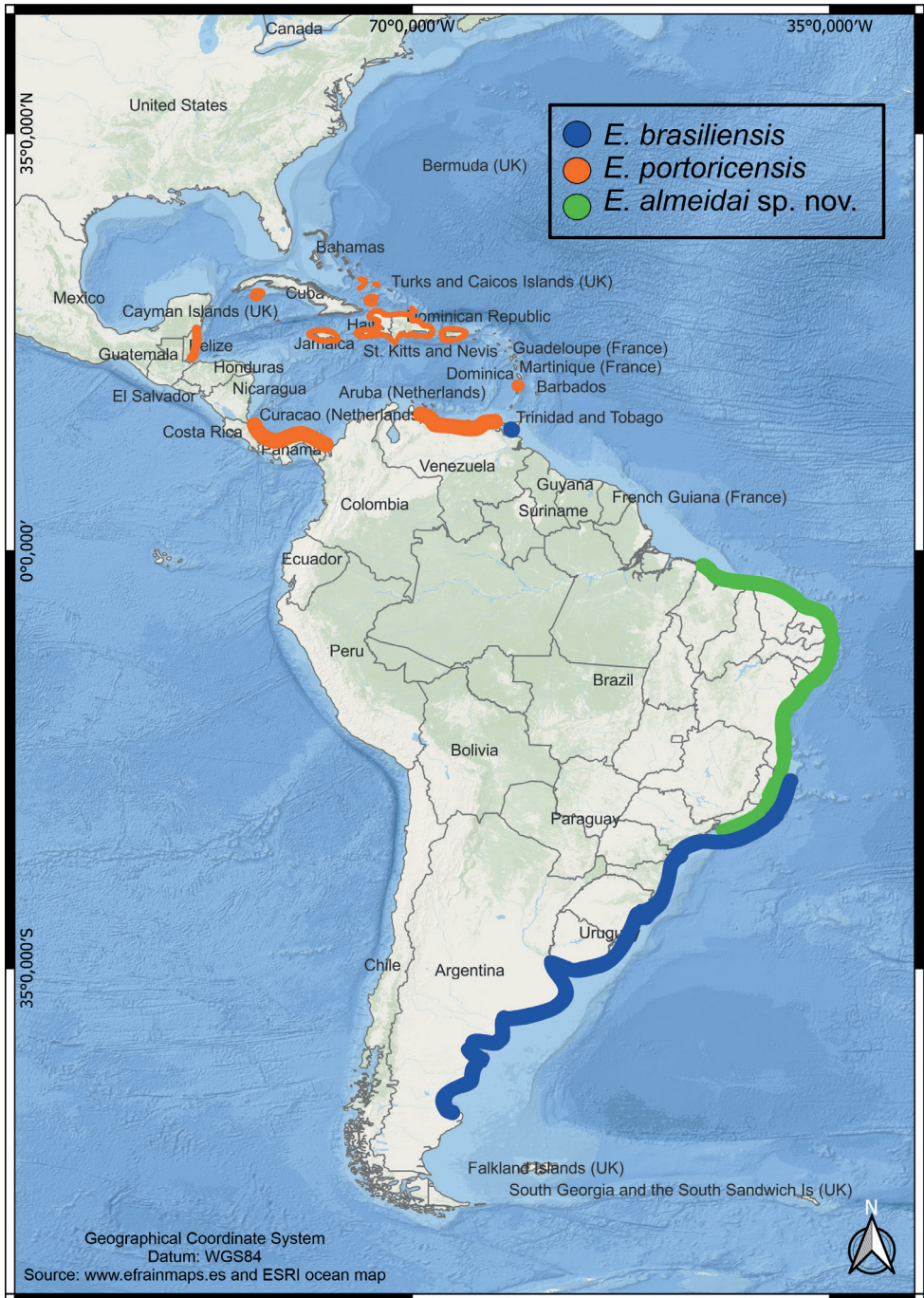


**Figure 7.** The updated geographic distribution of *Emerita brasiliensis*, *E. portoricensis*, and *E. almeidai* sp. nov. according to the literature (Efford 1976; Melo 1999; Veloso and Cardoso 1999; Felder et al. 2023) and the present study.

neário Camboriú, Camboriú (SC), Brazil, 04 December 2012, colls. Carvalho, F.L., Souza-Carvalho, E.A.; *Emerita portoricensis*: ovigerous ♀ (holotype, USNM 65731, photos), Mayaguez, Puerto Rico, 19–20 January 1899; 3 ♀s, CCDB 3525, Playa Boca Del Drago, Bocas Del Toro, Panamá, 06 August 2011, colls. Mantelatto, F.L., Negri, M.P., Rossi, N., Magalhães, T.; *Emerita rathbunae*: 3 ♀s, CCDB 1029, Playa Del Revolcadero, Granjas Del Marquez, Acapulco, México, 06 May 2012, coll. Mantelatto, F.L.; *Emerita talpoida*: 9 ♀s, CCDB 4675, Playa Escondida, Los Tuxtlas, México, 07 February 2013, coll. Robles, R.

**Diagnosis.** Carapace dorsally convex, 1.42–1.54× longer than wide, surface densely covered by microcrenulate rugae; most rugae elongate and continuous across carapace median line not forming rows or lines; 17 or more rugae crossing median line, rugae obsolete laterally on epimeral lobes. Front with three distinct subacute lobes consisting of rostrum and two lateral projections, rostrum visibly shorter than lateral projections. Antennular flagellum dorsal ramus with 30 articles. Antennal peduncle second article large, with three distal spines, median spine the longest, antennal flagellum with 74–104 articles. First maxilla proximal endite rounded, subcircular with margins visibly convex; endopodal palp wide, short, distal end upturned. Third maxilliped without exopod, endopod with merus distal inner margin projected into strong subtriangular lobe, lateral margins of merus sinuous, outer distal margin ending on acute angle. First pereopod merus large, inflated, broad truncate lobe on inferior margin of merus, carpus distal end with large spine, propodus ca. as long as dactylus; dactylus elongate, more than twice as long as wide, superior surface almost straight, inferior surface convex with low, moderate, and regularly spaced serrations, dactylus lined by long plumose setae and short spiniform setae or spinules, terminus of dactylus with single short spine, terminus subacute. Pleon with second pleonite larger than others, tergite as wide as carapace, sides of second pleonite forming wide flanges laterally, second and third pleonite with two pairs of rugae extending from junction with next pleonite almost to ventrolateral margin. Overall coloration olive grey, white laterally, rugae distinctly white in coloration, few thin white bars or stripes near posterolateral regions of carapace.

**Description.** *Carapace* (Figs 1A, 5D, 6B, 8A, 11, 12A) elongate, 1.42–1.54× longer than wide, subcylindrical, overall dorsally convex, highly convex transversely, slightly convex longitudinally; carapace surface densely covered by low transverse microcrenulate to microdenticulate rugae, many of which are continuously elongate, not forming proper lines or rows of rugae, many continuous across middorsal region on anterior and posterior portions of carapace, usually 17 or more rugae extending across postcervical middorsal line; pterygostomial region with ventrolateral rugae; rugae separating small, anteriorly curved ridges; anterior margin of broad epimeral lobe of carapace with serrated appearance due to presence of such ridges. Pterygostomial plates densely punctate, separated from carapace by post-gastric groove; low slightly rugose ridge extending from median portion almost to distal end of plate, parallel to carapace margin for most of its extension, slightly deflected inwards near distal end. Front

(Figs 5D, 6F) with three subacute dentiform projections; median projection forming broad triangular or subtriangular rostrum surrounded by relatively long plumose setae, distal end of rostrum sharply pointed, rostrum visibly shorter than lateral projections; lateral projections subtriangular with concave sides proximally and straight sides distally, visibly longer than rostrum, also surrounded by relatively long plumose setae; rostrum and lateral projections separated by wide U-shaped sulcus. Anterolateral margins of carapace just to the side of frontal projections surrounded by short plumose setae. Transverse frontal groove parallel to front, mostly straight, slightly bent at lateral extremes. Cervical groove just anterior to midlength of carapace, crescent shaped with convex face facing posteriorly, slight anteriorly facing notch on cervical groove on carapace midline. Most rugae broken, obsolete or absent on lower broad epimeral lobe.

**Eyes** (Fig. 5D) swollen at end of very narrow and elongated peduncles, reaching anteriorly past distal portion of fifth antennal peduncle article when extended and past spines of second antennal article when retracted; ocular peduncles composed of three articles; first article arcuate, longer than wide, convex on internal face and concave on external face; second article deflected downwards, longer than first article; third article long, first third wider, other two thirds very narrow, widening near eye.

**Antennules** (Fig. 8C) short; antennular peduncle composed of three articles; first article wider than others, external surface with large dentiform projection near base of article; second article densely setose, trapezoid in shape, dorsal surface shorter, ventral surface longer; third article short, also trapezoid in shape, dorsal surface longer, ventral surface shorter; flagellum dorsal ramus longer, with 30 articles, ventral ramus shorter, with 12 articles.

**Antenna** (Figs 6J, 8D) long; antennal peduncle composed of five articles; first article trapezoidal, longer than wide; second article large, covered by sparse rugae, distal end with three large spiniform projections, median projection longest, dorsal and ventral projections ca. the same size as each other, sulcus extending across dorsolateral surface from proximal end to base of dorsal spiniform projection, microdenticulate ridge separating ventral projection from median projection, one row of setose rugae present on mesial ventral portion; third article inserted on lateral portion of second article, completely concealed by second article in lateral view, trapezoidal in shape, proximal portion rectangular in shape, distal portion triangular, short line of setae parallel to distal margin; fourth article dorsally convex, ventrally Y-shaped; fifth article elongate, slimmer near base, inflated distally, row of setae on ventral margin; flagellum long, composed of 74–104 articles with dense long setae ventrally in adult specimens, number of articles smaller in juveniles, first article longest,  $\sim 3\times$  as long as other articles.

**Mandible** (Fig. 9A) membranous, mostly fused with posterior margin of epistome; gnathal lobe short, kidney-shaped, inserted basally on mandible, projected inwards, external margin convex, internal margin concave, long plumose setae along mesial and distal margins; palpus composed of two articles, longer than gnathal lobe; first article subrectangular; terminal article suboval, lined by many long setae.

**First maxilla** (Fig. 9B) small; proximal endite loosely connected to rest of appendage, oval, flattened, lateral and distal margins surrounded by relatively long setae; distal endite elongate, narrow, distal end slightly wider, pin-shaped, margins lined by setae,

setae on proximal internal side very long, median and distal setae shorter, setae on proximal and median external portions shorter, longer subdistally; endopodal palp nearly as wide as long, tip slightly hooked upwards.

**Second maxilla** (Fig. 9C) exopod developed as scaphognathite attached to base, proximal and distal lobes flattened, lined by long setae, proximal lobe semi-oval in shape, broader, distal lobe semi-oval, slimmer; endopod short, wider proximally, narrowed towards distal end, subacute tip deflected distally.

**First maxilliped** (Fig. 9D) membranous; exopod larger, arched, composed of two articles; proximal article subrectangular, outer margin convex, inner margin concave, distal article subovoid, surrounded distally by many long plumose setae, outer margin proximally convex until ca. midpoint, where it becomes concave, inner margin convex throughout its extension; endopod minute, elongate, membranous, with small tuft of setae subterminally; distal endite crescent shaped, exceeding length of exopod first article, extensively covered by short setae on external surface, inner margin covered by dense long plumose setae, patch of relatively long plumose setae present on distal end.

**Second maxilliped** (Fig. 9E) membranous, exopod and endopod subequal; exopod composed of two articles; proximal article elongate, subtriangular, widest proximally, narrowing towards distal end, sparsely setose; distal article subovoid, margins surrounded by long plumose setae; endopod composed of four articles; ischio-merus narrow, arcuate in shape, proximal end wider, narrowing towards distal end, outer margin convex lined by several long setae, inner margin concave lined by several setae; carpus short, inflated, distal and lateral margins densely covered by long plumose setae; propodus short, less robust than carpus, margins covered by setae; dactylus long, narrow, elongate, widest at base, narrowing towards distal rounded end,  $\sim 2/3$  as long as ischio-merus, surrounded by long setae.

**Third maxilliped** (Fig. 9F, G) lacking exopod; endopod with coxa wider than long, small subtriangular projection on proximal inner side, base-ischium minute, much wider than long, merus broad, sparse setose rugae present on outer face, inner face mostly smooth with one large and distinct ridge crossing merus from base-ischium junction to carpus junction, margins lined by short setae, long plumose setae distally, nearly twice as long as wide, proximal third of inner margin very rounded, convex, distal two thirds straight, large subtriangular projection on distal end of inner portion of merus overlying part of carpus and propodus, outer margin slightly concave proximally, convex distally, distal end of outer portion of merus straight, carpus short, subquadrate, distal margin and inner face covered by long setae, propodus long, slightly curved inwards, outer face smooth, inner face densely covered in setae, dactylus long, shorter than propodus, slightly curved inwards, distal end rounded, outer face smooth inner face densely covered in setae.

**First pereopod** (Fig. 10A) coxa subtrapezoidal, sparsely covered by setose rugae on external face, setae on ventral margin and distal end, ventral dentiform projection proximally; base-ischium longer than wide, minute, lined by setae ventrally, with two lobes separated by median notch, ventral margin surrounded by setae; merus large, subcircular, sparsely covered by setose rugae, superior margin convex, inferior margin convex proximally, extended laterally forming truncate lobe with straight or almost straight lat-

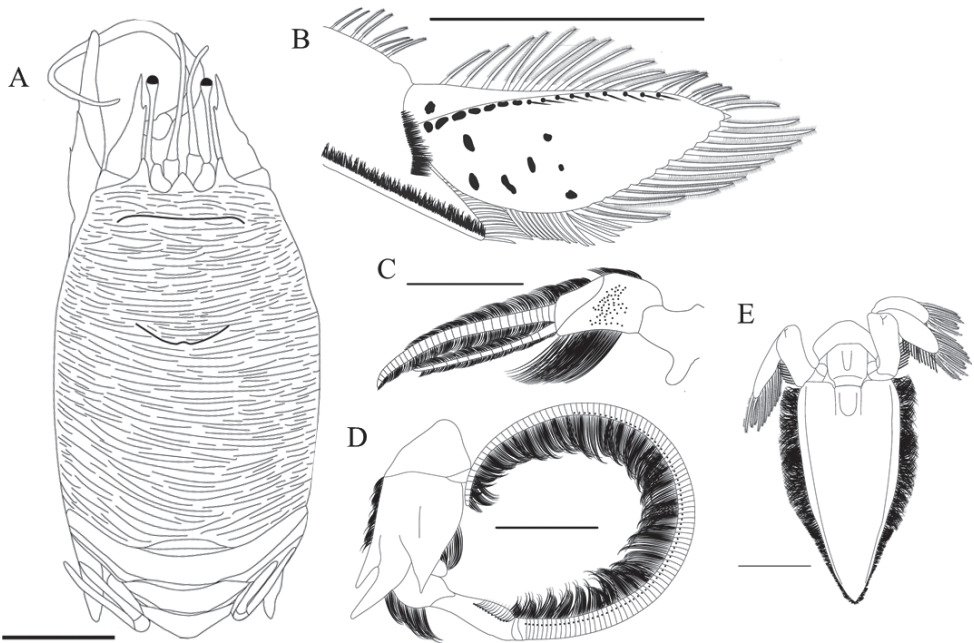


**Figure 8.** *Emerita almeidai* sp. nov. **A** ♀ paratype, cl. 14.67 mm (CCDB 5855) **B, E** ovigerous ♀ paratype, cl. 15.01 mm (CCDB 4937) **C, D** ovigerous ♀ paratype, cl. 17.31 mm (CCDB 5855) **A** dorsal view **B** lateral view of dactylus of pereopod 1 **C** lateral view of left antennule **D** lateral view of left antenna **E** dorsal view of telson and uropods. Scale bars: 6 mm (**A**); 4 mm (**B, E**); 3 mm (**C, D**).

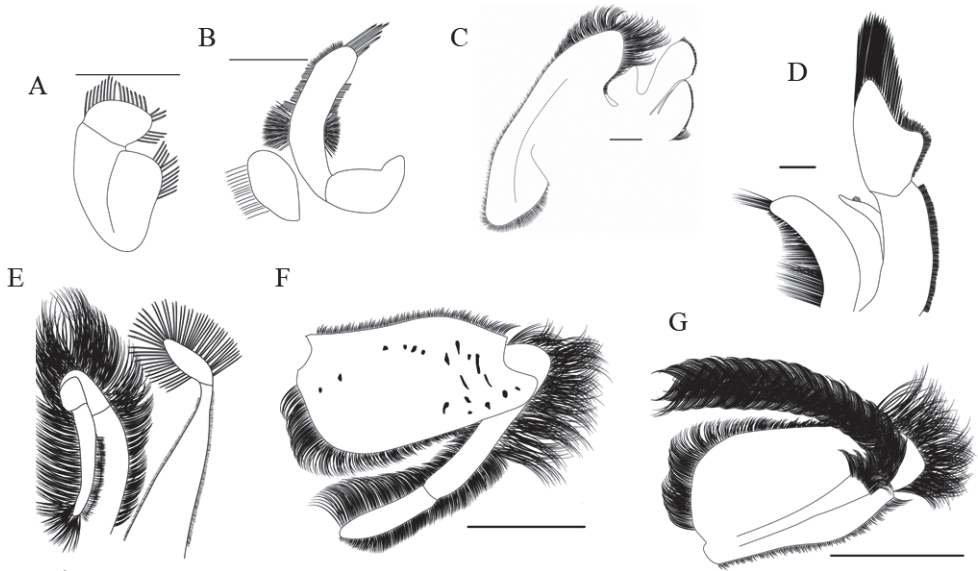


**Figure 9.** *Emerita almeidai* sp. nov. **A–E** ovigerous ♀ paratype, cl. 17.31 mm (CCDB 5855) **F, G** ovigerous ♀ paratype, cl. 15.01 mm (CCDB 4937) **A** right mandible **B** left first maxilla **C** right second maxilla **D** left first maxilliped **E** left second maxilliped **F** right third maxilliped external face **G** right third maxilliped internal face. Scale bars: 1 mm (**A–D**); 4 mm (**E–G**).

eral margin, small short sulcus on mesial portion of distal end of merus; carpus elongate, crossed by some oblique rows of setose rugae on distal ventral portion, three very distinct small perpendicular rows of setose rugae on dorsal surface separating article from large narrow distal spine, spine reaching to base of dactylus; propodus subtrapezoidal in shape, sparsely surrounded by setae, sparse setose rugae present, a transversal ridge running along most of ventrolateral portion of propodus, including distal process (Fig. 8B), dense short setae running along ridge, distal process long, subtriangular, strong oblique ridge running from dactylus junction to base of distal process, superolateral surface of distal process excavate, fits base of dactylus, long setae present on distal process; dactylus (Figs 5D, 6D, 8B) elongate, usually more than twice as long as wide, superior margin mostly straight, inferior surface convex, inferior surface moderately serrated from median portion to distal end, terminus of dactylus acute or subacute bearing one small spine, weakly arched oblique ridge across superior portion of dactylus, ridge originating near median portion of junction with propodus, running upwards towards superior margin, fusing with superior margin around median portion of dactylus, ridge lined by small setae, long plumose setae surrounding dactylus, small spiniform setae among them.

**Second through fourth pereopods** (Fig. 10B, C, D) similar in configuration. Second pereopod coxa subquadrate; base-ischium small, longer than wide, surrounded by setae; merus large, subrectangular, longer than wide, surface covered by sparse setose rugae, superior margin mostly straight, convex towards distal end, inferior margin slightly concave, large dentiform projection protruding ventrally from distal end of merus, inferior margin lined by setae; carpus subtriangular, external surface with two short ridges present, one on superior and one on inferior regions of article, internal surface setose, crossed mesially by single row of setae, inferior portion with small triangular projection distally lined by setae; propodus wider than long, subrectangular, superior margin oblique, external face with small triangular projection positioned distally on dorsal region overlying part of dactylus, transverse ridge near superior margin, internal face with large spiniform projection lined by large setae at ca. same position; dactylus large, flattened, hook-shaped, broad proximally, narrowing distally, superior margin concave, inferior margin convex, distal tip upturned, inferior margin surrounded by long setae. Third pereopod coxa and base-ischium similar to second pereopod; merus subrectangular, much longer than wide; carpus very large, subtriangular, superior and inferior ridges present, propodus wider than long, subrectangular, superior margin oblique, small ridge near superior margin present, small triangular projection positioned distally on superior margin overlying part of dactylus; dactylus large, hook-shaped, flattened, broad proximally, narrowing distally, superior margin concave, inferior margin convex, distal tip upturned, inferior margin surrounded by setae. Fourth pereopod coxa and base-ischium similar to that of second and third pereopods; merus elongate, much longer than wide, subrectangular; carpus large, longer than wide, inferior surface almost straight, superior surface convex; propodus subquadrate, nearly as wide as long, lacking triangular projection, line of short setae near superior margin; dactylus large, somewhat flattened, broad distally, narrowing towards distal end, proportionally smaller than in other pereopods, subtriangular, superior and inferior margins almost straight, tip not upturned, a line of short setae parallel to superior margin, inferior margin lined by setae.

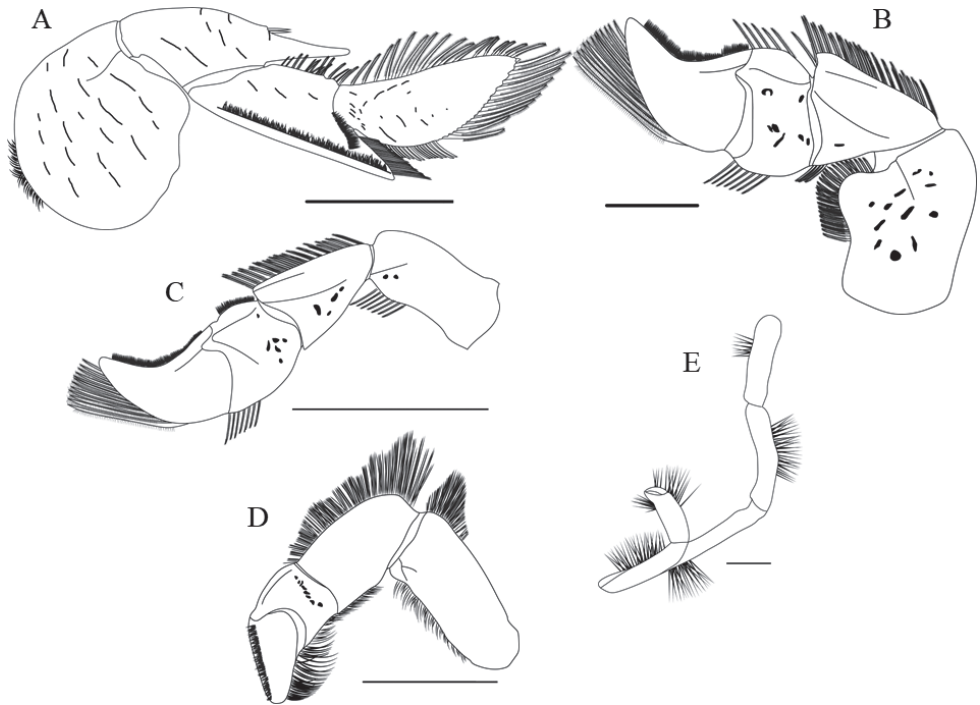


**Figure 10.** *Emerita almeidai* sp. nov. **A, D** ovigerous ♀ paratype, cl. 17.31 mm (CCDB 5855) **B, C, E** ovigerous ♀ paratype, cl. 15.01 mm (CCDB 4937) **A** lateral view of right pereopod 1 **B** lateral view of left pereopod 2 **C** lateral view of left pereopod 3 **D** lateral view of left pereopod 4 **E** lateral view of right pereopod 5. Scale bars: 4 mm (**A**); 2 mm (**B**); 5 mm (**C**); 3 mm (**D**); 1 mm (**E**).

**Fifth pereopod** (Fig. 10E) reduced, concealed under carapace; all articles except for dactylus elongate, much longer than wide, with small tufts of setae distally; propodus long, with distal projection that along with dactylus forms a small chela; dactylus short, deflected inwards; chela small, covered by setae.

**Pleon** short, partly recurved under carapace. First pleonite smallest, minute, much wider than long, fitting into posterior concavity of carapace; second pleonite larger than others, as wide as carapace, median portion of pleonite narrow, both sides of pleonite enlarged, forming two wide lateral flanges, flanges with pair of long transverse rugae extending from third pleonite junction almost to ventrolateral margins of tergite, distal portion of ventrolateral region of each pleonite with short transverse ruga extending from superior margin to inferior margin of narrowest portion of flange, wide lateral flanges forming space where third pleonite fits; third pleonite smaller than second, sides of pleonite somewhat enlarged forming flanges that are mostly covered by flanges of second pleonite, two transverse rugae extending from junction with fourth pleonite to junction with second on each flange; fourth pleonite smaller than third, sides slightly enlarged forming flanges which are mostly covered by flanges of third pleonite, one oblique ruga extending from junction with fifth pleonite to junction with third on each side of pleonite; fifth pleonite smaller than fourth, lateral flanges

small; sixth pleonite subpentagonal, lateral margins forming subtriangular projections, two short longitudinal grooves near articulation with telson, each groove joined to two much smaller transverse grooves. Female pleopods on second through fourth pleonites developed as three long and narrow articles, not developed on first and fifth pleonites; males without developed pleopods on first through fifth pleonites; uropods large, protopod subrectangular, endopod suboval, rounded, distal margin densely covered in setae, exopod suboval, more elongate, distal margin densely covered in setae.

**Telson** (Figs 6H, 8E) lanceolate, lateral margins setose, slightly convex proximally, very slight notches at  $\sim 3/4$  of length of telson, two short longitudinal grooves near junction with pleon, two long longitudinal ridges parallel to lateral margins of telson, distal end of telson subacute.

**Coloration in life.** Carapace overall olive grey dorsally, lateral regions white, rugae extending across carapace white, posterolateral regions of carapace with few slim white longitudinal lines or small white blotches; lines and blotches usually restricted to posterolateral region, but some specimens possess one white longitudinal line along posterior  $1/4$  of carapace median line. Pleonal somites olive-grey anteriorly, white posteriorly, forming a pattern of alternating olive-grey and white stripes (Fig. 12A).

**Habitat.** Shallow infaunal, lives in wave swash zone of sandy beaches or shallow subtidal sandy flats where it burrows shallowly in sand, moves with tidal rise and fall.

**Distribution.** Brazil: known from Maranhão, Ceará, Rio Grande do Norte, Paraíba, Pernambuco, Alagoas, Sergipe, Bahia, Espírito Santo, and Rio de Janeiro.

**Etymology.** The species name honors Alexandre O. Almeida, a valued friend and respected colleague who has contributed extensively to increase knowledge of the decapod crustaceans of Brazil.

**Remarks.** *Emerita almeidai* sp. nov. is closest to *E. portoricensis* and thus shares a wide range of morphological similarities, which is why for many years several specimens from Brazil were wrongly assigned to *E. portoricensis* (see Introduction). Both species have a carapace densely covered by microcrenulate rugae (Figs 1A, 5D, G, 6B, 8A, 11, 12) distributed in similar patterns, a front with three subacute lobes with the rostrum being distinctly shorter than lateral projections (Figs 5D, G, 6B), first pereopod dactyli more than twice as long as wide and not as rounded as in other species such as *Emerita brasiliensis* and *Emerita talpoida* (Figs 5, 6C, D), two pairs of rugae extending onto lateral flanges of the first two pleonites. However, some characters such as the carapace length and width ratio (cw./cl.), the number of articles on the antennal flagellum, the first maxilla, the dactylus of the first pereopod, and the coloration in life can be used to distinguish between these two species. The carapace in *E. almeidai* sp. nov. (Figs 1A, 5D, 6B, 8A, 11, 12A) tends to be more oblong than that of *E. portoricensis* (Figs 5G, 12B), usually being 1.42–1.54 $\times$  as wide as long in adult specimens (vs. 1.49–1.64 $\times$  in *E. portoricensis*, present study), although there is some overlap. The number of articles on the antennal flagellum of *E. almeidai* sp. nov. (Fig. 8D) also tends to be more variable than that of *E. portoricensis*, varying from 74 to 104 articles in adult specimens, while *E. portoricensis* usually has 76–86 (Felder et al. 2023; present study). Although there is still some overlap, this character is still useful to distinguish between the two species. However, juvenile specimens (see details in Materials and

methods) may have many fewer articles on the antennal flagellum in both species, and thus this character is only useful for adult specimens. The first maxilla of *E. almeidai* sp. nov. (Fig. 9B) also differs from that of *E. portoricensis* (Felder et al. 2023: 349, fig. 3): in *E. almeidai* sp. nov. the proximal endite is wider, rounder and with more convex margins, and the endopodal palp is proportionally wider and shorter. The first pereopod dactylus (Figs 5D, 6D, 8B) is also distinct, with *E. almeidai* sp. nov. having low, moderately and regularly spaced serrations on the inferior surface of the dactylus, while *E. portoricensis* has a slight and irregular serrations, which in many cases can be absent. The coloration of these two species can also be used to distinguish between live specimens. As shown in a recent redescription of *E. portoricensis* (Felder et al. 2023: 345, fig. 1) and in the present work (Fig. 12B), this species has very wide white bars on the posterolateral regions of carapace along with a wide white bar along the posterior 1/4 of the carapace median line. Although *E. almeidai* sp. nov. shares some of these characteristics (Fig. 12A), the white bars are usually slimmer and the white bar along the carapace median line is usually absent; however, it was observed only in one freshly collected paratype specimen (MZUSP 43536). The white colored rugae, which were observed in all of the freshly collected specimens of *E. almeidai* sp. nov. (Fig. 12A), however, are not present in either of the specimens shown in the recent redescription of *E. portoricensis* (Felder et al. 2023: 345, fig. 1) or in the specimen analyzed in this study (Fig. 12B), suggesting that this character might be unique to *E. almeidai* sp. nov. The southernmost record for *E. portoricensis* (Venezuela and Trinidad) and the northernmost record for *E. almeidai* sp. nov. (Maranhão, Brazil) are very far apart and there is a strong marine barrier, the Amazon–Orinoco plume (see Curtin 1986 for physical characteristics) that can promote some isolation between northern and southern decapod populations (see Peres et al. 2022), and this is possibly the reason there are no records of these species coexisting in the same environment.

*Emerita almeidai* sp. nov. has been observed to co-occur with *E. brasiliensis* in Praia de Iriri, in the state of Espírito Santo, Brazil (CCDB 3992 and 7226), with specimens of both species being collected at the same locality and on the same day. The distribution of these two species overlaps along the coast of the states of Espírito Santo and Rio de Janeiro, and it is possible that they co-occur in more locations in these states. *Emerita almeidai* sp. nov. can be distinguished from *E. brasiliensis* by the shape of the dactylus, which is elongated and has a serrated ventral margin in *E. almeidai* sp. nov. (Figs 5D, 6D, 8B) and ovate and non-serrated in *E. brasiliensis* (Figs 5C, 6C). The dactylus length and width ratio (dl./dw.) is also a robust parameter to distinguish the two species, especially in individuals of similar size. In *E. almeidai* sp. nov., the dactylus is proportionally longer and narrower than that of *E. brasiliensis*. The front is also different (Figs 5C, D, 6C, D): in *E. brasiliensis* the lateral projections and the rostrum are ca. as long as each other. The patterns of distribution of the microcrenulate rugae are also distinct between these two species (Figs 5C, D, 6A, B), with *E. almeidai* sp. nov. having very dense and non-broken rugae across much of the carapace, while *E. brasiliensis* has rugae that

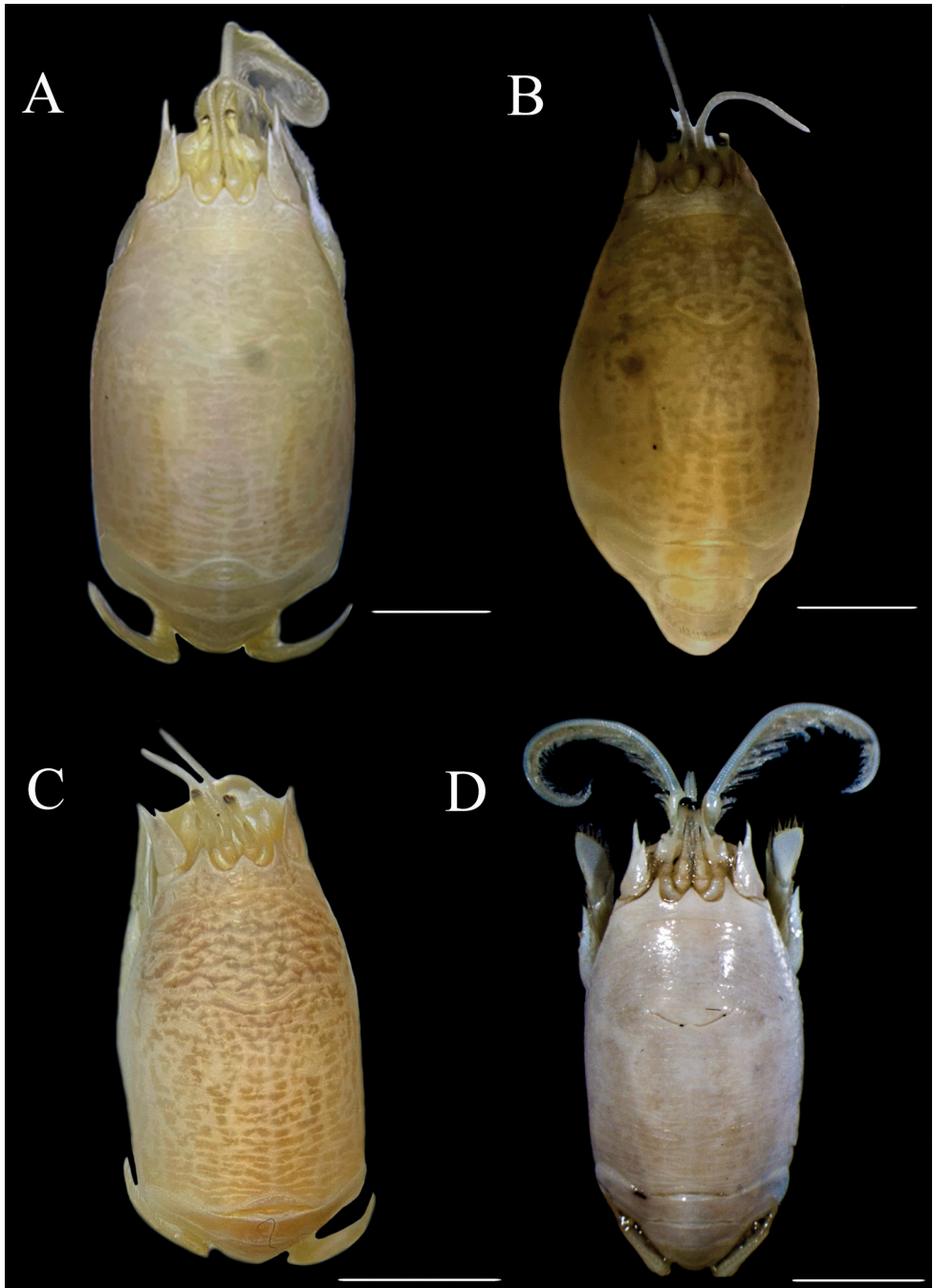


**Figure 11.** *Emerita almeidai* sp. nov. **A** ovigerous ♀ holotype, cl. 13.52 mm (CCDB 7233) **B** ♂ paratype, cl. 7.29 mm (MZUSP 43536) **C** ♀ paratype, cl. 10.49 mm (MOUFPE 20112) **D** ♀, cl. 10.20 mm (CCDB 3369). Scale bars: 4 mm (**A, B**); 2 mm (**C**); 5 mm (**D**).

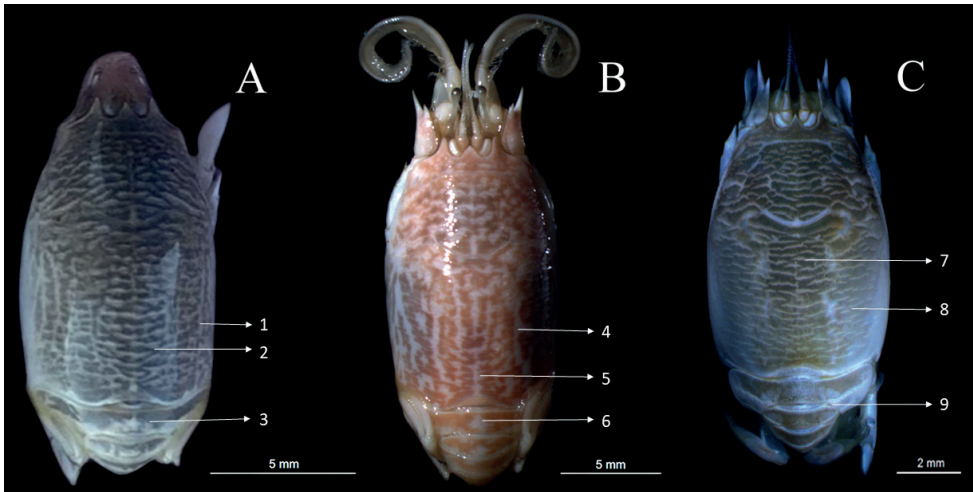


**Figure 12.** Fresh coloration of *Emerita almeidai* sp. nov., *E. portoricensis* and *E. brasiliensis* **A** *E. almeidai* sp. nov., ovigerous ♀ (not deposited), live specimen, Porto de Galinhas, PE, Brazil **B** *E. portoricensis*, ♀ (CCDB 3525), freshly collected specimen, Boca del Drago, Panama **C** *Emerita brasiliensis*, ♀ (CCDB 7301), freshly collected specimen, Praia de Guaratuba, Bertioga (SP), Brazil. Coloring details: 1. Thin white stripes on posterolateral portions of carapace; 2. Rugae clearly surrounded by white coloration; 3. Striped pattern on pleon; 4. Wide white bars on posterolateral portions of carapace; 5. White bar along posterior 1/4<sup>th</sup> of median line of carapace; 6. Striped pattern on pleon; 7. Olive brown or brownish white color overall; 8. Rugae broken into cusps; 9. Absence of striped pattern on pleon.

are more broken into cusps (Felder et al. 2023). Furthermore, the cw./cl. ratio is also useful to distinguish these two species since *E. almeidai* sp. nov. has an overall longer and narrower carapace when compared to *E. brasiliensis*. The antennae (Figs 6I, J, 8D) is another character that can be used to distinguish between the two species, because *E. almeidai* sp. nov. has 74–104 articles, while *E. brasiliensis* has 103–134 articles; however, there is a small overlap. The differences between the telson measurements obtained between the telson length and width ratio (tl./tw.) showed a tendency for telson growth in *E. almeidai* sp. nov. in relation to the increase in carapace length, while in *E. brasiliensis* this ratio tends to remain stable with increasing carapace length. Melo (1999) did not highlight significant differences for this structure, but Calado (1990) described the telson of *E. brasiliensis* as being lanceolate, larger than the pleon, with all margins with short bristles, and that of *E. almeidai* sp. nov. with a triangular shape, larger than the pleon, wider in the proximal portion, with margins also supporting short bristles, which corroborates the biometric data found in our analyses.

The other species of *Emerita* found in the western Atlantic Ocean, *E. talpoida* and *E. benedicti*, are not known to co-occur with *E. almeidai* sp. nov.; *Emerita talpoida* can be distinguished from the new species by the rounded and ovate dactylus of the first pereopod (Fig. 5D, F), while *E. benedicti* (Fig. 5B) has a very acute terminus of the dactylus compared to a more subacute and slightly rounded terminus for *E. almeidai* sp.

nov. The morphology of the first pereopod dactylus can also be used to distinguish the new species from other congeners in the Indian Ocean, Indo-Pacific and eastern Pacific.

Previous descriptions of mouthparts of species of *Emerita* are scarce, only existing for two species, *E. talpoida* and *E. portoricensis* (see Snodgrass 1952 and Felder et al. 2023). Thus, comparative studies of the mouthpart morphology of *Emerita* are lacking and could be of great importance. At least for *E. almeidai* sp. nov. and *E. portoricensis*, it has been noted that the morphology of certain articles of the mouthparts, in this case the first maxilla, can be successfully used to distinguish between species. Thus, future descriptions and redescrptions of species of *Emerita* should include such characters, which might be valuable for comparative taxonomic studies.

The number of species in the genus *Emerita* is now raised to 12, with five occurring in the western Atlantic (*E. almeidai* sp. nov., *E. benedicti*, *E. brasiliensis*, *E. portoricensis*, *E. talpoida*), five in the Indian Ocean or Indo-Pacific (*E. austroafricana*, *E. emeritus*, *E. holthuisi*, *E. karachiensis*, *E. taiwanensis*) and two in the Eastern Pacific (*E. analoga* and *E. rathbunae*). The actual number might even be higher, given that there is a large distribution hiatus between the populations of *E. analoga* from North and South America and genetic differences between the northern and southern populations of *E. talpoida*. The record of *E. brasiliensis* from Venezuela is doubtful and may be a misidentification or may represent a separate species given the large geographic hiatus (Fig. 7). All of these cases require a thorough study, as made herein for some congeners, to determine whether these actually represent different, yet very similar, species.

## Discussion

The combination of morphological and molecular methods confirms the validity of each species of *Emerita* included in the analysis and showed a clear division of *E. talpoida* into two subgroups that should be studied in the future. In addition, our phylogenetic trees based on two molecular markers confirmed the presence of a cryptic species previously misidentified as *E. portoricensis*, which we described in detail as *E. almeidai* sp. nov. For more than eight decades, a group of Brazilian specimens of *Emerita* was treated as *E. portoricensis* by several authors (see Introduction). The distribution of *E. almeidai* sp. nov. from Maranhão to Rio de Janeiro (Brazil) in combination with the redescription of *E. portoricensis* by Felder et al. (2023) answered questions that were raised in the past by some authors (Efford 1976; Calado 1990; Melo 1999) about the gap/discontinuity that existed in the distribution of *E. portoricensis*. These questions were clarified by the recognition of two different species, one in each hemisphere along the western Atlantic.

Species in the genus *Emerita* are known to have relatively long planktonic larval stages (i.e., *E. talpoida* lasting 30 days and *E. rathbunae* lasting 90 days, Efford 1970; *E. holthuisi* lasting 52 days, Siddiqi and Ghory 2006), thus favoring the chances of dispersion to suitable habitats. This extended larval development plays a critical role in governing the genetic structure, phylogeography, and dispersion of mole crabs of the

genus *Emerita* (Dawson et al. 2011), factors which are also influenced and defined by other influences such as currents, transport effects, and sea level changes as observed in other groups (Doherty et al. 1995; Bohonak 1999; Cowen et al. 2000; Dawson 2001; Byers and Pringle 2006; Lester et al. 2007; Lessios 2008). Although the dispersal potential is high for species that present this larval profile (Palumbi and Benzie 1991), it does not always lead to strong gene flow, since physical or biological barriers can interfere with this dispersal process. Thus, disjunct populations can accumulate substantial genetic differences over time (Tam et al. 1996) that can result in the appearance of species that are not recognized as such due to the absence of studies covering all the different populations within the area of distribution as well as the lack of a representative set of specimens from these populations. The newly described species *E. almeidai* sp. nov. fits within this pattern, since it is a southern population that appears to be separated geographically by the Amazon–Orinoco plume, which has been shown to be an important physiological barrier for larval dispersal of many marine taxa, including decapod crustaceans (see Mandai et al. 2018 and Peres et al. 2022 for references and details).

There are some examples to support this hypothesis of separation for marine decapod crustaceans with a wide distribution along the western Atlantic, as noted in *E. almeidai* sp. nov. Using shrimps as an example, a recent study expanded the diversity of seabob shrimps of the genus *Xiphopenaeus* Smith, 1869 with descriptions of two new species (Carvalho-Batista et al. 2019), and a new species of *Latreutes* Stimpson, 1860 was described for a population from Brazil (Terossi et al. 2019). Considering the low number of integrative studies devoted to the huge diversity of decapods in the western Atlantic, these cases might not be exceptional, and we expect that a considerable number of cryptic and undescribed species may be revealed in the future.

### Insights on the evolution of the genus

There are no known fossils that provide information about the evolutionary history of *Emerita* or the paleontological origins of the genus. Molecular clock-based studies have suggested that all species of the genus evolved before the mid- to late Pliocene, although no centers of origin or biogeographic scenarios have been suggested. The hypothesis that *Emerita* species evolved at least before the late Neogene was raised by Tam et al. (1996). Vicariance and dispersal events probably played an important role in the speciation of *Emerita*. Other ecological, physiological, and oceanographic processes likely contributed to the final geographic distribution of the populations that gave rise to the different species of the genus seen today. The expansion and colonization of new geographic areas with subsequent reduction of gene flow were probably the mechanisms by which most of these species originated (Haye et al. 2002).

Species of *Emerita* present a geographic distribution in disjunctive regions, apparently with separate conspecific populations and/or with species that may coexist (see Tam et al. 1996 and Felder et al. 2023 for reviews). In the Americas, *Emerita analoga* is one of two species that inhabit the Pacific coast, recorded in both hemispheres, while *Emerita rathbunae* is restricted to the tropical region. In the western

Atlantic, *Emerita talpoida* is found from Massachusetts to Florida and also in the Gulf of Mexico; *Emerita benedicti* occurs mainly in the inner part of the Gulf of Mexico; *Emerita portoricensis* inhabits the tropical sandy islands and Central American mainland shorelines of the Caribbean Sea; *Emerita brasiliensis* is distributed along the coast of southern South America, and *Emerita almeidai* sp. nov. is endemic to the Brazilian coast. These examples demonstrate that the vast majority of these species have wide geographic ranges and, thus, disjunct populations can be naturally genetically isolated (Tam et al. 1996), especially when natural barriers are present.

Outside of the Americas, *Emerita holthuisi* has a very wide distribution, from the easternmost part of Africa to the southernmost part of India. It can also occur along the east coast of Africa, but so far there are few records for this region. *Emerita emeritus* overlaps with *E. holthuisi* along the western coast of southern India and also occurs in the Indo-Pacific on the eastern coast of India, Malaysia, Indonesia (Efford 1976), and possibly in between. In the present study, these two species grouped together in a separate clade from the one composed of specimens from the Americas. *Emerita austroafricana* can be found along the southern portion of the east coast of Africa, in Mozambique, Madagascar, and South Africa (Schmitt 1937; Efford 1976). The molecular phylogenetic analysis using the COI gene carried out by Haye et al. (2002) recovered *E. austroafricana* as the sister species of *E. emeritus*, although *E. holthuisi*, the sister species of *E. emeritus* recovered in their phylogenetic analysis with the 16S rRNA gene and in the present study, was not included in the analysis. This suggests a close relationship between these three species, but the precise topology of the clade formed by these taxa cannot be determined at present. *Emerita karachiensis* occurs on the west coast of the Indo-Pak subcontinent (Niazi and Haque 1974) and has not been included in any molecular analyses. However, Niazi and Haque (1974) mentioned morphological similarities between *E. karachiensis* and *E. holthuisi*, suggesting a close relationship between these species. Therefore, it is likely that this species is also part of the clade encompassing the Indo-Pacific species, although its exact position within this clade remains to be determined. *Emerita taiwanensis* is known only from two localities in Taiwan (Hsueh 2015) and has not been included in molecular phylogenetic analysis either. Hsueh (2015) suggested a close relationship between species that possess an acute and elongate pereopod 1 dactylus, such as *E. portoricensis*, *E. benedicti*, *E. holthuisi*, and *E. karachiensis*. However, as indicated by our phylogenetic analysis, this character does not seem to be phylogenetically informative, as it does not define any clades and appeared and was lost at least several times during the evolution of the species in the genus. Thus, the phylogenetic relationships of *E. taiwanensis* remain uncertain.

In the hypothesis proposed by Tam et al. (1996) on the evolution of the *Emerita* species from the Americas, it was suggested that *E. analoga* (Pacific species) was diverged from the other five New World species and was distant from *E. rathbunae* (the other Pacific species). Furthermore, *E. rathbunae* was clustered as sister species of the other species of *Emerita* found in the western Atlantic instead of with *E. analoga* that inhabits the Pacific coast. This hypothesis also suggests that *Emerita* species in the Americas evolved from an ancestral stock that was split into two branches, one leading

to *E. analoga* and the other leading to the five remaining species. Our phylogenetic analysis corroborates this hypothesis, as *E. analoga* was recovered as the sister taxon to all other species of *Emerita*. Furthermore, it is likely that after splitting from *E. analoga*, the other populations of *Emerita* were divided into two groups, one that gave rise to the western Atlantic species and another that gave rise to the Indo-Pacific species. Consequently, with this scenario in mind, it can be assumed that the ornamentation of the second joint of the antennal peduncle present in *E. analoga* and some of the Indo-Pacific species (Schmitt 1937) is plesiomorphic, while the apomorphic condition is found in the clade composed of the other American species.

The biogeographic scenarios for the origin of *E. analoga* are not clear, and two hypotheses have been proposed (see references below): in the first, the genus *Emerita* originated on the western side of the Atlantic Ocean. If the center of origin is the Atlantic Ocean, it can be assumed that the species currently distributed in the eastern Pacific (*E. analoga* and *E. rathbunae*) evolved from Atlantic ancestors that dispersed into the Pacific and became isolated due to the closing of the Isthmus of Panama. The isthmus was closed to surface marine water circulation ~ 3 Mya (Late Neogene) but closed to deep-water circulation much earlier (Malfait and Dinkelman 1972; Keigwin 1982). In the second scenario, the center of origin of the genus *Emerita* was the Pacific Ocean. The Atlantic may have been colonized through the isthmus and taxa that differentiated in the Atlantic were likely to be ancestors of the species that later recolonized the Pacific, in this case *E. rathbunae* (Haye et al. 2002). At the end of the Cretaceous (~ 65 Mya), South America and Africa were completely separated (Dietz and Holden 1970). Although it is not possible to know how many species of *Emerita* inhabited the Tethys Sea before the complete separation of South America and Africa, it can be inferred that the separation of the continents was an important event in the speciation of these animals.

The clade composed of the northwest Atlantic species (*E. benedicti*, *E. talpoida*, *E. portoricensis*) and *E. almeidai* sp. nov. from the southwest Atlantic, as recovered in the 16S rRNA analysis, underwent extensive species diversification compared to the clade formed by *E. rathbunae* from the Pacific and *E. brasiliensis*, from the southwestern Atlantic, since the separation of the Pacific and Atlantic oceans ~ 3 Mya. This is consistent with other studies suggesting that the marine biota (mollusks, corals, and foraminiferans) of the western Atlantic were dramatically transformed ~ 2–3 Mya (Jackson and Budd 1996; Allmon 2001). Some hypotheses postulate that this change occurred as a result of the environmental disturbance associated with glaciation in the northern hemisphere and the formation of the Isthmus of Panama (Harrison 2004).

The closure of the Isthmus of Panama strongly affected ocean circulation, nutrient distribution, temperature, and salinity of the western Atlantic, and therefore had a significant influence on the evolution of marine fauna (Coates and Obando 1996; Allmon 2001). The flow of the Gulf Stream through the Yucatan Strait became more intense than it was before the closure of the Isthmus (Richards 1968) with an intense upwelling of cold deep waters (Stanley 1986). Therefore, this type of current may be a significant

factor acting as a barrier to separate the group of species from the Gulf of Mexico from those located in the western side of the Atlantic, as observed in the *E. talpoida* clade, composed of specimens from Florida and Mexico in one group and individuals from Massachusetts and South Carolina in another group. There have been some suggestions of the occurrence of *E. talpoida* in Caribbean waters (see Felder et al. 2023, who say there is no confirmed evidence of this distribution). Previous usage of crabs as models of study (Felder and Staton 1994; Scheineider-Broussard et al. 1998) have identified the Florida Peninsula as a geographic barrier between the western Atlantic and Gulf of Mexico populations, raising awareness about the presence of cryptic species resulting from genetic isolation between populations distributed in these regions.

## Acknowledgements

The present study is part of a long-term project to evaluate the taxonomy and genetic variability of decapods in the western Atlantic, including the Brazilian coast, and was supported by scientific grants provided to FLM by Fundação de Amparo à Pesquisa do Estado de São Paulo – FAPESP (Temáticos Biota 2010/50188-8 and INTERCRUSTA 2018/13685-5; Coleções Científicas 2009/54931-0; PROTAX 2016/50376-5 and 2021/08075-6); Conselho Nacional de Desenvolvimento Científico e Tecnológico – CNPq (Edital Universal 471011/2011-8; International Cooperative Project CNPq 490353/2007-0, 490314/2011-2; and PQ 302748/2015-5, 302253/2019-0); and Coordenação de Aperfeiçoamento de Pessoal de Nível Superior – CAPES (Código de financiamento 001, Ciências do Mar II Proc. 2005/2014 –23038.004308/2014-14). JMP received support by scientific fellowships from CNPq (Proc. 139656/2012-0) and FAPESP (Proc. 2013/20688-7), RR received post-doctoral scholarships from CNPq (Proc. 500460/2010-8) and FAPESP (Proc. 2013/05663-8), JNT received a PhD fellowship from CNPq (Proc. 140957/2020-0) and FCB received a scientific fellowship from FAPESP (Proc. 2022/11860-0). Among many colleagues who assisted with field sampling, loans, donations, logistics, and discussion, we thank Alexandre O. Almeida (UFPE, Brazil), Darryl Felder (ULLZ, USA), Fernando Álvarez and José Luis Villalobos (CNCR, UNAM, Mexico), Javier Luque (Yale University, USA), Luis M. Pardo (Universidad Austral, Chile), Raquel Collins (STRI, Panama), and all members of LBSC for their contributions during the development of this research. The collection and access to genetic heritage of species conducted in this study complied with current applicable state and federal laws of Brazil (permanent license to FLM for collection of Zoological Material No. 11777-2 MMA/IBAMA/SISBIO and SISGEN A4CCD88). The authors, especially FLM, are honored to recognize the many achievements of Dr. Tereza Calado (retired professor of UFAL, Brazil) to the study of mole crabs of Brazil in past and for this reason dedicate this contribution to her. We also thank Christopher Boyko, Dian Baghawati, Ingo S. Wehrtmann, and Nathalie Yonow for the useful comments during the review process.

## References

- Allmon WD (2001) Nutrients, temperature, disturbance, and evolution: A model for the late Cenozoic marine record of the western Atlantic. *Palaeogeography, Palaeoclimatology, Palaeoecology* 166(1–2): 9–26. [https://doi.org/10.1016/S0031-0182\(00\)00199-1](https://doi.org/10.1016/S0031-0182(00)00199-1)
- Bhagawati D, Winarni ET, Nuryanto A (2020) Molecular barcoding reveal the existence of mole crabs *Emerita emeritus* in north coast of Central Java. *Biosaintifika. Journal of Biology & Biology Education* 12(1): 104–110. <https://doi.org/10.15294/biosaintifika.v12i1.20497>
- Bhagawati D, Nuryanto A, Winarni ET, Pulungsari AE (2022) Morphological and molecular characterization of mole crab (Genus: *Emerita*) in the Cilacap coastlines of Indonesia, with particular focus on genetic diversity of *Emerita* sp. nov. *Biodiversitas (Surakarta)* 23(5): 2395–2404. <https://doi.org/10.13057/biodiv/d230517>
- Bohonak AJ (1999) Dispersal, gene flow, and population structure. *The Quarterly Review of Biology* 74(1): 21–45. <https://doi.org/10.1086/392950>
- Boyko CB (2002) A worldwide revision of the recent and fossil sand crabs of the Albuneidae Stimpson and Blepharipodidae, new family (Crustacea: Decapoda: Anomura: Hippoidea). *Bulletin of the American Museum of Natural History* 272: 1–396. [https://doi.org/10.1206/0003-0090\(2002\)272<0001:AWROTR>2.0.CO;2](https://doi.org/10.1206/0003-0090(2002)272<0001:AWROTR>2.0.CO;2)
- Boyko CB, McLaughlin PA (2010) Annotated checklist of anomuran decapod crustaceans of the world (exclusive of the Kiwaoidea and families Chirostylidae and Galatheidae of the Galatheoidea) Part IV – Hippoidea. *The Raffles Bulletin of Zoology (Supplement 23)*: 139–151.
- Byers JE, Pringle JM (2006) Going against the flow: Retention, range limits and invasions in advective environments. *Marine Ecology Progress Series* 313: 27–41. <https://doi.org/10.3354/meps313027>
- Calado TS (1990) Redescritção do gênero *Emerita* Scopoli, 1777 e as espécies brasileiras (Decapoda, Anomura, Hippidae). *Trabalhos Oceanográficos da Universidade Federal de Pernambuco* 21: 263–290. <https://doi.org/10.5914/tropocean.v21i1.2649>
- Calado TS (1998) Biogeografia dos Hippoidea no Atlântico (Crustacea: Decapoda) com ênfase ao Brasil. *Boletim de Estudos de Ciência do Mar* 10: 83–85.
- Carvalho-Batista A, Terossi M, Zara FJ, Mantelatto FL, Costa RC (2019) A multigene and morphological analysis expands the diversity of the seabob shrimp *Xiphopenaeus* Smith 1869 (Decapoda: Penaeidae), with descriptions of two new species. *Scientific Reports* 9(1): e15281. <https://doi.org/10.1038/s41598-019-51484-3>
- Coates AG, Obando JA (1996) The Geologic Evolution of the Central American Isthmus. In: Jackson JBC (Eds) *Evolution and Environment in Tropical America*. University of Chicago Press, Chicago, 21–57.
- Cowen RK, Lwiza KMM, Sponaugle S, Paris CB, Olson DB (2000) Connectivity of marine populations: Open or closed? *Science* 287(5454): 857–859. <https://doi.org/10.1126/science.287.5454.857>
- Crandall KA, Fitzpatrick Jr JE (1996) Crayfish molecular systematic: Using a combination of procedures to estimate phylogeny. *Systematic Biology* 45(1): 1–26. <https://doi.org/10.1093/sysbio/45.1.1>

- Curtin TB (1986) Physical observations in the plume region of the Amazon River during peak discharge—II. Water masses. *Continental Shelf Research* 6(1–2): 53–71. [https://doi.org/10.1016/0278-4343\(86\)90053-1](https://doi.org/10.1016/0278-4343(86)90053-1)
- Dawson MN (2001) Phylogeography in coastal marine animals: A solution from California? *Journal of Biogeography* 28(6): 723–736. <https://doi.org/10.1046/j.1365-2699.2001.00572.x>
- Dawson MN, Barber PH, González-Gusmán LI, Toonen RJ, Dugan JE, Grosberg RK (2011) Phylogeography of *Emerita analoga* (Crustacea, Decapoda, Hippidae), an eastern Pacific Ocean sand crab with long-lived pelagic larvae. *Journal of Biogeography* 38(8): 1600–1612. <https://doi.org/10.1111/j.1365-2699.2011.02499.x>
- Delgado E, Defeo O (2006) A complex sexual cycle in sandy beaches: the reproductive strategy of *Emerita brasiliensis* (Decapoda: Anomura). *Journal of the Marine Biological Association of the United Kingdom* 86(2): 361–368. <https://doi.org/10.1017/S002531540601321X>
- Dietz RS, Holden JC (1970) The breakup of Pangaea. *Scientific American* 223(4): 30–41. <https://doi.org/10.1038/scientificamerican1070-30>
- Doherty PJ, Planes S, Mather P (1995) Gene flow and larval duration in seven species of fish from the Great Barrier Reef. *Ecology* 76(8): 2373–2391. <https://doi.org/10.2307/2265814>
- Efford IE (1970) Recruitment to sedentary marine populations as exemplified by the sand crab, *Emerita analoga* (Decapoda, Hippidae). *Crustaceana* 18(3): 293–308. <https://doi.org/10.1163/156854070X00248>
- Efford IE (1976) Distribution of the sand crabs in the genus *Emerita* (Decapoda, Hippidae). *Crustaceana* 30(2): 169–183. <https://doi.org/10.1163/156854076X00558>
- Felder DL, Staton JL (1994) Genetic differentiation in Trans-Floridian species complexes of *Sesarma* and *Uca* (Decapoda: Brachyura). *Journal of Crustacean Biology* 14(2): 191–209. <https://doi.org/10.2307/1548900>
- Felder DL, Lemaitre R, Mantelatto FL (2023) Redescription of the mole crab *Emerita portoricensis* Schmitt, 1935 (Crustacea: Decapoda: Hippidae), based on Caribbean populations from Puerto Rico, Belize, Costa Rica, and Panama. *Zootaxa* 5227(3): 341–354. <https://doi.org/10.11646/zootaxa.5227.3.3>
- Folmer O, Black M, Hoeh W, Lutz R, Vrijenhoek R (1994) DNA primers for amplification of mitochondrial cytochrome c oxidase subunit I from diverse metazoan invertebrates. *Molecular Marine Biology and Biotechnology* 3: 294–297.
- Hall TA (2005) BioEdit version 7.0.5. Biological sequence alignment editor for windows 95/98/NT/2000/XP. <http://www.mbio.ncsu.edu/BioEdit/bioedit.html> [Accessed 11 Dec 2018]
- Harrison JS (2004) Evolution, biogeography, and the utility of mitochondrial 16s and COI genes in phylogenetic analysis of the crab genus *Austinixia* (Decapoda: Pinnotheridae). *Molecular Phylogenetics and Evolution* 30(3): 743–754. [https://doi.org/10.1016/S1055-7903\(03\)00250-1](https://doi.org/10.1016/S1055-7903(03)00250-1)
- Haye PA, Tam YK, Kornfield I (2002) Molecular phylogenetics of mole crabs (Hippidae, *Emerita*). *Journal of Crustacean Biology* 22(4): 903–915. <https://doi.org/10.1163/20021975-99990302>
- Hsueh PW (2015) A new species of *Emerita* (Decapoda, Anomura, Hippidae) from Taiwan, with a key to species of the genus. *Crustaceana* 88(3): 247–258. <https://doi.org/10.1163/15685403-00003413>

- Hubbard DM, Dugan JE (2003) Shorebird use of an exposed sandy beach in Southern California. *Estuarine, Coastal and Shelf Science* 58: 41–54. [https://doi.org/10.1016/S0272-7714\(03\)00048-9](https://doi.org/10.1016/S0272-7714(03)00048-9)
- Jackson JBC, Budd AF (1996) Evolution and environment: introduction and overview. In: Jackson JBC, Budd AF, Coates AG (Eds) *Evolution and Environment in Tropical America*. University of Chicago Press, Chicago, 20 pp.
- Katoh K, Standley DM (2016) A simple method to control over-alignment in the MAFFT multiple sequence alignment program. *Bioinformatics* 32: 1933–1942. <https://doi.org/10.1093/bioinformatics/btw108>
- Kearse M, Moir R, Wilson A, Stones-Havas S, Cheung M, Sturrock S, Buxton S, Cooper A, Markowitz S, Duran C, Thierer T, Ashton B, Meintjes P, Drummond A (2012) Geneious Basic: An integrated and extendable desktop software platform for the organization and analysis of sequence data. *Bioinformatics* 28(12): 1647–1649. <https://doi.org/10.1093/bioinformatics/bts199>
- Keigwin Jr LD (1982) Isotopic paleoceanography of the Caribbean and East Pacific: Role of the Panama uplift in Late Neogene time. *Science* 217(4557): 350–353. <https://doi.org/10.1126/science.217.4557.350>
- Lercari D, Defeo O (1999) Effects of freshwater discharge in sandy beach populations: The mole crab *Emerita brasiliensis* in Uruguay. *Estuarine, Coastal and Shelf Science* 49(4): 457–468. <https://doi.org/10.1006/ecss.1999.0521>
- Lessios HA (2008) The great American schism: Divergence of marine organisms after the rise of the central American isthmus. *Annual Review of Ecology, Evolution, and Systematics* 39(1): 63–91. <https://doi.org/10.1146/annurev.ecolsys.38.091206.095815>
- Lester SE, Ruttenberg BI, Gaines SD, Kinlan BP (2007) The relationship between dispersal ability and geographic range size. *Ecology Letters* 10(8): 745–758. <https://doi.org/10.1111/j.1461-0248.2007.01070.x>
- Luo A, Qiao H, Zhang Y, Shi W, Ho SY, Xu W, Zhang A, Zhu C (2010) Performance of criteria for selecting evolutionary models in phylogenetics: A comprehensive study based on simulated datasets. *BMC Evolutionary Biology* 10(242): 1–13. <https://doi.org/10.1186/1471-2148-10-242>
- Malfait BT, Dinkelman MG (1972) Circumcaribbean tectonic and igneous activity and the evolution of the Caribbean Plate. *Geological Society of America Bulletin* 83(2): 251–272. [https://doi.org/10.1130/0016-7606\(1972\)83\[251:CTAIAA\]2.0.CO;2](https://doi.org/10.1130/0016-7606(1972)83[251:CTAIAA]2.0.CO;2)
- Mandai SS, Buranelli RC, Schubart CD, Mantelatto FL (2018) Phylogenetic and phylogeographic inferences based on two DNA markers reveal geographic structure of the orange claw hermit crab *Calcinus tibicen* (Anomura: Diogenidae) in the western Atlantic. *Marine Biology Research* 14(6): 565–580. <https://doi.org/10.1080/17451000.2018.1497184>
- Mantelatto FL, Robles R, Biagi R, Felder DL (2006) Molecular analysis of the taxonomic and distributional status for the hermit crab genera *Loxopagurus* Forest, 1964, and *Isocheles* Stimpson, 1858 (Decapoda, Anomura, Diogenidae). *Zoosystema* 28(2): 495–506.
- Mantelatto FL, Robles R, Felder DL (2007) Molecular phylogeny of the western Atlantic species of the genus *Portunus* (Crustacea, Brachyura, Portunidae). *Zoological Journal of the Linnean Society* 150(1): 211–220. <https://doi.org/10.1111/j.1096-3642.2007.00298.x>

- Mantelatto FL, Pardo LM, Pileggi LG, Felder DL (2009) Taxonomic re-examination of the hermit crab species *Pagurus forceps* and *Pagurus comptus* (Decapoda: Paguridae) by molecular analysis. *Zootaxa* 2133(16): 20–32. <https://doi.org/10.11646/zootaxa.2133.1.2>
- Mantelatto FL, Miranda I, Vera-Silva AL, Negri M, Buranelli RC, Terossi M, Magalhães T, Costa RC, Zara FJ, Castilho AL (2021) Checklist of decapod crustaceans from the coast of the São Paulo state (Brazil) supported by integrative molecular and morphological data: IV. Infraorder Anomura: Superfamilies Chirostyloidea, Galatheoidea, Hippoidea and Paguroidea. *Zootaxa* 4965(3): 558–600. <https://doi.org/10.11646/zootaxa.4965.3.9>
- Melo GAS (1999) Manual de identificação dos Crustacea Decapoda do litoral Brasileiro: Anomura, Thalassinidea, Palinuridea, Astacidea. Ed. Plêiade/FAPESP, São Paulo, 551 pp.
- Miller S, Dykes D, Polesky H (1988) A simple salting out procedure for extracting DNA from human nucleated cells. *Nucleic Acids Research* 16(3): e1215. <https://doi.org/10.1093/nar/16.3.1215>
- Miller MA, Pfeiffer W, Schwartz T (2010) Creating the CIPRES Science Gateway for inference of large phylogenetic trees. Gateway Computing Environments Workshop (GCE). <https://doi.org/10.1109/GCE.2010.5676129>
- Miranda I, Peres P, Tavares MDS, Mantelatto FL (2020) New molecular data on squat lobster from the coast of São Paulo State (Brazil) (Anomura: *Munida* and *Agononida*) and insights on the systematics of the Family Munididae. Chapter 14. In: Hendrickx M (Ed.) Deep-Sea Pycnogonids and Crustaceans of the Americas. Springer Nature, Cham, 343–356. [https://doi.org/10.1007/978-3-030-58410-8\\_14](https://doi.org/10.1007/978-3-030-58410-8_14)
- Niazi MS, Haque MM (1974) On a new species of mole-crab (*Emerita karachiensis* sp. nov.) with a key to common Indo-Pacific species. *Records of the Zoological Survey of Pakistan* 5: 1–6.
- Palumbi SR, Benzie J (1991) Large mitochondrial DNA differences between morphologically similar penaeid shrimp. *Molecular Marine Biology and Biotechnology* 1: 27–34.
- Peres PA, Bracken-Grissom H, Timm LE, Mantelatto FL (2022) Genomic analyses implicate the Amazon–Orinoco Plume as the driver of cryptic speciation in a swimming crab. *Genes* 13(12): e2263. <https://doi.org/10.3390/genes13122263>
- Pérez D (2003) Mercury levels in mole crabs *Hippa cubensis*, *Emerita brasiliensis*, *Emerita portoricensis* and *Lepidopa richmondi* (Crustacea: Decapoda: Hippidae) from a sandy beach at Venezuela. *Bulletin of Environmental Contamination and Toxicology* 63: 320–326. <https://doi.org/10.1007/s001289900983>
- Petracco M, Veloso VG, Cardoso RS (2003) Population dynamics and secondary production of *Emerita brasiliensis* (Crustacea: Hippidae) at Prainha Beach, Brazil. *Marine Ecology (Berlin)* 24(3): 231–245. <https://doi.org/10.1046/j.0173-9565.2003.00837.x>
- Richards HG (1968) The tertiary history of the Atlantic coast between Cape Cod and Cape Hatteras. *Palaeogeography, Palaeoclimatology, Palaeoecology* 5(1): 95–104. [https://doi.org/10.1016/0031-0182\(68\)90063-1](https://doi.org/10.1016/0031-0182(68)90063-1)
- Robles R, Schubart CD, Conde JE, Carmona-Suárez C, Álvarez F, Villalobos JL, Felder DL (2007) Molecular phylogeny of the American *Callinectes* Stimpson, 1860 (Brachyura: Portunidae), based on two partial mitochondrial genes. *Marine Biology* 150(6): 1265–1274. <https://doi.org/10.1007/s00227-006-0437-7>

- Rodgers JA (1987) The foraging behavior of gray gulls at a sandy beach. *The Wilson Bulletin* 99: 271–273.
- Scheineider-Broussard R, Felder DL, Chlan CA, Neigel JE (1998) Tests of phylogeographic models with nuclear and mitochondrial DNA sequences variation in stone crabs, *Menippe adina* and *Menippe mercenaria*. *Evolution; International Journal of Organic Evolution* 52(6): 1671–1678. <https://doi.org/10.2307/2411339>
- Schmitt WL (1935) Crustacea Macrura and Anomura of Porto Rico and the Virgin Islands. *Scientific Survey of Puerto Rico and the Virgin Islands, New York Academy of Science* 15(2): 125–227. <https://doi.org/10.5962/bhl.title.10217>
- Schmitt WL (1937) A new species of *Emerita* (Crustacea) from South Africa. *Annals of the South African Museum* 32: 25–29. [pl. 3.]
- Schubart CD, Neigel JE, Felder DL (2000) Use of the mitochondrial 16S rRNA gene for phylogenetic and population studies of Crustacea. *Crustacean Issues* 12: 817–830.
- Siddiqi FA, Ghory FS (2006) Complete larval development of *Emerita holthuisi* Sankolli, 1965 (Crustacea: Decapoda: Hippidae) reared in the laboratory. *Turkish Journal of Zoology* 30: 121–135.
- Snodgrass RE (1952) The sand crab *Emerita talpoida* (Say) and some of its relatives. *Smithsonian Miscellaneous Collections* 117(8): 1–34.
- Spivak ED, Fariás NE, Ocampo EH, Lovrich GA, Luppi TA (2019) Annotated catalogue and bibliography of marine and estuarine shrimps, lobsters, crabs and their allies (Crustacea: Decapoda) of Argentina and Uruguay (Southwestern Atlantic Ocean). *Frente Marítimo* 26: 1–164.
- Stanley SM (1986) Anatomy of a regional mass extinction: Plio-Pleistocene decimation of western Atlantic bivalve fauna. *Palaios* 1(1): 17–36. <https://doi.org/10.2307/3514456>
- Tam YK, Kornfield I, Ojeda FP (1996) Divergence and zoogeography of mole crabs, *Emerita* spp. (Decapoda: Hippidae) in the Americas. *Marine Biology* 125(3): 489–497. <https://doi.org/10.1007/BF00353262>
- Terossi M, Almeida AO, Mantelatto FL (2019) Morphology and DNA data reveal a new shrimp species of genus *Latreutes* Stimpson, 1860 (Decapoda: Hippolytidae) from the western Atlantic. *Zoological Science* 36(5): 440–447. <https://doi.org/10.2108/zs190016>
- Timm L, Bracken-Grissom HD (2015) The forest for the trees: Evaluating molecular phylogenies with an emphasis on higher-level Decapoda. *Journal of Crustacean Biology* 35(5): 577–592. <https://doi.org/10.1163/1937240X-00002371>
- Veloso VG, Cardoso RS (1999) Population biology of the mole crab *Emerita brasiliensis* (Decapoda: Hippidae) at Fora Beach, Brazil. *Journal of Crustacean Biology* 19(1): 147–153. <https://doi.org/10.1163/193724099X00349>
- WoRMS (2023) Hippoidea Latreille, 1825. World Register of Marine Species. <https://www.marinespecies.org/aphia.php?p=taxdetails&id=106686> [Accessed 23 Feb 2023]